An investigation of the dynamic behavior of a hybrid life support system and an experiment on plant cultivation with a urine-derived nutrient solution

Bei der Fakultät Maschinenwesen

der Technischen Universität Dresden

zur

Erlangung des akademischen Grades

Doktoringenieur (Dr.-Ing.)

angenommene Dissertation

von

Dipl.-Ing. Paul Zabel

geboren am 10.06.1987 in Altdöbern.

Tag der Einreichung: 11.10.2017

Tag der Verteidigung: 02.04.2019

Gutachter: Prof. Dr. techn. Martin Tajmar, TU Dresden

Prof. Dr.-Ing. Markus Czupalla, FH Aachen

Vorsitzender der Promotionskommission:

Prof. Dipl.-Ing. Dr. nat. techn. habil. Harald Rohm

Acknowledgements

I would like to thank Prof. Martin Tajmar for his continuous support and advices during the work on this thesis. Furthermore, I would like to thank Prof. Markus Czupalla for providing the second review on the thesis and the fruitful discussions at the past International Conferences on Environmental Systems.

I thank Christel Paille from ESA's MELiSSA bio-regenerative life support research group who helped me to secure funding for this thesis through ESA's Networking and Partnering Initiative (NPI).

Special thanks go to my colleagues of the EDEN research group and the department for system analysis space segment at the DLR Institute of Space Systems in Bremen. It was a pleasure to be part of such a motivated team and the wonderful work environment. First among them I would like to thank Daniel Schubert who supervised my diploma thesis and then hired me for his research team. I also thank Dr. Matthew Bamsey, Conrad Zeidler and Vincent Vrakking for talks about life support systems and plant cultivation in space. Great thanks also to the interns Andreas Hadjistyllis, Alexander Bell, Hendrik Kolvenbach, Etienne David and Dominik von Borell who supported me building the growth chambers for the experiments and helped me out with the experiment execution when I was busy with other projects.

Above all I want to thank my parents and my family! You are the biggest source of inspiration I could think of. You always motivated me to go my own way. You were always listening to my complaints and providing good advices in hard times. Thank you so much!

Danksagung

Ich möchte Prof. Martin Tajmar für seine kontinuierliche Unterstützung und seine Ratschläge während der Arbeit an dieser Dissertation danken. Außerdem danke ich Prof. Markus Czupala dafür, dass er das zweite Gutachten für diese Arbeit verfasst hat und auch für die anregenden Diskussionen während der letzten International Conferences on Environmental Systems.

Ich danke Christel Paille von ESA's MELiSSA Forschungsgruppe für bio-regenerative Lebenserhaltungssysteme für ihre Unterstützung bei meinem Antrag für Fördermittel bei ESA's Networking and Partnering Initiative.

Besonderer Dank geht an meine Kollegen der EDEN Forschungsgruppe und der Abteilung System Analyse Raumsegment am DLR Institut für Raumfahrtsysteme in Bremen. Es war mir eine Freude Teil eines so motivierten Teams zu sein. Als erstem aus dem Team möchte ich Daniel Schubert danken. Er betreute bereits meine Diplomarbeit und holte mich dann in sein Forschungsteam. Ich danke außerdem Dr. Matthew Bamsey, Conrad Zeidler und Vincent Vrakking für die zahlreichen Gespräche über Lebenserhaltungssysteme und Pflanzenanbau im Weltraum. Großer Dank geht auch an meine Praktikanten Andreas Hadjistyllis, Alexander Bell, Hendrik Kolvenbach, Etienne David und Dominik von Borell, welche mir halfen die Pflanzenkammern für die Experimente aufzubauen und zu betreiben.

Von allen gehört meinen Eltern und meiner Familie der größte Dank! Ihr seid die größte Quelle an Inspiration die ich haben konnte. Ihr habt mich immer motiviert meinen eigenen

Weg zu gehen. Ihr habt immer meinen Beschwerden zugehört und mir gute Ratschläge in harten Zeiten gegeben. Vielen herzlichen Dank!

Abstract

Earth's biosphere is sustained by its biological diversity, which forms an intricate network of biological, physical and chemical pathways. This network has many fail-safe redundant functions including buffer stocks of inert biomass, huge amounts of water and the large volume of gases in the atmosphere. By contrast, manmade habitats for human space exploration are closed ecosystems that represent only a trivial fraction of Earth's biosphere.

The employment of bio-regenerative processes complemented with physical-chemical technologies is thought to have numerous advantages from the perspective of redundancy and reducing resupply mass for the sustained human presence in space or on other planetary surfaces. However, the combination of bio-regenerative processes, such as plant cultivation, with physical-chemical processes to form hybrid life support systems is challenging. Such systems are a concert of many interdependencies and interacting feedback loops, which are difficult to operate in a desired range of set points. Furthermore, the complexity of such systems makes them vulnerable to perturbations.

Applying system dynamics modelling to study hybrid life support systems is a promising approach. System dynamics is a methodology used to study the dynamic behavior of complex systems and how such systems can be defended against, or made to benefit from, the perturbations that fall upon them. This thesis describes the development of a system dynamics model to run exploratory simulations, which can lead to new insights into the complex behavior of hybrid life support systems. An improved understanding of the overall system behavior also helps to develop sustainable, reliable and resilient life support architectures for future human space exploration.

A set of simulations with a hybrid life support system integrated into a Mars habitat has been executed and the results show a strong impact of space greenhouses on the life support system behavior and the different matter flows. It is also evident from the simulation results that a hybrid life support system can recover from a perturbation event in most cases without a fatal mission end.

Recycling urine to produce a plant nutrient solution is a novel approach in further closing loops in space life support systems. Within this thesis, a number of experiments have been executed in order to determine the effectiveness of a urine-derived nutrient solution compared to a standard reference solution. The results show that in principle plants can be grown with a nutrient solution made of human urine, but that the yield is lower compared to the reference solution. However, the urine-derived solution might be tuned by adding small amounts of additional nutrients to remove the imbalance of certain elements. This way the nutrient salts supplied from Earth could be reduced.

Table of Content

Table of Content

Table of Content

1 Scope

1.1 Motivation

Humanity will eventually leave Earth to explore the solar system and what lies beyond. These journeys require the construction of advanced hybrid life support systems, a combination of physical-chemical technologies and bio-regenerative systems. These system mimic the functions of Earth's biosphere to keep the travelling humans alive. Earth's biosphere is sustained by its biological diversity, which forms an intricate network of biological, physical and chemical pathways. This network has many fail-safe redundant functions including buffer stocks of inert biomass, huge amounts of water and the large volume of gases in the atmosphere. By contrast, manmade habitats for space exploration are closed ecosystems that represent only a trivial fraction of Earth's biosphere.

Bio-regenerative systems are often incorporated in the ideas of long duration crewed space missions and also in ideas of habitats on the Moon, Mars or other planetary bodies. Most concepts incorporate a space greenhouse for food production, air revitalization and also for psychological benefits. Other bio-regenerative systems are algae photo bioreactors for food production and air revitalization, or systems with mono- or polycultures of microorganisms for waste treatment and water recycling. While all of these systems have been advanced in recent years by various research and development teams all over the world, there is still a strong need for more research in area of bio-regenerative life support systems. This need was also identified in a study for the European Space Agency (ESA):

> *'It will be practically impossible within the foreseeable future to replace completely the physicochemical Life Support technologies by biological processes. However, the need for progressing in bio-regenerative technologies is obvious.'*

<div align="right">

Dussap (2003, p. 22)

</div>

The employment of bio-regenerative processes complemented with physical-chemical technologies is thought to have numerous advantages from the perspective of redundancy and reduction of resupply mass for the sustained human presence in space or on other planetary bodies. However, the combination of bio-regenerative processes, such as plant cultivation, with physical-chemical processes is challenging. Such systems are a concert of many interdependencies and interacting feedback loops, which are thought to be difficult to operate in a desired range of set points. The complexity of hybrid life support systems makes the prediction of the system behavior under nominal and off-nominal conditions problematic.

> *'Life Support Systems must be conceived as an integrated sum of unit operations. This requires on one hand, a systemic approach of complex, highly branched systems with important feed-back loops and, on the other hand, the study of a set of unit operations (physico-chemical and biological compartments) in charge of the elementary functions constitutive of the entire Life Support System.'*

<div align="right">

Dussap (2003, p. 22)

</div>

Profound knowledge of the performance of hybrid life support systems as a whole and their components is essential to the development of sustainable, reliable and resilient life support architectures for future human space exploration missions. Such knowledge can be either gathered with an appropriate test facility, which incorporates all aspects of a life support sys-

tem. Constructing, building and operating such a facility is, however, expensive and also challenging from a technical and political point of view. Another way to improve the understanding of hybrid life support systems is dynamic modelling. The need for dynamic modelling was already identified by Babcock *et al.* (1984) several years ago.

The first goal of this dissertation is therefore the investigation of the behavior of hybrid life support systems, primarily the combination of physical-chemical technologies and plant cultivation in space greenhouses through dynamic simulations.

Space greenhouses also require a certain amount of mineral nutrients for plant cultivation. For exploration missions planned in the near-term, these nutrients can be supplied by premixed crystalline or liquid fertilizers brought from Earth. Long duration mission and eventually permanently crewed habitats incorporating a greenhouse, however, require a more sustainable way of supplying nutrients. One possible approach is the production of plant nutrients out of waste products such as inedible biomass, feces and urine. The latter has the highest potential, because human urine is rich in elements required for plant nutrition and the elements are already dissolved in water. Techniques for recycling urine into a nutrient solution for plants are still in an early development stage and have not been tested within a space life support system context.

The second goal of this thesis is therefore the verification of a urine-derived nutrient solution for plant cultivation. The urine-derived solution is produced by a microbiological filter, which is under development at the Institute of Space Medicine of the German Aerospace Center (DLR). Plant cultivation experiments have been conducted for this thesis in order to improve the understanding on how plants grow and behave when fed with a nutrient solution produced from recycled urine.

1.2   Thesis Objectives

Two main objectives have been defined for this thesis, which are explained in the following paragraphs.

Objective 1: Dynamic simulation of a hybrid life support system

The first objective of this thesis is to improve the understanding of the behavior of hybrid life support systems containing physical-chemical technologies and plant cultivation. Therefore a life support system model is developed, when necessary, to simulate a hybrid life support system under nominal and off-nominal conditions to investigate the dynamic behavior of the system with all its feedback loops and interdependencies. The simulations should include:

- **Full mission simulations for nominal and off-nominal conditions to understand the overall system behavior.**
- **Investigations of the effects of a greenhouse on the life support system architecture.**
- **Sensitivity analyses to investigate the effects of e.g.:**
  - **Physical-chemical technologies capacities,**
  - **Plant growth performance.**
- **Perturbation analyses to investigate the effects of e.g.:**
  - **Physical-chemical system failures,**

> - o **Greenhouse failures.**
> - **Studies of events or specific situations that might arise from the abovementioned simulations.**

Objective 2: Plant cultivation experiments with a urine-derived nutrient solution

> **The second objective of this thesis is the setup and execution of plant cultivation experiments with a nutrient solution derived from microbiologically processed urine. The experiments shall clarify if plants grow when fed with such a nutrient solution at all and how the plant development and food production is affected.**

1.3   Thesis Approach

The dissertation is structured into six chapters with various subchapters as shown in Figure 1-1. Chapter 1 describes the motivation behind this thesis, the thesis objectives and the structure of the thesis.

In Chapter 2 the scientific background of this thesis is explained. The chapter begins with a summary of life support definitions and a review of regenerative physical-chemical life support technologies. The main focus of Chapter 2 is on explaining plant cultivation in space and its requirements in Chapter 2.3. The benefits of plant cultivation in space are highlighted followed by a brief explanation of plant metabolism. Understanding how plants live and grow is an important prerequisite for modeling a space greenhouse. This subchapter also includes a definition of space greenhouse subsystems, inputs and outputs, and a review of plant selection methodologies. Chapter 2.3 concludes with a review of greenhouse research facilities and a summary of constraints for space greenhouse. The last subchapter of Chapter 2 describes the challenges of designing and operating hybrid life support systems.

Chapter 3 starts with a description of life support modeling guidelines, a review of past and present life support models and the implications for this dissertation. Chapter 3.2 describes the modelling approach that is used in the development of the model. The model itself is briefly described in Chapter 3.3, followed by detailed descriptions for each model part (Chapter 3.4 to 3.9. The model consists of three layers (one for gases, one for liquids and one for solids), a crew model, a greenhouse model and models for different physical-chemical technologies. Chapter 3.10 summarizes the model inputs which have to be defined prior to performing simulations. The developed model has also been validated. This process is described in Chapter 3.11.

A number of simulations have been conducted with the model, which are described in Chapter 4. The chapter starts with an overview of the simulations performed in Chapter 4.1. Chapter 4.2 describes simulations performed only with the greenhouse model in order to determine the effects of changing environmental parameters on the output of the model. Chapter 4.3 contains simulations with the full model. The simulations use a defined life support architecture with a nominal greenhouse (~60 % of food requirement met) based on values found in Anderson *et al.* (2015). The simulations resemble a Mars surface habitat mission with a

surface stay of 500 days on Mars. A simulation under nominal conditions was performed in order to determine the behavior of the system. This simulation was followed by a number of sensitivity and perturbation analyses in order to determine the system behavior under off-nominal conditions. The simulations described in Chapter 4.4 are in principle the same as in those of Chapter 4.3, but this time the greenhouse was scaled up to produce almost 100 % of the food required for the survival of the crew. Again sensitivity and perturbation analyses were conducted. Chapter 4.5 and 4.6 describe simulations of scenarios of particular interest, namely the effects of the greenhouse production schedule on the system behavior and the effects of different greenhouse startup scenarios.

Chapter 5 of this thesis illustrates the plant cultivation experiments with a urine-derived nutrient solution. The first subchapter describes in detail the experiment background and purpose. The experiment hardware and software is explained in the second subchapter. The experiments have been setup and conducted at the EDEN laboratory of the DLR Institute for Space Systems in Bremen, Germany. Over the course of three years, several experiment runs have been conducted in order to gather enough data for a solid evaluation. The experiment setup was designed and built by the author from 2013 to 2014. In 2015, the experiment facility was first tested with a growth cycle of lettuce and then with a growth cycle of super-dwarf tomatoes (the target crop for the experiments). The latter is described in Chapter 5.3. A number of technical and procedural issues were identified during the test growth cycle and the experiment setup was adjusted accordingly. The final experiment procedures are described in Chapter 5.4 and the experiment set points in Chapter 5.5. The results of the various experiment runs are described in detail and evaluated in Chapter 5.6.

Chapter 6, the last chapter of the thesis, contains a summary of the work conducted for this dissertation. The results of the hybrid life support system modeling and simulations, as well as the results of the plant cultivation experiments with a urine-derived nutrient solution are discussed in detail in Chapter 6.2. Chapter 6.3 describes ideas for future work, which include improvements to the model and suggestions for additional simulations. Ideas for future experiments and improvements to the urine-derived nutrient solution are mentioned as well.

Scope	•Motivation (Chapter 1.1) •Thesis Objectives (Chapter 1.2) •Thesis Approach (Chapter 1.3)
Scientific Background	•Life Support Definitions (Chapter 2.1) •Regenerative Physical-Chemical Life Support Technologies (Chapter 2.2) •Space Greenhouse Systems (Chapter 2.3) •Challenges of Hybrid Life Support Systems (Chapter 2.4)
Modeling	•Space Life Support Models (Chapter 3.1) •The System Dynamics Approach (Chapter 3.2) •Overview of the Model (Chapter 3.3) •Model Modules (Chapter 3.4 to 3.9) •Overview of Model Inputs (Chapter 3.10) •Model Validation (Chapter 3.11)
Simulations	•Outline (chapter 4.1) •Effects of Environmental Conditions on Crop Inputs and Outputs (Chapter 4.2) •Mars Surface Habitat Simulation Scenario (Chapter 4.3) •Habitat with Full Nutrition Greenhouse (Chapter 4.4) •Greenhouse Production schedule Improvement (Chapter 4.5) •Greenhouse Startup Phase Analyses (Chapter 4.6)
Experiment	•Background and Purpose (Chapter 5.1) •Hardware and Software (Chapter 5.2) •Test Growth Cycle (Chapter 5.3) •Experiment Procedures (Chapter 5.4) •Experiment Set Points Chapter 5.5) •Experiment Results and Evaluation (Chapter 5.6)
Conclusion	•Summary (Chapter 6.1) •Discussion (Chapter 6.2) •Future Work (Chapter 6.3)

Figure 1-1: Thesis structure.

2 Background

2.1 Life Support Definitions

Several similar-sounding terms for the classification of life support systems (LSS) exist. A short review of the most commonly used variations shall clarify the different meanings and definitions, because most of the terms are frequently used in this thesis.

Environmental control and life support system (ECLSS) is the general term for the subsystems required to maintain crew life and workability in spacecraft. These subsystems are the atmosphere management, water management, food production and storage, waste management, crew safety and extravehicular activities (EVAs) (Messerschmid and Bertrand, 1999). ECLSS can also be categorized depending on the implemented technologies (P/C LSS, BLSS, hybrid LSS), the level of regeneration (non-RLSS, RLSS) and the level of loop closure (open, partially closed, closed), see scheme in Figure 2-1.

ECLSS

Technologies used — P/C LSS, BLSS, Hybrid LSS

Level of regeneration — RLSS, Non-RLSS

Level of loop closure — Open loop, Partially closed loop, Closed loop
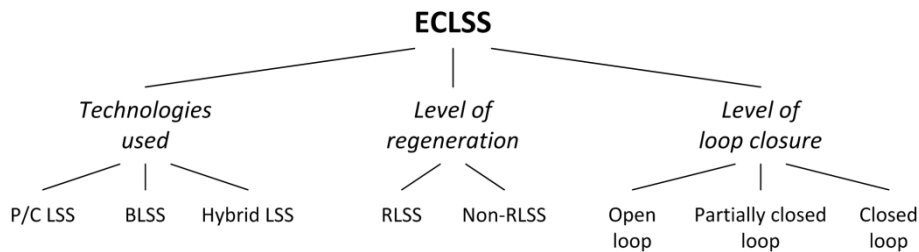
Figure 2-1: Classification of Environmental Control and Life Support Systems (ECLSS).

Physical-chemical life support systems (P/C LSS) utilize mechanical, physical and chemical processes to manage atmosphere, water and waste. Food production with P/C LSS is not possible. A broad variety of P/C technologies are already in use onboard the International Space Station (ISS) and other spacecraft.

Biological life support systems (BLSS) utilize metabolic needs and products of biological components besides humans. Plants, algae, microorganisms and animals can be considered to fulfill different tasks within an ECLSS. Depending on the utilized component, BLSS are capable of producing food, oxygen and other materials, reducing atmospheric carbon dioxide, treating waste and purifying water.

Hybrid life support systems combine P/C technologies with biological components to increase loop-closure. Furthermore, hybrid life support systems have a potentially higher degree of reliability and resilience, because their components work with fundamentally different functionalities. Controlling life support systems made of physical, chemical and biological components however is more challenging than either of them by themselves.

Regenerative life support systems (RLSS) are capable of recycling matter produced in spacecraft to regenerate required resources. RLSS need none or only little resupply (e.g. spare parts, filters) to fulfill their tasks, which reduces the overall resupply mass and therefore the mission costs.

Non-regenerative life support systems (non-RLSS) can only be used until their resources are depleted. They are usually used to makeup leakages or to provide resources in case of emergencies or to maintain human requirements in transfer vehicles during short missions.

An open loop ECLSS needs a constant resupply of all goods required for the survival of the crew. Traditionally, open loop ECLSS are used in transfer vehicles and during short missions.

Partly closed ECLSS can be achieved by closing one or more of the water, oxygen and carbon loops. Each closed loop reduces the required resupply mass, but increases the initial launch mass and complexity of the system.

A closed loop system recycles and reuses all matter produces within the system and consequently has the lowest resupply needs of all ECLSS. Since closed loop systems have only little exchange with their environment (e.g. leakage), they are often called CELSS (Closed/Controlled Ecological Life Support Systems). Despite the same abbreviation, there is a difference between closed and controlled systems. Closed systems regulate themselves and naturally strive for equilibrium, but over time the productivity and species diversity declines. On the contrary, controlled systems are under constant influence of humans respectively control devices, which allow maintaining the ecosystem at desired conditions (MacElroy and Averner, 1978).

2.2 Regenerative Physical-Chemical Life Support Technologies

This chapter gives a brief overview of regenerative physical-chemical life support technologies. Each technology is only described very briefly. References are given for further information. The functional categorization of the technologies is mainly based on Wydeven (1988) with minor alterations. Bubenheim and Wydeven (1994), Wieland (1994), Eckart (1996) and Schubert *et al.* (1984) provide summaries of almost all known physical-chemical life support technologies. The following descriptions are based on these references if not mentioned otherwise. Table 2-1 shows the physical-chemical technologies described in the following sections and the life support functions they can address.

2.2.1 Carbon Dioxide Removal and Concentration

The technologies mentioned in this section remove CO_2 from the spacecraft/habitat atmosphere and concentrate the gas for further processing.

Electrochemical Depolarized CO_2 Concentrator (EDC)

An EDC removes CO_2 from moist cabin air by an electrochemical reaction with H_2 and exhausts processed air with a reduced CO_2 partial pressure in one stream and concentrated CO_2 with unprocessed H_2 in another stream. Furthermore, the EDC generates direct current and heat.

Air Polarized Concentrator (APC)

An APC is a special form of EDC, which requires no H_2 and includes an O_2/CO_2 separator. Due to the absence of H_2 the APC generates no electrical energy and becomes a net power consumer. However, an APC can also operate with H_2.

Molecular Sieves (MS)

MS reduce the amount of CO_2 present in the air stream by using zeolites to adsorb CO_2. Once the adsorption material is saturated, it is exposed to vacuum for desorption and regeneration of the zeolite. For a continuous operation multiple adsorption beds are necessary.

Solid Amine Resin CO_2 Removal (SAWD)

SAWD systems are based on absorption and desorption of CO_2, similar to MS. Instead of zeolites, solid amine resins are used as absorption material scrubbing CO_2 from the cabin air. Heated water vapor is used to desorb CO_2 from the resins. SAWD systems also require multiple beds or canisters for a continuous operation.

Table 2-1: Physical-chemical technologies for different LSS functions.

	CO_2 removal and concentration	CO_2 reduction	O_2 generation	O_2 concentration	Concentrated water feed processing	Diluted water feeds processing	Solid waste processing
EDC	X						
APC	X						
MS	X						
SAWD	X						
Bosch		X					
Sabatier		X					
CO_2 electrolysis		X	X				
SFWE			X			X	
SPWE			X			X	
WVE			X				
VCD					X		
TIMES					X		
VPCAR					X	X	
RO						X	
MF						X	
Electrodialysis						X	
Dry incineration							X
WO							X
SCWO							X
Electrochemical oxidation							X

2.2.2 Carbon Dioxide Reduction

Technologies described in this section process carbon dioxide with the purpose to recover the oxygen.

Bosch Reactor

Bosch CO_2 reduction systems are fed with inflows of CO_2 and H_2. The mixture is heated (700-1000 K) and compressed (130 kPa) before it reaches the catalyst bed. The CO_2 and H_2 react to H_2O, heat and solid carbon. The latter is formed on the catalyst (e.g. activated steel wool, ruthenium-iron alloys). Consequently, the catalyst material has to be replaced periodically to maintain its functionality.

Sabatier Reactor

Sabatier CO_2 reduction systems require inlet streams of CO_2 and H_2 to start a catalytic reaction. In the presence of a catalyst (e.g. ruthenium) and under high temperatures (450-800 K) CO_2 and H_2 react to methane, water and heat. The conversion efficiency and the production

of by-products (e.g. C, CO) can be controlled by the reaction temperature and the molar ratio of the H_2/CO_2 inlet.

Carbon dioxide electrolysis

This technology combines CO_2 reduction and O_2 production in a single process using solid oxide electrolytes. The CO_2 reacts catalytically under high temperatures (1400-1600 K) to O_2 and CO. The latter is then decomposed to solid carbon and CO_2, which is fed to the electrolysis again. The process can also handle water vapor as input, with H_2 and O_2 as process products.

2.2.3 Oxygen Generation

The following technologies produce oxygen by electrolyzing water in different ways.

Static-Feed Water Electrolysis (SFWE)

SFWE systems convert hygiene water into O_2 and H_2. Water vapor diffuses as vapor through a membrane into an electrolyte (e.g. potassium hydroxide (KOH)). Under energy input provided as direct current power, H_2 is produced at the cathode and O_2 at the anode.

Solid Polymer Water Electrolysis (SPWE)

SPWE is a similar process to SFWE. Instead of KOH, the SPWE uses a solid plastic sheet/membrane or a perfluorinated sulfonic acid polymer.

Water Vapor Electrolysis (WVE)

WVE directly uses the water vapor contained in cabin air, which is fed to the anode side of the system. The water vapor is electrolyzed producing separated streams of H_2 and O_2 enriched air as output. Thus WVE can be used to regulate the humidity of the habitat air. Furthermore, WVE has only few interfaces and can be designed as a portable system.

2.2.4 Oxygen Concentration

Oxygen concentration has not been part of a life support system yet. However, for a future LSS architecture such a technology might be required. Oxygen concentrators allow the concentration/separation of O_2 from the normal spacecraft/habitat atmosphere for further processing. Graf (2011) describes a process to produce high purity oxygen for EVAs. A similar technology can also be envisioned as an interface between a space greenhouse and the habitat to better control the oxygen concentration in the atmosphere of both the greenhouse and the habitat.

2.2.5 Water Recycling

The water recycling system in spacecraft and habitats must provide the required potable and hygiene water to the crew. It treats the accumulating waste water (e.g. urine) and condensate water. Water recycling technologies can be classified either as phase change or filtration processes. The former are mainly suitable for treating urine and flush water, so called concentrated feeds, while the latter are considered to process dilute feeds such as hygiene (e.g. wash, shower, and laundry water) and potable water.

Vapor Compression Distillation (VCD)

VCD is a phase change water recovery process which can recover more than 96 % H_2O from urine. The urine is concentrated to over 50 % solids. Pre- and post-processing is necessary to achieve high water quality. The VCD system has to be evacuated periodically to remove undesired volatiles.

Thermoelectric Integrated Membrane Evaporation System (TIMES)

TIMES is a phase change process using thermoelectric heat pumps to transfer heat from a water condenser to an evaporator. The urine and flush water is heated to 339 K and afterwards pumped through hollow fiber membranes. Up to 93 % of the H_2O can be recovered or until the concentration of solids reaches 38 %. Pre- and post-treatment of the processed water are required.

Vapor Phase Catalytic Ammonia Removal (VPCAR)

VPCAR is a phase change process which combines vaporization with high-temperature catalytic oxidation to eliminate the need of pre- and post-processing and the related expendable chemicals. Volatiles like ammonia, hydrocarbons and N_2O present in the water are oxidized and decomposed in two catalyst beds during the process.

Reverse Osmosis (RO)

RO is a filtration technique using a pressure-driven membrane separation process. The feed stream is pressurized (690-5500 kPa) and forced through a semipermeable membrane. Water passes through the membrane, while volatiles and organics are separated, which leads to a relatively pure stream of H_2O and a concentrated solution of residues.

Multifiltration (MF)

MF systems use filters and packed columns connected in series to purify H_2O. MF can be split into three steps, the removal of particles by filtration, the removal of organics by adsorption and the removal of inorganic salts by ion-exchange. Expendables for the regeneration of activated charcoal and the ion-exchange beds are required.

Electrodialysis

This process is a combination of electrodeionization and filtration. The inlet H_2O stream flows through a diluting compartment which is separated from adjacent concentrating compartments by ion exchange membranes. Ions present in the H_2O feed are forced through the resins and membranes by an electrical potential gradient. Pre- and post-treatment has to be applied for removing volatiles not extracted by the electrodeionization,

2.2.6 Solid Waste Processing

In current LSS waste usually is collected, then stabilized and stored, before returned to Earth or burned in atmospheric re-entries of supply vehicles. Future LSS, especially, when food is provided through plant cultivation, will have to recycle inedible biomass produced in greenhouse modules. Waste recycling allows the regeneration of gases, fluids and provision of nutrients for the greenhouse module.

Dry incineration

During this process solid waste is combusted in air or preferable pure O_2 under temperatures of about 813 K. The waste feed must be dried before the combustion at least until the solid content is about 50 %. The product streams of dry incineration are water condensate, inorganic ash, CO_2 and trace gases. Post-treatment with catalytic afterburners may be required to further increase the efficiency of the process and to reduce products from incomplete combustion (Bubenheim and Wydeven, 1994).

Wet Oxidation (WO)

WO uses high temperatures (473-573 K) and high atmospheric pressure (14 MPa) to oxidize diluted or concentrated waste streams. The process takes place in air or pure O_2 and requires no pre-drying, unlike incineration processes. WO regenerates H_2O and essential nutrient salts for plants, produces CO_2 and reduces solid wastes to small amounts of sterile, non-degradable ash (Bubenheim and Wydeven, 1994).

Supercritical Water Oxidation (SCWO)

SCWO utilizes the unique abilities of water in its supercritical state (temperature above 647 K and pressure above 21.5 MPa). Since organic substances and oxygen are completely soluble and inorganic salts only sparingly soluble in supercritical water, SCWO can be used to separate salts from the aqueous product phase. The recycling of organic wastes with SCWO results in efficiencies greater than 99.99 % in less than 1 minute reaction time (Bubenheim and Wydeven, 1994).

Electrochemical oxidation

This technology utilizes a non-thermal waste treatment process. Organics and other solid wastes are recycled by oxidization to CO_2, N_2 and H_2. The oxidization takes place on the surface of catalytic electrodes under a relatively low operating temperature of about 422 K. CO_2 and N_2 will be produced at the anode and H_2 at the cathode. No atmospheric oxygen is consumed during the process and the power demand is relatively low (Bubenheim and Wydeven, 1994).

2.2.7 Other Technology Areas

The previous subchapter focuses entirely on technologies and life support functions related to the provision and recycling of a number of vital substances. However, there are other life support technology areas which are of equal importance such as:

- Trace gas monitoring and removal,
- Humidity control,
- Nitrogen supply,
- Air quality monitoring,
- Water quality monitoring,
- Food quality monitoring,
- Crew health monitoring.

While these technology areas are important for spacecraft life support systems in general, they are of minor interest for this thesis. That is why these areas are not explained in more detail.

2.3   Space Greenhouse Systems

2.3.1   Benefits of Plants in Life Support Systems

Plants offer a wide range of advantages when used in life support systems. On Earth plants function as the backbone of the land-based ecosystem. They provide food and other products to many other life forms. Plants also bind carbon dioxide and produce oxygen. Plants act as a water filtration system with their water uptake and transpiration. Consequently, cultivating plants during long duration space mission on spacecraft or in planetary habitats has a high potential for human space exploration.

The production of a wide variety of food is unique to plants. While algae are able to produce high quantities of protein in a small space, plants can produce proteins as well as carbohydrates and fats. Furthermore, most plants produce a wide range of vitamins and minerals which are all beneficial to humans. Currently, human space missions rely on dehydrated, freeze-dried and pre-packed food with the occasional provision of fresh produce for a short time after resupply. During future human space exploration missions to the Moon, Mars or beyond, the resupply intervals will be much longer and consequently the supply of fresh food is very limited. Space greenhouses have a lot of potential for this kind of mission as they can produce fresh vegetables during the mission. Furthermore, depending on the size of the space greenhouse and the crop composition, the greenhouse can contribute a significant amount of food supply which in turn reduces the amount of resupply to be brought from Earth.

The metabolism of plants is based on photosynthesis. Photosynthesis is a bio-chemical reaction which uses carbon dioxide, water and light energy to produce carbohydrates, fats, proteins and oxygen. On Earth plants are the main consumers of carbon dioxide and the main producers of oxygen, whereas the human metabolism requires oxygen and produces carbon dioxide. Mimicking this process in space life support systems is self-evident. Plant cultivation in space greenhouse could significantly contribute to the atmosphere management of the life support system.

Plants require water not only for their metabolism. In fact, over 99 % of the water consumed by plants is evaporated over the leaves. While the water evaporates, minerals and other substances remain in the plant material. This makes plants to very effective water filtration systems. If the evaporated water is condensed on a sterile surface, the produced liquid is very close to potable water standards. The water can either be fed again to the plants or with minor processing be made consumable for humans.

The biomass produced by plants can also be used to create replacements for broken items. There are already a lot of commercially available products made out of bio-plastic a compound made from biological materials based on plant biomass. Although the idea to produce small spare parts and tools made out of plant material seems very ambitions, the rapid development of adhesive manufacturing and other production techniques will allow the production of small parts out of biomass in the near future. Transferring these technologies to space exploration will open up more means to reduce the resupply mass required for long duration space missions.

Besides the production of different resources, plant cultivation during long periods of isolation has a positive effect on the psychological well-being of the crew. In an environment in which

survival depends to a very high degree on technology, plants resemble the natural environment of Earth. Past experiments on space station Mir and the ISS have shown that even a very small amount of plants is highly appreciated by the astronauts (Haeuplik-Meusburger *et al.*, 2014).

2.3.2 Plant Metabolism at a Glance

Plants' metabolism is an aggregation of several complex interacting biological, physical and chemical processes. Knowing these processes is necessary to understand the functionality of space greenhouses and why plants in controlled environment perform better than in their natural environment. Therefore, some of the processes (e.g. photosynthesis, mineral nutrition) are shortly explained in the following.

2.3.2.1 Photosynthesis

Photosynthesis is the only biological process which is capable of harvesting the Sun's energy to produce complex chemical compounds. The whole process is a chemical redox reaction. Electrons are removed from one compound (oxidation) and added to another compound (reduction).

Plants assimilate atmospheric carbon dioxide (CO_2), which is reacted with water (H_2O) in a series of physical and biochemical processes to produce carbohydrates ($C_6H_{12}O_6$), water and oxygen (O_2):

$$6\ CO_2 + 12\ H_2O \xrightarrow{light} C_6H_{12}O_6 + 6\ H_2O + 6\ O_2 \qquad (2\text{-}1)$$
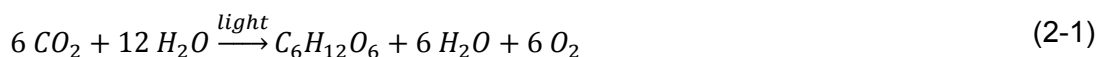
The required energy for the reaction is given by photons of specific wavelengths. The energy is stored in carbohydrate molecules and can be used to power the plant's cellular activities or the metabolism of other forms of life.

The formula (2-1) shown above is the simplest form of describing photosynthesis and disregards the more than 50 intermediate steps (Blankenship, 2010). First of all, photosynthesis can be divided into two basic series of reactions:

- Thylakoid reactions

$$12\ H_2O \xrightarrow{light} 12\ [H_2] + 6\ O_2, \text{ and} \qquad (2\text{-}2)$$

- Stroma reactions

$$6\ CO_2 + 12\ [H_2] \longrightarrow C_6H_{12}O_6 + 6\ H_2O. \qquad (2\text{-}3)$$

Both take place inside two different organelles of plants' chloroplasts, see Figure 2-2. The Thylakoid reactions, also known as light-driven reactions, are named after the Thylakoid membranes in which light is used in Photosystem I + II (PSI resp. PSII) to separate H_2O into O_2 and H^+, nicotinamide adenine dinucleotide phosphate ($NADP^+$) is reduced to NADPH and adenosine triphosphate (ATP) is formed out of adenosine diphosphate (ADP) and an additional phosphate ion (P_i). NADPH is a reducing agent which is required for the carbon fixation processes during the Calvin-Benson Cycle. ATP is an important energy carrier for metabolic processes. By adding an additional phosphate molecule to ADP, potential energy is stored and can be transported for the utilization in other processes.

Inside stromas, the carbon fixation reactions occur, also known as Calvin-Benson Cycle. This cycle does not require light as energy source, but is only regulated by illumination (Buchanan and Wolosiuk, 2010).
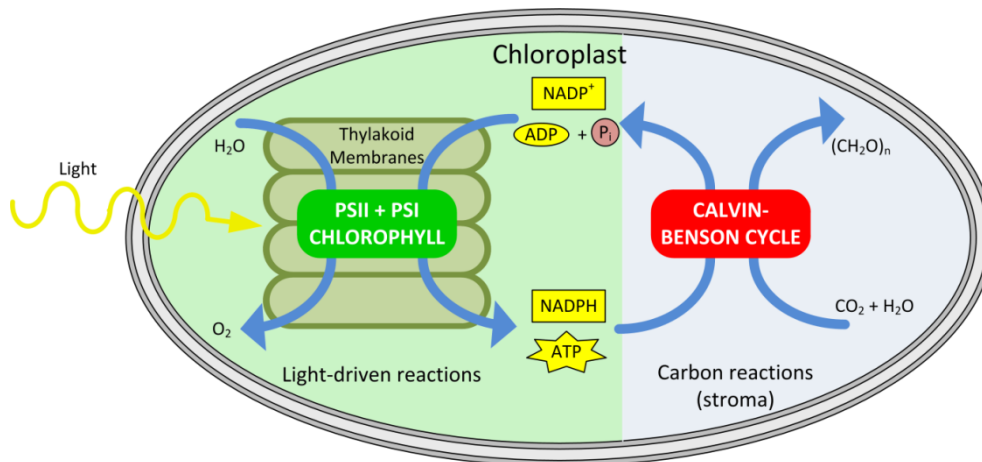
Figure 2-2: Chloroplast scheme including reactions, redrawn from Buchanan and Wolosiuk (2010).

Thylakoid reactions

Inside the Thylakoid membranes, two complexes known as Photosystem I and Photosystem II harvest and concentrate the energy of light. The illustration of the electron flow and related reactions in these photosystems is known as Z-scheme of photosynthesis, see Figure 2-3. Both systems consist of a reaction center and a light-absorbing antenna system. The latter collect and concentrate photons before they are directed to the reaction center.
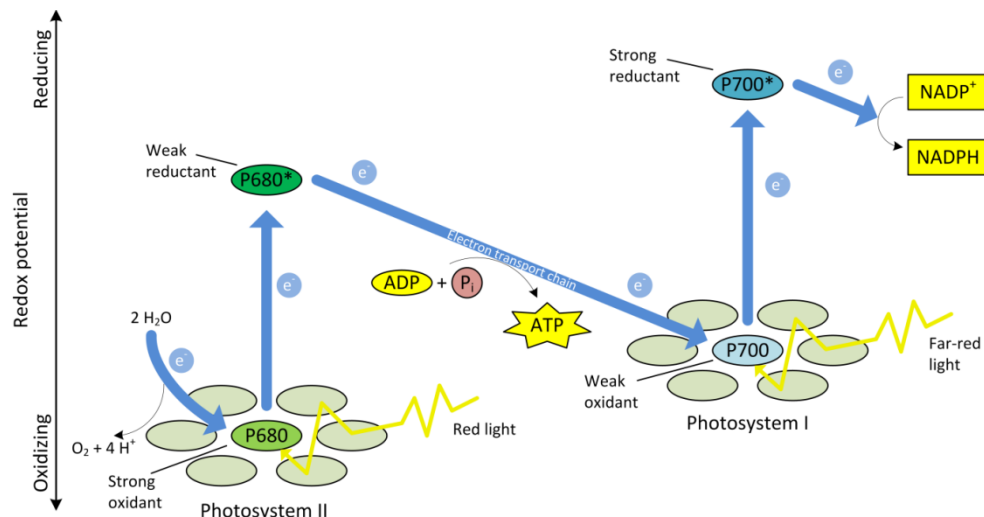
Figure 2-3: Z-scheme of photosynthesis, redrawn from Blankenship (2010).

PSII mainly absorbs red light with a wavelength of 680 nm. Inside the reaction center P680, the energy of the collected photons is used to produce a strong oxidant, which oxidizes H_2O to O_2 and H^+, and a weak reductant, which reduces the oxidant generated by PSI. The peak of absorption of PSI is in far-red light at a wavelength of 700 nm. The reaction center P700 produces a strong reductant, which reduces $NADP^+$ to NADPH, and a weak oxidant. Both photosystems are linked by an electron transport chain (Blankenship, 2010).

Another complex of the Thylakoid membranes is responsible for ATP synthesis, also known as photophosphorylation. ATP formation requires the transport of hydrogen ions (H^+). Inside

the membranes is an excess of H^+ produced by PSII which is about 1000 times greater than in the stroma. This high concentration gradient is a source of chemical-potential energy, which is used by the ATP synthesis. Therefore, H^+ moves through channels in the Thylakoid membrane to form ATP out of ADP + P_i (Ross, 1992b).

Stroma reactions

NADPH and ATP produced by the Thylakoid reactions flow from the membranes to the stroma, a fluid surrounding them. In the stroma both substances are used in the enzyme-catalyzed reduction of CO_2 to carbohydrates and other compounds. This process is known as the Calvin-Benson Cycle which is a 3-stage cyclic process and encompasses several intermediate reaction steps, see Figure 2-4.

The first stage is the carboxylation, where 3 CO_2 and 3 H_2O enzymatically react with 3 molecules of ribulose 1,5-biphosphate to 6 molecules of 3-phosphoglycerate. During the second stage, the reduction, the 6 3-phosphoglycerate molecules are reduced to 6 triose phosphate using 6 NADPH as the reducing agents and consuming the energy provided by 6 ATP. The NADPH molecules react to NADP$^+$, while ADP and P_i are formed out of ATP:

$$3\,CO_2 + 3\,ribulose\,1,5 - bisphosphate + 3\,H_2O + 6\,NADPH + 6\,H^+ + 6\,ATP \\ \rightarrow 6\,Triose\,phosphates + 6\,NADP^+ + 6\,ADP + 6\,P_i. \tag{2-4}$$
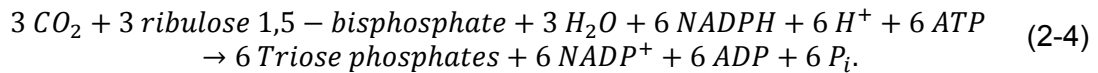
The third stage is the regeneration of ribulose 1,5-biphosphate to ensure a continuous uptake of atmospheric CO_2. This stage is more complex than the other two and involves 10 intermediate reactions. During these reactions 5 molecules of the formerly produced triose phosphates are consumed in addition to 3 ATP molecules to regenerate 3 molecules of ribulose 1,5-biphosphate, 3 ADP and 3 P_i:

$$5\,Triose\,phosphates + 3\,ATP \\ \rightarrow 3\,ribulose\,1,5 - bisphosphate + 3\,ADP + 3\,P_i. \tag{2-5}$$

The sixth triose phosphate is the net production of assimilating 3 CO_2 and is used as the basis of forming more complex molecules such as starch and sucrose.
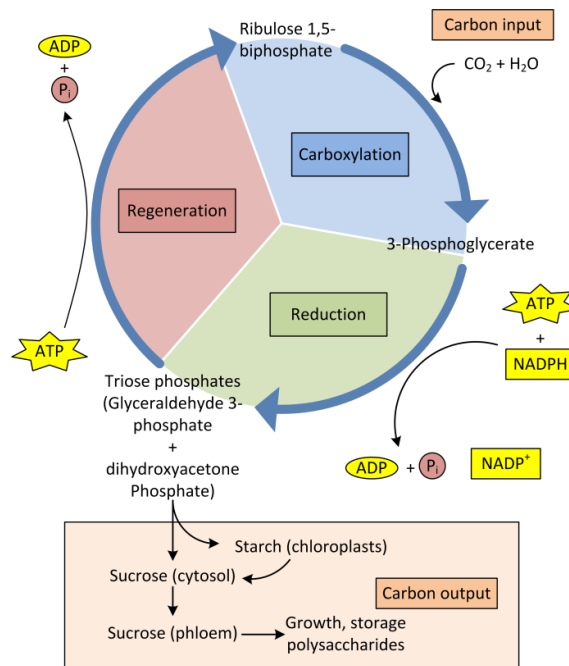
Figure 2-4: The three stages of the Calvin-Benson Cycle, redrawn from Buchanan and Wolosiuk (2010).

2.3.2.2 Photosynthetic Response to Light

The description in the previous chapter indicates that illumination conditions have a high impact on the photosynthetic processes. The light's spectrum and intensity are of great importance.

The photosynthetically active radiation (PAR) is defined as the wavelength zone between 400 and 700 nm (Sager and Mc Farlane, 1997). Plants show the highest photosynthetic response within this spectrum, see Figure 2-5. Other wavelengths do not contribute to the photosynthesis.
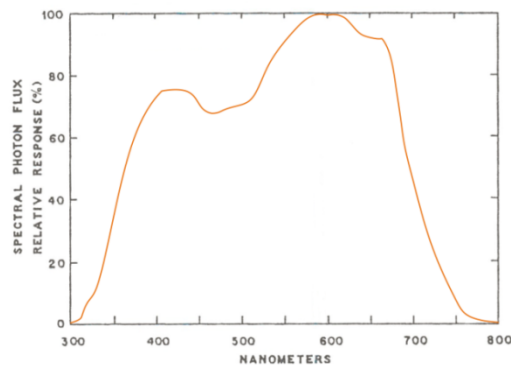
Figure 2-5: Spectrum of the Photosynthetic Active Radiation (PAR) (Sager and Mc Farlane, 1997).

Photosynthesis is not only driven by light of the right wavelength, but also by the amount of absorbed photons of PAR, photosynthetic photon flux (PPF). It is defined as the light quantity effective in photosynthesis and is expressed in µmol/(m²*s). Most plants saturate at a PPF between 500 and 1000 µmol/(m²*s) for an optimal growth (Sager and Mc Farlane, 1997).

Under normal CO_2 concentrations in air (350 ppm), photosynthesis is light limited. Exposing plants to higher PPF levels increase the assimilation of CO_2 and consequently the growth rate. After reaching the light saturation point, a further increase in PPF does not enhance photosynthesis anymore. Photosynthesis is then CO_2 limited (Ehleringer and Sandquist, 2010; Salisbury, 1992c). Figure 2-6 illustrates the relation between absorbed light and CO_2 assimilation.
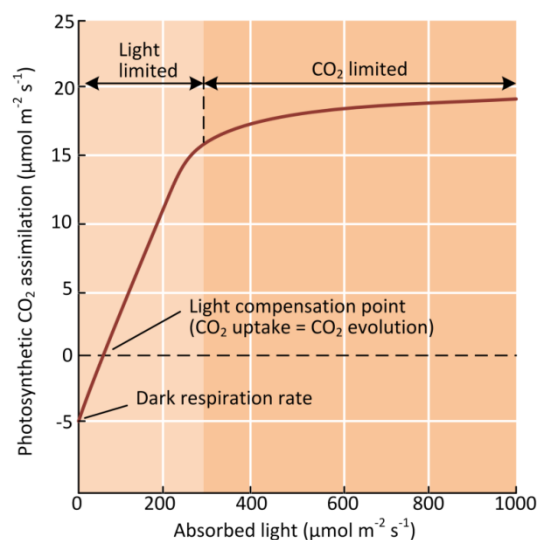
Figure 2-6: Response of photosynthesis to light, redrawn from Ehleringer and Sandquist (2010).

2.3.2.3 Photosynthetic Response to Carbon Dioxide

Carbon dioxide as one of the main reactants influences the photosynthesis depended on the atmospheric concentration. Higher levels of CO_2 increase the ratio of CO_2 to O_2 reacting with rubisco leading to a better net assimilation. The saturation point at which a higher CO_2 concentration does not enhance photosynthesis is lower under nominal irradiance levels. Plants exposed to high PPF benefit from high CO_2 concentrations. Most plants benefit from CO_2 concentrations of 1000 to 1200 ppm with sufficient irradiance. Higher concentrations are not beneficial anymore, because the fixation point is reached. Figure 2-7 shows the relation between the CO_2 concentration and net CO_2 fixation at different irradiance levels (Ehleringer and Sandquist, 2010; Salisbury, 1992a).
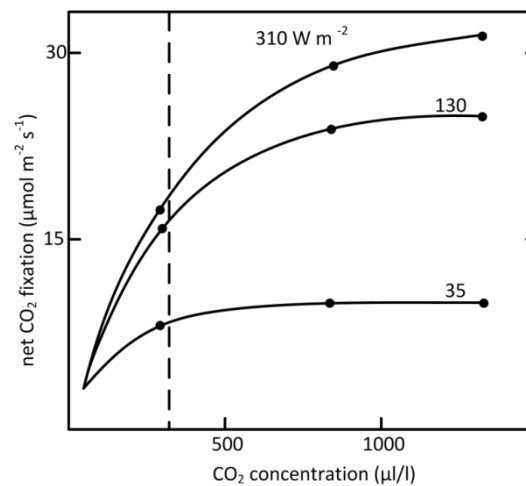
Figure 2-7: Effects of atmospheric CO_2 enrichment on CO_2 fixation (atmospheric CO_2 concentration highlighted as dashed line), redrawn from Salisbury (1992a).

2.3.2.4 Photosynthetic Response to Temperature

Photosynthesis is temperature sensitive. Plants under illumination also experience radiative heat transfer from the lighting source. The heat dissipates from the leaves through radiative heat loss, conduction and convection to the air, and through evaporative cooling. The latter occurs through water diffusion out of the leaves. This process is regulated by stomatal opening which also affects CO_2 uptake. The effects of temperature on photosynthetic processes are various and nearly every process step is temperature dependent. High temperatures reduce, among others, the rubisco activity and therefore the CO_2 assimilation. At low temperatures photosynthesis is limited by phosphate uptake into the chloroplasts. Every plant species has its own optimal temperature range. Within this range, all photosynthetic steps are optimally balanced. Figure 2-8 illustrates the plant growth of four species as a function of temperature (Ehleringer and Sandquist, 2010; Salisbury, 1992b).
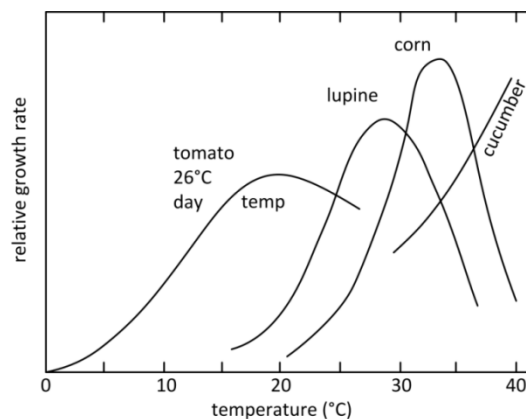
Figure 2-8: Plant growth as a function of temperature for four species. With tomato, day temperature was constant and night temperature varied. Redrawn from Salisbury (1992b).

2.3.2.5 Mineral Nutrition of Plants

While light, CO_2 and temperature directly affect photosynthesis, mineral nutrition is a limiting factor for plant growth in general. The yield of plants increases nearly linear with the amount of absorbed nutrients. Nutrients are naturally found in terrestrial soil in form of inorganic ions. The roots of plants absorb them and provide them to the food chain.

The list of mineral nutrients encompasses 16 essential elements. They are classified as macro- or micronutrients. The former can be found in plant tissue in concentrations from 0.1 to 1.5 % and the latter from 0.1 to 100 ppm. Macronutrients are Nitrogen (N), Potassium (K), Calcium (Ca), Magnesium (Mg), Phosphorus (P), Sulfur (S) and Silicon (Si). Micronutrients are Chlorine (Cl), Iron (Fe), Boron (B), Manganese (Mn), Sodium (Na), Zinc (Zn), Copper (Cu), Nickel (Ni), and Molybdenum (Mo) (Bloom, 2010; Ross, 1992a). They can also be classified by their biochemical role and physiological function, see Table 2-2.

Deficiencies in mineral nutrition cause metabolic disorders and limit plant development. Inadequate supply of specific nutrients produces characteristic symptoms which are extensively described by Bloom (2010) and Ross (1992a). Above plant specific concentrations, mineral nutrients are toxic. Especially the root system is sensitive to an overexposure of nutrients and is easily damaged. Figure 2-9 shows the relationship between nutrient concentration in plant tissue and growth respectively yields.
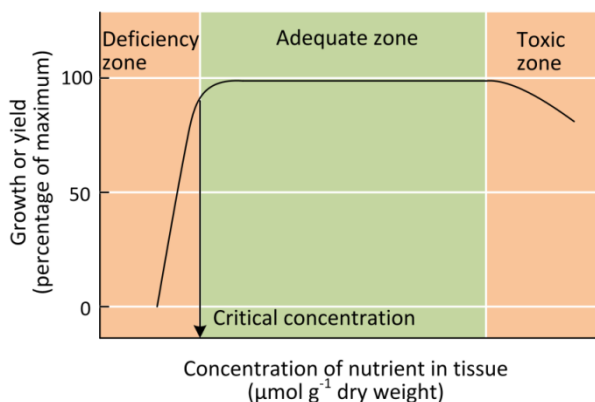
Figure 2-9: Relationship between yield and nutrient supply, redrawn and modified from Bloom (2010).

Table 2-2: Classification of plant mineral nutrients according to biochemical function (Ross, 1992a).

Mineral nutrient	Functions
Group 1	**Nutrients that are part of carbon compounds**
N	Constituent of amino acids, amides, proteins, nucleic acids, nucleotides, coenzymes, hexosamines, etc.
S	Component of cysteine, cysteine, methionine. Constituent of lipoic acid, coenzyme A, thiamine pyrophosphate, glutathione, biotin, 5´-adenylylsulfate, and 3´-phosphoadenosine
Group 2	**Nutrients that are important in energy storage or structural integrity**
P	Component of sugar phosphates, nucleic acids, nucleotides, coenzymes, phospholipids, phytic acid, etc. Has a key role in reactions that involve ATP.
Si	Deposited as amorphous silica in cell walls. Contributes to cell wall mechanical properties, including rigidity and elasticity.
B	Complexes with mannitol, mannan, polymannuronic acid, and other constituents of cell walls. Involved in cell elongation and nucleic acid metabolism.
Group 3	**Nutrients that remain in ionic form**
K	Required as a cofactor for more than 40 enzymes. Principal cation in establishing cell turgor and maintaining cell electro neutrality.
Ca	Constituent of the middle lamella of cell walls. Required as a cofactor by some enzymes involved in the hydrolysis of ATP and phospholipids. Acts as a second messenger in metabolic regulation.
Mg	Required by many enzymes involved in phosphate transfer. Constituent of the chlorophyll molecule.
Cl	Required for the photosynthetic reactions involved in O_2 evolution.
Mn	Required for activity of some dehydrogenases, decarboxylases, kinases, oxidases, and peroxidases. Involved with other cation-activated enzymes and photosynthetic O_2 evolution.
Na	Involved with the regeneration of phosphoenolpyruvate in C_4 and CAM plants. Substitutes for potassium in some functions.
Group 4	**Nutrients that are involved in redox reactions**
Fe	Constituent of cytochromes and nonheme iron proteins involved in photosynthesis, N_2 fixation, and respiration.
Zn	Constituent of alcohol dehydrogenase, glutamic dehydrogenase, carbonic anhydrase, etc.
Cu	Component of ascorbic acid oxidase, tyrosinase, monoamine oxidase, uricase, cytochrome oxidase, phenolase, laccase, and plastocyanin.
Ni	Constituent of urease. In N_2-fixing bacteria, constituent of hydrogenase.
Mo	Constituent of nitrogenase, nitrate reductase and xanthine dehydrogenase.

2.3.2.6 Water and Humidity

The water demand of plants is high compared to the demands of CO_2 and nutrients. For every CO_2 molecule diffusing into the leaf, on average 400 molecules of water diffuses out. This unbalance leads to the evaporation of around 97 % of water gathered by the root system. Only 2 % of the water is used to supply growth and 1 % for photosynthetic reactions. Water is also a good solvent for ionic substances and molecules such as sugar and proteins. Water deficit is a major limiting factor for plant growth and development. It inhibits photosynthesis and causes physiological changes. Insufficient water supply leads to reduced shoot growth and leaf expansion, but enhances root elongation. Plants gather mineral nutrients dissolved in water through their roots. The root hairs, filamentous outgrowths of root epidermal cells, provide the necessary surface area for water uptake. Especially the root tips absorb water while the rest of the root is less permeable to water (Holbrook, 2010).

The humidity or more precise the difference in water vapor pressure between the atmosphere surrounding the leaves and the inner air spaces of the leaves drives the transpiration

of plants. Transpiration occurs by diffusion through the stomata of the leaves (Taiz and Zeiger, 2010).

2.3.3 Subsystems

Space greenhouse can be divided into several subsystems. The definition of subsystems and the explanation of their purposes shown in Table 2-3 are based on Schubert (2011). However, the information given by the reference is modified by the author of the thesis. The air management and the thermal subsystem are combined to utilize the synergies in equipment and function. The lighting and power subsystems are separated. The power distribution system has a high complexity and coverage, because of the different voltage levels, kind of currents and power levels of the other subsystems. The purposes' descriptions and exemplary equipment of all subsystems were adapted when necessary to reflect the modified subsystem classification.

Table 2-3: Description of greenhouse module subsystems; based on (Schubert *et al.*, 2011).

Subsystem	Purpose	Equipment
Structures and Mechanisms	Various structures to provide support for other subsystems, to withstand all applied loads during the whole mission and to act as radiation shielding	e.g. primary and secondary structural elements, shielding, interfaces, walkways, access ladder, conveying system
Plant Cultivation Subsystem	Containment of root zone and growth medium, as well as providing support for the shoot zone. Environmentally closed compartments to maintain desired levels of T, RH, and CO_2.	e.g. adjustable height root/shoot box, grow lid, plant support structures, germination unit
Air and Thermal Control Subsystem	Provision of O_2 and CO_2, dehumidification, extraction and removal of trace gases, control of air temperature and humidity	e.g. fans, H_2O recovery system, temperature and humidity control system, trace gas removal system, piping, CO_2 injection system, T-/RH-/gas-sensors
Lighting Subsystem	Illumination of plants with the necessary intensity of PAR during the whole life cycle	e.g. electrical or natural lighting systems, cooling system, light pipes, illumination sensors
Power Distribution Subsystem	Provision and distribution of electrical energy to all subsystems	e.g. harness, interface to power generation equipment, voltmeter
Nutrient and Fluid Delivery Subsystem	Storage, mixing, and transportation of H_2O and nutrients. Ability to create individual mixtures for different purposes	e.g. H_2O tank, nutrient mix computer, filters, pumps, nutrient tanks (N,P,K), other tanks, ph-/EC-/T- and water flow sensors
Harvest and Cleaning Subsystem	Workstation and equipment for separation of edible and non-edible plant material, as well as cleaning and sterilization of other subsystems	e.g. washing sink, piping, sterilization unit, harvest tools, initial storage locations for edible and non-edible materials
Command and Data Handling Subsystem	General data handling and control system, receiving of sensor signals, distribution of control signals	e.g. computers, control units, harness, cameras

The Plant Cultivation Subsystem needs further explanation in addition to the brief description in Table 2-3, because the definition of its subdivision is not always consistent between different research groups. The following definition is based on work performed for the ESA project *'Greenhouse Module for Space'* by researchers of the DLR Institute of Space Systems in Bremen, with whom the author worked together.

According to this definition the greenhouse is integrated into the habitat or into a separate module, which is then connected to the habitat. The greenhouse can consist out of several growth chambers to divide the greenhouse volume into different segments. A growth chamber itself contains a number of growth compartments to separate different species from each other or to provide different lighting conditions between compartments. One growth compartment holds several growth pallets, which provide a suitable root zone for the plants. Each grow pallet is connected to the nutrient and fluid delivery subsystem and typically supports a number of plants of the same species (Poulet *et al.*, 2013). Figure 2-10 shows an exemplary scenario of a greenhouse and its subunits containing multiple species compartments.
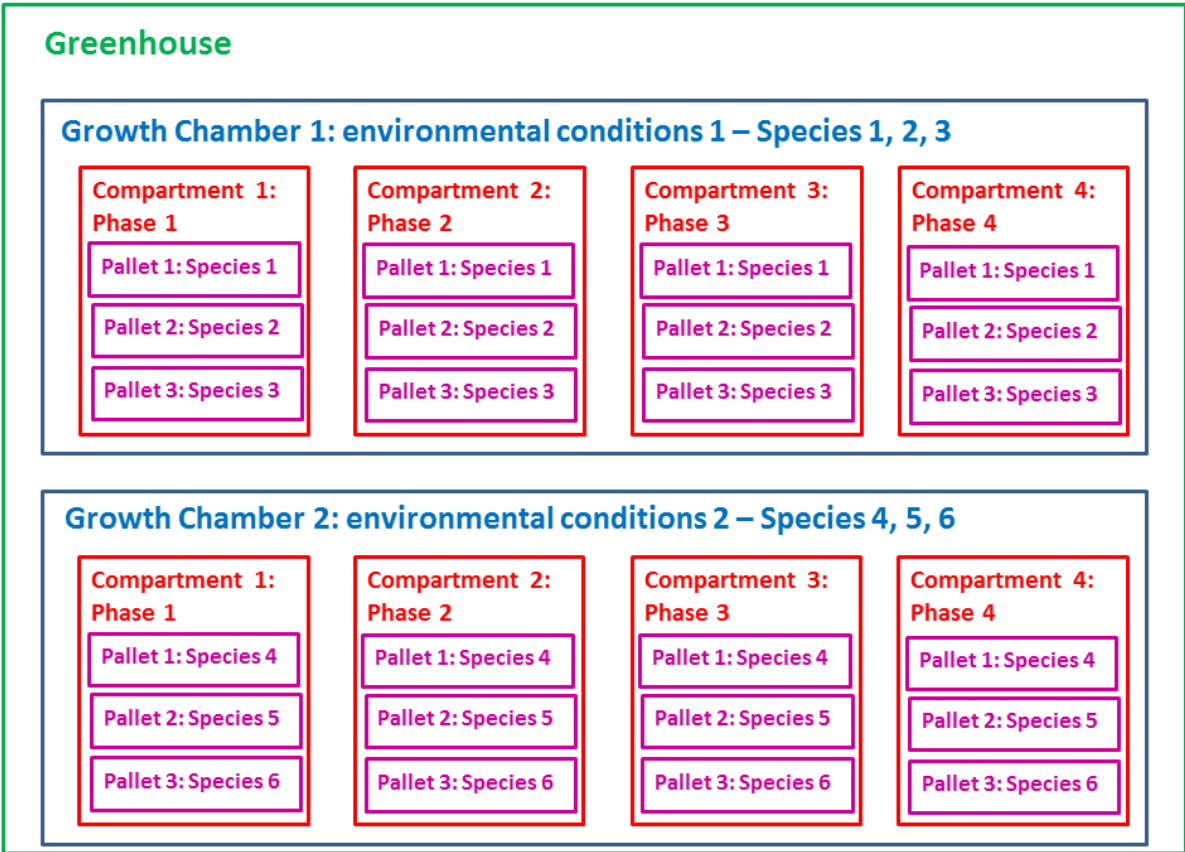
Figure 2-10: Organization of a greenhouse, with different subunits. Scenario with multiple species chambers (Poulet *et al.*, 2013).

2.3.4 Inputs and Outputs

Greenhouse modules incorporated into a habitat have several inputs and outputs to the habitat infrastructure subsystems. The quality and quantity of the in- and outputs greatly depend on the system architecture of the greenhouse. Figure 2-11 shows all possible in- and outputs of a greenhouse module arranged by type in the four groups: gases, liquids, solids and energy.

Gaseous inputs are inert gas for compensating the loss of atmosphere through leakage and carbon dioxide as metabolic input for plant photosynthesis. Gaseous outputs are oxygen produced by plant photosynthesis and atmospheric leakage to the environment.

Liquid inputs are potable water and wastewater for plant growth. The outputs are waste nutrient solution and potable water. The liquid in- and outputs may vary in different greenhouse setups, depending on the design of the water loops. The greenhouse may recycle the water transpired by the plants and directly feed it back to the plants or provide it as potable water to the habitat. Depending on how much water is taken from the greenhouse in terms of recovered transpiration water and fresh biomass, water has to be supplied to the greenhouse. The supplied water might be potable water or even slightly polluted water, depending on the crops grown in the greenhouse.

Solid inputs are nutrient salts and potentially biological solid waste to supply the crops with macro- and micronutrients. Solid outputs of the greenhouse are usually biomass (edible and inedible) and general waste (e.g. tools, consumables, growth media).

Greenhouse modules require energetic inputs in terms of electrical energy, workforce and heat. However, there is also the need for heat extraction from the greenhouse depending on the atmospheric conditions (especially temperature and relative humidity).
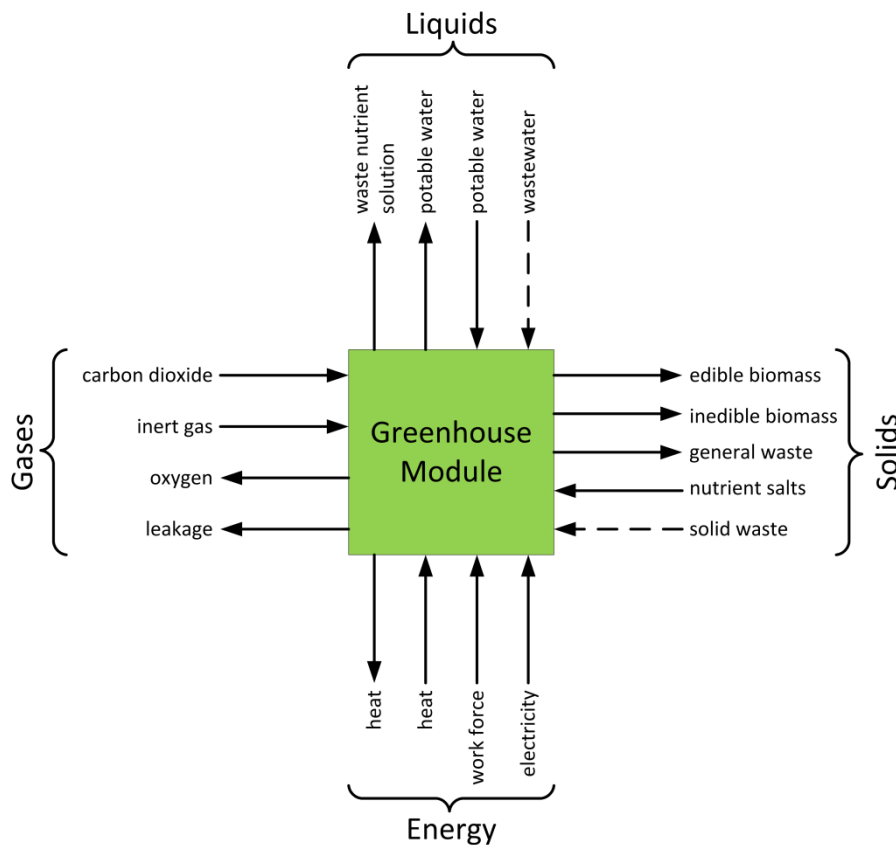
Figure 2-11: Greenhouse module inputs and outputs arranged by type (solid arrows indicate necessary inputs and outputs; dashed arrows indicate potential inputs and outputs).

2.3.5 Plant Selection

Selecting the right plants and cultivars for space greenhouse modules is a complicated process, which is so far not satisfactorily finished. A number of criteria exist to evaluate plants on their suitability for the cultivation in BLSS. Among them are biomass production and nutritional aspects, plant requirements, growth conditions and others. Table 2-4 shows an overview of selection criteria by Eckart (1996).

Table 2-4: Overview of plant selection criteria (Eckart, 1996).

Biomass Production and Nutritional Aspects	Plant Requirements	Growth Conditions	Others
• Proportion of edible biomass • Yield of edible plant biomass • Energy concentration • Nutritional composition • Palatability • Acceptable serving size and frequency • Flexibility of usage • Storage stability • Toxicity • Degree of human nutritional experience	• Volume of space required • Labor requirements • Weight of the plant-growing system • Electrical energy utilized • Purchase and maintenance cost of plant-growing system	• Environmental tolerance • Photoperiodic and temperature requirements • Pollination and propagation • Vegetation period • Harvesting methods • Continuous harvesting • Possibility of using low quality water • Compatibility with other plant species • Ecological and genetic stability • Resistance against infections • Degree of loop closure of the whole system • Water consumption and transpiration rate • O_2 production and CO_2 assimilation	• Atmosphere regeneration capability • Water regeneration capability • Waste regeneration Capability • Behavior under extra-terrestrial conditions • Interaction with other Systems

Wheeler (2004b) reviewed and collected a number of plant selections from different sources (Pilgrim and Johnson, 1962; Tibbits and Alford, 1982; Gitelson *et al.*, 1989; Salisbury and Clark, 1996; NASA, 1998; Waters *et al.*, 2002; Hoff *et al.*, 1982), as shown in Table 2-5.

Table 2-5: Collection of plant lists from different sources (Wheeler, 2004a).

Pilgrim and Johnson (1962)	Tibbitts and Alford (1982)*	Hoff et al. (1982)*	Gitelson and Okladnikov (1989)	Salisbury and Clark (1996)*	Vegetable Unit for ISS (NASA, 1998)	Waters et al. (2002)*
Sweet Potato	Wheat	Wheat	Wheat	Wheat	Lettuce	Wheat
Tambala	Soybean	Soybean	Salad Spec.	Soybean	Spinach	Soybean
Chinese Gab.	Lettuce	Potato	Potato	Lettuce	Radish	Lettuce
Cabbage	Sweet Potato	Carrot	Radish	Sweet Potato	Cabbage	Sweet Potato
Cauliflower	Peanut	Peanut	Beet	Kale	Green Onion	Rice
Kale	Rice	Rice	Nut Sedge	Broccoli	Carrot	Bean
Collards	Sugar Beet	Tomato	Onion	Carrot	Tomato	Beet
Turnip	Taro	Dry Bean	Cabbage	Canola	Pepper	Cabbage
Swiss Chard	Winged Bean	Chard	Tomato	Rice	Strawberry	Broccoli
Endive	Broccoli	Cabbage	Pea	Peanut	Different	Cauliflower
Dandelion	Onion		Dill	Chickpea	Herbs	Carrot
Radish	Strawberry		Cucumber	Lentil		Kale
New Zealand			Carrot	Tomato		Spinach
Spinach				Onion		Potato
				Chili Pepper		Onion

*Listing do not show the complete range of species suggested for a more complete diet

2.3.6 A Brief History of Greenhouse Module Research

The Soviet Union was the first among the space faring nations to begin with research in BLSS in the early 1960s. First experiments began in 1961 and led to the construction of the Bios-1 facility in 1965 (Salisbury *et al.*, 1997). It can be seen as the beginning of space greenhouse research. From there on various flight experiments were flown, ground test facilities operated and design studies performed. This chapter gives an overview of the history of greenhouse module development and research.

2.3.6.1 Flight Experiments

There has been a consistent effort on-orbit to grow higher plants and to assess the effects of the spaceflight environment upon them. These efforts have included free-flyer experiments (Halstead and Dutcher, 1984), short duration crewed missions (e.g. Shuttle, Shenzhou) (Hoehn *et al.*, 1998; Preu and Braun, 2014) as well as those typically of longer duration conducted in Salyut, Mir and the International Space Station (ISS) (Porterfield *et al.*, 2003). In particular, plant growth experiments have been an important part of each space station program since their incorporation into the Soviet/Russian Salyut 1, the first space station. Early on-orbit production systems were quite exploratory in nature in that they focused on the fundamental investigations related to the effect of the spaceflight environment on plant growth or technology development associated with providing an appropriately controlled environment on-orbit.
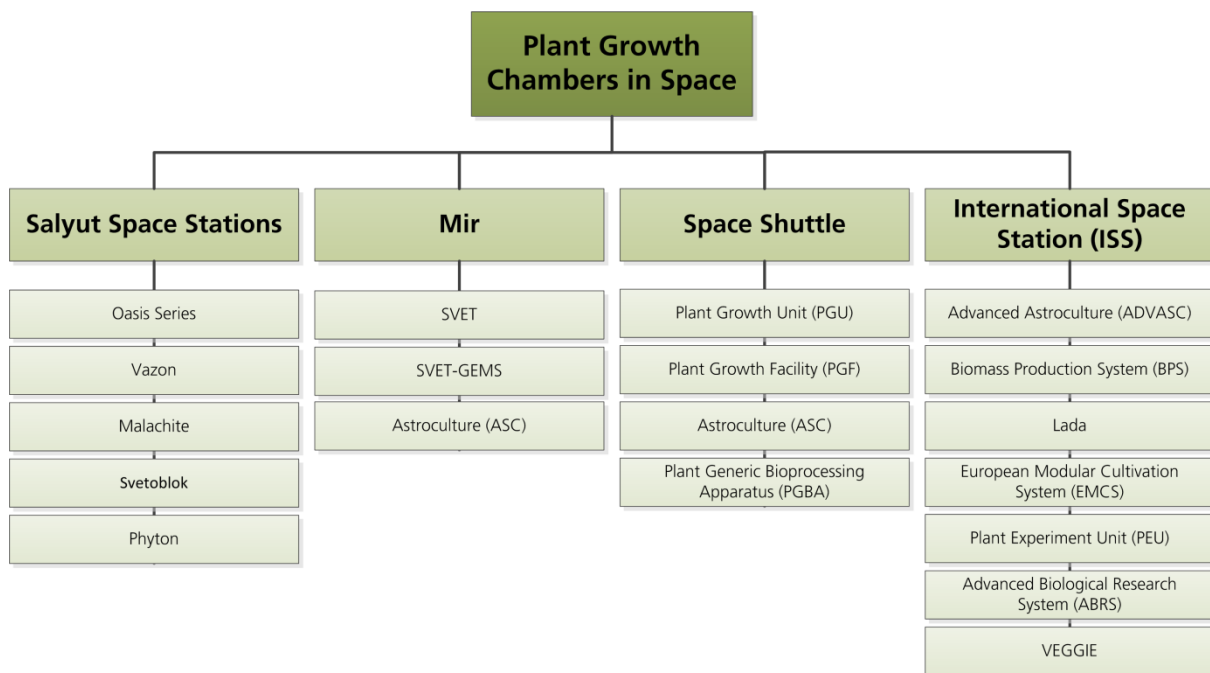
Figure 2-12: Overview of plant cultivation flight experiment systems.

Plant cultivation flight experiments are usually small chambers that are not an active part of the life support system. They are typically utilized to study plant behavior and development under reduced gravity and in closed environments. Summaries of plant growth chambers have been published in recent years (Hoehn *et al.*, 1998; Porterfield *et al.*, 2003; Berkovitch, 1996; Haeuplik-Meusburger *et al.*, 2011; Haeuplik-Meusburger *et al.*, 2014; Paul *et al.*, 2013a). The most up-to-date paper was published by this thesis' author and his co-authors

(Zabel *et al.*, 2016a). The following paragraphs give a short summary of the review presented in the paper.

Figure 2-12 provides an overview of the plant growth chambers described in the following subchapters. Although not explicitly mentioned as a category, the author is aware of the experiments conducted on-board Skylab (Floyd, 1974; Kleinknecht and Powers, 1973) and Shenzhou (Preu and Braun, 2014).

Salyut Space Stations

The first Soviet Union flight experiment was executed within the **Oasis 1** plant growth system. It was part of the Salyut 1 mission in 1971. During the mission *Brassica capital*, *Linum usitatissimum* and *Allium porrum* were grown in the eight cultivation slots of Oasis 1. Fluorescent lamps provided the necessary illumination. Oasis 1 was the first in a number of successful Oasis series chambers. Oasis 1M, an upgraded version of Oasis 1 was operated on Salyut 4. Oasis 1AM was the next plant growth system of the Oasis family and was flown on Salyut 6. Oasis 1A was installed in the Salyut 7 station and was the last of the Oasis experiments. Compared to its predecessors, Oasis 1A was capable of providing increased aeration to the root zone (Halstead and Dutcher, 1984; Porterfield *et al.*, 2003; Haeuplik-Meusburger *et al.*, 2014).

Figure 2-13: Oasis 1 as exhibited in the Memorial Museum of Astronautics in Moscow (Encyclopedia of Safety, 2012).

Vazon is another plant growth system of the Soviet Union. Its first flight was on Soyuz 12 in 1973. Unlike Oasis, Vazon had no separate lighting system. Illumination was provided by the lighting system of the spacecraft. The system was designed to grow bulbous plants. Vazon was modified several times and was also operated onboard Salyut 6, Salyut 7 and the Mir space station (Porterfield *et al.*, 2003).

Malachite, flown on Salyut 6, was the first experiment specifically designed to investigate the psychological benefits of crew interaction with plants. From that perspective, orchids were the chosen crop and were grown in four Malachite planting boxes (Porterfield *et al.*, 2003).

Svetoblok, on Salyut 7, was the first plant growth system capable of growing plants in a sterile environment. According to Porterfield, et al. (2003), this advantage led to the first successful flowering of plants grown in space during a 65-day experiment. However, no viable seeds were produced. Updated versions of Svetoblok were also flown on the Mir space station (Haeuplik-Meusburger *et al.*, 2014; Musgrave and Kuang, 2003).

The success of Svetoblok led to the initiation of the **Phyton** project, which was used to conduct the first seed-to-seed cycle in space during a mission on Salyut 7 (Porterfield *et al.*, 2003).

Mir Space Station

The Russians continued their bio-regenerative life support system research efforts on the Mir space station with the **SVET** space greenhouse. The first SVET experiment conducted in collaboration with Bulgaria was launched on the 31st of May in 1990. The module successfully docked to the Mir station on the 10th of June and was subsequently installed inside the Kristall (Kvant 3) module. SVET was initiated on the 15th of June with a number of system tests that proved the functionality of the system (Ivanova *et al.*, 1993; Ivanova *et al.*, 1994).

The first plants were grown in a 53-day experiment in the summer of 1990. Radish and Chinese cabbage were selected for this experiment. During the experiment plant samples were taken and brought back to Earth together with the crops harvested on the last day. According to Ivanova (1993), the plants had a healthy appearance, but were stunted compared to the control plants grown on Earth. The leaves had a characteristic dark green color and a rough surface. The arrangement of the leaves was normal.

In 1995 the Space Shuttle successfully docked to the Mir station. During this mission the SVET space greenhouse was reinitiated as part of the Shuttle-Mir Program. Some of the old equipment was updated and new systems provided by the Americans were added to SVET. The new equipment consisted of an Environmental Measurement System (EMS) and a Gas Exchange Monitoring System (GEMS), leading to the name **SVET-GEMS** for the new system (Bingham *et al.*, 1996).

Between 1995 and 1997 several experiments with super-dwarf wheat were conducted and the SVET greenhouse received small design updates with each subsequent experiment. According to Ivanova (1998) and Salisbury (2003), the results of the 1996/97 experiments were better than expected. The produced biomass was much higher than expected and the plant health, especially root health, was much better than in any previous experiment. The leaves had a healthy green color and 280 wheat heads were produced. However, none of them contained any seeds. It was assumed, that pollen was either not formed or not released. Another finding during the 1996/1997 experiments led to the conclusion, that high levels of ethylene led to aborted seed production in wheat. As a result all subsequent plant experiments included ethylene filters and trace contaminant control (Campbell *et al.*, 2001).

Space Shuttle

The Space Shuttle Program was the first opportunity for American BLSS researchers to perform regular flight experiments. The **Plant Growth Unit (PGU)** was the first experiment and was flown on STS-3 in 1982. The system was designed to study seedling growth and lignification and fit into a middeck locker. The PGU system was used for experiments over the next 15 years (Porterfield *et al.*, 2003; Cowles *et al.*, 1984).

In 1997 the **Plant Growth Facility (PGF)** had its first flight on STS-87. The PGF was an updated PGU with the same dimensions, but enhanced equipment (Porterfield *et al.*, 2003; Kuang *et al.*, 2000). The PGU and PGF were also used to investigate plant reproduction in microgravity during the CHROMEX experiments that showed that CO_2 enrichment and adequate ventilation were required for ensuring normal seed production in microgravity. This

work led to the notion that secondary effects of microgravity can significantly affect normal plant development (Musgrave *et al.*, 1997).

The **Astroculture** series was another plant growth chamber designed for the Space Shuttle. Its first flight (ASC-1) was on STS-50 in 1992, followed by continuous updates and corresponding qualification flights (STS-57, -60, -63, -73, -89, -95) (Zhou *et al.*, 2000). At one time an ASC chamber was also operated on board the Mir space station. The first three ASC experiments were designed to perform system tests and verification (Morrow *et al.*, 1993; Morrow *et al.*, 1994; Bula *et al.*, 1994; Duffie *et al.*, 1994; Duffie *et al.*, 1995). The last experiment with the Astroculture system was performed in 1998. ASC-8, as shown in Figure 2-14, grew roses and investigated the effects of microgravity on the production of essential oils (Musgrave *et al.*, 1997).

Figure 2-14: ASC-8 flight hardware installed in a middeck locker (Musgrave *et al.*, 1997).

The first flight of the **Plant Generic Bioprocessing Apparatus (PGBA)** was on STS-77 in 1996. The PGBA was designed to fit into two middeck lockers. A containment structure, a plant growth chamber, a thermal control system and an electrical subsystem were part of the PGBA (Hoehn *et al.*, 1997). The PGBA was operated during three Space Shuttle missions (STS-77, STS-83, STS-94) with durations of 4, 10 and 16 days respectively (Hoehn *et al.*, 1998). In 2002 the PGBA was also used for experiments onboard ISS during Expedition 5 (Evans *et al.*, 2009).

The International Space Station

The **Advanced Astroculture (ADVASC)** experiment was the first plant growth chamber flown on the ISS. The design is based on the original Astroculture system, but with twice the size. Due to its increased size, ADVASC required two single middeck lockers inserts which could be installed into an EXPRESS Rack. One insert contains all support systems, lower insert shown in Figure 2-15, while the other contains the plant growth chamber, top insert in Figure 2-15 (Zhou *et al.*, 2002). During the ADVASC-1 experiment (2001), a seed-to-seed experiment with *Arabidopsis Thaliana* was performed. Several seeds were gathered (Link *et al.*, 2003). These 1st generation seeds were used for the ADVASC-2 (2001/2002) experiment to investigate whether they are able to complete another full life cycle under microgravity and how the genes were affected. At the end of the experiment, 2nd generation seeds were gathered. ADVASC-3 (2002) was the first experiment to grow soybean plants in space (Zhou, 2005).

Figure 2-15: Advanced Astroculture™ ISS plant growth chamber (Link *et al.*, 2003).

The **Biomass Production System (BPS)** was a plant growth chamber operated on the ISS in 2002 during Expedition 4. Two experiments were carried-out during this mission, the Technology Validation Test (TVT) and the Photosynthesis Experiment and System Testing and Operation (PESTO) experiments. PESTO demonstrated that plants grown in space do not differ from ground controls when the secondary effects of the spaceflight environment are mitigated. Evidence was identical rates of photosynthesis and transpiration which were proven with identical biomass production between spaceflight and ground control plants (Evans *et al.*, 2009; Stutte *et al.*, 2005). The subsystems and technologies validated with the BPS were later used within the Plant Research Unit (PRU) (Kern *et al.*, 2001).

The **Lada** greenhouse is a plant growth system developed for the ISS and flown in 2002 (Ivanova, 2002). The system partly reused equipment from SVET-GEMS. The subsystems of Lada are spread amongst four modules: the control and display module (Figure 2-16 upper center), two growth modules (Figure 2-16 left and right) and a water tank (Figure 2-16 bottom center) (Bingham *et al.*, 2002). For the first time in on-orbit greenhouse module research the psychological effects of the interaction between the crew and plants were investigated (Bingham *et al.*, 2002). Some reactions of the ISS crew to the consumption of space-grown plants are cited by Bingham (2003). From 2003 to 2005, genetically modified dwarf pea plants were grown during five experiments with Lada. These experiments investigated morphological and genetic parameters over several generations of space grown plants (Sychev *et al.*, 2007). LADA was also used to develop the hazard analysis and critical control point (HACCP) plan for vegetable production units (Hummerick *et al.*, 2011; Hummerick *et al.*, 2010).

Figure 2-16: Lada; control and display module (upper center), growth modules (left and right), water tank (bottom center) (Bingham *et al.*, 2002).

The **European Modular Cultivation System (EMCS)** was launched on STS-121 in July 2006 (Solheim, 2009). The EMCS contains two rotors to apply different levels of gravity (0.001 g to 2.0 g) to the contained experiment containers (EC). Each rotor can hold up to four ECs. One EC is 60 mm high, 60 mm wide and 160 mm long with an internal volume of 0.58 liters (Brinckmann, 1999). The EMCS was used to carry out different European plant growth and plant physiology experiments (e.g. GRAVI, GENARA, MULTIGEN and TROPI) (Brinckmann, 2005). It was also utilized by the Japanese Aerospace Exploration Agency (JAXA) (Kamada *et al.*, 2007).

The Japanese **Plant Experiment Unit (PEU)** is an experiment container to be mounted within the Cell Biology Experiment Facility (CBEF) inside the Kibo laboratory module of the ISS. In 2009, eight PEUs were launched with STS-128 and implemented into the CBEF. The experiment was called Space Seed and had the purpose to grow Arabidopsis from seed to seed under different conditions. The plants were grown for 62 days inside the PEU mounted in the CBEF (Yano *et al.*, 2013).

The **Advanced Biological Research System (ABRS)** was launched in 2009 on STS-129. The main parts of ABRS are two Experimental Research Chambers (ERCs) that provide a controlled environment for experiments with plants, microbes and other small specimens (Levine *et al.*, 2009). One of the first experiments conducted within the ABRS was the investigation of the Transgenic Arabidopsis Gene Expression System (TAGES) (Paul *et al.*, 2012; Paul *et al.*, 2013b).

The **VEGGIE Food Production System** is NASA's latest achievement in developing BLSS. It was launched in early 2014. VEGGIE is the first system designed for food production rather than plant experiments under microgravity. A deployable design allows VEGGIE to be stowed to 10% of its nominal deployed volume. In collapsed configuration, six VEGGIE units can be stored in a single middeck locker. Each unit consists of three major subsystems, the lighting subsystem, the bellows enclosure and the root mat and provides 0.17 m² growth area with a variable height of 5 to 45 cm. A customized LED panel with red, blue and green LEDs is used as the lighting subsystem. The panel is able to provide more than 300 µmol/(m²*s) of illumination to the plants. The bellows enclosure separates the plant environment from the cabin to provide containment for the plants and to maintain elevated humidity. The enclosure is supported by a foldable structure, which allows adjustment of the distance between the lighting subsystem and the root mat while maintaining containment. The root mat serves as a

passive nutrient delivery system, which requires only a small amount of crew time to be supplied with water and nutrient solution (Morrow *et al.*, 2005). Several different growth media have been investigated (Massa *et al.*, 2013; Stutte *et al.*, 2011a) and in the end specially developed rooting pillows were selected.

Crops produced by the VEGGIE system shall be used as supplemental food for the ISS crew. Achieving this objective is challenging and requires compliance with NASA's microbiological standards for food. The project team developed a HACCP plan, based on the plans tested with Lada, to minimize the risk of consuming produced vegetables. The selected sanitizer demonstrated functionality and applicability during a test campaign at NASA's Desert Research and Technology Studies (DRATS). For the demonstration a VEGGIE unit was installed in the Habitat Demonstration Unit (HDU) Pressurized Excursion Module (PEM), see Figure 2-17. After a 28 day growth cycle the harvested lettuce plants were sanitized and more than 99 % of the microbial load was removed. The microbial load of the produce was well within the NASA standards (Stutte *et al.*, 2011b).

Figure 2-17: VEGGIE prototype during ground tests (left); NASA astronaut Steve Swanson next to VEGGIE after the deployment on-board ISS (right) (Stromberg, 2014).

On August 10 in 2015 NASA astronauts were, for the first time ever, officially allowed to eat their space-grown vegetables. The astronauts Kelly, Lindgren, Yui, Kononenko and after their spacewalk Padalka und Kornijenko ate lettuce of the variety Outrageous grown within the Veggie growth system, see Figure 2-18 (NASA Kennedy Space Center, 2015).

Additional Systems and Designs

The **Vitacycle** is a Russian plant growth chamber concept with a novel approach for the arrangement of the growth area. The design incorporates a convex growth area combined with a conveyor, which leads to a savings in occupied volume compared to a standard flat growth area. Prototypes of the chamber were built and tested in advance of a proposed utilization in the Russian compartment of the ISS (Berkovich *et al.*, 1997; Berkovich *et al.*, 1998; Berkovich *et al.*, 2004; Berkovich *et al.*, 2009). The concept was also part of the Mars500 experiment (Berkovich *et al.*, 2009).

The **Salad Machine** concept was initially investigated by NASA's Ames Research Center (Kliss and MacElroy, 1990) and further developed over the following years (Kliss *et al.*, 2000a; Kliss *et al.*, 2000b). The production unit was planned to occupy a standard rack and provide around 5% of the total caloric intake of the crew.

The **Plant Research Unit (PRU)** was supposed to fly to ISS in its early years. It was the direct predecessor of the BPS. The PRU was designed as a closed system to generate a reliable plant growth environment. Although extensive effort was put into the design of the PRU (Turner *et al.*, 1995; Crabb *et al.*, 2001; Stadler and Brideau, 2004; Stadler *et al.*, 2004; Heathcote *et al.*, 1997), the program was canceled in 2005 (Forehand, 2005).

Figure 2-18: Astronauts Kelly, Lindgren and Yui eating self-grown lettuce (image made by the authors from reference (NASA Kennedy Space Center, 2015)).

The **Portable Astroculture Chamber (PASC)** was a planned follow-on to the ADVASC. Although it did not fly, the PASC was designed for installation within an ISS EXPRESS rack. Compared to its predecessors, PASC planned to reduce complexity by utilizing ISS ambient air and included four transparent sides to permit easy viewing by the crew (NASA, 2014).

Astro Garden (later termed Education Payload Operations - Kit C Plant Growth Chambers) was developed as an educational tool and hobby garden for on orbit plant growth. The relatively simple apparatus which flew to the ISS on STS-118 in 2007 required no supplemental power and utilized existing ISS light sources for growth (Morrow *et al.*, 2007).

CPBF (Commercial Plant Biotechnology Facility), although never flown was a quad middeck locker based system. It was being developed to provide a facility for long-term scientific and commercial plant trials onboard the ISS (Hoehn *et al.*, 1998).

The NASA **Advanced Plant Habitat (APH)** is a planned four middeck locker plant growth system being developed at the Kennedy Space Center in cooperation with ORBITEC. The APH is based upon some of the design heritage of the CPBF. The project is divided into several phases with the final goal to deploy an EXPRESS rack based plant growth chamber onboard the ISS (Spaceref, 2012; Wheeler, 2012).

Small-scale plant growth hardware has also flown on Shenzhou. In particular, the DLR developed **Science in Microgravity Box (SIMBOX)** flew on a late 2011 Shenzhou flight and within it contained 17 different bio-medical experiments in collaboration between German and Chinese researchers. Included were a number of plant seedlings under LED illumination (Preu and Braun, 2014).

2.3.6.2 Ground Research Facilities

Plant growth chambers in space are necessary to study plant physiology and development under microgravity. However, they are usually restricted in their size, energy consumption and by other means. Ground research facilities do not have these limitations. Consequently, various such facilities were built and operated in the past. They can be divided into greenhouses in human isolation tests, pure plant cultivation facilities and greenhouses at analogue test sites, see Figure 2-19.
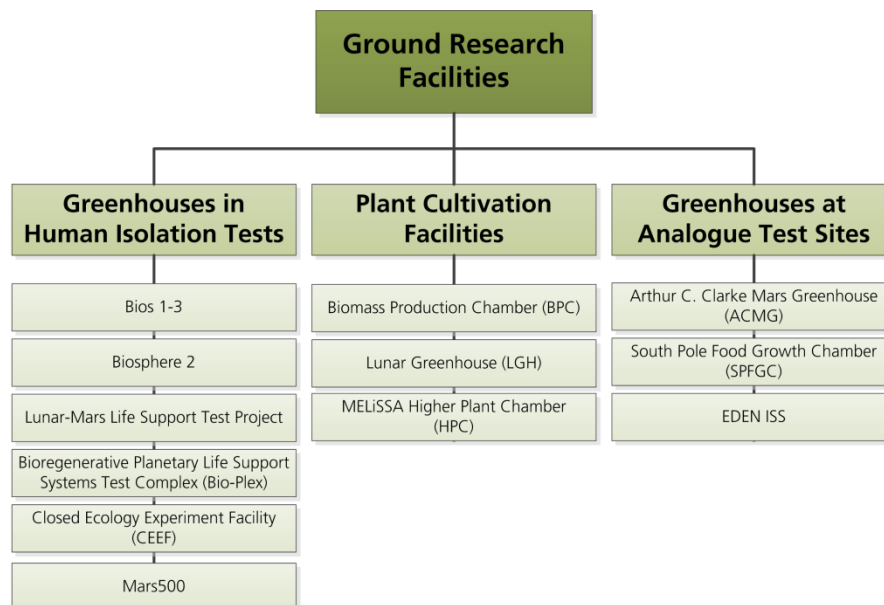
Figure 2-19: Overview of ground research facilities.

Greenhouses in Human Isolation Tests

Even before the first flight experiments were performed onboard the Salyut stations, the Soviet Union had started their ground research on biological life support systems. **Bios-1** (1965-1968) was the first test facility of the Soviet research program in closed life support systems. In 1968 a greenhouse for the cultivation of higher plants was attached to Bios-1. The new complex was named **Bios-2** (1968-1972) (Salisbury *et al.*, 1997). The design and construction of **Bios-3** began during the last experiments of Bios-2 and was finished in 1972. Bios-3 was a human isolation research facility for the investigation of closed ecological life support systems. The facility was located at the Institute of Physics of the Soviet Academy of Sciences in Krasnoyarsk. The purpose of Bios-3 was the development of life support systems capable of supporting a crew of two to three persons with clean water, fresh air and a sufficient amount of food. All systems are designed to be maintained by the crew during the experiments (Gitelson *et al.*, 2003).

Biosphere 2 was a research facility for human isolation tests and closed ecosystems. The facility is located in the USA near Tuscon, Arizona, its construction began in 1986 (Marino *et al.*, 1999). The purpose was the design and construction of a human controlled mesocosm with similarities to Earth. Therefore, seven biomes with different layouts and climates were established. The interesting part for greenhouse module research is the Intensive Agriculture Biome (IAB), which consists of an animal bay, an orchard and a two floor greenhouse for crop growth and is designed to provide food for humans and feed for the animals during the closed habitation missions. The dimensions of the greenhouse are 41 x 54 x 24 m³, which

results in an area of 2200 m² and a volume of 38000 m³ (Marino *et al.*, 1999). In the early 1990s, two closed habitation missions were accomplished within the Biosphere 2 facility. The first mission started in September 1991 with a crew of eight and ended in September 1993. After mission one, improvements were made to the systems of Biosphere 2, especially to the IAB. Mission two went from March 1994 to September 1994; the crew consisted of seven people (Marino *et al.*, 1999).

The crew of Biosphere 2 encountered a number of problems such as disputes between the crew members, decreasing oxygen levels caused by microorganism activity, a collapse of the animal ecosystem (only 6 out of 25 small inset species survived), the water system became polluted with too many nutrients and imbalances in the atmosphere let to a dangerous increase in dinitrogen oxide (Alling *et al.*, 1993).

Figure 2-20: Overview of the Biosphere 2 complex (Marino *et al.*, 1999).

The **Lunar-Mars Life Support Test Project (LMLSTP)** was conducted from 1995 to 1997 at NASA's Johnson Space Center in Houston, Texas. The main objective was the testing and integration of a closed-loop system which incorporates biological and physical-chemical technologies for water recycling, waste processing and air revitalization (Williams, 2002). The project was divided into four separate phases respectively tests. Phase I demonstrated the utilization of higher plants for air revitalization by providing enough O_2 for one crew member by simultaneously removing the CO_2. The Phase I test lasted 15 days. For Phase II the test duration was increased to 30 days and the number of crew members accounted for four. During the test physical-chemical LSS were used for air revitalization, water recovery and thermal control. Furthermore, a number of studies were conducted with respect to psychology, human factors and the microbiological environment. Phase IIa utilized life support systems built for the ISS. During a 60 day study, four crew members operated the systems in a confined environment. They were permanently monitored throughout the experiments. Phase III, the final experiment, combined biological and physical-chemical technologies in an integrated system. It was capable of continuously recycle air, water and partly solid waste of four humans during a 91 days confinement (Lane, 2002).

The **Bioregenerative Planetary Life Support Systems Test Complex (BIO-Plex)** was one of NASA's projects of the Advanced Life Support (ALS) program and was located at the Johnson Space Center in Houston. BIO-Plex was designed as test facility for human isolation experiments and as a testbed for life support systems. The design was influenced by the

findings of the LMLSTP. Systems regarding the food production, water purification and air revitalization and other key elements of an ECLSS were planned to be integrated and evaluated during long duration experiments. The design of the facility began in the early 1990s, but the project was directed to suspend ongoing activities in 2001 due to the declining NASA budget. Since 2001, the already constructed parts of the facility are placed in a "stand-by" mode (Villareal and Tri, 2001). Although BIO-Plex was neither finished nor operated, the design shows a new approach for human isolation test facilities and was the first one with a cylindrical module structure similar to space stations.

The **Closed Ecology Experiment Facility (CEEF)** was constructed for the investigation of carbon transfer in the area around the Rokkasho nuclear fuel reprocessing plant in Japan. In 2000 the facility was rebuild for research in closed life support system for space application (Nitta, 1999). Figure 2-21 shows an outside view on the CEEF. Inside the plant cultivation building, 150 m² are used for the cultivation of plants. The cultivation area is allocated in four chambers (Nitta, 2005). The closed habitation experiments started in 2005 with three 1-week closures of two humans and two goats. During these first experiments, only the oxygen, carbon dioxide and food loops were closed, while water and waste were treated outside the test facility. The water recycling system was installed and active in the experiments in 2006. In this year the habitations were extended to three 1-month closures. In 2007 the waste processing system was integrated in the habitations, which were further extended to two 1-month and one 2-month closure. The Japanese scientists consequently extended the habitation to a four-month closure in 2009 (Tako *et al.*, 2008). The food loop closure was between 91.8 % and 94.6 % during four different closures. A value of 96 % was estimated during simulations. However, the harvested edible biomass was less than expected (Masuda, 2007).

Figure 2-21: Outside view of the CEEF (Nitta, 2005).

The **Mars-500** project, a joint venture between Russia, ESA and China, was a psychosocial isolation experiment. Between 2007 and 2011 different crews were confined in a test facility located at the Russian Academy of Sciences' Institutes of Biomedical Problems (IBMP) in Moscow. Although the main purpose of the project was to simulate a flight to Mars and investigate the psychological and social issues related to such a voyage, there was also a small plant growth facility (Belakovsky *et al.*, 2010).

Plant Cultivation Facilities

The **Biomass Production Chamber (BPC)** of NASA's Closed Ecology Life Support System (CELSS) program was the most powerful and successful research facility for plant cultivation under controlled environment so far. Figure 2-22 shows the BPC in a building of the Kennedy

Space Center in 1986. Plants could be cultivated on two floors with two levels each, leading to a total growth area of 20 m². The dimensions of the chamber were designed to suit the food production, water and air generation for one person (Wheeler *et al.*, 2003). Plants were cultivated in special trays which fit into the cylindrical shape of the BPC. Figure 2-23 shows wheat plants growing inside the BPC. Nutrient film technology (NFT) was used to provide the required nutrition for the crops (Knott, 1992). Illumination was provided by high-pressure sodium (HPS) lamps, but metal halide lamps (Wheeler *et al.*, 1996) and fluorescent lamps (Wheeler *et al.*, 2003) were also used for different experiments. In 2001 the BPC was decommissioned after 13 years of extensive research. During this time, several experiments with wheat, soybean, lettuce, potato and tomato were performed (Knott, 1992; Wheeler *et al.*, 1996; Wheeler *et al.*, 2003).

Figure 2-22: BPC at the Kennedy Space Center in 1986 (Wheeler *et al.*, 2003).
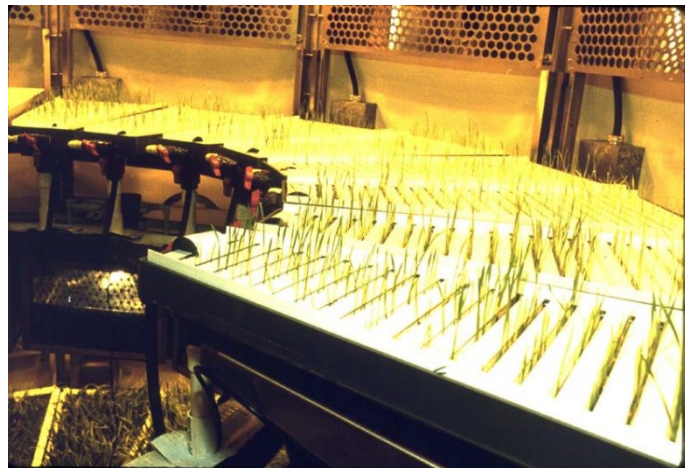
Figure 2-23: Wheat growing plants in BPC trays (Wheeler *et al.*, 2003).

The **Lunar Greenhouse (LGH)** is a BLSS developed by an U.S.-Italian corporation under the leadership of the University of Arizona's Controlled Environment Agriculture Center (UA-CEAC). The project started in 2005 with a feasibility study and is still running. According to Sadler (2009), the purpose of the Lunar Greenhouse project is the demonstration of biomass and food production, air and water revitalization, and waste recycling within a poly-culture deployable cropping system. The aim of the greenhouse is full water purification and air revitalization, and the provision of up to 50 % of the required crew's daily energy intake. The greenhouse module concept is able to fulfill these requirements for one human. Consequently, four modules are required to meet the requirements for the lunar outpost scenario (Sadler *et al.*, 2009).

The **Micro-Ecological Life Support Alternative (MELiSSA)** is a project of ESA that began in the 1990s. The objective of the project is to improve understanding and knowledge of artificial ecosystems to foster development of bio-regenerative life support systems. MELiSSA investigates a closed loop with multiple compartments each containing a certain organism. The five compartments are: an anaerobic composter to recycle plant material and human feces, a photoheterotrophic bacteria compartment to absorb volatile organic acids, an aerobic nitrification compartment to recycle ammonium to nitrate, a photosynthetic compartment consisting of an algae photo bioreactor and a plant compartment for food production, air revitalization and water recycling, and a crew compartment for the astronauts (Lasseur *et al.*, 2010;

Lasseur *et al.*, 2005; Lasseur *et al.*, 2000; Lasseur *et al.*, 1996). The complete MELiSSA loop is shown in Figure 2-26.

Figure 2-24: Folded Configuration of the LGH (Sadler *et al.*, 2011).

Figure 2-25: Deployed Configuration of the LGH during a test period (Sadler *et al.*, 2011).
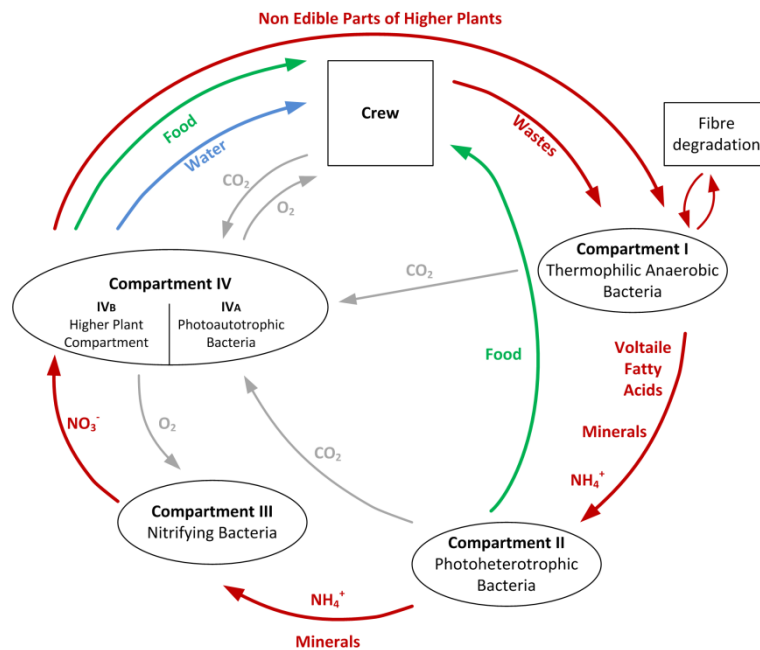
Figure 2-26: The MELiSSA loop compartmentalized structure, redrawn from Lasseur *et al.* (2010).

The MELiSSA pilot plant is located at the Autonomous University of Barcelona and is used to integrate the different compartments into a test facility. The pilot plant also has a small plant growth chamber. The higher plant chamber (HPC) is a down-scaled version of the higher plant compartment of the MELiSSA loop. The chamber is primarily used for plant cultivation studies on e.g. plant health monitoring, determination of growth parameters and characterization of crops.

Greenhouses at Earth-Analogue Test Sites

The **Arthur C. Clarke Mars Greenhouse (ACMG)** is a research facility of the Canadian Space Agency (CSA), the University of Guelph and the University of Florida. The facility is located at the Haughton Mars Project Research Station (HMPRS) on Devon Island in the Canadian Arctic, see Figure 2-27. The purpose of the ACMG is to study greenhouse engineering, plant growth and autonomous functionality under extreme operational conditions. The main achievement of a prosperous year of autonomous operations with a spring and a fall crop successfully grown to maturity (Bamsey *et al.*, 2009b). The greenhouse is operational since 2002, mainly during the summer periods. The ACMG has seen enhancements in 2005 (Bamsey *et al.*, 2009a). The plant growth system consists of two commercial drip-line systems. One drip-line system is used for spring plants and one for fall plants. A pump delivers water and nutrients to the plants every hour. The remaining water is collected in a tank and reused for the next watering (Giroux *et al.*, 2006).

Figure 2-27: Outside view of the ACMG (Bamsey *et al.*, 2009b).

The **South Pole Food Growth Chamber (SPFG)** is located at the American Amundsen-Scott South Pole Station. The SPFG was built by the University of Arizona in Tucson and the Sadler Machine Company from 2002-2004. The chamber is outfitted with a hydroponic, semi-automated plant cultivation system. SPFG is located in a climate-controlled room at the South Pole Station and consists of a utility room and the actual plant production room. The latter is roughly 54.7 m² large with a production area of 21.9 m². The edible biomass production averaged 2.8 kg/day (±1.0 kg/day) during the season from January to October 2006 (Patterson *et al.*, 2008; Giacomelli *et al.*, 2006). In total 32 different crops were grown in that season. Six zones with 1.72 m² were assigned for lettuces, three zones with 2.43 m² each were used to grow tall crops such as tomato, cucumber and cantaloupe, in another three zones with 1.29 m² each different types of herbs were cultivated and one zone with 1.29 m² was used as nursery area for seedlings (Patterson *et al.*, 2012).

EDEN ISS is a project funded by the European Horizon 2020 research framework and is lead by the German Aerospace Center (DLR) Institute of Space Systems in Bremen, Germany. The project consortium consists of the major players in bio-regenerative life support systems in Europe, Canada and the United States. The project aims to design, develop and test a container-sized greenhouse at the Germany Neumayer III Antarctic research station. The project started in March 2015 and plans to deploy the greenhouse in December 2017. From there on it will be operated for 12 months continuously (Zabel *et al.*, 2015; Zabel *et al.*, 2016b; Vrakking *et al.*, 2017; Zabel *et al.*, 2017).

The greenhouse consists of a small cold porch, a service section, an ISPR cultivation system and the future exploration greenhouse. The cold porch functions as a buffer room between the outside environment and the work area of the facility. Here crew members change their winter gear to laboratory cloths. The service section houses all the different subsystem (e.g. nutrient delivery, atmosphere management), which are necessary to operate the green-house. The ISPR cultivation system is a stand-alone plant growth unit in the size of a stand-ard ISPR including standard interfaces. It is located within the service section and is a pre-cursor for an ISS plant growth system (Boscheri *et al.*, 2016; Boscheri *et al.*, 2017b). The fu-ture exploration greenhouse is the main plant cultivation area and takes up almost 50 % of the complete facility. Within the future exploration greenhouse are two rows of shelf-like culti-vation units, which can be rearranged in order to outfit the greenhouse to the selected crops, see Figure 2-28 and Figure 2-29.
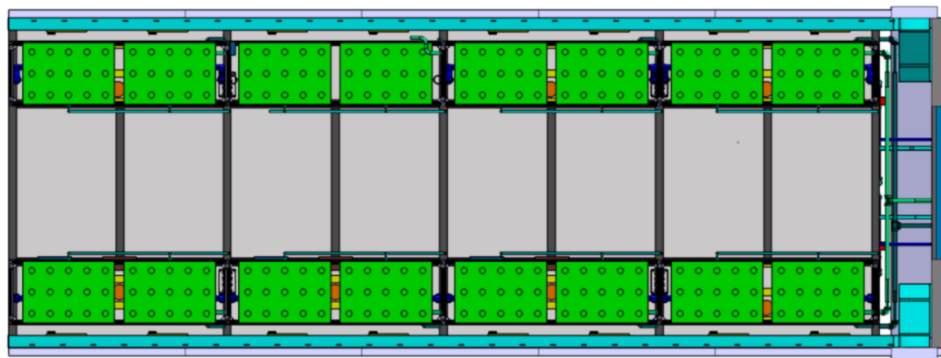
Figure 2-28: Top view of the EDEN ISS Future Exploration Greenhouse (Zabel *et al.*, 2016b).

In total the EDEN ISS greenhouse has a cultivation area of 10-12 m² and a fresh biomass production rate of roughly 176 kg/year respectively 3.4 kg/week, depending on the cultivated crops. EDEN ISS focuses on the production of pick-and-eat crops (e.g. tomatoes, cucum-bers, lettuce). More than 15 different crops and cultivars were selected (Dueck *et al.*, 2016).

Figure 2-29: Future Exploration Greenhouse – Plant tray configuration including illustration of the rele-vant definitions of chamber, rack, unit, level and tray (Zabel *et al.*, 2016b).

Miscellaneous facilities

There are small greenhouse system installed at analogue test sites such as the Mars Desert Research Station (**MDRS**) and at the Habitat Demonstration Unit of the NASA Desert Research and Technology Studies (**Desert RATS**) research site. They are not explicitly explained here, as they are operated infrequently and only for short durations.

2.3.7   Constraints

Despite the accomplishments in growing plants in space so far and the ongoing development of closed environment agriculture systems there are still some obstacles to overcome before greenhouses can be a vital part of LSS. There are technological challenges:

- the low TRL of mid to large sized greenhouse subsystems,
- the relatively high system mass,
- the relatively high power demand,
- the large pressurized volume required,
- system and component reliability.

There are biological and microbiological challenges among others in the areas of:

- monitoring of the microbial environment,
- food quality and safety monitoring,
- plant compositions for different mission scenarios and
- plant growth parameter definition.

Furthermore incorporating a space greenhouse into the overall life support system also results in a number of challenges, namely:

- the need for an effective overall LSS control,
- interactions between physical-chemical technologies, greenhouses and other biological technologies,
- the reliability of a hybrid LSS,
- the resilience of a hybrid LSS,
- the long-term system behavior of a hybrid LSS.

This thesis addresses the last five bullet points of this list.

2.4   Challenges of Hybrid Life Support Systems

Jones (2009) provides an extensive list of questions with respect to designing space life support systems, see Table 2-6. There are a number of design issues and questions a life support system engineer needs to answer during the development of a system architecture for a given mission scenario. The questions can be categorized in steady state design, dynamic design, expected external events, internal life support events and external off-nominal events.

All of the issues and questions listed in Table 2-6 are also greatly affected when other biological components besides the crew (e.g. plants, algae) are incorporated into the life support system architecture. This makes the design of hybrid life support systems more complex than designing a system purely consisting of physical-chemical technologies.

A number of design issues and questions specific to life support systems working with a space greenhouse have been identified which are not covered in the previous table.

Crop under- and overperformance

Greenhouse Modules are designed not only to keep plants alive, but especially to provide conditions for an optimal plant growth in a predefined range. However, unforeseen events (e.g. poor or old seeds, system malfunctions) can lead to an unanticipated development of plants, which can be a delayed or extended growth cycle, abnormal fruiting or diseases. Consequently the underperformance affects the desired greenhouse module production cycle, which should be avoided or at least reduced to a tolerable level. The same is true if crops perform better than anticipated, because plants act as resource consumers, producers and sinks. If the plants in the greenhouse perform much better than anticipated, this will have an effect on the matter balance and flows, which might not be desirable.

Table 2-6: Life support design issues and questions.

	Design questions according to Jones (2009)
Steady state design	Extent of waste processing and recycling
	Extent of ISRU
	Recycling system architecture
	Hydrated or dehydrated food
	Steady state material flow rates, margins
	Required recycling efficiencies
	Recycling processor technology selection
Dynamic design	Maximum material flow rates
	Storage buffer sizing
	System material flow controls
	Operations scheduling
	Maintenance scheduling
Expected external events	How does the system handle the mission scenario
	Start-up and shut-down
	EVA
	Resupply
	Crew changeover and overlap
	Power availability cycle
	Mars/Moon environmental conditions
Internal life support system failures	Processor failures
	Storage failures
	Failure to meet requirements
	Multiple life support failures
External off-nominal events	Depressurization
	Resupply delay
	Power failure
	Crew changeover delay
	Mission scenario failures, delays and changes
	Interface failures, off-nominal inputs
	Multiple external off-nominal events

Crop failure

An extreme case of crop underperformance, which should be avoided at any time, is a complete crop failure. Crop failures can have a high impact on the productivity of the greenhouse module, depending on the amount of plants included. A loss of a few lettuce plants might be

overcome by other food sources whereas the failure of batches of wheat or the whole plant community inside the GHM would destabilize the balance of the whole life support system.

Photoperiod schedule

Light energy is an essential element of plants' metabolism. Hence the illumination cycle in the plant compartments of the GHM directly governs photosynthesis. Typical illumination cycles of plants are 12 hours light followed by 12 hours dark (12/12), 16 h light 8 h dark (16/8) or constant light (24/0). When periods of natural sunlight are not sufficient to provide optimal lighting, electrical lighting should be considered. Even under optimal illumination conditions a variety of plants require periods without light for proper development and to avoid injuries (Velez-Ramirez *et al.*, 2011; Sysoeva *et al.*, 2010). During these dark periods plants do not consume CO_2, but exhale it leading to fluctuations of the partial pressure in the atmosphere.

Harvest events

After reaching the desired vegetable size or successful fruiting, the whole plant or plant parts are harvested. In case of fruit forming plants (e.g. tomato, pepper); harvest events only slightly affect the plant metabolism since the leaves, which are the photosynthetic parts of the plant, are still intact. However, in case of leafy vegetables and grain which are harvested as a whole (e.g. lettuce, wheat), photosynthesis ends with the harvest and new seedlings must be planted. Consequently, some harvest events lead to fluctuations in the production cycle of the greenhouse module. The impact depends on the amount of plants harvested at the same time. While lettuce can be harvested on demand and only in small portions causing only a small impact, wheat must be harvested in batches to alleviate the food processing and therefore causes a large impact, especially on the CO_2 intake and O_2 generation. Furthermore, batch harvesting burdens the waste recycling system with a high amount of inedible biomass.

Plant growth cycles

From seed to harvest, plants go through the development stages germination, juvenile vegetative phase, adult vegetative phase and generative phase (Schubert *et al.*, 2011). The germination phase takes place in a special climate controlled chamber with warm, high humidity conditions and only little or even without illumination. When the seed has developed its first cotyledons (germ layers) as well as first roots, ready to begin with the first photosynthesis processes, it is implanted in the primary grow area. During this juvenile vegetative phase the plant forms its first branches and leaves. Additionally, the root system is continuously evolving during this phase. Most of the plant growth takes place during the adult vegetative phase. Here the plant develops most of its branch and leaf system. During the generative phase the plant evolves one or more fruiting bodies.

From stage to stage and even during them, the plant's photosynthetic activity varies. Furthermore, each plant species has its own growth cycle with specific periods for the different stages. Greenhouse modules grow various crops in multiple development stages simultaneously to provide a continuously food provision for the crew. Consequently, the different growth cycles overlap each other leading to variations in the overall production cycle.

Greenhouse start-up phase

A special case of the aforementioned challenges occurring due to the plants' growth cycle is the start-up phase of the greenhouse module during which the subsystems are initiated and

the first crops are planted. The phase is finished, when the desired growth-harvest routines are established and the greenhouse module continuously delivers the desired outputs. Usually this state is reached after the first harvest of the plants with the longest period between seeding and harvesting.

Since no adult plants are present in the greenhouse at the beginning of the start-up phase, the CO_2 intake is negligible. At the time when more and more plants are planted and growing, the CO_2 demand increases and can be much higher than the daily CO_2 production by the crew. Technical solutions (e.g. stored CO_2, ISRU CO_2 generation) are required to compensate for the lack of carbon dioxide supply.

Influence on recycling systems

Plants are consumers, producers and sinks for resources. Although the primary purpose of a space greenhouse is food and oxygen production, plants also produce a number of byproducts that need to be recycled. Most of the water supplied to the plants is released as water vapor to the atmosphere through the plant's leaves. This transpiration water needs to be recovered from the atmosphere. Depending on the quality, the transpiration water might need additional post-processing to remove contaminants and to meet the water quality requirements. All plants produce inedible biomass (e.g. roots, leaves, stems). Although the ratio of edible to inedible biomass varies greatly between the crop species, one needs to consider recycling systems to recover material from the inedible biomass. Furthermore, plants also produce a number of VOCs that need to be filtered from the atmosphere.

How does a greenhouse affect the life support system?

All the aforementioned design issues and questions lead to the question stated above. Hybrid life support systems using a space greenhouse are complex dynamic systems, which are by nature hard to control. Various parameters, flows, buffers, tanks, delays and feedback loops affect each other.

The impact of the greenhouse on the life support system depends on various factors such as greenhouse volume, cultivation area, production schedule, crop species and many more. A greenhouse module providing a full vegetarian diet with around 36 different crops (Mitchell, 1994) would have a significant impact or might even dominate the behavior of the system. The crops would be in different development stages to assure a continuous food output. Furthermore, a significant amount of plant area would be occupied by batch planted crops like wheat and soybean to provide enough caloric energy and proteins to the crew. These crops are usually planted and harvested in batches to allow processing of large amounts which leads upon harvest to a significant impact on the system.

Short and long-term oscillations in the productivity can enforce each other and when not considered during the design phase, leading to instabilities in the finely adjusted balance of the hybrid life support system. A malfunction overlapping instabilities in the system's behavior could lead to mission critical events. The consequences can range from a slightly decreased oxygen level to perilous food and water deficits over long periods.

Nevertheless, some of the impacts can be reduced or even avoided with cultivation techniques such as timed planting/harvesting or coordinated staggered/batch planting. Crops can be planted time-delayed to avoid overlapping harvest events. The illumination cycles can be adjusted to each other to reduce the effects of dark respiration of CO_2. System maintenances

can also be scheduled in a way to avoid overlapping with other frequently occurring critical events. Another option is the possibility to slightly control plant development by regulating environmental conditions, which is a complex task in its own. However, plants are not man-made systems which continuously produce the same amount and can be switched on and off to react to different situations.

All of the abovementioned effects and interdependencies need to be investigated in order to guarantee the reliability, stability and resilience of a hybrid life support system. Test facilities that incorporate all the elements of hybrid life support systems are complex and very expensive. There have been attempts to build and operate such facilities in the past, as described in 2.3.6.2. Most of the facilities provided great insights into the behavior of closed habitats and corresponding life support systems and plant cultivation. However, they are all limited in some regard on which research objectives can be investigated with time being the strongest constraint.

An alternative way to investigate the dynamic behavior of a hybrid life support system under different nominal and off-nominal operational conditions is system modelling and simulation.

3 Modeling

3.1 Space Life Support Models

3.1.1 Guidelines for Modelling Space Life Support

A life support system model is usually a simplified mathematical representation of the real hardware setup. Models allow engineers and researchers to investigate life support architectures without the need to build and operate the actual system, which would be expensive and time consuming. Space life support systems can be modeled as spreadsheets using steady-state calculations or modeled dynamically to simulate changes within the system that occur over time. A dynamic model can simulate more realistically the actual behavior of the system. The need of dynamic modeling of space life support system was already identified several years ago by Babcock *et al.* (1984).

Jones (2009) has developed a number of questions and guidelines for developers of life support system models:

- What should be in a model?
- "Does the model include X?"
- What is the purpose of modeling?
- Should models be built up in layers?
- Failures are unanticipated because of incomplete models.
- A dynamic system modeling is needed.
- What elements should be included in a model of a space life support system?
- What questions should dynamic simulation of space life support answer?
- The standard design approach must be expanded with "What if?" modeling questions.

These guidelines should be used in order to determine whether the research questions one wants to investigate requires modeling and how the model should be set up.

Jones (2009) also suggests question-targeted models over all-inclusive models, which try to simulate all aspects of the life support system. Question-targeted models on the other hand are usually tailored to answer specific questions, which has a number of advantages such as reduced complexity, faster simulation times, etc.

3.1.2 Review of Past and Present Life Support Models

There have been numerous life support models in the past and some of them are still used and further developed today. Jones (2017) performed an extensive review of all modelling and simulation efforts for space life support systems with the early models dating back to the early 1980s. The complete list of life support modeling and simulation work is shown in Appendix A in Chapter 8. The ELISSA and V-HAB models are described more in detail in the following, because both models have been continuously developed in recent years.

ELISSA

The ELISSA (Environment for Life Support Systems Simulation and Analysis) software tool is a set of different models to simulate and analyze life support system architectures. The models have been developed at the Institute of Space Systems of the University of Stuttgart, Germany. Three separate and specialized models make up the software tool. PreLISSA is a

preliminary selection tool for physico-chemical life support systems. It is used to determine an optimized life support system architecture for a given mission scenario. PreLISSA uses a number of evaluation criteria (e.g. ESM, TRL) to compare different technological solutions. The so determined optimal life support system architecture is then implemented in the ELISSA model to perform dynamic simulations of the system. The simulations can be used to determine buffer and tank sizes and to calculate matter flows dynamically. ELISSA is primarily used to simulate physical-chemical life support systems, but it also contains a model for a photo-bioreactor. ELISSA comes with a programmed graphical user interface to allow students and other life support engineers the use of the model. The third model is called ReLISSA and focuses on reliability analysis of the life support system (Detrell and Belz, 2017; Detrell *et al.*, 2016; Detrell *et al.*, 2011). Drawbacks of the ELISSA software tool are the lack of a working greenhouse model and the relatively long simulation times of about 1 minute per simulation day (Do *et al.*, 2015).

V-HAB

The Virtual Habitat (V-HAB) model is developed at the Technical University of Munich. The work on V-HAB started with the development of a sophisticated human model for simulating space life support systems (Czupalla *et al.*, 2009) which was integrated into a dynamic simulation model (Czupalla, 2012; Czupalla *et al.*, 2011; Czupalla *et al.*, 2010). The human model represents whole body metabolic functions in mathematical terms. The human body is therefore broken down in different layers: the respiration layer, the metabolic layer, the water and electrolyte layer, the thermal layer and the cardiovascular layer. The model also includes a crew controller which allows for dynamic crew time characterization. The backbone of V-HAB is the closed environment module it connects the crew module to the physical-chemical module and the biological systems module (Czupalla, 2012).

V-HAB is programmed using the software MATLAB. While most life support models are using a top-down approach in modelling, V-HAB is developed with the bottom-up approach. V-HAB is being constantly improved. Olthoff *et al.* (2014) describes how the program code has been improved and how new solvers have been implemented. Furthermore, the biological module has been greatly improved by implementing an arthropod model, a rodent model, a microbiological filter system and several updates to the plant model. The module containing the models of physical-chemical technologies has been enhanced as well (Olthoff *et al.*, 2014; Czupalla *et al.*, 2015). Weber and Schnaitmann (2016) and Schnaitmann and Olthoff (2017) explain how the thermal layer of the crew model has been updated.

In recent years a number of simulations have been performed using V-HAB. Schnaitmann *et al.* (2015) used V-HAB to simulate air revitalization technologies developed by the Japanese Space Agency (JAXA). Pütz *et al.* (2016) and Pütz (2017) simulated the impact of the Advanced Closed Loop System (ACLS), which is developed in Europe, on the ISS environment and the life support systems already in place onboard the ISS.

In recent years a number of additional functions have been added to V-HAB. Olthoff *et al.* (2015) describe updates to the thermal simulations of V-HAB in general and additions that allow for thermal simulations during EVAs. Another addition to V-HAB is the Virtual Spacesuit (V-SUIT). This model allows the simulation of portable life support systems like those incorporated into spacesuits. Göser and Olthoff (2014), Cusick *et al.* (2016), Gierszewski and Olthoff (2016) and Olthoff (2017) describe the development and functionality of V-SUIT.

The simulation times of V-HAB are reported to be around one week simulation time for a 90 day mission (Do *et al.*, 2015).

3.1.3 Implications for this Dissertation

In this subchapter the guidelines for life support modeling described in Chapter 3.1.1 are used to define the model requirements for the thesis objectives mentioned in Chapter 1.2.

What should be in a model?

The research objectives of this thesis require a question-targeted model in order to simulate the behavior of a hybrid life support system. An all-inclusive model would probably be too complex to simulate the very specific questions mentioned in the objectives.

"Does the model include X?"

According to Jones (2009), this question can also be formulated as *"What effects does X have on the question being answered?"*. Only X important to answering the model's research questions should be implemented in the model to avoid overly complex model architectures.

What is the purpose of modeling?

In general modeling is used to improve understanding and to gather knowledge about a specific problem or scenario. The research questions defined for this thesis cannot be answered by experimentation, because currently no adequate test facility exists. Therefore a life support model is the logical solution to investigate the behavior of a hybrid life support system.

Should models be built up in layers?

Layers in this case mean a hierarchical system of piece parts, components, assemblies, subsystems, systems and supersystems. Jones (2009) argues to only include those layers in the model that are required to answer the defined research questions. The implications for the hybrid life support systems model are that systems such as the physical-chemical systems can be modeled on the system level. The greenhouse model on the other hand requires modeling on a lower hierarchical level in order to adequately simulate crop development. Although not every single plant needs to be simulated, but rather assemblies of a certain number of plants or a certain cultivation area. The crew model does not need to simulate every metabolic process of the involved humans, but only the inputs and outputs depending on the level of activity.

Failures are unanticipated because of incomplete models.

Modeling system failures is necessary to understand the life support system behavior also under off-nominal conditions. Some of the research questions defined for this thesis are already targeted at exactly the issue of system failures and their effects. Consequently the model used for the investigation of the thesis' research objectives needs to be able to implement failures of all relevant model parts.

Dynamic system modeling is needed.

Since hybrid life support systems have even more components with dynamic characteristics (e.g. biological systems), dynamic modeling is definitely required to answer the research questions defined for this thesis.

What elements should be included in a model of a space life support system?

The model to investigate the research objectives of this thesis needs at least the following components:

- A crew model.
- A greenhouse model including models for different crops.
- Models of physical-chemical systems.
- A habitat model to simulate the atmosphere conditions for the crew.
- Interfaces between all model parts to simulate exchange of matter and information.

What questions should dynamic simulation of space life support answer?

There are many questions that dynamic simulation of space life support can answer with appropriate modeling. The research questions for this thesis are defined in Chapter 1.2.

The standard design approach must be expanded with "What if?" modeling questions.

The dynamic behavior of a hybrid life support system is mostly unknown. Its components form intricate networks of feedback loops and interdependencies which can result in unexpected emergent behavior. Therefore the model of used in this thesis should be able to simulate a wide range of "What if?" questions without the need of big changes to the model itself. The more "What if?" questions the model can answer, the better gets the understanding of the system behavior.

Remark on simulation times

Every model requires a certain time to execute the mathematical formulas involved in the simulation. Although this aspect is not mentioned by Jones (2009), it has large implications on the investigations that can be performed. A model that requires long simulation times is rather impracticable to simulate a wide range of different simulation cases. Especially sensitivity analyses where a simulation is repeated multiple times with different starting conditions require fast simulation times in order to produce data in an adequate timespan. Do *et al.* (2015) have done an assessment of simulation times of different life support models. Depending on the model setup and strategy the simulation times range from 10 seconds to 1 week for a 90 day mission. The investigation of the research questions defined for this thesis should be in the range of 1 minute simulation time for 100 mission days in order to perform all the envisioned simulations and analyses.

Summary

The hybrid life support system model required to perform the simulation necessary to answer the research questions of this thesis should be a dynamic model. The model should include at least a crew model (system level), a greenhouse model (assembly level), models of physical-chemical technologies (system level) and a habitat including interfaces to connect the different model parts (system level). The model has to be capable of simulating a wide range of nominal and off-nominal conditions in order to understand the behavior of the hybrid life support system. The simulation time should be in the order of 1 minute per 100 mission days to investigate a wide range of simulation cases.

The review of past and present life support models described in Chapter 3.1.2 revealed that there is currently no model that meets all of the mentioned requirements. As a consequence

a new model has been developed for this thesis to investigate the research objectives defined in Chapter 1.2.

3.2 The System Dynamics Approach

3.2.1 Definition

System Dynamics can be understood by defining system as:

> *'A set of elements or parts that is coherently organized and interconnected in a pattern or structure that produces a characteristic set of behaviors, often classified as its function or purpose.'*

<div align="right">(Meadows and Wright, 2008, p. 188)</div>

and dynamics as:

> *'The behavior over time of a system or any of its components.'*

<div align="right">(Meadows and Wright, 2008, p. 187)</div>

However, these definitions are abstract and more pragmatic definitions exist.

Ford (2010, p. 7) defines System Dynamics as:

> *'a methodology for studying and managing complex systems that change over time. The method uses computer modeling to focus our attention on the information feedback loops that give rise to dynamic behavior.'*

He also quotes another popular definition by Coyle (1977, p. 2):

> *'System dynamics is a method of analyzing problems in which time is an important factor, and which involves the study of how a system can be defended against, or made to benefit from, the shocks which fall upon it from the outside world.'*

3.2.2 History

The origin of System Dynamics lays in the early works of Jay Forrester in the 1960s at the Massachusetts Institute of Technology. He suggested utilizing methods from feedback control theory to investigate industrial systems (Forrester, 1961). Later the same ideas were applied to the periodic population growths and declines of large cities in the United States (Forrester, 1969). He described a city as a system of industries, housing and people interacting with each other. The study was intended to help city planners in making the right decisions.

Some years later in 1972 the System Dynamics approach became popular when the Club of Rome, a non-profit think tank consisting of internationally renowned characters from diplomacy, science and economics, published the report 'The Limits to Growth' (Meadows, 1972). The study investigated the consequences of the raising growth in human population and industrial production. The results were broadly discussed all over the world, because they showed a worldwide collapse of the industrial system and the environment around the year 2100. The world would not sustain unlimited growth of population and industry forever. By altering parameters within the System Dynamic model the study authors found out, that stability in economic and ecology is feasible. However, the impact of a certain change or decision greatly depends on the moment they are made.
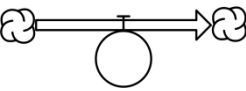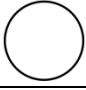
Since 'The Limits to Growth', System Dynamics is used in more and more research fields. Typical applications are the classical System Dynamics fields of economics, urban dynamics and models of the development of the world (Ruth and Hannon, 2012). In recent years System Dynamics is also used in investigating climate change (Robinson, 2001) and other environmental systems (Deaton and Winebrake, 1999). Modeling of biological systems (Hannon and Ruth, 1997) and health sciences (Hargrove, 1998) is possible. Studying the behavior of ecosystems by utilizing System Dynamics is also feasible and can lead to surprising insights. Typical ecosystem models are predator-prey models (e.g. the overshoot of the Kaibab deer population) (Ford, 2010), Conway's Game of Life and Daisyworld (Hannon and Ruth, 1997).

3.2.3 Building Blocks

System Dynamics models are built with only five components: stocks, flows, sources/sinks, converters and interrelationships. By combining these components in different ways, various system behaviors can be modelled. Table 3-1 gives a short description of each component and the symbols used in the software tool Stella Professional.

A **stock** is the place of a system where something you can see, feel, count or measure at any given time are accumulated. This accumulation can represent physical material, but also information. Examples for a stock are water in a tank, money in a bank account or the amount of knowledge about a given situation (Meadows and Wright, 2008).

Table 3-1: The five building blocks of System Dynamics models (Deaton and Winebrake, 1999).

Name	Short Description	Stella Symbol
Stock or reservoir	A component of a system where something is accumulated. The contents of the reservoir may go up or down over time.	The *stock*
Flow or process	Activity that determines the values of reservoirs over time.	The *flow*
Source and sink*	Display flows across the boundary of the system (open system).	The *sink/source*
Converter	System quantity that dictates the rates at which the process operate and the reservoir change.	The *converter*
Connector	Defines the cause-effect relationships between system elements.	The *connector*

* Explained according to (Ford, 2010).

Flows are the tools to change the amount of material or information contained in stocks. They can be inflows, filling the stocks or outflows, depleting stocks over time. Typical flows are births and deaths, purchases and sales, growth and decay (Meadows and Wright, 2008).
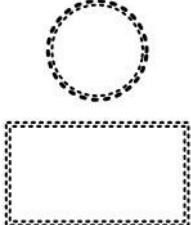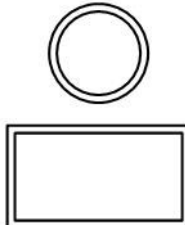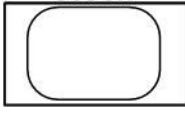
Sources and sinks show flows across the boundary of the system. Whenever there is a source or sink in the model the system is called an open system. Models of closed systems on the contrary do not contain any sources or sinks (Ford, 2010).
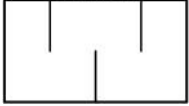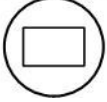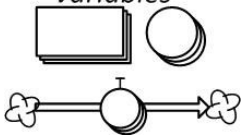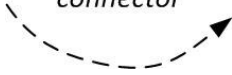
Converters are used to direct the flows and stocks through defining limits, demands and other parameters. They influence the rates at which flows run and stocks change.

Interrelationships connect the different blocks of the model with each other. While flows always have to be connected to stocks, interrelationships can be used to connect converters with stocks and flows. Connectors can also display interrelationships between stocks and flows.

In addition to the basic buildings blocks, the software tool Stella Professional (used for this dissertation) offers a number of advanced buildings blocks. Those are implemented to ease the construction of models. The advanced building blocks combine a certain combination of basic buildings and mathematical functions. They can be then directly integrated into to the model, making it easier to construct and clearly arranged models.

Table 3-2: Advanced building blocks provided by Stella Professional.

Name	Related Basic Build Block	Short Description**	Stella Symbol
Module	n.a.	Used to separate parts of the overall model. Modules can be computed independently from the overall model.	The *module*
Module input	Converter, stock	Receives input from another module. Indicated by a double-thick gray border. Input building block name includes the origin module name followed by a dot.	Module inputs
Module output	Converter, stock	Provides output to another module. Indicated by a double-line border.	Module outputs
Conveyor stock	Stock	A conveyor stock is similar to moving sidewalk or a conveyor belt. Material gets on the conveyor, rides for a period of time, and then gets off.	The *conveyor stock*
Oven stock	Stock	An oven stock is similar to a processor of discrete batches of stuff. The oven opens its doors, fills (either to capacity or until it is time to close the door), bakes its contents for a time (as defined by its outflow logic), and then unloads them in an instant.	The *oven stock*

Name	Related Basic Build Block	Short Description**	Stella Symbol
Queue stock	Stock	A queue stock is similar to a normal queue, a line of items awaiting entry into some process or activity.	The *queue stock*
Delay converter	Converter, stock	This converter can change over time in response to changes in input. Because it has properties of a stock, it is possible for Delay Converters to be involved in feedback loops in which no explicit Stock exists.	The *delay converter*
Summing converter	Converter	This converter adds together values for a set of model variables, without the need to draw connectors from inputs to the converter.	The *summing converter*
Arrayed variables	Converter, stock, flow	Arrays are used to combine parallel calculations (e.g. the calculation of different plant compartments) in one building block, which increases visibility of the model.	*Arrayed variables*
Information connector	Connector	Information connectors carry information that is used to arrive at decisions.	The *information connector*

** Description in Stella Professional documentation (http://iseesystems.com/resources/help/v1-1/)

3.2.4 Dynamic Patterns in System Dynamics

Combinations of a few basic building blocks can be used to represent typical behavioral patterns, as presented in Chapters 3.2.4 to 3.2.6. Linear and exponential growth or decay, logistic growth, overshoot and oscillations are part of nearly every model. Recognizing those blocks leads to a faster and better understanding of the overall system behavior.

Linear growth or decay represents a constant change of a stock over time. Figure 3-1 shows a typical graph of linear growth or decay. The formula for linear behavior is:

$$\frac{dR(t)}{dt} = k. \qquad (3\text{-}1)$$

Where R(t) represents the stock at a given time t and k the rate of change. The value k is independent of the number of inflows and outflows. However, k is the difference between the sum of all inflows and the sum of all outflows:

$$k = (sum\ of\ all\ inflows) - (sum\ of\ all\ outflows). \qquad (3\text{-}2)$$

When k > 0 the stock experiences a linear growth, while k = 0 means that the stock does not change at all. Linear decay appears when k < 0. Figure 3-2 shows a typical stock and flow

diagram of a simple System Dynamics model with linear behavior (Deaton and Winebrake, 1999).
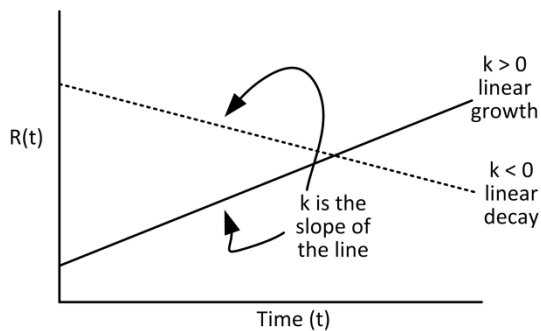
Figure 3-1: Linear growth or decay (Deaton and Winebrake, 1999).
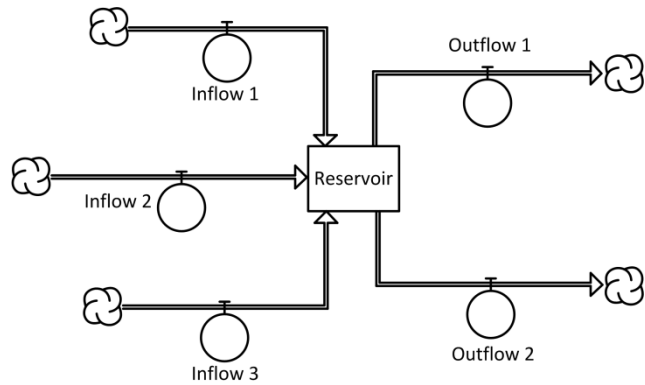
Figure 3-2: Generic system diagram for linear growth or decay (Deaton and Winebrake, 1999).

Exponential growth or decay occurs more often in natural systems than linear behavior. When the rate of change of a stock depends on the stock itself, exponential behavior is the result. Figure 3-3 displays the related graphs. Exponential growth or decay is described by the formula:

$$\frac{dR(t)}{dt} = k * R(t).$$ (3-3)

The constant k is calculated with the formula:

$$k = inflow\ rate - outflow\ rate.$$ (3-4)

The larger |k| is, the more rapid is the growth or decay and vice versa. A generic model for exponential growth or decay is shown in Figure 3-4. Hereby exponential behavior occurs on each side, inflow and outflow, of the stock (Deaton and Winebrake, 1999).
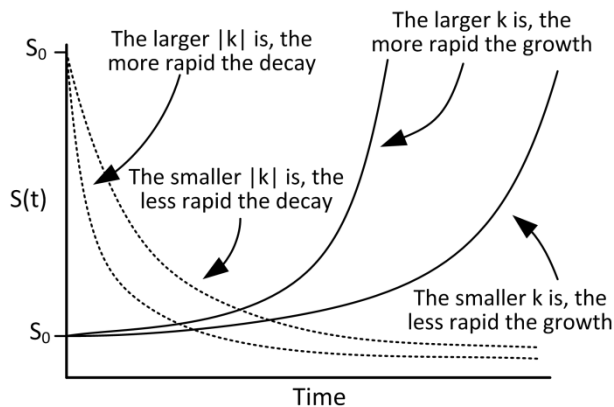
Figure 3-3: Exponential growth or decay (Deaton and Winebrake, 1999).
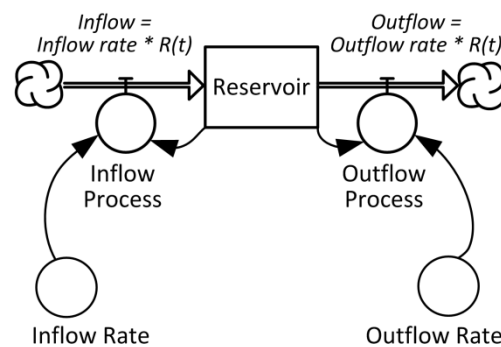
Figure 3-4: Generic system diagram for exponential growth or decay (Deaton and Winebrake, 1999).

Logistic growth, also known as S-shaped growth or S-curve occurs when a system with exponential growth is constrained at a certain level. Figure 3-5 shows a logistic S-curve. First the stock grows exponentially, but when approaching the maximum level the growth slows down until the steady state is reached. When comparing the system diagram of logistic growth, Figure 3-6, with the one of exponential growth, Figure 3-4, one can notice the similarity on the inflow side and the difference on the outflow side. The formula for s-shaped growth;

$$\frac{dR(t)}{dt} = k(t) * R(t), \tag{3-5}$$

is more complicated than the one of exponential behavior, since k is time dependent. The formula for k(t) is:

$$k(t) = unconstrained\ growth\ rate * \left\{1 - \frac{R(t)}{carrying\ capacity}\right\}. \tag{3-6}$$

The carrying capacity is the value of R(t) at which the system is in its steady state. The initial rate of change of the system is defined as the unconstrained growth rate. The system will approach its steady state faster with a larger unconstrained growth rate (Deaton and Winebrake, 1999).
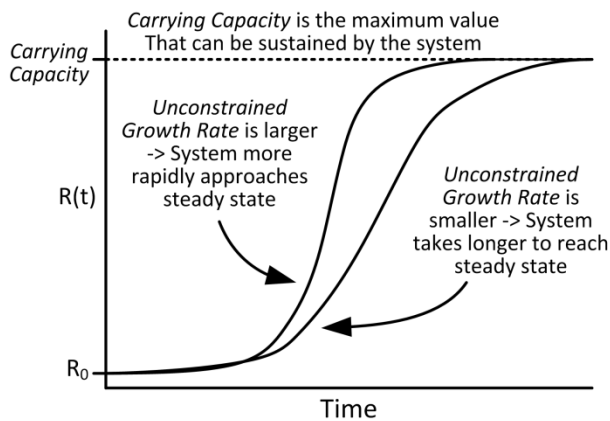
Figure 3-5: Logistic growth (Deaton and Winebrake, 1999).
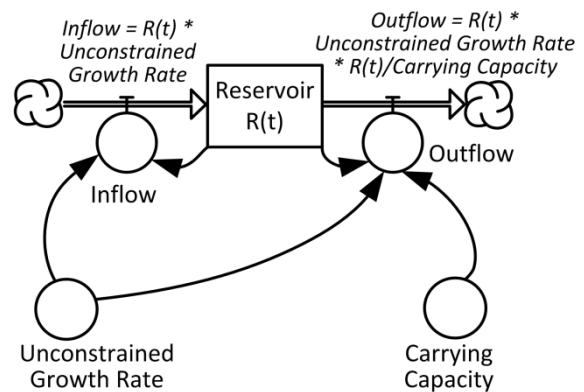
Figure 3-6: Generic system diagram for logistic growth (Deaton and Winebrake, 1999).

Overshoot and collapse is a typical behavior of systems containing a non-renewable resource and a population consuming the resource. Figure 3-7 shows the graphs for an overshoot of a population, followed by a collapse. As long as resources are available the population will grow exponentially, consuming more and more resources. At a point where the resources are too low to sustain the population any longer, the population exponentially decays. Resources and population decline until both reach a steady state. This kind of system collapse can be often observed in malfunctioning ecosystems. The system incorporates two interconnected stocks, leading to the stock and flow diagram in Figure 3-8.

The formula for calculating the population stock is:

$$\frac{dP(t)}{dt} = \left\{per\ capita\ birth\ rate - \left[1 - \frac{R(t)}{R_0}\right]\right\} * P(t). \tag{3-7}$$

R_0 represents the initial value of the resource stock and the per capita birth rate is the rate at which the population grows per unit of time. R(t) is the value of the resource stock at a given time and is calculated with the formula:

$$\frac{dR(t)}{dt} = -per\ capita\ consumption\ rate * P(t). \tag{3-8}$$

Where the per capita consumption rate represents the rate at which the resource are consumed per unit of time. When looking on the two formulas, one notices that they are coupled. The change of the population P(t) is a function of the resource R(t) and vice versa (Deaton and Winebrake, 1999).
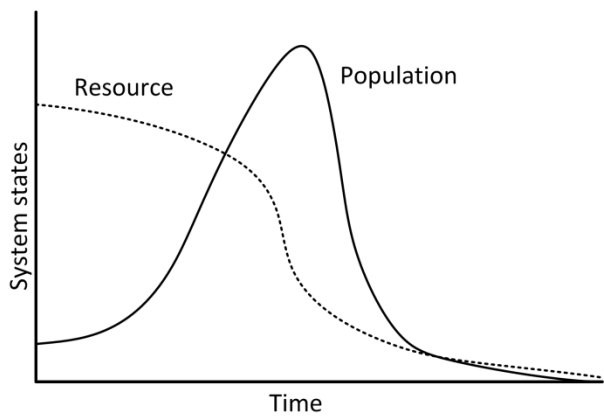
Figure 3-7: Overshoot and collapse (Deaton and Winebrake, 1999).
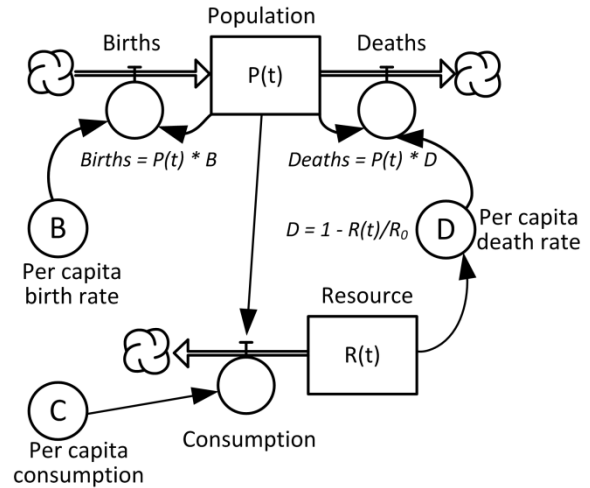
Figure 3-8: Generic system diagram for overshoot and collapse (Deaton and Winebrake, 1999).

Oscillations are another dynamic pattern observed in systems. Such systems contain at least two interconnected stocks, a consumer (or predator) and a resource (or prey). Both stocks have an equilibrium around which their values oscillate, see Figure 3-9. The more the value of one stock (e.g. prey) is away from its equilibrium the larger is the impact of the other stock (e.g. predator) pulling the prey stock towards the equilibrium. The value of the prey stock does not approach the equilibrium, but generates an overshoot it in the opposite direction and is then pulled back again. A system diagram for a simple oscillating system is shown in Figure 3-10.

The value of the consumer stock C(t) is calculated with the formula:

$$\frac{dC(t)}{dt} = consumer\ growth\ rate * R(t) - consumer\ deaths. \qquad (3\text{-}9)$$

The formula for the resource stock R(t) is:

$$\frac{dR(t)}{dt} = resource\ growth - resource\ consumption\ rate * C(t). \qquad (3\text{-}10)$$

Both stocks are again coupled to each, influencing the behavior of each other. The consumer stock C(t) is a function of the resource stock R(t) and vice versa (Deaton and Winebrake, 1999).
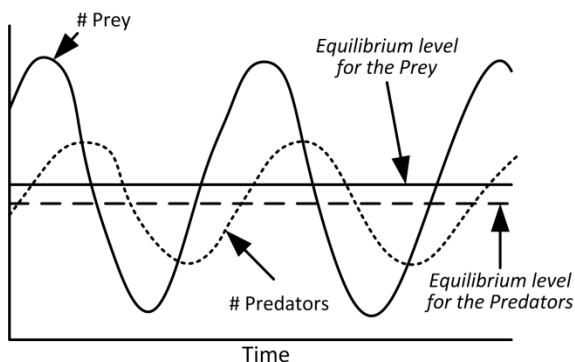
Figure 3-9: Oscillations (Deaton and Winebrake, 1999).
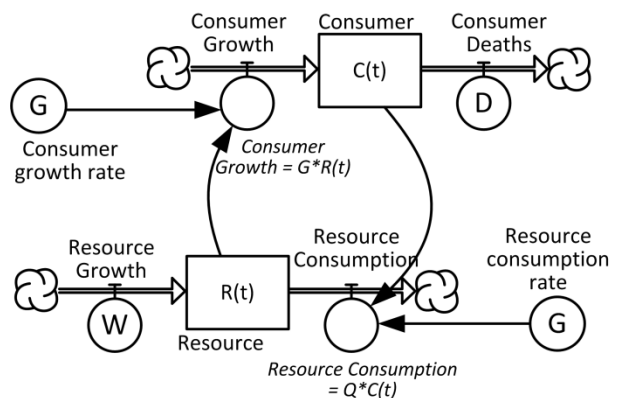
Figure 3-10: Generic system diagram for oscillations (Deaton and Winebrake, 1999).

3.2.5 Feedback in System Dynamics Models

Feedback loops are part of a broad variety of dynamic systems. A system contains a feedback loop when one part of the system affects another part, which in turn influences the first one. These closed-loop circles of cause and effect are the origin of common system performance such as reinforcing and counteracting feedback. Both types are very common in nature, but also in manmade systems such as economy (Deaton and Winebrake, 1999).

Reinforcing feedback, also known as positive feedback or runaway loop, exists when a change of a condition within the feedback loop amplifies or reinforces itself over time. A common example is an interest-bearing bank account as most people in the industrial world possess (see Figure 3-11 and Figure 3-12). The interest added depends on the money in the bank account and the interest rate. The interest earned is added to the money in the bank account. Assuming, that no money is removed from the account, interest added after the next interval is higher than the original one. The interest added per interval is always higher than that of the previous interval (Deaton and Winebrake, 1999).
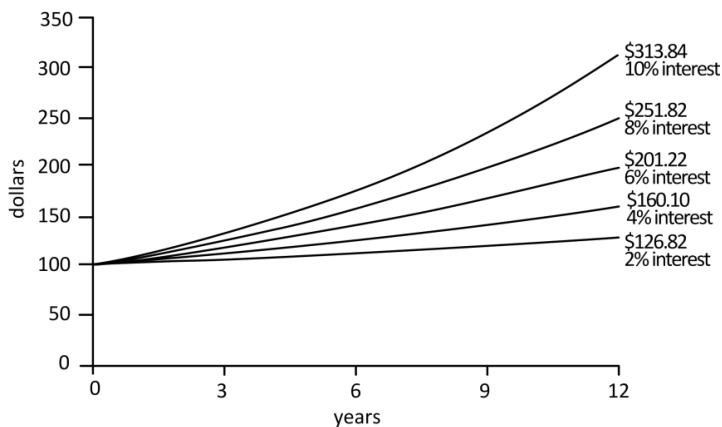
Figure 3-11: Growth in savings with various interest rates (Meadows and Wright, 2008).
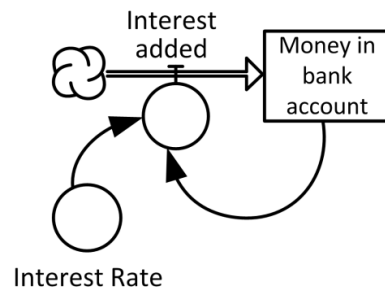
Figure 3-12: Interest-bearing bank account (Meadows and Wright, 2008).

Reinforcing feedback is often underestimated in its effect on a system. A simple example helps to better understand the effects. Ford (2010) calls the example the "rule of 70" which estimates the doubling time (the time after which the initial stock is doubled) for a given growth using the formula:

$$growth\,rate\,(\%/year) * doubling\,time\,(years) \sim 70. \qquad (3\text{-}11)$$

The formula results in a doubling time of 20 years for a growth rate of 3.5 % per year, 10 years for a growth rate of 7 % per year and so forth.

Counteracting feedback, also known as negative or balancing feedback, exists when a change of a condition within the feedback loop counteracts or dampens itself over time. The cooling and heating of a cup of coffee in a room with a certain temperature is a common example (see Figure 3-13 and Figure 3-14). The cooling/heating depends on the discrepancy between the coffee temperature and the room temperature. The larger the discrepancy, the larger is the change of the coffee temperature in a certain time interval. The coffee temperature will eventually approach the room temperature. However, the cooling/heating will slow down over time.
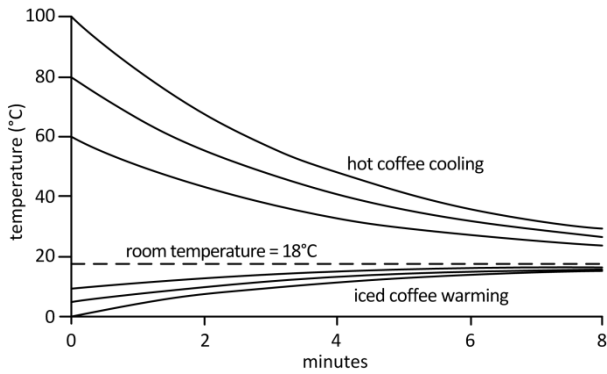
Figure 3-13: Coffee temperature as it approaches a room temperature of 18°C (Meadows and Wright, 2008).
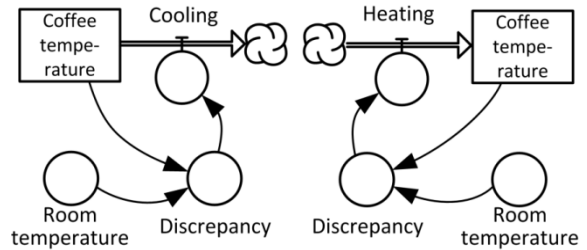
Figure 3-14: A cup of coffee cooling (left) and warming (right) (Meadows and Wright, 2008).

The previously shown examples for feedback loops are similar to the ones shown for the exponential behavior in Chapter 3.2.4. That is a result of the simple examples chosen for the explanation. Feedback loops in larger models are usually more complex and often hard to identify, because they consists of a larger number of interdepending elements.

3.2.6 Perturbations in System Dynamics Models

A system will eventually be perturbed from the outside at one point, either by purpose or accidentally. System Dynamics allows the simulation of certain perturbations and the investigations of their effects on the system. Therefore the elements of a system can be perturbed with pulse, step and ramp functions.

Pulse functions, see Figure 3-15, are usually used to introduce a short period change of a flow or converter at a certain time point during the simulation. The perturbation can occur solely or multiple times during a simulation. The system reacts on the perturbation depending on the system architecture and the strength of the pulse. Resilient systems will eventually return to a steady state over time, while non-resilient systems will most likely collapse (Deaton and Winebrake, 1999).
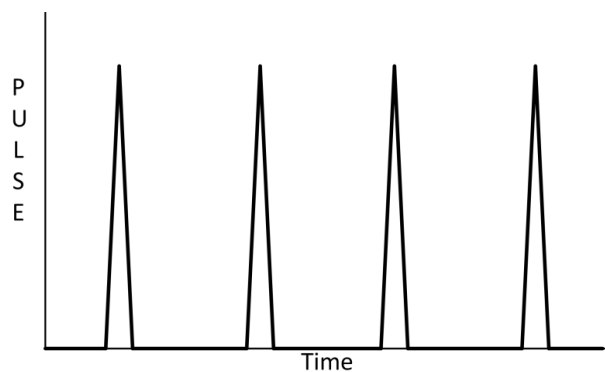
Figure 3-15: Graph of a multiple pulse perturbations (Deaton and Winebrake, 1999).

Step functions, see Figure 3-16, change the value of a flow or converter at a defined time by a certain degree. While a pulse perturbation introduces a one-time change, a step perturbation creates a permanent change in one the system element. The system reacts on the perturbation depending on the system architecture and the height of the step. Since the step perturbation introduces a permanent change, the system will eventually show different be-

havior than before. For example the system might find a new steady-state or it will show un-expected behavior, which might lead to a system collapse (Deaton and Winebrake, 1999).
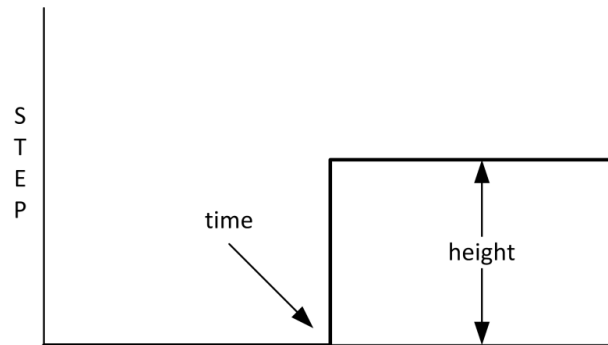
Figure 3-16: Graph of a step perturbation (Deaton and Winebrake, 1999).

Ramp functions introduce a permanent increase or decrease of a flow or converter over time, see Figure 3-17. Again, the system reacts on the perturbation depending on the system architecture and on the slope of the ramp. The introduced change is not constant, but itself changing over time, which makes the resulting system behavior hard to predict (Deaton and Winebrake, 1999).
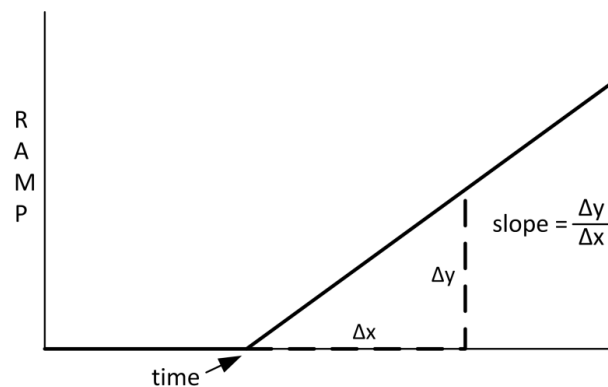
Figure 3-17: Graph of a ramp perturbation (Deaton and Winebrake, 1999).

3.2.7 System Dynamics Software

Ford (2010) has done an extensive review of different software tools to develop System Dynamics models. A comparison is made between the widely used spreadsheets with special System Dynamics software (Dynamo, Stella, Vensim, Powersim and Simile), with multipurpose modeling software (Simulink, GoldSim) and with individual-based modeling. Based on this analysis and extensive testing of different software packages, the model described in the following chapters was developed using the program Stella Professional.

3.3   Overview of the Model

The model described in the following chapters is organized in modules and sub modules. The root model contains the six main modules of the model, namely:

- Crew model,
- Physical-chemical systems,
- Greenhouse model,
- Gases layer,

- Liquids layer and
- Solids layer.

All modules are connected to other modules as shown in Figure 3-18. One should note that the arrows shown in Figure 3-18 not always represent matter flows, as described earlier these arrows are used to indicate interaction between model components. The interaction can be an exchange of actual matter (e.g. water) but also an exchange of information (e.g. number of crew member).

The crew model module, the physical-chemical systems module and the greenhouse model module represent actual components of a life support system. The three layer modules are managing the interaction between the other modules and represent the habitat. Each layer module is only simulating matter in the same aggregation state, e.g. the gases layer module calculates the mass flows of all gases like oxygen and carbon dioxide.

The three layer approach was pursued in order to improve the graphical representation of the model. Furthermore, the separate module approach allows for simulating only parts of the model by only running selected modules. Another approach would have been with a single core module which would contain all formulas now represented in the three layers.
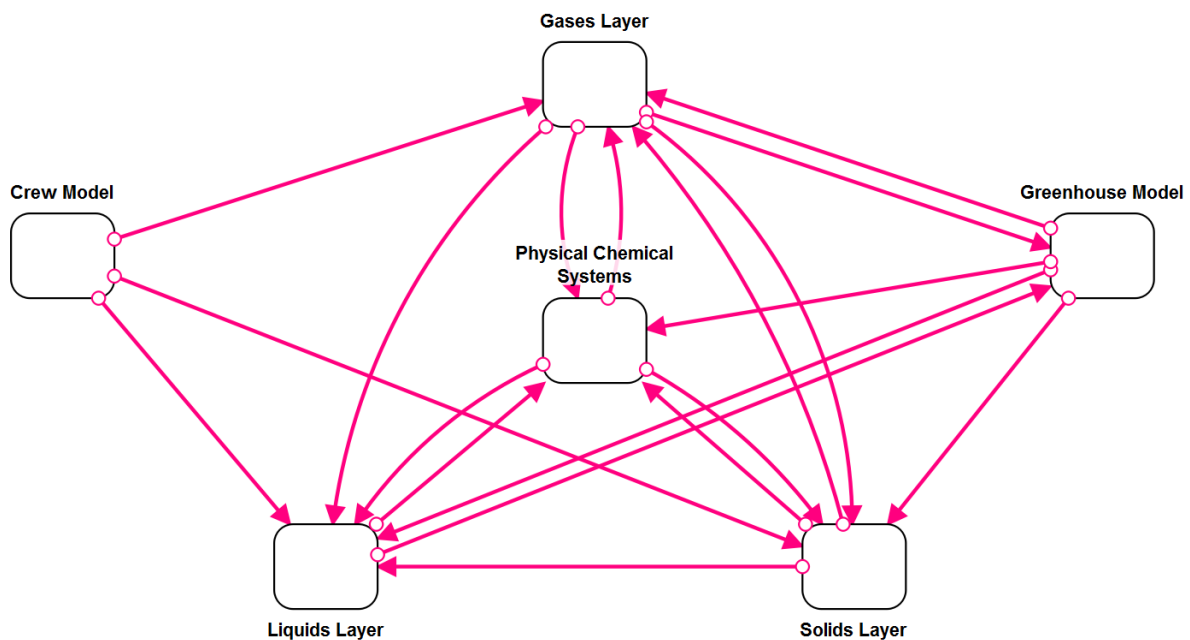
Figure 3-18: Root model layout in Stella.

Each of the six main modules in the root model has a number of different submodules respectively subparts which are all described in detail in the following chapters. Figure 3-19 outlines the structure of the following subchapters.
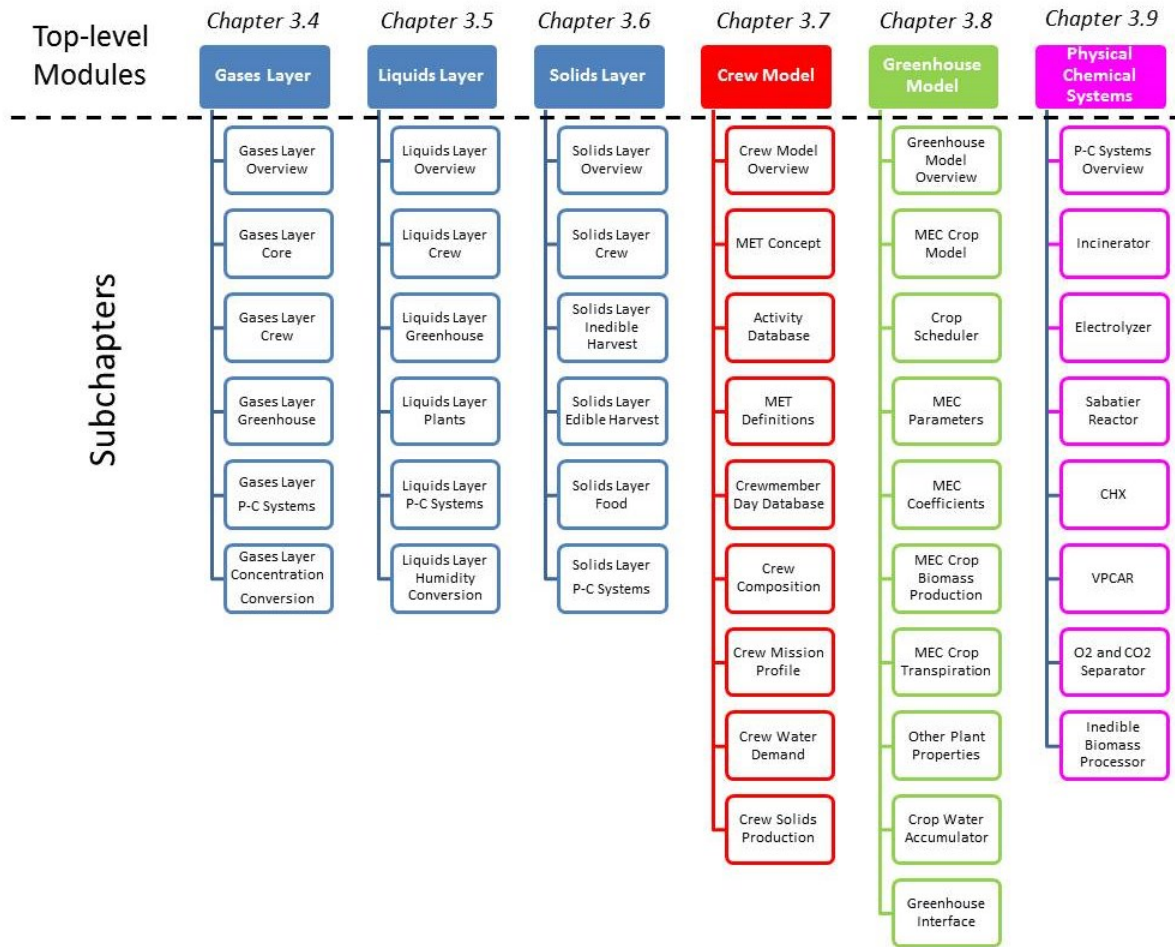
Figure 3-19: Module hierarchy within the Stella model and the chapter number of the description in this thesis.

3.4 Gases Layer

3.4.1 Gases Layer - Overview

The gases layer module calculates the gas flows of the life support system mainly oxygen and carbon dioxide, but also hydrogen, methane and carbon monoxide. Each of the gases has its own stocks and flows which are calculated and controlled by inputs from the other modules of the root model.

The gases layer module is divided into six frames with the core of the layer in the middle (black frame), see Figure 3-20. The interfaces to the crew model are on the left side (orange frame), the interfaces to the greenhouse model on the right side (green frame) and the interfaces to the physical-chemical systems in top mid and bottom (purple frames). The bottommost frame is used to convert the concentration of oxygen and carbon dioxide, which are in kilograms for the mass flow calculations in and around the core module, into percent for oxygen and parts per million for carbon dioxide. All frames are described in detail in the following subchapters.
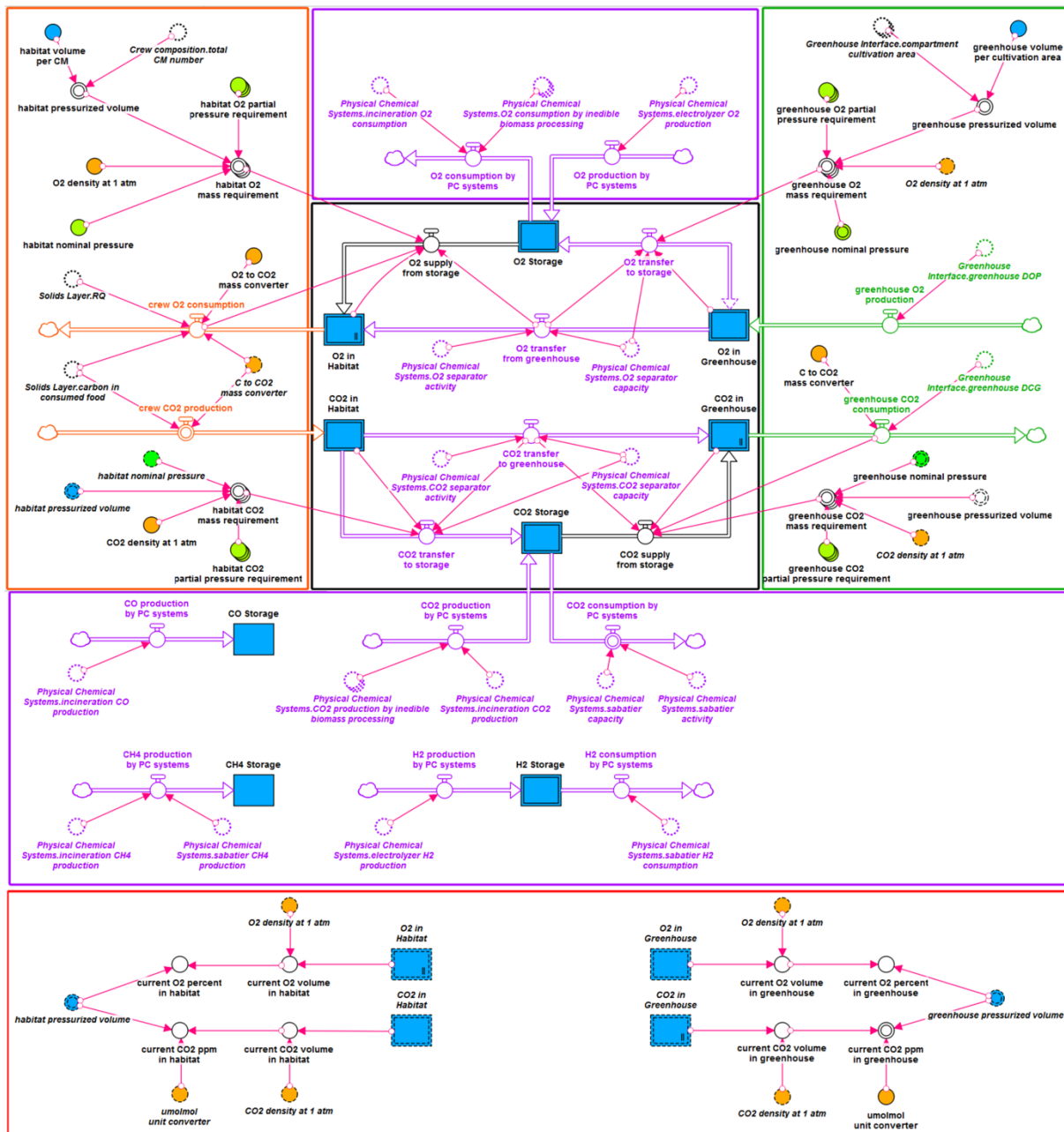
Figure 3-20: Overview of the gases layer module. Frames indicate different parts of the module. Black frame: Core; Orange frame: Crew; Green frame: Greenhouse; Purple frames: Physical-chemical systems; Red frame: Atmospheric composition conversions.

3.4.2 Gases Layer - Core

The core frame of the gases layer module contains the stocks for the two most important gases, oxygen and carbon dioxide. For each of the two gases there are three stocks which are connected to each other in a loop, as shown in Figure 3-21. The oxygen and the carbon dioxide loops have the same setup but in reverse directions. Oxygen flows from the production inside the greenhouse to the consumers inside the habitat, whereas the carbon dioxide flows from the production inside the habitat to the consumers inside the greenhouse. As a simplification it is assumed that oxygen is only produced in the greenhouse and only consumed inside the habitat. A similar simplification was made for carbon dioxide, which is only produced inside the habitat and consumed inside the greenhouse. Although in a real space

habitat setup there will be oxygen consumption and carbon dioxide production inside the greenhouse when humans are present.

Both parts of the frame consist of three stocks. One stock represents the partial pressure of the gas in the habitat atmosphere and another stock the partial pressure of the gas in the greenhouse atmosphere. The third stock represents storage for the gas. This stock acts as a buffer between the habitat and the greenhouse to dampen the effects of uneven production and consumption and also acts as the interface to the physical-chemical life support systems. The inputs from the crew model are applied to the habitat side of the core frame and the greenhouse inputs to the greenhouse side of the core frame.

The primary flow is always between the habitat and the greenhouse or vice versa. The flows to and from the storage stocks are only active if certain thresholds e.g. too low oxygen in the habitat despite oxygen supply by the greenhouse are met. The oxygen transfer from the greenhouse to either the habitat or to the storage is controlled by the activity of an oxygen separator, which is implemented in the physical-chemical systems module. A carbon dioxide separator is performing the same task for the carbon dioxide produced inside the habitat.

The balance between the three stocks is defined by control parameters such as the minimum, nominal and maximum concentrations of the gases inside the habitat and the greenhouse. These control parameters are implemented in the crew and greenhouse frames.

All formulas of the gases layer core frame are shown in Appendix 9.1.1.
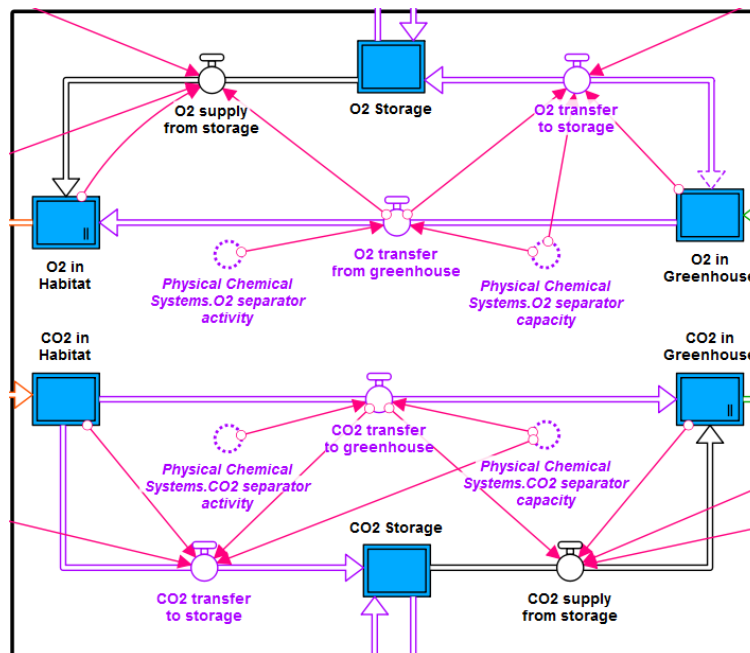
Figure 3-21: The gases layer core frame.

3.4.3 Gases Layer - Crew

The crew frame of the gases layer module manages the input from the model and converts the unit of the inputs where necessary. This frame also contains the oxygen and carbon dioxide partial pressure requirements for the habitat, see top and bottom part of the frame in Figure 3-22. The partial pressure requirements are based on Anderson *et al.* (2015). The corresponding converters in the frame are arrays containing the minimum, nominal and maximum value of the oxygen and carbon dioxide partial pressure in the habitat. The partial pressure

values are given in kilopascal and need to be converted to kilograms of gas contained in the pressurized volume of the habitat.

The middle part of the frame handles the oxygen consumption by the crew. This value is calculated within the crew model. For further information see chapter 3.7. The carbon dioxide production by the crew depends on the oxygen consumption and the respiratory quotient (RQ), which is the ratio between oxygen inhaled and carbon dioxide exhaled. The respiratory quotient depends on the ratio of fats, carbohydrates and proteins in the consumed food. Consequently the RQ is calculated in the Solids Layer of the model, which handles all solid mass flows including food (see chapter 3.6). The two flows crew O2 consumption and crew CO2 production are connected to the habitat stocks of the Core frame, which calculate the amount of oxygen respectively carbon dioxide inside the habitat atmosphere.

All formulas of the gases layer crew frame are shown in Appendix 9.1.2.
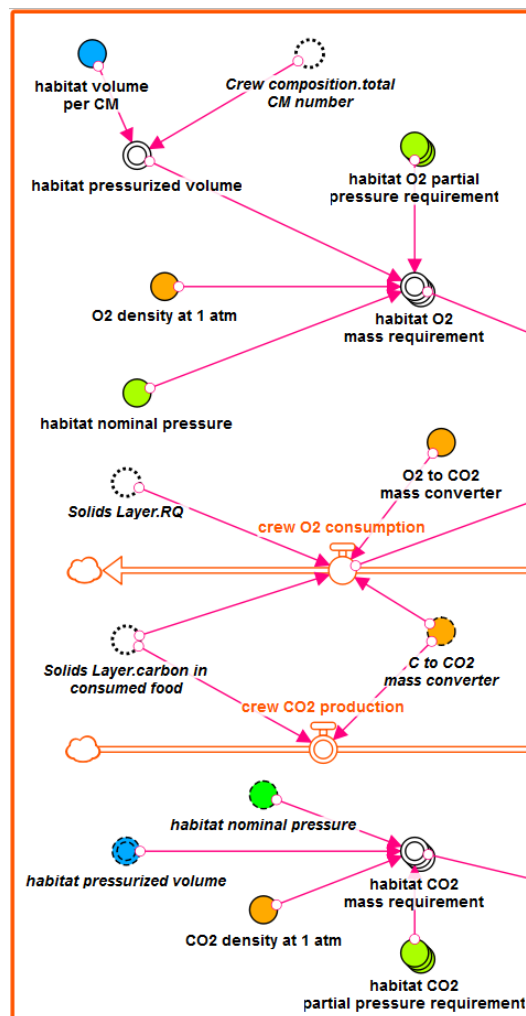
Figure 3-22: The gases layer crew frame.

3.4.4 Gases Layer - Greenhouse

The greenhouse frame of the gases layer module looks very similar to the crew frame, because it performs the same set of calculations (see Figure 3-23). However, the inputs for the greenhouse frame are the oxygen production and the carbon dioxide consumption by the plants. The greenhouse frame contains the partial pressure requirements for oxygen and

carbon dioxide in the greenhouse atmosphere. The oxygen requirements are based on Anderson *et al.* (2015). The carbon dioxide requirements on the other hand are based on the needs of the plants and should be set to the desired set point for plant cultivation. The two converters for the partial pressure requirements are arrays containing a value for the minimum, nominal and maximum partial pressure of the respective gas.

There are two inputs provided by the Greenhouse model, the daily oxygen production (DOP) and the daily carbon gain (DCG). While the DOP value can be directly used to define the greenhouse O2 production flow, the DCG value needs to be converted. The DCG input by the Greenhouse model is the mass of carbon bound per day. The carbon for plant growth is mainly provided by the consumed carbon dioxide. Consequently, the DCG value can be converted to the greenhouse CO2 consumption value by the mass ratio of carbon in carbon dioxide.

All formulas of the gases layer greenhouse frame are shown in Appendix 9.1.3.
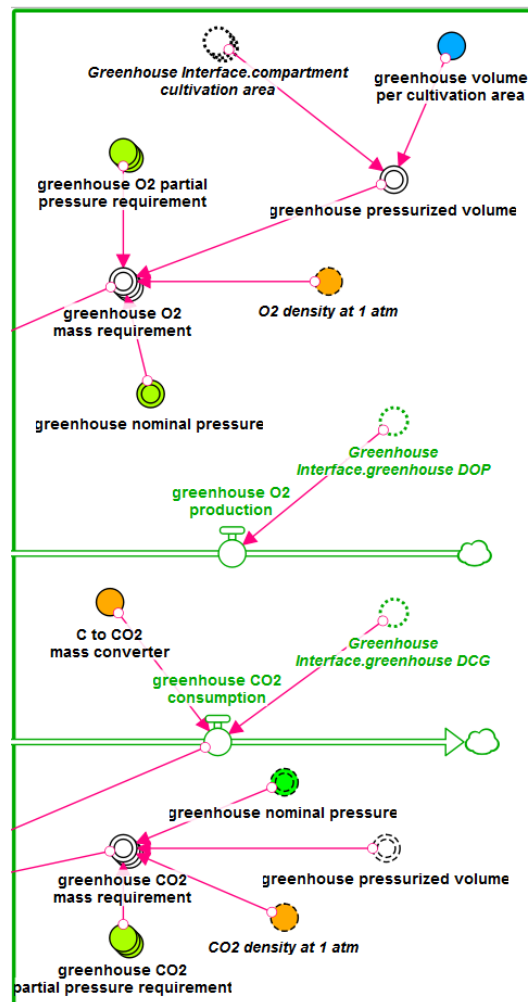
Figure 3-23: The gases layer greenhouse frame.

3.4.5 Gases Layer - Physical-Chemical Systems

There are two physical-chemical systems frames in the gases layer module. The top frame, see Figure 3-24, handles the oxygen interface to the physical-chemical systems module. The bottom frame, see Figure 3-25, handles all other gas interfaces (carbon dioxide, hydrogen, carbon monoxide, methane) to the physical-chemical systems module.

The oxygen interface in the top frame consists of an inflow and an outflow of the oxygen storage stock in the core frame of the gases layer module. The inflow is the sum of oxygen produced by the electrolyzer. The outflow is defined by the oxygen consumption of the incinerator and the inedible biomass processor.
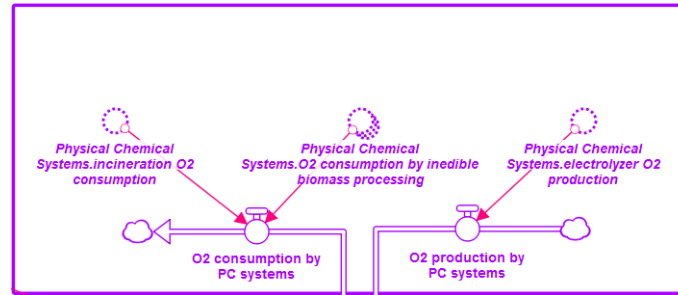
Figure 3-24: The gases layer physical-chemical systems top frame.

The bottom frame contains a carbon dioxide interface which is made of an inflow and an outflow to the carbon dioxide storage stock of the core frame of the gases Layer module. The carbon dioxide production of the physical-chemical systems module is the sum of the carbon dioxide production of the incinerator and the inedible biomass processor. The carbon dioxide consumption is defined by the activity and capacity of the Sabatier reactor.

Furthermore the bottom frame manages the secondary gases which are produced and consumed by the physical-chemical life support systems. Carbon monoxide is a by-product of the incineration process and is stored in its own stock. Hydrogen is produced by the electrolyzer, then stored and consumed by the Sabatier reactor when active. The methane which is also a by-product of the incineration process, but is also produced by the Sabatier reactor, is stored in its own stock as well.

There is the theoretical possibility to burn methane with oxygen to recover water and carbon dioxide if necessary. A fuel cell would allow to combine the hydrogen with oxygen to water. However, both mechanisms are not yet implemented in the model. The implemented life support system architecture does not require those functions, because it is assumed that the amount of produced hydrogen and methane is rather small.

All formulas of the gases layer physical-chemical systems frame are shown in Appendix 9.1.4.
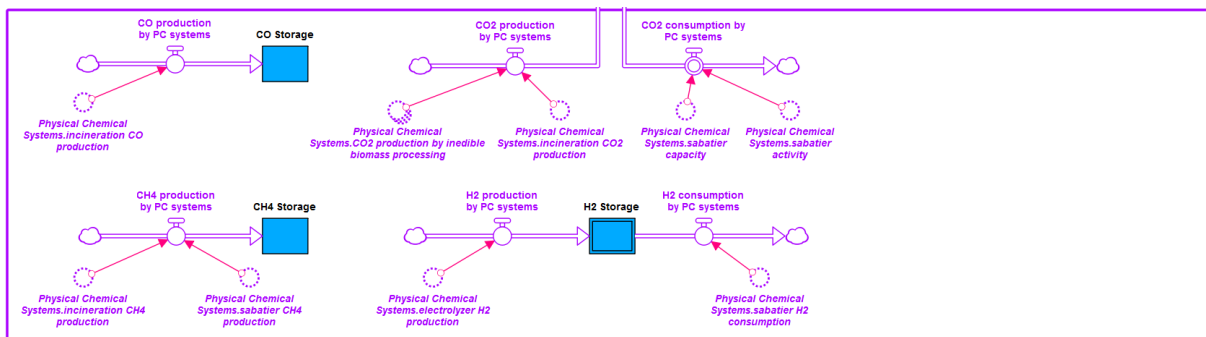
Figure 3-25: The gases layer physical-chemical systems bottom frame.

3.4.6 Gases Layer - Atmospheric Composition Conversions

The stocks and flows of the different gases implemented in the gases layer module are based on kilograms respectively kilograms per day. While using kilograms and kilograms per day is perfect for matter flows, this unit is inadequate to check whether the concentration in the atmosphere is within the desired ranges. Consequently, the stocks O2 in Habitat, O2 in Greenhouse, CO2 in Habitat and CO2 in Greenhouse need to be converted to more adequate units. The requirements for oxygen in spacecraft are usually given in percent and the values of carbon dioxide in parts per million. The Atmospheric composition conversions frame is doing exactly that. The values of the mentioned stocks are converted using the set-up shown in Figure 3-26. Other inputs are the density of oxygen and carbon dioxide at one atmosphere pressure and the pressurized volume of the habitat and the greenhouse.

All formulas of the gases layer atmospheric composition conversion frame are shown in Appendix 9.1.5.
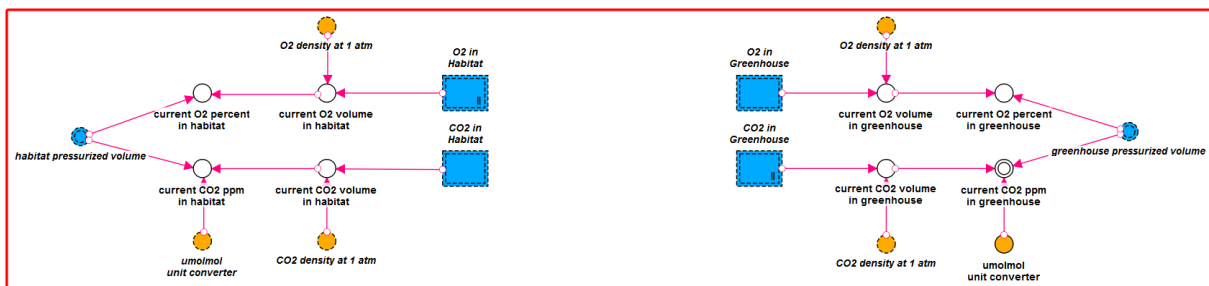
Figure 3-26: The gases layer atmospheric composition conversions frame.

3.5   Liquids Layer

3.5.1 Liquids Layer - Overview

The Liquids Layer module manages all water reservoirs and flows of the life support system. This includes the potable water, the wastewater and the water bound in the crew and the living plants. The water present as humidity in the habitat and greenhouse atmosphere is also calculated by this module.

The liquids layer module is divided into six frames see Figure 3-27. The blue frame is the crew frame and calculates the water balance of the astronauts, the potable water storage and the water in the habitat atmosphere. The potable water storage of the greenhouse and the water in the greenhouse atmosphere are managed by the green frame. The water bound in living plants is calculated by the red frame. The two purple frames contain the interfaces to the physical-chemical life support systems. The water in the habitat atmosphere and in the greenhouse atmosphere is calculated in kilograms. The relative humidity requirements are given as percentage. The orange frame converts kilograms to percent of relative humidity based on the habitat and greenhouse volumes. All frames are described in detail in the following subchapters.
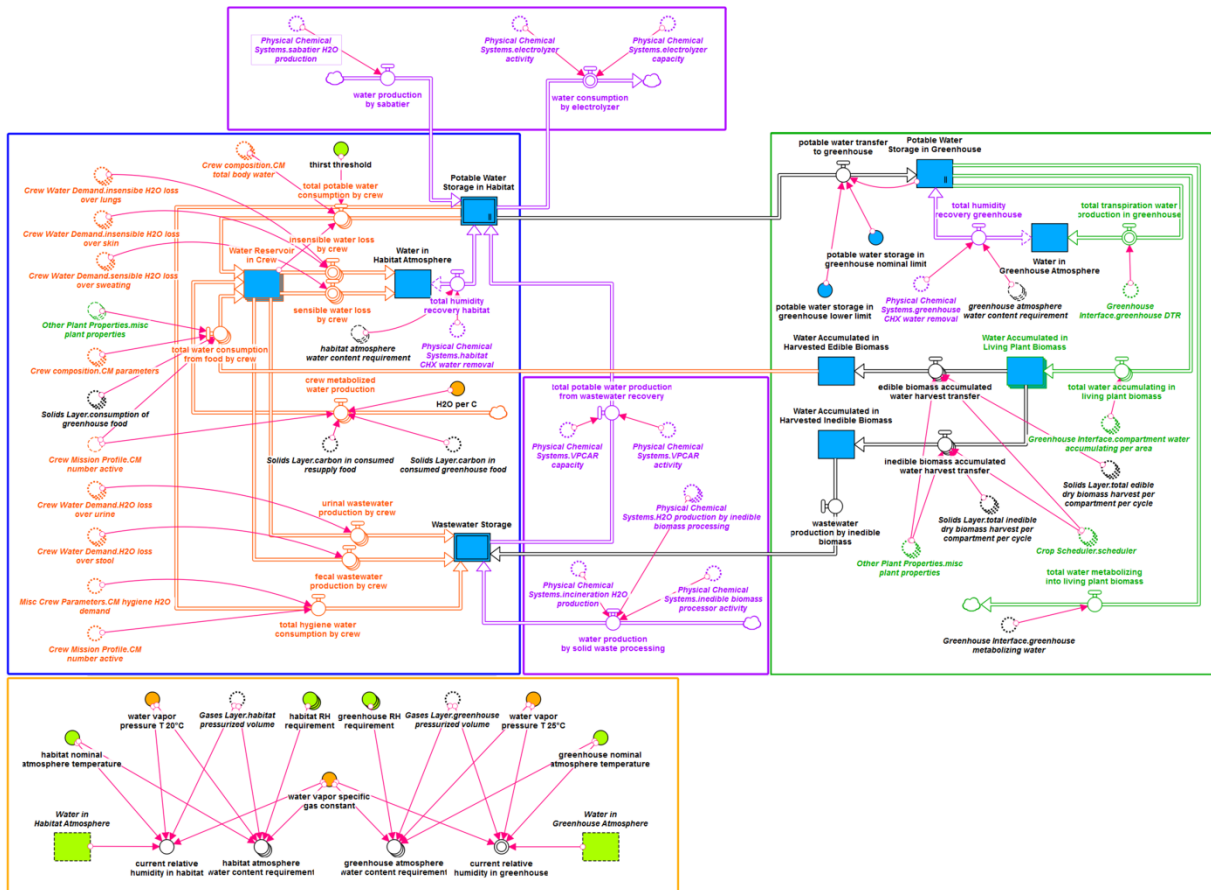
Figure 3-27: Overview of the liquids layer module. Frames indicate different parts of the module. Blue frame: Crew; Green frame: Greenhouse; Purple frames: Physical-chemical systems; Orange frame: Humidity conversion.

3.5.2 Liquids Layer - Crew

The liquids layer crew frame's main function is the calculation of the water balance of the crew. Furthermore this frame contains the potable water storage of the habitat, the water in the habitat atmosphere and the wastewater storage stock.

The human body loses water and these water losses need to be compensated by fluid intake in order to guarantee health and work efficiency of the crew. The human water balance implemented in the model is shown in Figure 3-28. Five ways are generally considered how the human body loses water: Insensible water loss via the lungs and via the skin, sensible water loss via sweating, fecal water loss and urinal water loss. The amount of water lost through the different pathways depends strongly on the environmental conditions and the physical activity of the person. In a comfortable environment with normal physical activity, urine causes the largest water loss whereas losses via sweat are almost negligible. The water losses need to be compensated through fluid intake, the water contained in food and the metabolic water production.

Figure 3-29 shows how the human water balance is implemented in the model. The inputs for the different stocks and flows are mainly calculated in the crew model, see Chapter 3.7. The insensible and sensible water loss to the habitat atmosphere is recovered by a condensing heat exchange (CHX) system, see Chapter 3.9.5. Besides the metabolic related water flows, the crew also requires hygiene water which is transferred from the potable water stor-

age stock to the wastewater storage stock depending on the amount that is required per crew member per day.

All formulas of the liquids layer crew frame are shown in Appendix 9.2.1.
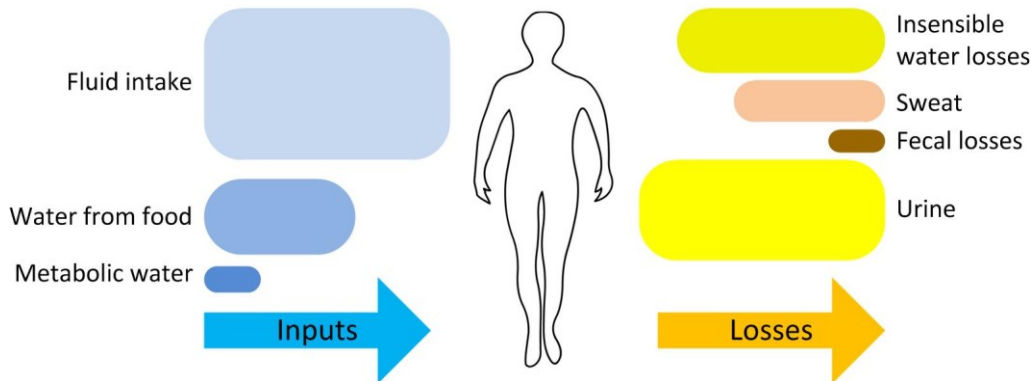
Figure 3-28: Human water balance in a comfortable environment with nominal physical activity. Ratio of block sizes is roughly to scale.
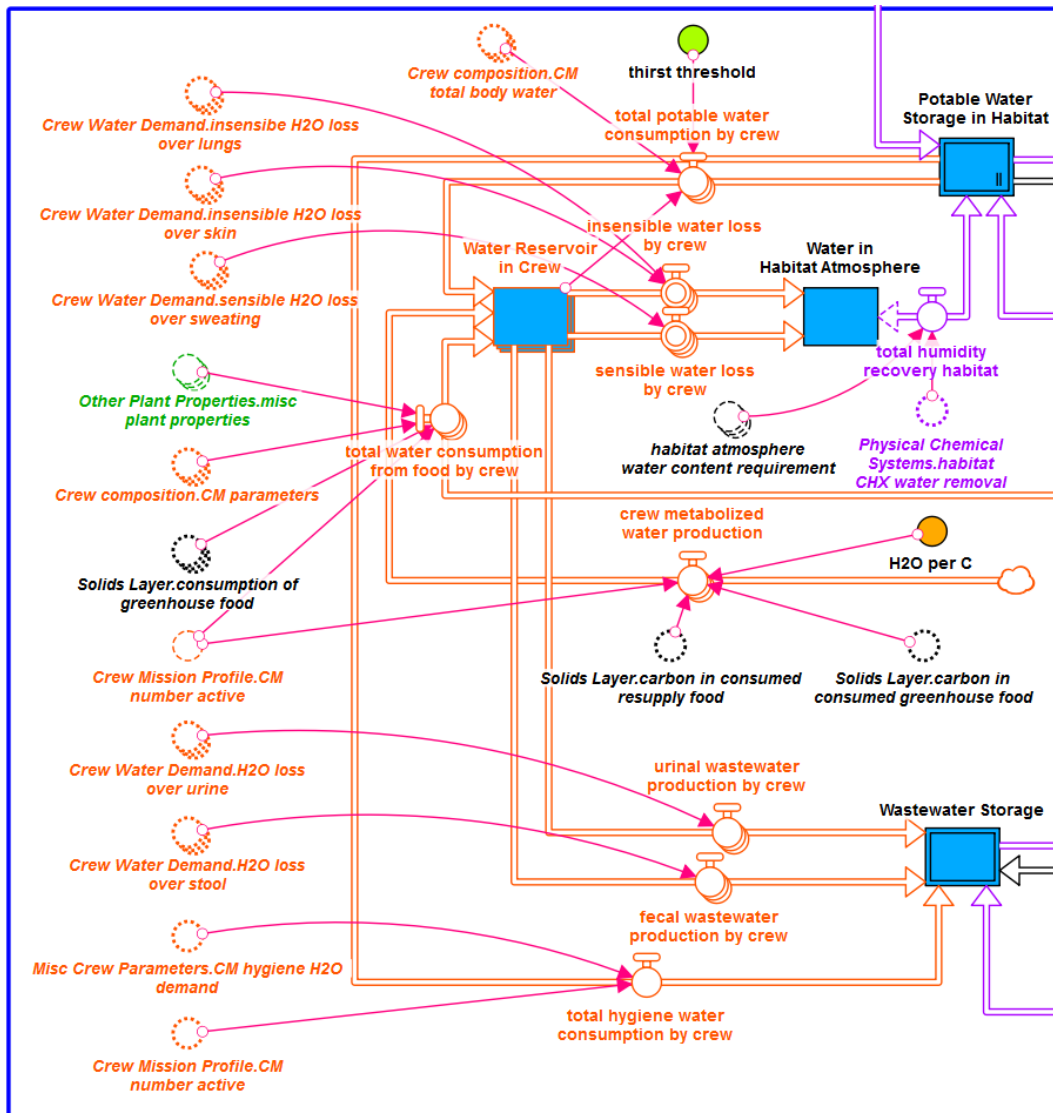
Figure 3-29: The liquids layer crew frame.

3.5.3 Liquids Layer - Greenhouse

The liquids layer greenhouse frame calculates the potable water storage in the greenhouse, the water present in the greenhouse atmosphere and the water flows related to plant cultivation, see Figure 3-31. The potable water storage inside the greenhouse is filled from the potable water storage inside the habitat when certain thresholds are met. The water uptake by the plants is the sum of the three green outflows of the potable water storage in greenhouse stock in Figure 3-31. A large amount of the plant's water uptake is transpired over the leaves and increases the water in the greenhouse atmosphere. Plants also bind water in their biomass. Depending on the crop species the water bound in the biomass can be up to 90 % of the fresh weight. Some water is also metabolized in plant material by photosynthesis. Figure 3-30 shows the plant water balance implemented in this model.

While the transpiration water can be recovered relative fast, the water bound in the biomass is only available after harvesting. The metabolized water is recovered through human metabolic processes as described in Chapter 3.5.2 or through incineration. The ratio between the three flows depends on the crop species and several other factors. For example the ratio of transpiration to accumulating to metabolizing water is roughly 11:1:0.08 for dry bean plants.
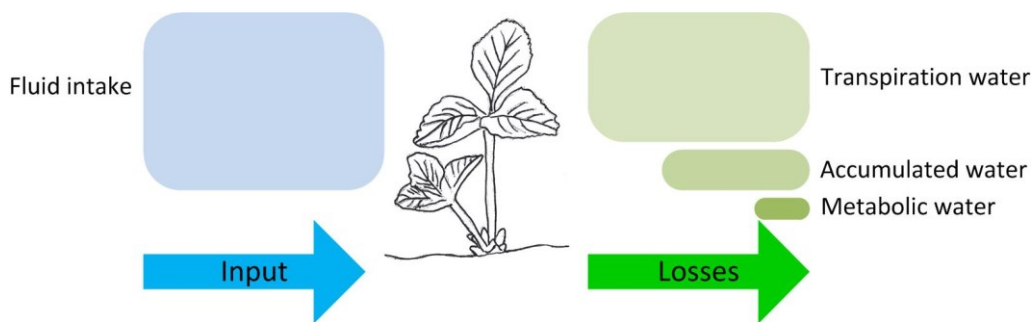
Figure 3-30: Plant water balance. Ratio of block sizes is roughly to scale.

The transpiration water is recovered through a condensing heat exchanger (CHX) (see Chapter 3.9.5) and fed back to the potable water storage of the greenhouse. The water bound in the living plant biomass is transferred upon harvest. Hereby the different water content of edible and inedible biomass is taken into account.

All formulas of the liquids layer greenhouse frame are shown in Appendix 9.2.2.
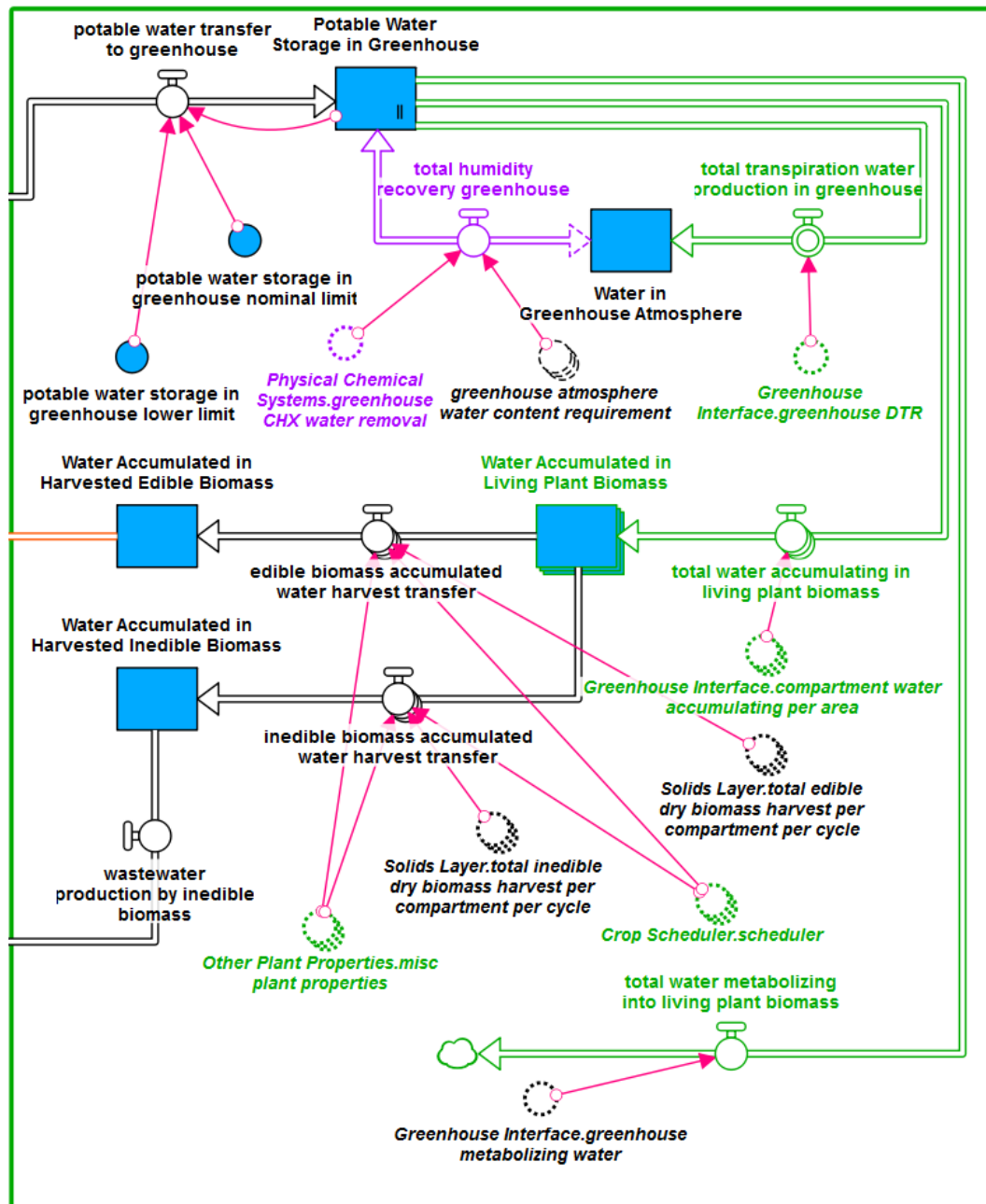
Figure 3-31: The liquids layer greenhouse frame.

3.5.4 Liquids Layer - Physical-Chemical Systems

Similar to the other two layer modules, the liquids layer module has interfaces to the physical- chemical technologies. These interfaces are contained in two frames. The top frame in the liquids layer module is shown in Figure 3-32. This frame manages the interaction with the potable water storage of the habitat. The water produced by the Sabatier reactor and the water consumed by the electrolyzer are calculated in this frame. The inflow and outflow are connected to the potable water storage stock in the crew frame.
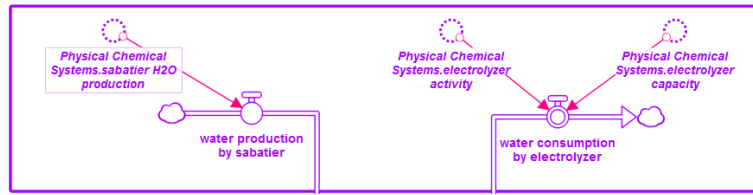
Figure 3-32: The liquids layer top physical-chemical systems frame.

The bottom physical-chemical systems frame of the liquids layer module, see Figure 3-33, contains the wastewater recycling flow and the interface to the water produced by the solid waste processing. The wastewater recycling is performed by a VPCAR (see Chapter 3.9.6) into potable water. The water produced by the incinerator and the inedible biomass processor is directed into the wastewater storage in the crew frame as it may still contain volatiles from the incineration process which can be filtered by the water recycling system.

All formulas of the liquids layer physical-chemical systems frame are shown in Appendix 9.2.3.
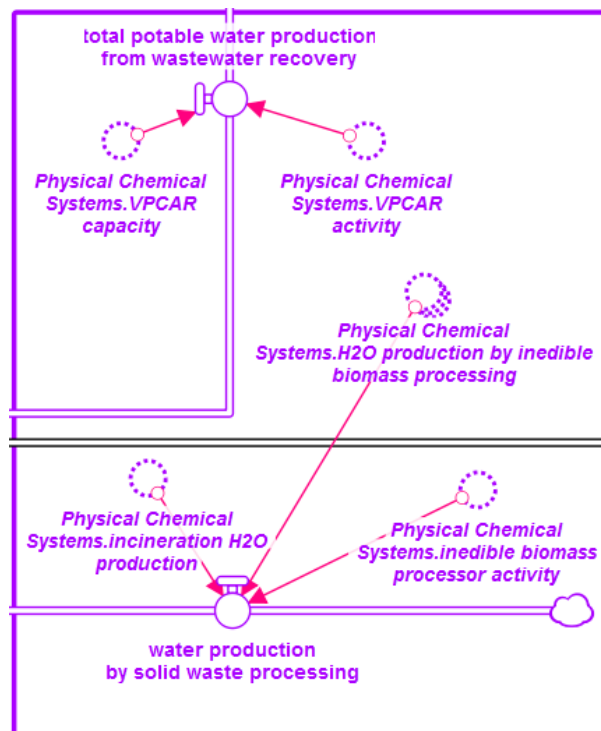
Figure 3-33: The liquids layer bottom physical-chemical systems frame.

3.5.5 Liquids Layer - Humidity Conversions

The humidity conversions frame, see Figure 3-34, converts the absolute water content contained in the habitat atmosphere and in the greenhouse atmosphere from kilograms to a relative humidity in percent and vice versa.

All formulas of the liquids layer humidity conversion frame are shown in Appendix 9.2.4.
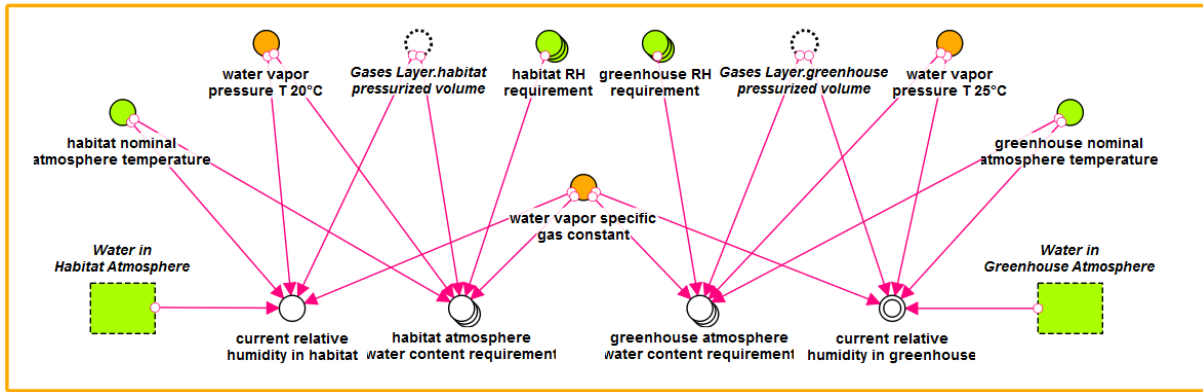
Figure 3-34: The liquids layer humidity conversions frame.

3.6 Solids Layer

3.6.1 Solids Layer - Overview

The solids layer module simulates the solid mass flows of the life support system. This module receives inputs from the crew model, the greenhouse model and the physical-chemical systems module. Outputs are provided to the gases layer, liquids layer and physical-chemical systems module.
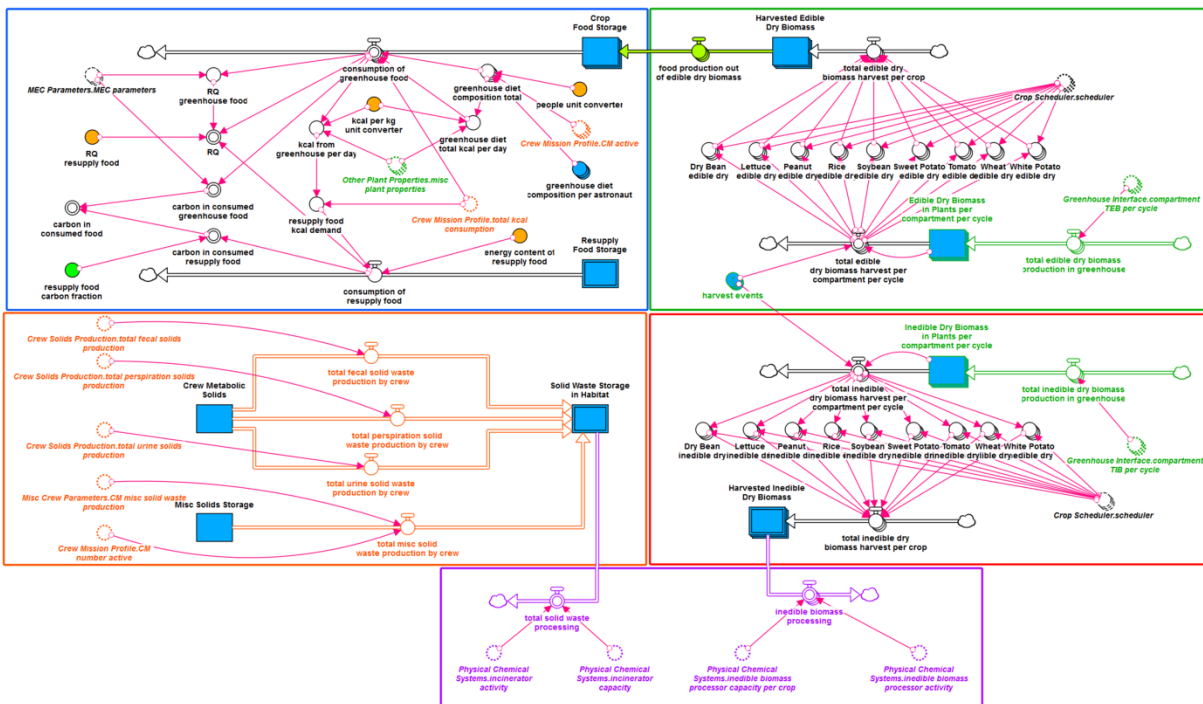
Figure 3-35: Overview of the Solids Layer module. Frames indicate different parts of the module. Blue frame: Crew food; Orange frame: Crew waste; Green frame: Edible biomass harvest; Red frame: Inedible biomass harvest; Purple frame: Physical-chemical systems.

The module is divided into five frames to distinguish the flows of the different material flows calculated in this module, see Figure 3-35. The blue frame in the top left corner deals with the crew food. The green frame with the edible biomass produced in the greenhouse. The inedible biomass harvest is treated in the red frame. The orange frame contains the calculations for the crew solid waste and the central solid waste storage stock. The purple frame shows the inputs and outputs from and to the physical-chemical systems.

3.6.2 Solids Layer - Crew Food

The crew food frame contains two stocks, one for food brought by resupply missions (which also includes the initial food stock at mission start) and one for the food produced by the edible biomass harvest of the greenhouse, see Figure 3-36. The crew model provides an input on how many kilocalories each astronaut requires per day. The crew's diet is a mix of the food produced by the greenhouse and the food from the resupply stock. The crew first consumes a dedicated amount of greenhouse food. The remaining kilocalorie demand is filled with food from the resupply storage stock. The composition of the food (percentage of total kilocalories supplied by carbohydrates, fat and protein) is not taken into consideration.

The crew food frame also calculates the respiratory quotient which is the ratio of oxygen inhaled and carbon dioxide exhaled by a person, because the respiratory quotient depends on the ratio of macronutrients consumed. The macronutrient composition of the greenhouse food is calculated based on the amount of food consumed and the composition of the greenhouse food. The resupply food is assumed to be pure glucose ($C_6H_{12}O_6$) with an RQ of 1.0. This simplification for the resupply food was made in order to ease the calculations related to the mass closure validation of the simulation (see Chapter 3.11).

All formulas of this frame are shown in Appendix 9.3.1.
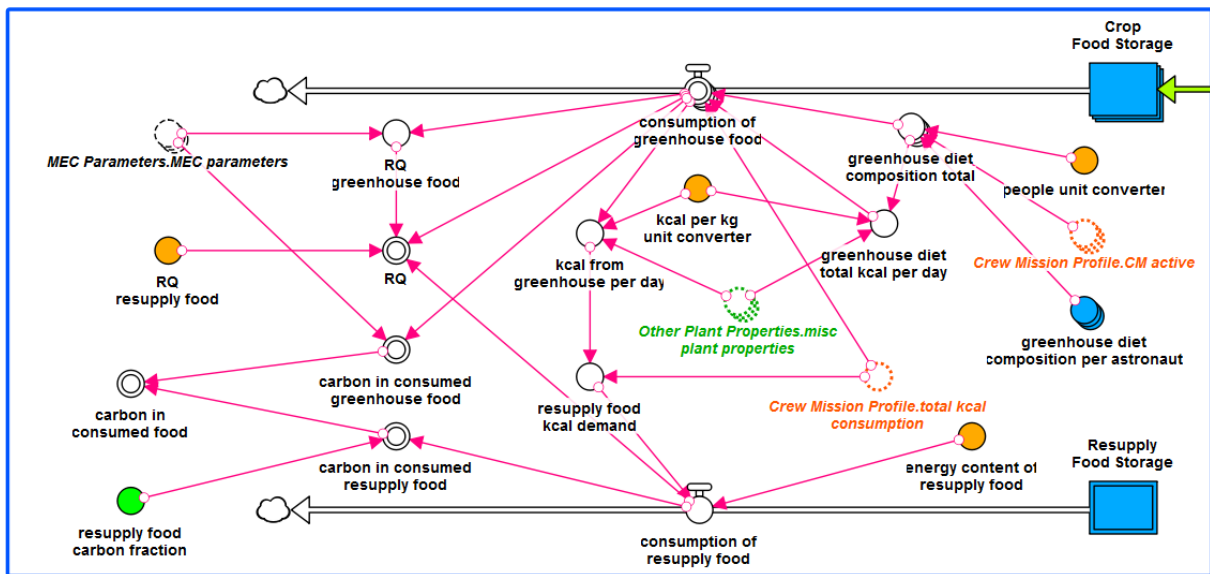
Figure 3-36: The solids layer crew food frame.

3.6.3 Solids Layer - Edible Biomass Harvest

The edible biomass harvest frame looks relatively complex (see Figure 3-37) but is rather straight forward. The frame calculates the edible dry biomass bound in the plants growing in the greenhouse. An input table with harvest dates for the different compartments and growth cycles controls the edible biomass harvest.

The harvest of the greenhouse plants is calculated in arrays with the dimensions compartment and cycle (for explanation see Chapter 3.8) to allow the user of the model for full flexibility on arranging the plant production schedule. The crew food frame however works with arrays with the dimension crop which is the list of crops available in the model. Stella Professional does not allow calculations of arrays with different dimensions. Consequently, the edi-

ble biomass harvest per compartment per cycle flow is converted to the total edible dry biomass harvest per crop flow by using the converter structure in the center of the frame, see Figure 3-37. The harvested edible dry biomass per crop is then handed over to the crew food frame.

All formulas of the edible biomass harvest frame are shown in Appendix 9.3.2.
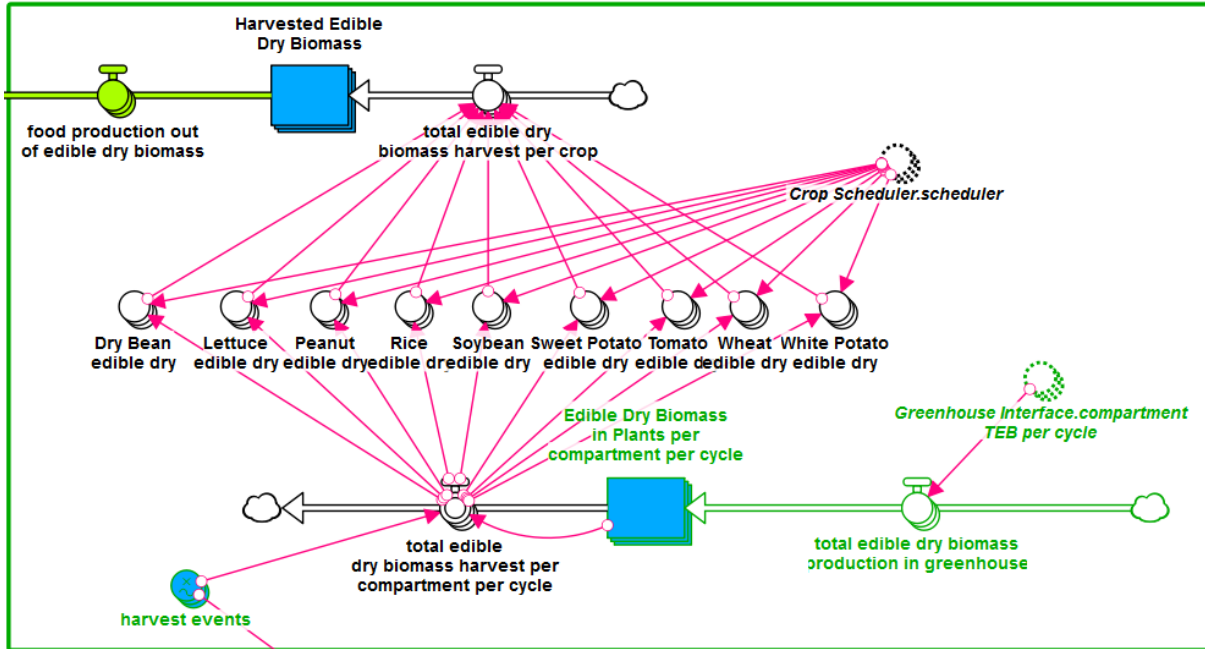
Figure 3-37: The solids layer edible harvest frame.

3.6.4 Solids Layer - Inedible Biomass Harvest

The inedible biomass harvest frame manages the calculation of all the biomass that cannot be eaten by the crew, see Figure 3-38. The frame has a structure similar to the edible biomass harvest frame, because also for the inedible biomass a conversion from arrays per compartment per cycle to arrays per crop is necessary. The arrayed stock in the center of the frame simulates the inedible dry biomass bound in the living plants cultivated in the greenhouse. The frame also has as input the harvest events arrayed converter of the edible biomass frame. This converter controls the harvest of the plants and therefore the inedible dry biomass flow from the living plants to the harvested inedible dry biomass stock. This stock has an output flow which is controlled by the inedible biomass processor (see Chapter 3.9.8).

All formulas of this frame are shown in Appendix 9.3.3.
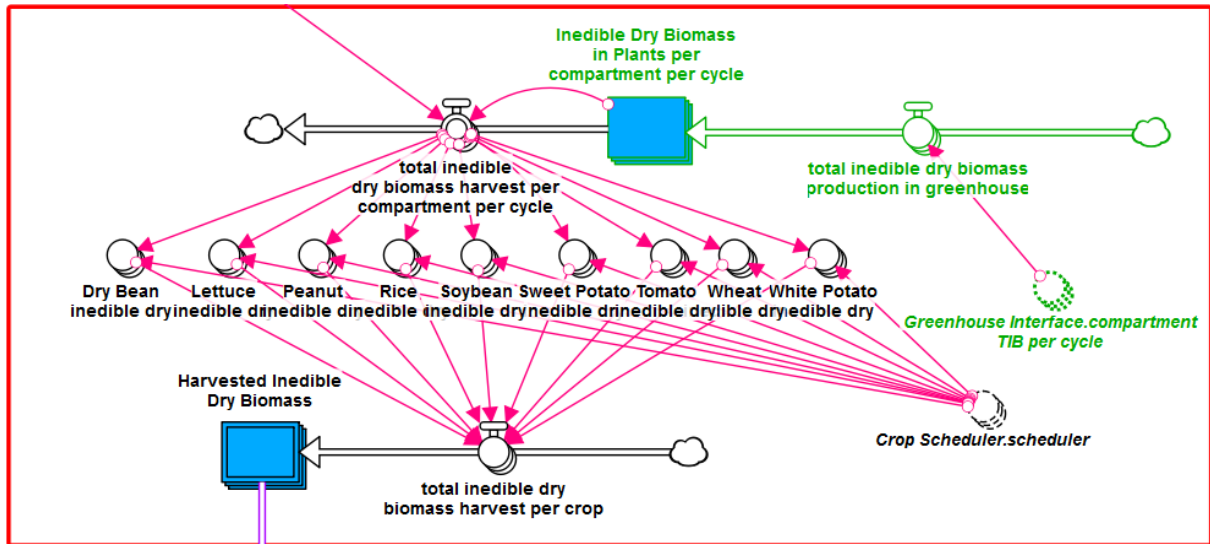
Figure 3-38: The solids layer inedible biomass harvest frame.

3.6.5 Solids Layer - Crew Waste

The crew waste frame manages the crew solid waste production and also contains the central solid waste storage stock, see Figure 3-39. The crew produces fecal, perspiration and urine solids based on their daily kilocalorie demand and therefore based on their activity. These three values are inputs from the crew model. The production of metabolic solids in the current model is not linked to a matter transformation from food to metabolic waste solids. Consequently, a supply stock named Crew Metabolic Solids is necessary so that the metabolic solids do not appear out of nowhere which would bring the mass closure calculations (see Chapter 3.11) out of balance.

The crew also produces a number of miscellaneous solid wastes (e.g. old cloths, experiment equipment, packaging), which come from the misc solids storage stock and are transferred to the solid waste storage stock based on the average daily production per person. The solid waste storage stock contains all solid wastes as dry mass. The only outflow from this stock is the amount of solid waste recycling performed by the physical-chemical systems like the incinerator.

All formulas of this frame are shown in Appendix 9.3.4.
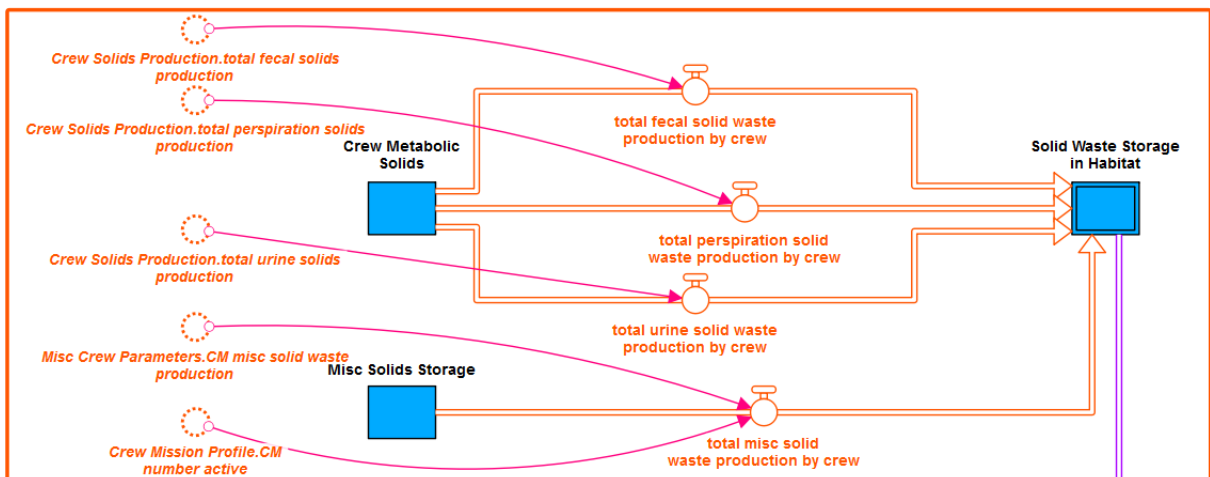
Figure 3-39: The solids layer crew waste frame.

3.6.6 Solids Layer - Physical-Chemical Systems

The physical-chemical systems frame of the solids layer module is shown in Figure 3-40. On the right side of the frame is the inedible biomass processing flow which receives inputs from the inedible biomass processor frame (Chapter 3.9.8) of the physical-chemical systems module. The total solid waste processing on the left side of the frame is done with an incinerator as described in Chapter 3.9.2.

Formulas of the solids layer physical-chemical systems frame are shown in Appendix 9.3.5.
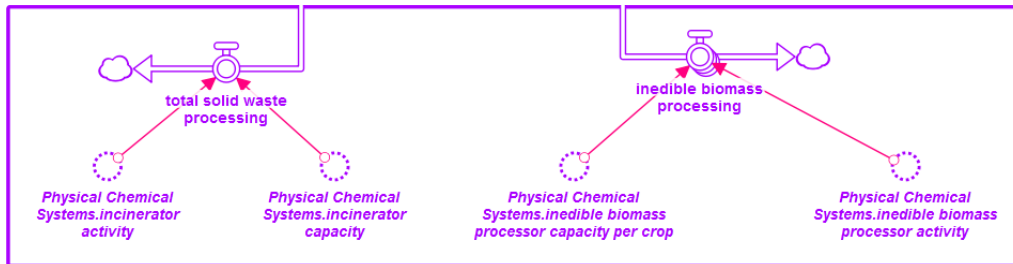
Figure 3-40: The solids layer physical-chemical systems frame.

3.7 Crew Model

3.7.1 Crew Model Module Overview

Purpose of the crew model is the calculation of human inputs and outputs depending on the crew composition and the daily schedule of activities. The model is divided into eight modules as shown in Figure 3-41. Each of the modules is described in the following subchapters. Model inputs are parameters concerning the crew composition (e.g. number of crew members, crew member weight), crew baseline values (e.g. waste production rates) and an activity database, which is used to generate specific crew member days. Different crew member days are then combined to a mission profile for each crew member. The crew mission profile then provides total values for the daily oxygen consumption and calorie demand to the gases and solids layer modules. The crew water demand module calculates the daily water intake of the crew and provides the results to the liquids layer module. The crew solids production module uses the information on the daily water demands to calculate the daily solids production. The misc. crew parameters module contains baseline values not directly related to the human metabolism (e.g. hygiene water demand).
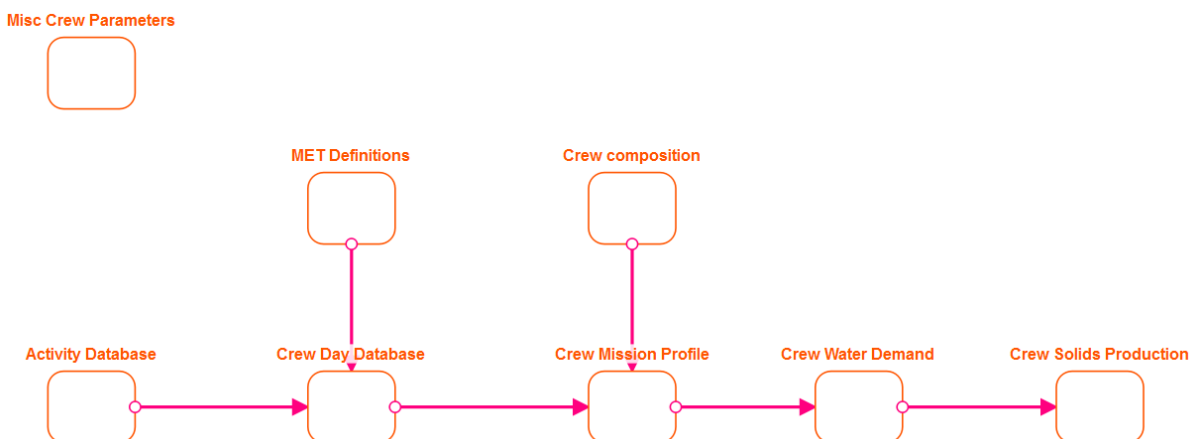
Figure 3-41: Crew model module.

3.7.2 The Metabolic Equivalent of Tasks (MET) Concept

Calculations of daily oxygen consumption and calorie demand are based on the Metabolic Equivalent of Tasks (MET) concept. Jetté *et al.* (1990) introduces the MET as a method to calculate human energy expenditure for different activities as a multiple of the resting metabolic rate. In that definition the resting metabolic rate is the amount of oxygen consumed at rest, sitting quietly in a chair. One MET is defined as 3.5 mL oxygen consumption per kilogram body weight in one minute. One liter of consumed oxygen is equal to 5 kcal of energy expenditure. Consequently, one MET also equals 0.0175 kcal of energy expenditure per kilogram of body weight in one minute.

Sleeping is generally considered to have a value of 0.9 MET. The MET approach can also be used to classify the intensity of exercises in five levels, see Table 3-3. Summary tables of MET values for a large amount of household, occupational, recreational and sports activities depending on body mass are available (McArdle *et al.*, 2014).

Table 3-3: Five-level classification of physical activity for men and women (McArdle et al., 2014).

	Men	Women
Light	1.6-3.9	1.2-2.7
Moderate	4.0-5.9	2.8-4.3
Heavy	6.0-7.9	4.4-5.9
Very heavy	8.0-9.9	6.0-7.5
Unduly heavy	>10.0	>7.6

3.7.3 Activity Database Module

The activity database module contains a converter with MET values for different space mission related activities. MET values for typical astronaut activities (e.g. science, EVA) are not available. For the model, activities listed in McArdle *et al.* (2014) are converted to astronaut activities as shown in Table 3-4. More activities can be added to the model and MET values adjusted, if necessary.

All formulas of the crew model activity database module are shown in Appendix 9.4.1.

Table 3-4: Crew member activity as implemented in the activity database module and their corresponding MET values.

Crew member activity in model	Corresponding task in McArdle *et al.* (2014)	MET value (mean value based on tables in McArdle *et al.* (2014))
Sleeping	n.a.	0.900
Leisure	Lying at ease, resting	1.260
Eating	Eating (sitting)	1.319
Personal hygiene	Eating (sitting)	1.319
Science	Writing (sitting)	1.660
Communication	Eating (sitting)	1.319
Normal maintenance	Writing (sitting)	1.660
Repair	Heavy house work, repairing*	4.500
Greenhouse maintenance	Cooking (F)	2.573
Training/exercise	1/3x Cycling (leisure, 5.5 mph) 2/3x Cycling (leisure, 9.4 mph)	5.034
Emergency	Heavy housework, carpentry*	7.000
EVA	Running on flat surface (9 min/mile)	10.477
Recreation	Eating (sitting)	1.319

*based on Jetté *et al.* (1990)

3.7.4 MET Definitions Module

The MET definitions module contains one converter with a value to transform MET into units used by the model. The converter is MET kcal conversion with a value of 0.0175 kcal per kilogram of body mass per minute of activity per MET. The concrete value is based on the description of the MET approach in chapter 3.7.2.

3.7.5 Crew Day Database Module

This module contains a set of predefined characteristic crew member day sets as shown in Table 3-5. Each of those days is a combination of time spent on the previously defined crew member activities. Existing sets can be modified and new sets can be added on demand. The module uses the MET values for each activity and the MET unit converter to calculate the kilocalories consumption per body mass for each of the predefined crew member days. The setup of the module within Stella is shown in Figure 3-42.

The BVAD weekday and the BVAD weekend day are based on Anderson *et al.* (2015). The total daily energy expenditure for an 82 kg astronaut performing a BVAD weekday as shown in Table 3-5 is around 13.03 MJ which is similar to the 12.99 MJ per crewmember listed in Anderson *et al.* (2015). The former is also very similar to an exemplary daily schedule of German astronaut Alexander Gerst (Fleischmann *et al.*, 2015). The Nominal day schedule is an adaption of the BVAD weekday with increased science and greenhouse maintenance and less normal maintenance. The Emergency day activity list includes an emergency situation (e.g. an equipment failure) and repair work. The EVA day incorporates a three hour EVA and three hour recreation time and has the highest energy expenditure per crewmember.

All formulas of the crew model crew day database module are shown in Appendix 9.4.2.

Table 3-5: Predefined set of characteristic crew member days. Energy expenditure values for an 82 kg male astronaut.

Crew member activity	Amount of time in minutes spend per activity per day				
	BVAD weekday	BVAD weekend day	Nominal day	Emergency day	EVA day
Sleeping	510	510	510	510	510
Leisure	60	60	60	60	60
Eating	180	180	180	180	180
Personal hygiene	60	60	60	60	60
Science	30	0	60	0	60
Communication	90	90	90	120	90
Normal maintenance	420	180	270	120	120
Repair	0	0	0	180	0
Greenhouse maintenance	0	0	120	0	0
Training/Exercise	90	0	90	0	0
Emergency	0	0	0	60	0
EVA	0	0	0	0	180
Recreation	0	360	0	150	180
Total kcal per day	**3113.85**	**2501.94**	**3271.07**	**3783.36**	**4867.45**
Total MJ per day	**13.03**	**10.47**	**13.69**	**15.83**	**20.37**
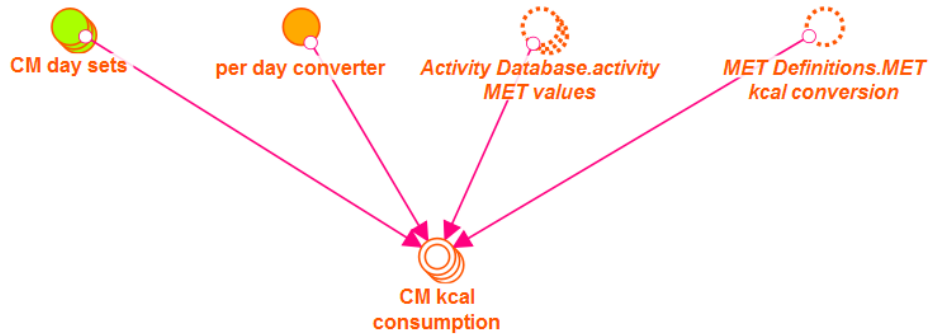
Figure 3-42: Crew day database module.

3.7.6 Crew Composition Module

The crew composition module contains an arrayed converter which is used to provide crew member parameters and other converters to calculate total body water and the total number of crew members, see Figure 4-39. Table 3-6 shows the table setup. The content of the converter has to be adjusted to the specific crew composition of the space mission to be investigated. The CM total body water converter calculates the mass of the total body water per astronaut based on their weight and sex. Total body water is around 62.5% (for men) and 52.5% (for women) of the total weight. Another converter calculates the number of crew members active for the current simulation case based on the values of the first column in the crew member parameters converter.

All formulas of the crew model crew composition module are shown in Appendix 9.4.3.

Table 3-6: Crew member parameters converter.

	Active (1 = active; 0 = inactive)	Height [m]	Weight [kg]	Sex (10 = male; 20 = female)	Age [y]
astronaut 1	1	1.7	70	10	40
astronaut 2	0	…	…	…	…
astronaut 3	…	…	…	…	…
…					
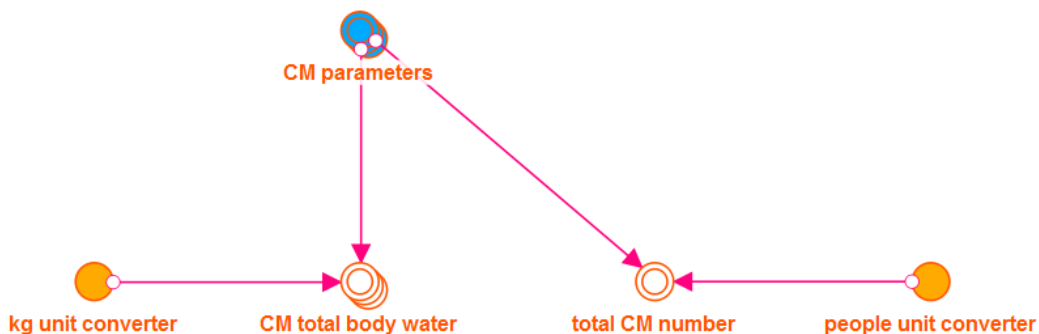
Figure 3-43: Crew composition module.

3.7.7 Crew Mission Profile Module

The predefined characteristic days for each crew member are combined to a complete mission profile within this module. Therefore in the converter crew member mission profile each crew member and each day of the mission duration is assigned a characteristic crew member day from the database. Together with the kilocalorie consumption calculation from the previous modules, consumption values per body mass per day for each crew member are calculated. Those values in turn are multiplied by the specific weight of each crew member to have the final consumption values. The output values to the gases, liquids and solids layers are then the sum of the consumption values of all crew members per day. The formulas of each converter of the module are shown in Appendix 9.4.4.
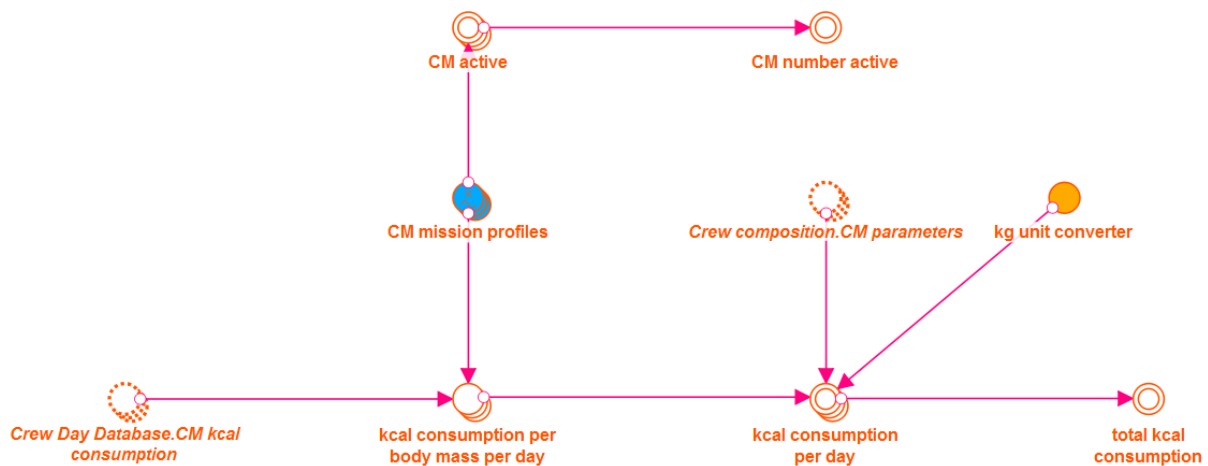
Figure 3-44: Crew mission profile module.

3.7.8 Crew Water Demand Module

The water demand of the crew is calculated by summing up the water a human loses per day due to various processes. Humans can only produce a very small amount of water per day and consequently need to intake water regularly to compensate the deficit, as explained in Chapter 3.5.

Determining the exact values for those processes, however, is rather complicated. Holliday and Segar (1957) explain the relationship between the basal energy expenditure of a given person and the water balance on a per 100 kilocalorie basis. The insensible water loss is reported to be around 50 mL per 100 kcal, the water loss via urine to be around 66.7 mL per 100 kcal and the water loss through stool to be negligible. When summing up the water loses and adding 16.7 mL of metabolically produced water per 100 kcal, Holliday and Segar (1957) estimate the water demand of a human in a comfortable environment to be around 100 mL per 100 kcal.

The work of Hellerstein (1993) extends the principle further. Insensible water loss is now separated into loses via the lungs and loses via the skin. Furthermore, the water loss via stool, although relatively small, is also included. Table 3-7 summarizes the values.

The crew water demand module uses the values from Table 3-7 to calculate the daily water loses. The daily production of metabolic water is directly calculated in the liquids layer crew frame. Therefore, the daily kilocalorie consumption values per crew member based on the

mission schedule from the crew mission profile module are used, see Figure 3-45. The formulas for this module are shown in Appendix 9.4.5.

Table 3-7: Usual maintenance of water expenditure per 100 kcal metabolized (Hellerstein, 1993).

		mL of water per 100 kcal
Insensible		45
Lungs	15	
Skin	30	
Sensible		
Sweat		10
Stool		5
Urine		50
	Total water loss	**110**
Water produced by oxidation		-10
Water needed from external sources		**100**

The values shown in Table 3-7 are average values for an adult person in a comfortable environment. They do not take into account the differences between male and female body constitution and metabolism. Furthermore, the values are not appropriate for very young (infants, children) and old humans. Several medical conditions have an effect on the water demand. For example Diarrhea greatly increases the water loss through stool and the increased body temperature caused by infections and fever results in more water loss through sweating. Cox (1987) reports these and some other factors influencing the water loss of a person.

Furthermore, increased activity (e.g. training) results in an increase of water loss through sweating. Rehrer and Burke (1996) summarize sweat rates for various sport activities and ambient conditions. Sweat production is again affected by the constitution of the person, by the ambient temperature and humidity and therefore rather hard to determine on a general basis. Within the model the increased water demand due to sport activities is compensated to some degree by the increased kilocalorie demand which results in a higher water intake of the crew member doing training.
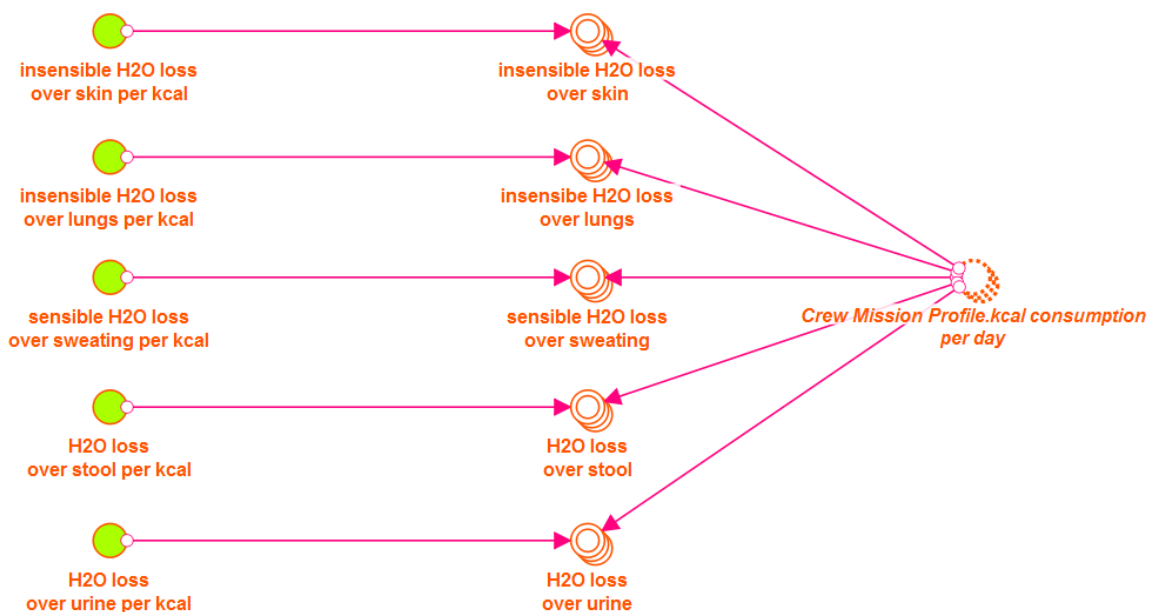
Figure 3-45: Crew water demand module.

3.7.9 Crew Solids Production Module

This module calculates the daily production of solids per crew member. The calculation is based on a linear approximation of the BVAD (Anderson *et al.*, 2015) average production values for fecal solid waste, urine solid waste and perspiration solid waste per crew member per day. It is assumed that there is a linear correlation between the water loss and the corresponding solids under nominal conditions (e.g. no sickness). Consequently, this module provides a dynamic output of solids production, summed up over the whole crew, to the solids layer based on the daily water demand which is based on the activity level, see Figure 3-46. The formulas for this module are shown in Appendix 9.4.6.
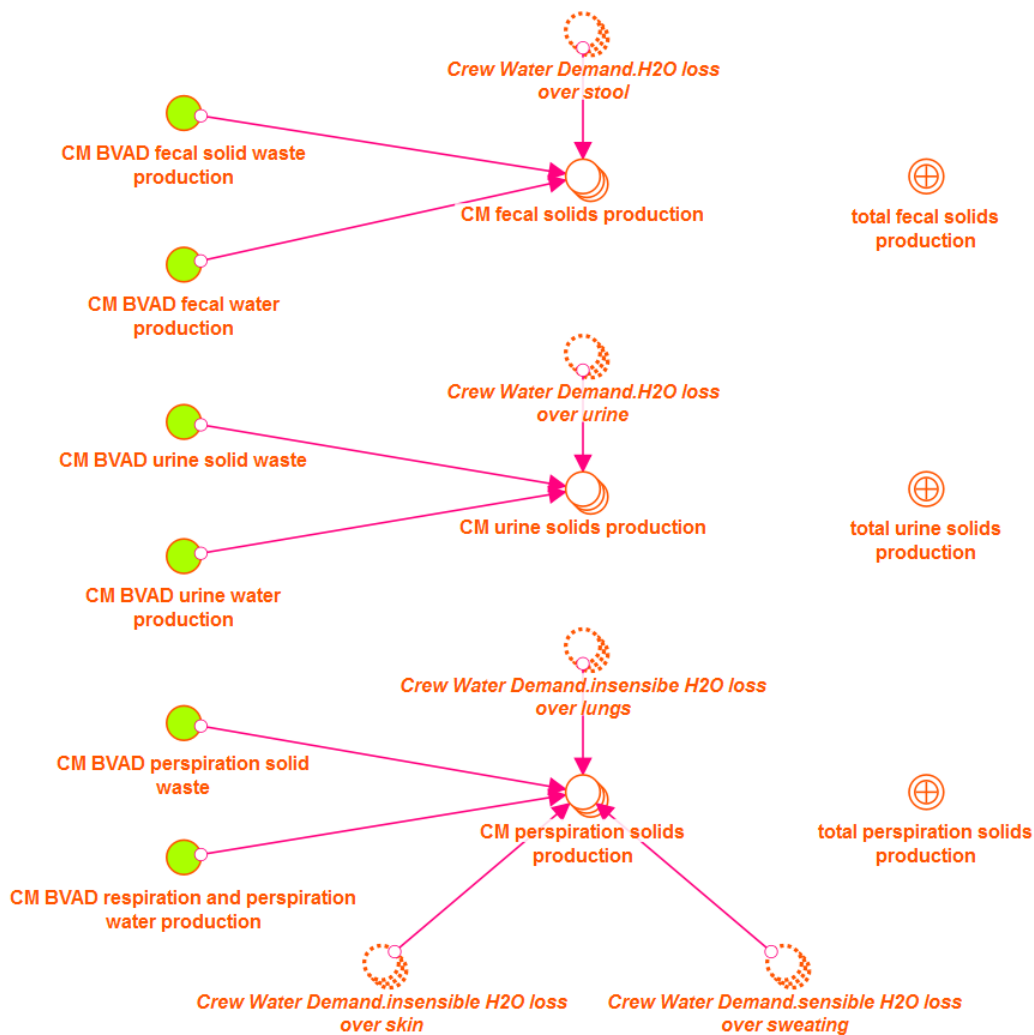
Figure 3-46: Crew solids production module.

3.8   Greenhouse Model

3.8.1 Greenhouse Model Module Overview

The greenhouse model module consists of eight modules, which calculate intermediate parameters or function as input or output interface. Figure 3-47 shows the setup of the greenhouse model module in Stella Professional. The crop scheduler provides input to the MEC (Modified-Energy-Cascade) crop model, which provides outputs for the greenhouse interface module. The crop water accumulator module calculates the daily water accumulation of the

plants, which is not part of the original MEC model. The other plant properties module contains an arrayed converter which holds certain parameters such as harvest index, water content in biomass and amount of macronutrients (fat, protein, carbohydrates). Each of the different modules is described in the following subchapters. In Figure 3-47 the interconnections between the different modules are shown as they are in the Stella.
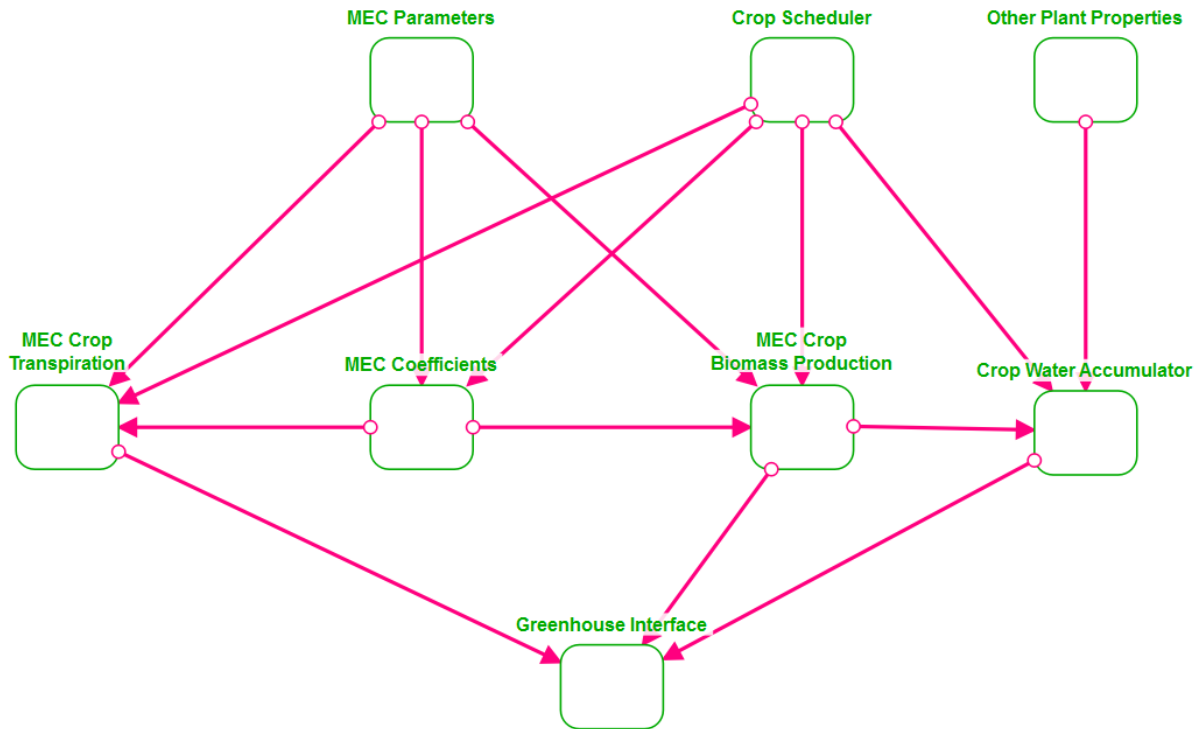
Figure 3-47: Greenhouse model module interconnections in Stella.

3.8.2 MEC Crop Model Description

The Modified Energy Cascade (MEC) crop production model was developed to calculate biomass production and transpiration rates depending on environmental conditions (e.g. light intensity, carbon dioxide concentration). The model is based on a multivariate polynomial regression (MPR) of experimental data acquired and links plant metabolic and growth processes on a general level.

The model was first created in 1995 and named Energy Cascade (EC) model (Volk *et al.*, 1995). This first model simulated the growth of wheat, but did not included formulas for transpiration. The model was then evolved to the Top-level Energy Cascade (TLEC) model in 2000 (Jones and Cavazzoni, 2000), which increased the number of crop species to nine, including most of the preferred cultivars at that time. Furthermore, the formulas in the model were adapted to better fit the experimental observations. The TLEC also included formulas for canopy transpiration. In 2002, the TLEC was improved to the MEC by adjusting the formulas again and by adding the calculation of daily oxygen production (Jones et al., 2002). Table 3-8 summarizes the characteristics of each of the three models.

Table 3-8: Characteristics of the EC, the TLEC and the MEC.

EC	• Absorption of light - The irradiance of photosynthetic active radiation, which denotes the spectral range from 400 to 700nm, is specified as photosynthetic photon flux (PPF), using quantum units. Despite its name, the PPF is actually a density, since its unit is usually µmol/(m²*s). The corresponding model variable for the absorption of light is A, which specifies the fraction of the incident PPF that is absorbed by the plant canopy. • Photosynthesis - During photosynthesis, the energy of the absorbed light quanta is used to fix carbon in carbohydrates. The corresponding model variable is CQY (canopy quantum yield), which specifies the number of moles of carbon that are fixed in sucrose for each mole of PPF absorbed. • Respiration - Plants respire in order to convert sucrose to biomass and for maintenance and therefore lose a portion of the assimilated carbon. The corresponding model variable for this process is CUE (carbon use efficiency), which is the fraction of sucrose carbon that is converted to biomass.
TLEC	• A variety of other crops was incorporated, adding up to a total of 9 cultivars. • The prediction of tA (time until canopy closure), tQ (time until onset of canopy senescence) and tM (time at crop maturity), dependent on environmental conditions, was added. • The parameter CUE was redefined to be computed on a daily basis and a time dependency of legumes for the same value was incorporated. • The net photosynthesis (PNET) was also redefined to be computed on a daily basis. • CQYMAX was described as a function of PPF and the CO_2 level. • A model for canopy transpiration that depends on environmental conditions was added.
MEC	• The model variable for PPF absorption (A) was redefined to represent a more realistic, crop specific exponential growth. • CQYMAX and tA were defined as functions of the CO_2 level and PPF using the above mentioned MPR fits. • The simulation of edible biomass production was implemented. Before, a fixed harvest index was applied at the end of a simulation run. • The calculation of daily oxygen production (DOP) was added. • The light integral (H), the CO_2 level and thus also CQY can vary from day to day, but have to stay fixed over the course of one day and must not exceed a certain range for the equations to be applicable.

Anderson et al. (2015) is a very good documentation of all MEC formulas and parameters and also lists the allowable ranges of the environmental input parameters (see Table 3-9) in which the model is validated.

Table 3-9: Allowed ranges for the environmental input parameters (Anderson *et al.*, 2015).

Crop	PPF [μmol/(m²*s)]	CO2 level [ppm]	light/dark temperature [°C]
Bean (dry)	200-1000	330-1300	32/28-23/19
Lettuce	200-500	330-1300	28/28-18/18
Peanut	200-1000	330-1300	32/28-23/19
White Potato	200-1000	330-1300	25/21-15/11
Rice	200-2000	330-1300	34/26-24/16
Soybean	200-1000	330-1300	32/28-23/19
Sweet Potato	200-1000	330-1300	33/27-21/17
Tomato	200-1000	330-1300	31/27-21/17
Wheat	200-2000	330-1300	28/28-18/18

3.8.3 Crop Scheduler Module

The crop scheduler module consists of only one arrayed converter named scheduler. The converter allows the user to implement a planting schedule for the greenhouse. The greenhouse is therefore divided in up to 10 compartments. A compartment in this case is an environmentally separated part of the greenhouse with its own internal conditions (e.g. light intensity, photoperiod). For each compartment up to 10 consecutive growth cycles can be defined. The number of compartments and growth cycles can be increased, if necessary, by modifying a few formulas and array dimensions. Each growth cycle can be assigned a starting day, a crop species, a light intensity and a photoperiod. Table 3-11 shows the described setup. The crop scheduler module provides the flexibility to investigate different crop combinations inside the greenhouse at different times of the simulation.

Each crop species available in the MEC model is assigned an index according to Table 3-10. These indices are then put into the second column of Table 3-11.

All formulas of the greenhouse model crop scheduler module are shown in Appendix 9.5.1.

Table 3-10: Crop species indices used in the Stella model.

Dry Bean	Lettuce	Peanut	Rice	Soybean	Sweet Potato	Tomato	Wheat	White Potato
1	2	3	4	5	6	7	8	9

Table 3-11: Crop scheduler arrayed converter.

Compartment 1				
Cycle No.	Cycle start [d]	Crop species	Light intensity [µmol/(m²*s)]	Photoperiod [h]
1				
2				
…	…	…	…	…
10				

Compartment …				
Cycle No.	Cycle start [d]	Crop species	Light intensity [µmol/(m²*s)]	Photoperiod [h]
1				
2				
…	…	…	…	…
10				

Compartment 10				
Cycle No.	Cycle start [d]	Crop species	Light intensity [µmol/(m²*s)]	Photoperiod [h]
1				
2				
…	…	…	…	…
10				

3.8.4 MEC Parameters Module

The MEC parameters module contains a number of static parameters and coefficients of the MEC crop model. Four converters, three of them arrayed, are used to provide those values.

- *Amax* is the maximum value for the fraction of *PPF* absorbed by the plant canopy, *A*. Amax is crop independent. *PPF* and *A* are variables later used in the calculations.
- *CQY max coefficients* contains crop specific matrixes with maximum values for the canopy quantum yield, *CQY*.
- *tA coefficients* contains crop specific matrixes for the time of canopy closure, *tA*.
- *MEC parameter per crop* contains the following crop specific constants:
    - *H0*, nominal photoperiod,
    - *OPF*, oxygen production fraction,
    - *BCF*, biomass carbon fraction,
    - *XFRT*, fraction of daily carbon gain allocated to edible biomass after *tE,*
    - *tE*, time at onset of organ formation,
    - *tQ*, time until onset of canopy senescence,

- ○ *tM*, time at harvest or crop maturity,
- ○ *n*, exponent to calculate *A* based on *Amax*, *t* and *tA,*
- ○ *CQYmin*, minimum value for *CQY* that applies until *tQ,*
- ○ *CUEmin*, minimum value for *CUE24* that applies until *tQ,*
- ○ *CUEmax*, maximum value for *CUE24* at *tM,*
- ○ *gA*, atmospheric aerodynamic conductance and
- ○ *Tlight*, canopy surface conductance.

The formulas and values for the above listed converters can be found in Appendix 9.5.2.

3.8.5 MEC Coefficients Module

The MEC coefficients module calculates the three values:

- - **A** the fraction of *PPF* absorbed by the plant canopy,
- - **CUE24** the carbon use efficiency in a 24 hour period and
- - **CQY** the canopy quantum yield

per compartment per growth cycle using inputs from the earlier described modules and the current carbon dioxide concentration in each compartment. Therefore three intermediate parameters (*tA* - time until canopy closure, *PPFe* - effective photosynthetic photon flux, *CQYmax* - maximum value for CQY that applies until *tQ*) are calculated first.

Figure 3-48 shows the calculation order of the MEC coefficients module. The exact formulas can be found in Appendix 9.5.3.
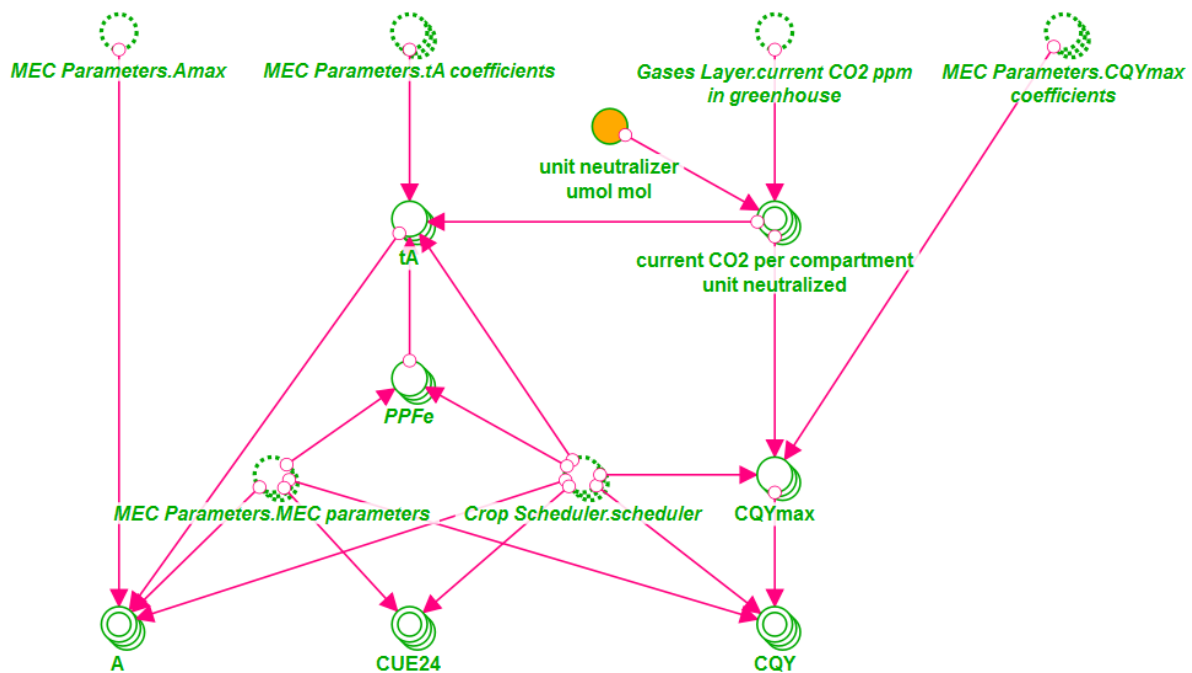
Figure 3-48: MEC coefficients module.

3.8.6 MEC Crop Biomass Production Module

The MEC crop biomass production module uses the output of the MEC coefficients module, the MEC parameters per crop and the crop scheduler to first calculate the daily carbon gain (DCG) and the daily oxygen production (DOP). Those two values are the input to calculate the crop growth rate (CGR), which is in turn used to calculate the total crop biomass on a dry basis (TCB), the total edible biomass (TEB) and the total inedible biomass (TIB). All three values are calculated per compartment per cycle. DCG, DOP, TEB, TCB and TIB are exported to the greenhouse interface module. Figure 3-49 shows the calculation order of the MEC coefficients module. The exact formulas can be found in Appendix 9.5.4.
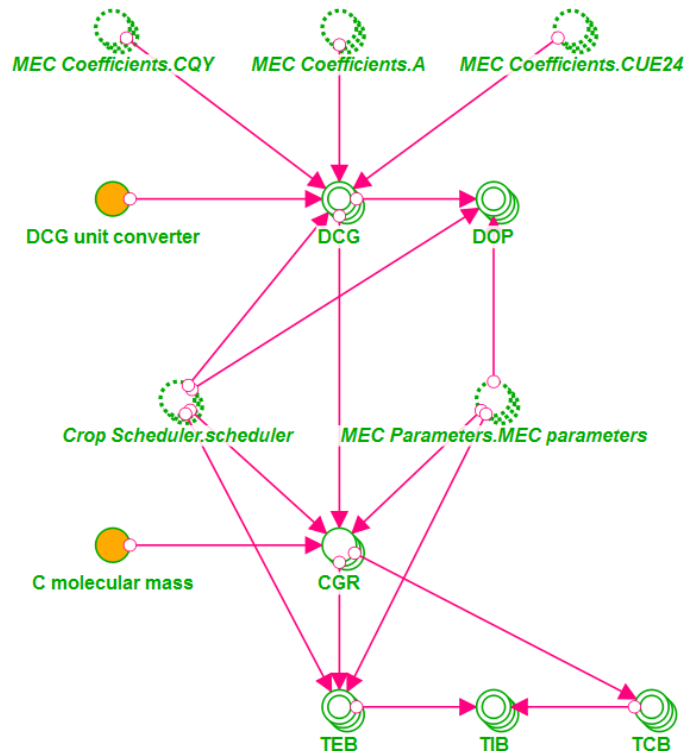
Figure 3-49: MEC crop biomass production module.

3.8.7 MEC Crop Transpiration Module

The MEC crop transpiration module uses a number of inputs from the earlier described modules (see Figure 3-50) and the current carbon dioxide concentration and relative humidity in each compartment. The module then calculates seven intermediate parameters:

- *PGross,* the gross canopy photosynthesis,
- *PNET,* the net canopy photosynthesis,
- *VPSAT,* the saturated moisture vapor pressure,
- *VPAIR,* the actual moisture vapor pressure,
- *VPD,* vapor pressure deficit,
- *gS,* canopy stomatal conductance,
- *gC,* canopy surface conductance.

The intermediate parameters are inputs to the calculation of the daily transpiration rate (DTR) per compartment per cycle, which is the module output to the greenhouse interface module. The exact formulas can be found in Appendix 9.5.5.
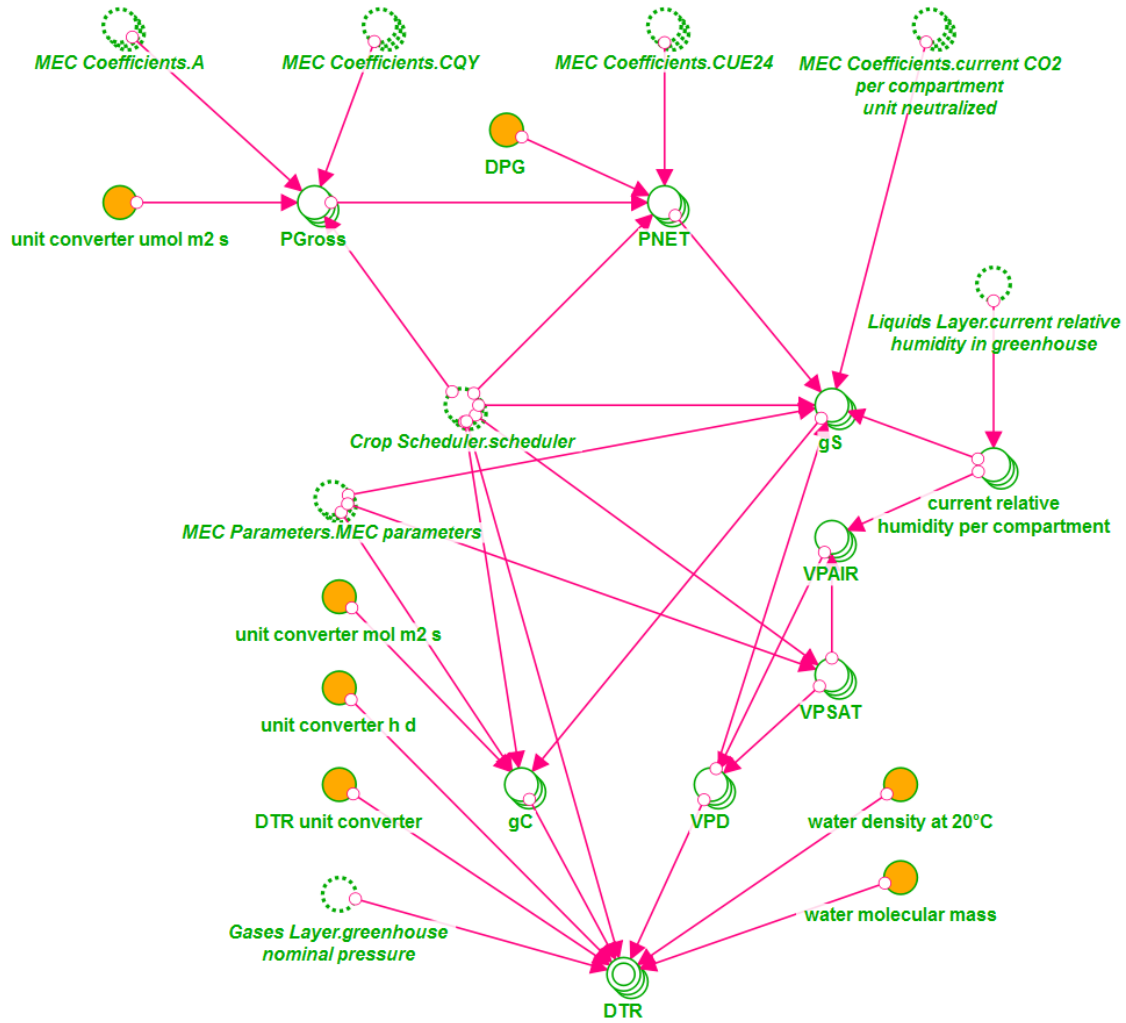
Figure 3-50: MEC crop transpiration module.

3.8.8 Other Plant Properties Module

This module contains an arrayed converter to provide miscellaneous plant properties to the greenhouse model and the solids layer. Table 3-12 shows the values of the converter.

All formulas of the greenhouse model other plant properties module are shown in Appendix 9.5.6.

Table 3-12: Misc plant properties converter. Harvest index and water content values according to Anderson *et al.* (2015), macronutrient values according to nutritionvalue.org.

Crop	Harvest index	Edible biomass water content	Inedible biomass water content	Carbo-hydrates [g/100 g]	Fats [g/100 g]	Proteins [g/100 g]
Dry Bean	0.40	0.100	0.9	61.0	1.5	22.0
Lettuce	0.90	0.950	0.9	3.0	0.1	0.9
Peanut	0.25	0.056	0.9	16.0	49.0	26.0
Rice	0.30	0.120	0.9	76.0	3.2	7.5
Soybean	0.40	0.100	0.9	30.0	20.0	36.0
Sweet Potato	0.40	0.710	0.9	20.0	0.1	1.6
Tomato	0.45	0.940	0.9	3.9	0.2	0.9
Wheat	0.40	0.120	0.9	75.0	2.0	11.0
White Potato	0.70	0.800	0.9	16.0	0.1	1.7

3.8.9 Crop Water Accumulator Module

The original MEC plant model adequately calculates the transpiration rate of the crops. However, the MEC model does not calculate the complete water balance of the plant which is needed for a precise greenhouse simulation. Especially the water accumulation inside living plants needs to be taken into account, because all plants consists mainly of water. Czupalla (2012) realized the same issue and developed a formula for the crop water accumulation, which is implemented in the crop water accumulator module. This module calculates the daily water accumulation for each crop depending on the biomass growth. The exact formulas can be found in Appendix 0.
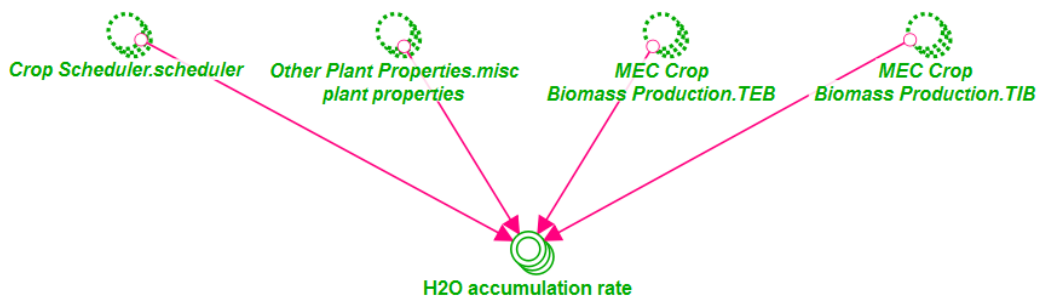
Figure 3-51: Crop water accumulator module.

3.8.10 Greenhouse Interface Module

The greenhouse interface module collects the outputs of the MEC crop biomass production module, the MEC crop transpiration module and the crop water accumulator module to transform them into values usable in the different layer modules described above. The outputs of the MEC modules are arrays with the dimensions compartment and cycle and are on a square meter basis. In a three step process (see Figure 3-52) the compartment DCG, DOP, DTR, TCB, TEB and TIB at the current time step are calculated by summing up the values of all growth cycles at the current time step. Those values are then multiplied by the actual compartment growth area to calculate the compartment total values. This step also includes unit transformation so that all parameters are in kilograms per day. The greenhouse DCG, DOP, DTR, TCB, TEB and TIB are the sum of all compartments inside the greenhouse. The same process is established for the crop water accumulation converters.

All formulas of the greenhouse model greenhouse interface module are shown in Appendix 9.5.8.
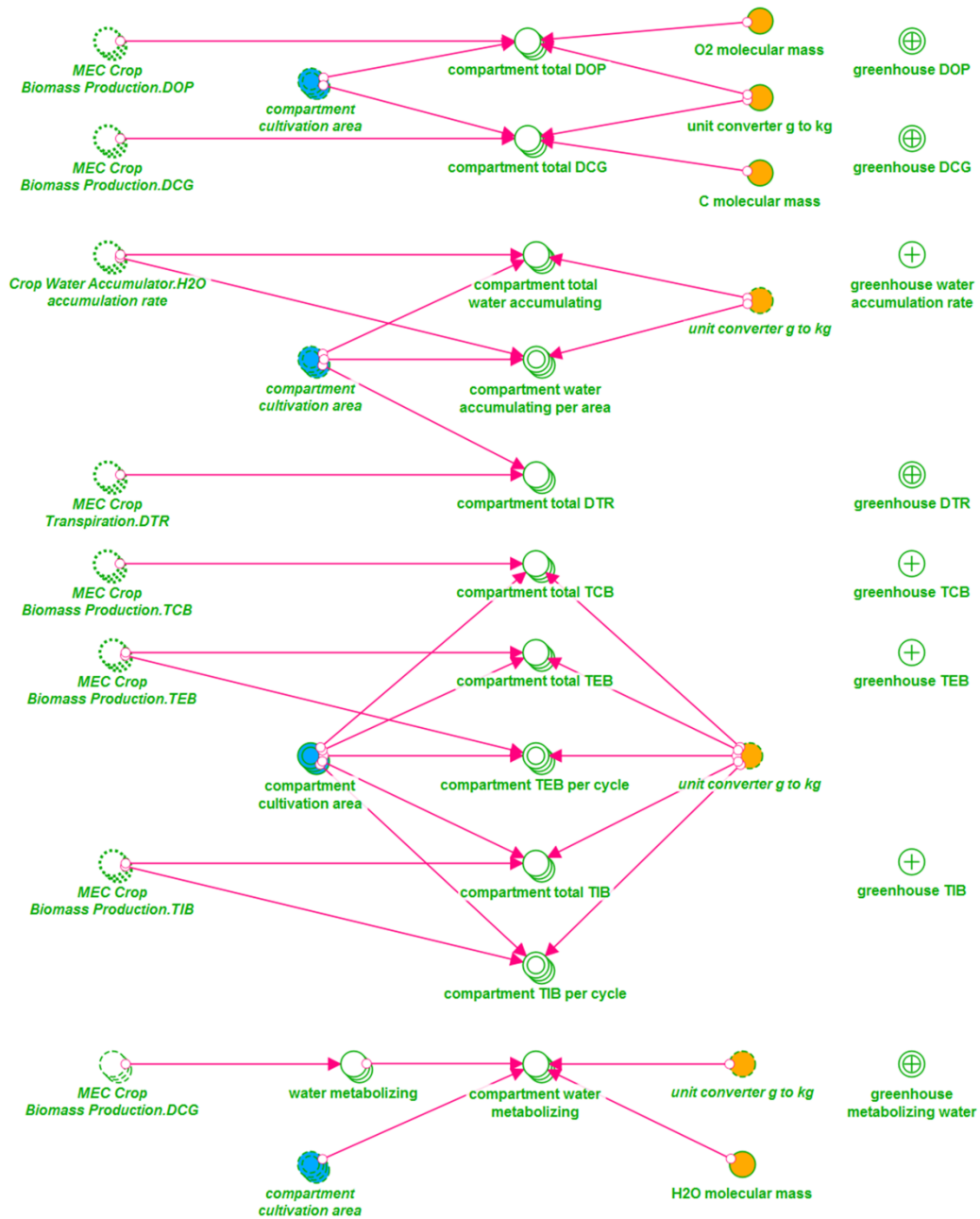
Figure 3-52: Greenhouse interface module.

3.9 Physical-Chemical Systems

3.9.1 Physical-Chemical Systems Module Overview

The physical-chemical systems module has no sub-modules like the previously described crew model and greenhouse model, because it contains several individual technologies rather than a complete model. The different physical-chemical technologies are represented by colored frames within the model, see Figure 3-53. Each frame contains only the components necessary to model the behavior of that specific technology and has its own inputs and outputs to the gases, liquids and solids layer of the root model.

Figure 3-53 shows a screenshot from the top part of the physical-chemical systems module as it is implemented. The red frame contains the calculation of the incinerator which is used

to recycle solid waste. This frame is described in detail in Chapter 3.9.2. The blue frame indicates the calculation of an electrolyzer which is used to break water into hydrogen and oxygen and is described in Chapter 3.9.3. The green frame represents the modelling components for a Sabatier reactor which is used to combine hydrogen and carbon dioxide to methane and water. The Sabatier reactor modelling is described in Chapter 3.9.4.
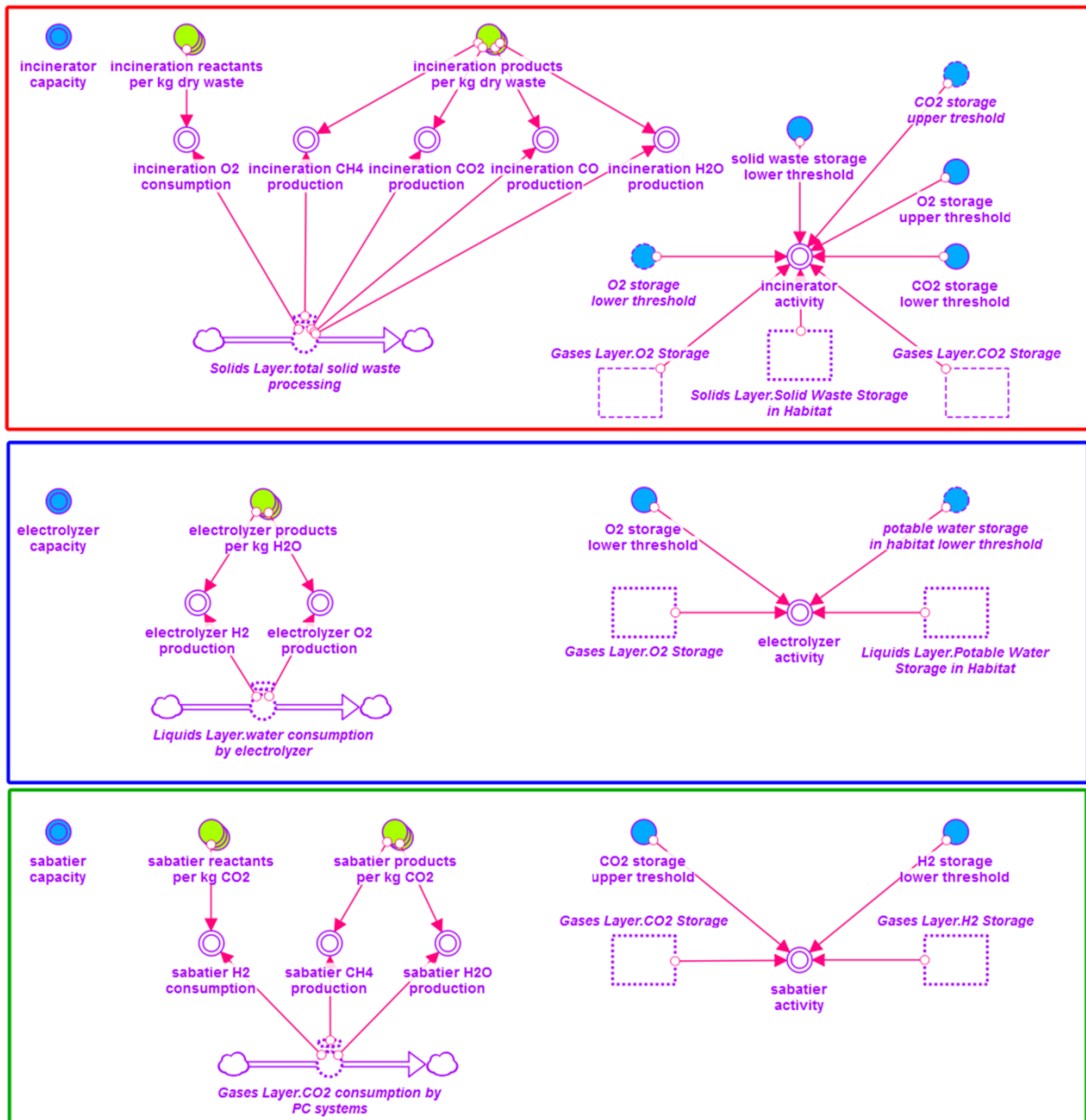
Figure 3-53: Overview of the top part of the physical-chemical systems module. Red frame: Incinerator calculations, blue frame: Electrolyzer calculations, green frame: Sabatier Reactor calculations.

Figure 3-54 shows the bottom part of the physical-chemical systems module which contains the calculations for the habitat and greenhouse condensing heat exchangers (CHX) in the teal frame, the calculations for the Vapor Phase Catalytic Ammonia Removal (VPCAR) in the purple frame, the calculations for the oxygen and carbon dioxide separators in the orange frame and the calculations of the inedible biomass processor in the black frame.

The technologies and all related calculations are described in detail in the following subchapters.
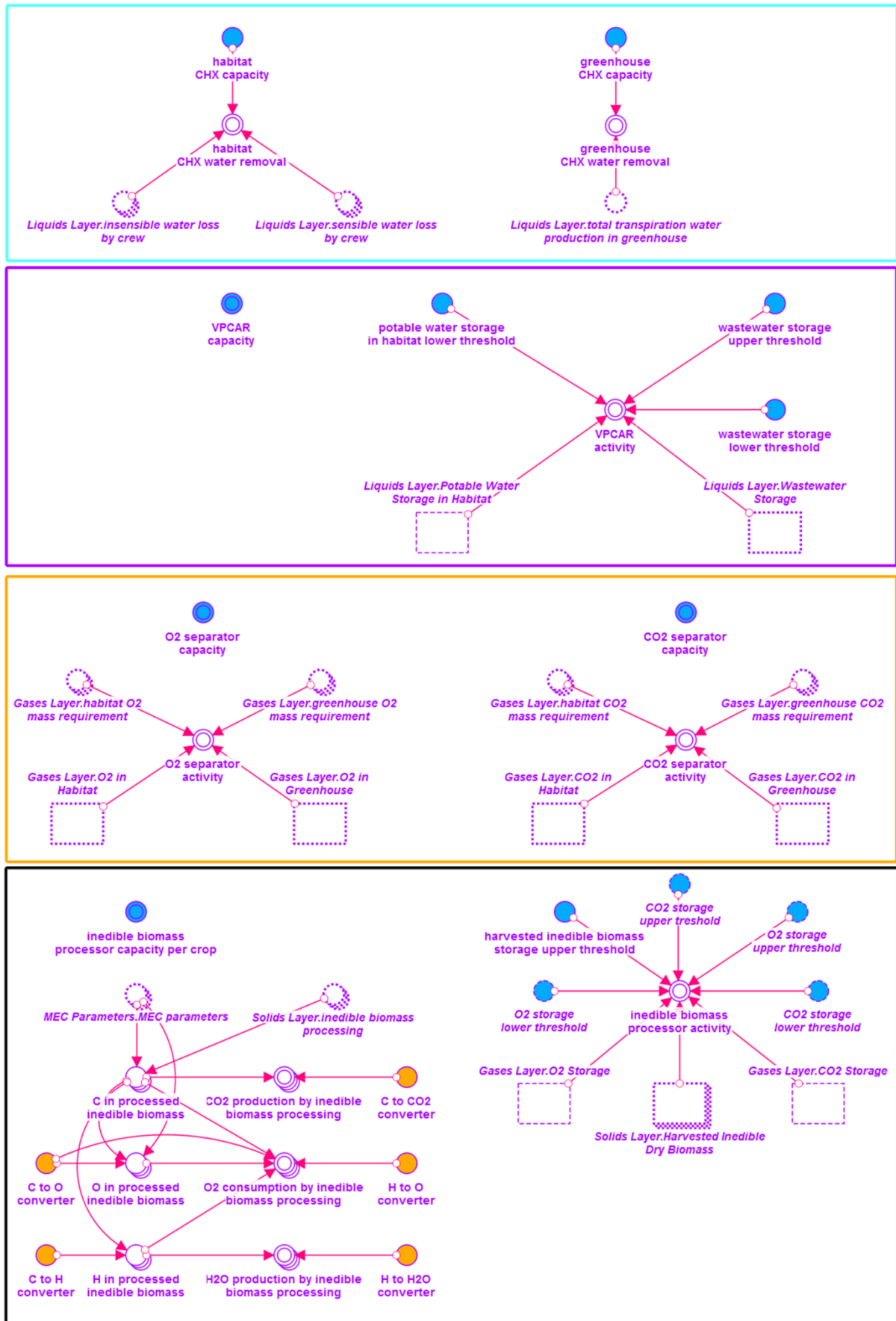
Figure 3-54: Overview of the bottom part of the physical-chemical systems module. Teal frame: CHX calculations, purple frame: VPCAR calculations, yellow frame: Oxygen and carbon dioxide separator calculations, black frame: Inedible biomass processor.

3.9.2 Incinerator

The incinerator is implemented into the model in order to recycle solid waste into useful products. Although it looks counterintuitive at first to expend precious oxygen on solid waste processing, this step is necessary to recover the carbon bound in the waste products so that the carbon can be supplied to the plants in the greenhouse for food and oxygen production.

Incineration is a combustion process under high temperatures and excess oxygen which converts complex carbohydrates into carbon dioxide and water. The choice to implement an incinerator over other solid waste recycling technologies is based on the evaluation described in Anthony and Hintze (2014). Steam reforming and incineration have shown 100% recovery of carbon from waste products, which is very important for a life support system architecture that includes a greenhouse. Steam reforming however produces methane and oxygen as end products, gases which cannot be used by the plants in the greenhouse. Incineration on the other side produces carbon dioxide and water as main products and carbon monoxide and methane as secondary products (see formula 3-12). The first two are among the supplies a greenhouse constantly needs. The amount of produced methane and carbon monoxide are relatively low compared to the amounts of carbon dioxide and water.

$$solid\ waste + O_2 + heat \rightarrow CO_2 + CO + CH_4 + H_2O \qquad (3\text{-}12)$$
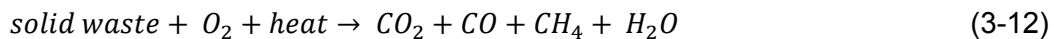
The incineration system described by Anthony and Hintze (2014) has a capacity to recycle 443 kg waste per year when run 16 hours per day and 350 days per year. The system produces 1.107 g carbon dioxide, 0.433 g water, 0.075 g carbon monoxide and 0.008 g methane per gram of solid waste. These values are implemented in the incinerator calculations of the model.
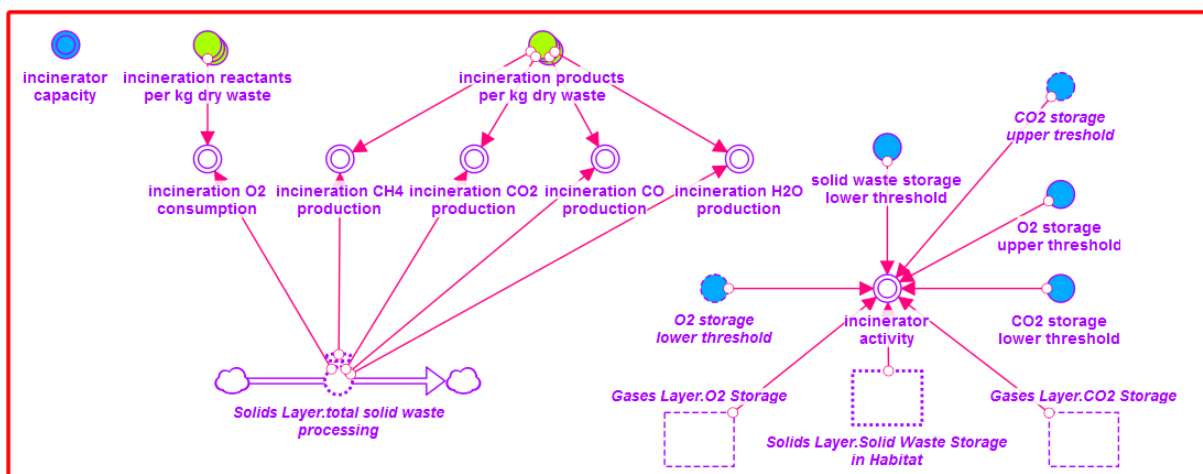
Figure 3-55: Incinerator frame.

The activity of the incinerator is controlled by the construct in the bottom right corner of the frame shown in Figure 3-53. The incinerator is active when the carbon dioxide in the CO_2 storage stock is below the lower threshold or the solid waste storage reached the upper threshold, and the oxygen in the O_2 storage stock is above the lower threshold. The CO_2 storage lower threshold is set to value which ensures that there is always enough carbon dioxide to supply the greenhouse. The O_2 storage lower threshold shall ensure that the incinerator is not consuming oxygen when there is not enough oxygen left for the crew to survive.

All formulas and values of the incinerator model are shown in Appendix 9.6.1.

3.9.3 Electrolyzer

An electrolyzer is a system that forces a redox reaction in a medium by applying electrical energy. When applying direct current to water, water is decomposed into hydrogen and oxygen, see chemical formula (3-13). Hydrogen is forming on the cathode and oxygen on the anode. In space life support systems water electrolysis is often considered to produce oxygen for the crew and hydrogen for a Sabatier reactor.

$$2H_2O + energy \rightarrow 2H_2 + O_2 \tag{3-13}$$

According to formula (3-13), 1 kg of water is converted to 0.112 kg of hydrogen and 0.888 kg of oxygen.

Within the model, the electrolyzer is implemented as shown in the frame in Figure 3-56. The electrolyzer activity is controlled by the need of oxygen, when the O_2 storage stock is below O_2 storage lower threshold. Furthermore, the electrolyzer can only work when there is enough water available. That is the case when the value of the potable water storage stock is greater than the potable water storage lower threshold value.

All formulas and values of the electrolyzer model are shown in Appendix9.6.2.
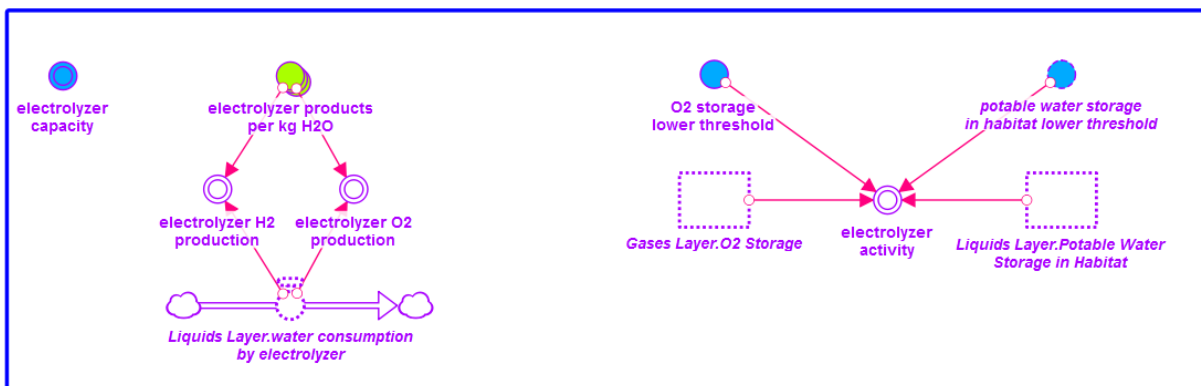
Figure 3-56: Electrolyzer frame.

3.9.4 Sabatier Reactor

The Sabatier reaction is an exothermic reaction at high temperatures (300-400 °C) in which carbon dioxide reacts with hydrogen under the presence of a catalyst to methane, water and heat, see formula (3-14). Current space life support systems use Sabatier reactors combined with an electrolyzer to recover oxygen from carbon dioxide.

$$CO_2 + 4H_2 \rightarrow CH_4 + 2H_2O + energy \tag{3-14}$$

Within the model the Sabatier reactor is implemented as shown in the frame in Figure 3-57. The Sabatier reactor is active when the CO_2 storage stock value is greater than the upper threshold and when there is enough hydrogen, H_2 storage stock greater than H_2 storage lower threshold.

All formulas and values of the Sabatier reactor model are shown in Appendix 9.6.3.
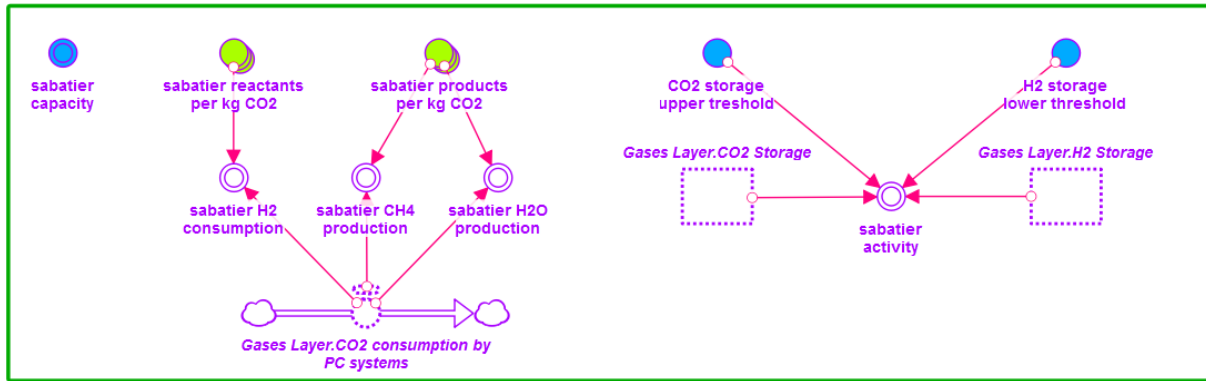
Figure 3-57: Sabatier reactor frame.

3.9.5 Condensing Heat Exchanger

A condensing heat exchanger (CHX) is a system that condensates the humidity of the atmosphere or of a gas stream on a cold surface. In closed systems such as a space station or a habitat the crew and plants emit water to the atmosphere through transpiration and perspiration. CHX systems are used to recover that water and to control the relative.

The current model has two CHX, one for the habitat and one for the greenhouse. Figure 3-58 shows the implementation. Each system has a defined maximum capacity. The actual water that is removed from the habitat atmosphere is equal to the sum of the insensible and sensible water loss of the crew. The water removal in the greenhouse is always equal to the water transpired by the plants. This setup assures that the relative humidity in the habitat and in the greenhouse is within the nominal requirements.

The formulas for the CHX frame can be found in Appendix 9.6.4.
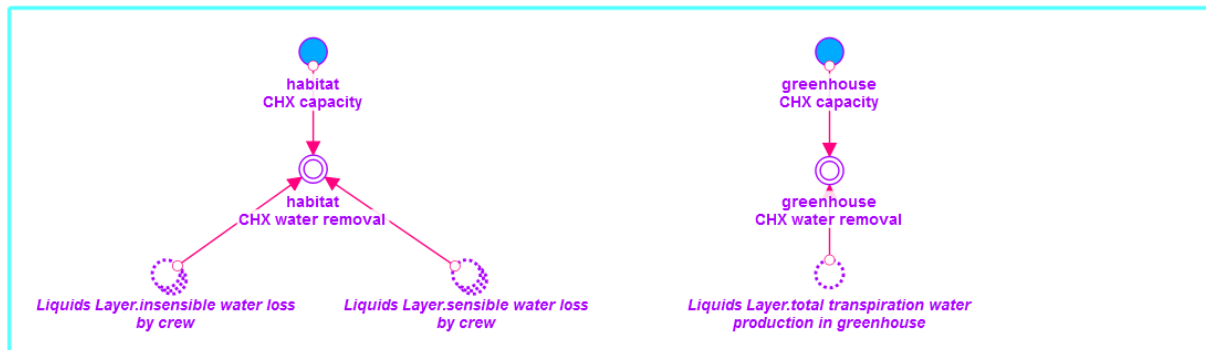
Figure 3-58: Habitat and greenhouse CHX frame.

3.9.6 VPCAR

The Vapor Phase Catalytic Ammonia Removal (VPCAR) is a water recycling system based on a phase change process. VPCAR has the advantage over other technologies such as vapor compression distillation or TIMES that it does not need expendable chemicals. Consequently VPCAR is more mass efficient and does not need resupply of expendables (Wydeven, 1988).

VPCAR systems evaporate wastewater to water vapor which is then condensed back to water. Volatiles that do not evaporate remain in the VPCAR and are discarded. Some volatiles (e.g. ammonia) evaporate together with the water. These volatiles are processed by the two

catalyst beds of the VPCAR to produce nitrogen, oxygen and carbon dioxide (Wydeven, 1988).

Figure 3-59 shows the VPCAR frame in the physical-chemical systems module. The implemented VPCAR has a defined capacity and its activity is controlled by thresholds of the potable water storage and the wastewater storage. The volatile processing and therefore the production of gases as mentioned above are not implemented in the model for simplification.

Appendix 9.6.5 shows the formulas of the VPCAR frame.
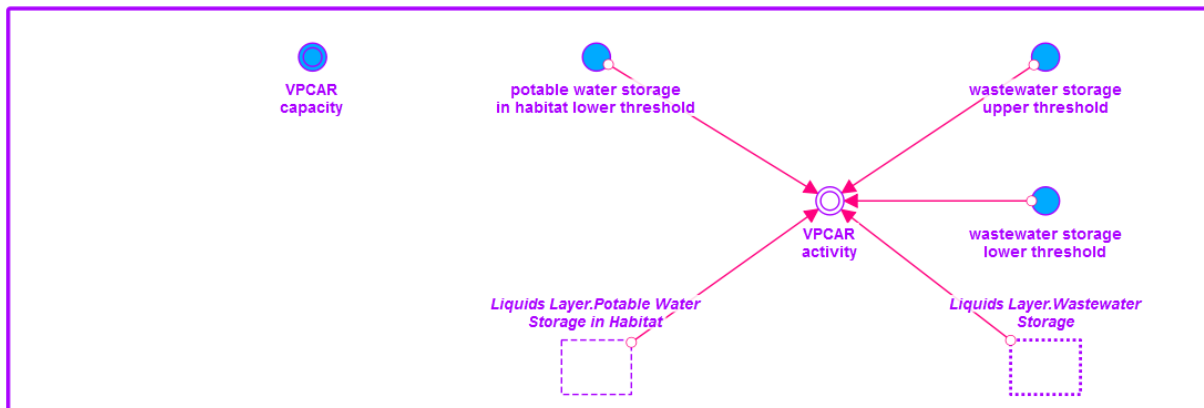
Figure 3-59: VPCAR frame.

3.9.7 Oxygen and Carbon Dioxide Separator

The model setup of the Gases Layer (see Chapter 3.4.2) requires the implementation of an oxygen separator and a carbon dioxide separator, because the habitat and the greenhouse have separated atmospheres.

The carbon dioxide separator deals with the carbon dioxide produced by the crew which would otherwise raise the level in the habitat atmosphere to a lethal level. The carbon dioxide separated from the habitat atmosphere is either moved to the greenhouse or the carbon dioxide storage. Several carbon dioxide separation systems such as molecular sieves, electrochemical depolarization and amine resin beds exist (Wydeven, 1988). There is no need to select a specific technology for the simulation, because the carbon dioxide separator within the model is only defined by the amount of carbon dioxide separated per day, see right side in Figure 3-60.

The oxygen separator is necessary in order to deal with the excess oxygen produced by the plants in the greenhouse. Space greenhouses typically have a large cultivation area in a small volume. The oxygen produced by the plants, when not removed, would increase the oxygen partial pressure inside the greenhouse to a level which would result in an increased fire risk. In current life support system architectures (e.g. ISS) without a greenhouse an oxygen separator is generally not necessary. Consequently the amount of available technologies is limited. Graf (2011) describes an oxygen separator system which separates oxygen from the cabin air in order to produce pure oxygen for EVAs. In principle the same system can be used to separate excess oxygen out of the greenhouse atmosphere.

The oxygen separator implemented in the model is shown in the left half of Figure 3-60. The system is only defined by its separation capacity per day. The activity of the oxygen separator is controlled by the oxygen partial pressure of the habitat and the greenhouse. The sys-

tem is active when the oxygen partial pressure of the habitat atmosphere is smaller than the nominal requirement or when the oxygen partial pressure of the greenhouse atmosphere is above the nominal requirement.

All formulas related to the oxygen and carbon dioxide separators are shown in Appendix 9.6.6.
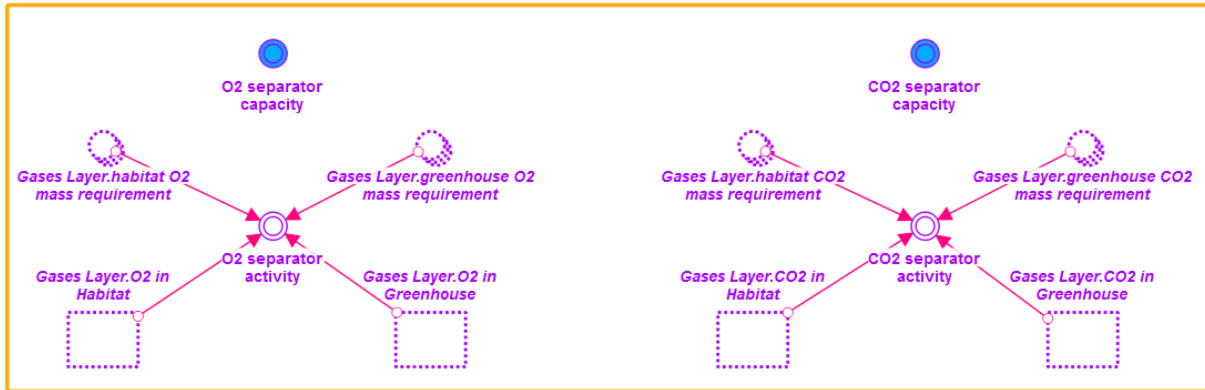
Figure 3-60: Oxygen and carbon dioxide separator frame.

3.9.8 Inedible Biomass Processor

The inedible biomass processor has the task to recycle the inedible biomass produced by the greenhouse. The processor is modeled as an optimal incineration process and is therefore similar to the incinerator described in Chapter 3.9.2. The difference to the incinerator is that the inedible biomass processor does not produce any carbon monoxide or methane. All carbon bound in the inedible biomass is converted to carbon dioxide through oxidation with pure oxygen, see formula 3-15. The hydrogen part of the inedible biomass is combined with oxygen to produce water.

$$inedible\ biomass + O_2 \rightarrow CO_2 + H_2O \tag{3-15}$$

Figure 3-61 shows the implementation of the inedible biomass processor within the model. The composition of the inedible biomass is defined by the plant parameters of the MEC model. Each crop has a different fraction of carbon in its biomass. With the assumption, that all carbon is converted to carbon dioxide one can calculate the amount of oxygen consumed and the amount of water and carbon dioxide produced by the inedible biomass processing.

The inedible biomass processor has a defined capacity. The activity of the system is controlled by a number of thresholds (right side in Figure 3-61). The inedible biomass processor is activated when the harvested inedible biomass storage reaches a defined upper threshold or the carbon dioxide storage reaches a lower threshold. Furthermore, there must be enough oxygen available for the process without putting the crew at risk. This condition is met as long as the O2 storage is higher than its lower threshold.

The formulas related to the inedible biomass processor are shown in Appendix 9.6.7.
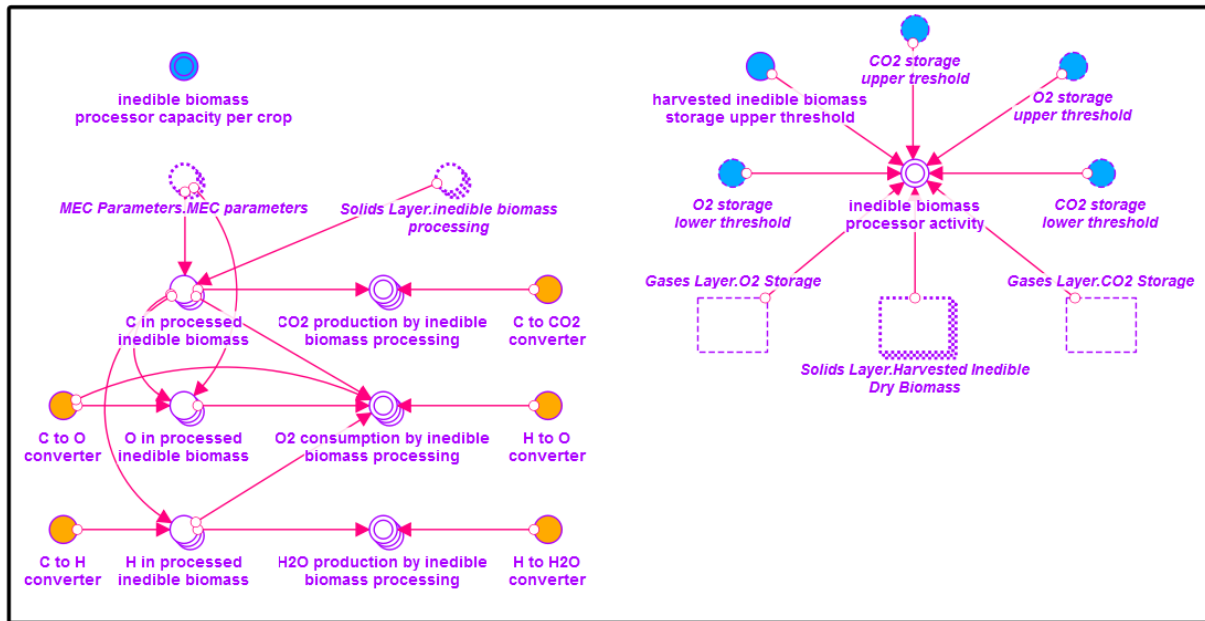
Figure 3-61: Inedible biomass processor frame.

3.10 Overview of Model Inputs

The developed model requires a set of inputs in order to simulate a desired scenario. The inputs are divided into constant simulation inputs and flexible simulation inputs. The flexible simulation inputs are variables which need to be adjusted for each simulation scenario individually. The values for these inputs are explained within the description of the different simulation scenarios in Chapter 4.

The constant simulation inputs are variables which can be kept constant for most scenarios and are usually based on standards and requirements documents such as NASA's Life Support Baseline Values and Assumptions Document (Anderson *et al.*, 2015). Table 3-13, Table 3-14 and Table 3-15 show all constant simulation inputs including variable type, model part, value and unit. References are given, when necessary. The values given for stocks are the initial values at simulation start.

Table 3-13: Constant simulation inputs (1).

Variable Name	Variable Type	Model Part	Value	Unit	Reference
habitat O2 partial pressure requirement	Converter, arrayed	Gases layer - crew	min: 18 nom: 21 max: 23.1	kPa	Anderson *et al.* (2015)
habitat nominal pressure	Converter	Gases layer - crew	101.325	kPa	Anderson *et al.* (2015)
habitat CO2 partial pressure requirement	Converter, arrayed	Gases layer - crew	min: 0.031 nom: 0.4 max: 0.71	kPa	Anderson *et al.* (2015)
greenhouse O2 partial pressure requirement	Converter, arrayed	Gases layer - greenhouse	min: 18 nom: 21 max: 23.1	kPa	Anderson *et al.* (2015)
greenhouse nominal pressure	Converter	Gases layer - greenhouse	101.325	kPa	Anderson *et al.* (2015)

Table 3-14: Constant simulation inputs (2).

Variable Name	Variable Type	Model Part	Value	Unit	Reference
greenhouse CO2 partial pressure requirement	Converter, arrayed	Gases layer - greenhouse	min: 0.060795 nom: 0.101325 max: 0.141855	kPa	Based on the experience of the author.
thirst threshold	Converter	Liquids layer - crew	0.005	-	Hellerstein (1993)
total wastewater production by inedible biomass processing	Flow	Liquids layer - physical-chemical systems	1000	kg/d	n.a
habitat nominal atmosphere temperature	Converter	Liquids layer - humidity conversion	293	K	Anderson *et al.* (2015)
habitat RH requirement	Converter, arrayed	Liquids layer - humidity conversion	min: 0.25 nom: 0.6 max: 0.7	-	Anderson *et al.* (2015)
greenhouse RH requirement	Converter, arrayed	Liquids layer - humidity conversion	0.6/0.7/0.8	-	Anderson *et al.* (2015)
greenhouse nominal atmosphere temperature	Converter	Liquids layer - humidity conversion	298	K	Anderson *et al.* (2015)
food production out of edible dry biomass	Flow, arrayed	Solids layer - edible biomass harvest	1000	kg/d	n.a.
activity MET values	Converter arrayed	Crew model - activity database	See Table 9-6.	MET	McArdle *et al.* (2014)
CM day sets	Converter, arrayed	Crew model - crew member day database	See Table 9-7.	min	n.a.
insensible H2O loss over skin per kcal	Converter	Crew model - crew water demand	0.030/100	kg/kcal	Hellerstein (1993)
insensible H2O loss over lungs per kcal	Converter	Crew model - crew water demand	0.015/100	kg/kcal	Hellerstein (1993)
sensible H2O loss over sweating per kcal	Converter	Crew model - crew water demand	0.010/100	kg/kcal	Hellerstein (1993)
H2O loss over stool per kcal	Converter	Crew model - crew water demand	0.005/100	kg/kcal	Hellerstein (1993)
H2O loss over urine per kcal	Converter	Crew model - crew water demand	0.050/100	kg/kcal	Hellerstein (1993)
CM BVAD fecal solid waste production	Converter	Crew model - solids production	0.032	kg/ (people*d)	Anderson *et al.* (2015)

Table 3-15: Constant simulation inputs (3).

Variable Name	Variable Type	Model Part	Value	Unit	Reference
CM BVAD fecal water production	Converter	Crew model - solids production	0.1	kg/ (people*d)	Anderson *et al.* (2015)
CM BVAD urine solid waste	Converter	Crew model - solids production	0.059	kg/ (people*d)	Anderson *et al.* (2015)
CM BVAD urine water production	Converter	Crew model - solids production	1.6	kg/ (people*d)	Anderson *et al.* (2015)
CM BVAD perspiration solid waste	Converter	Crew model - solids production	0.018	kg/ (people*d)	Anderson *et al.* (2015)
CM BVAD respiration and perspiration water production	Converter	Crew model - solids production	1.9	kg/ (people*d)	Anderson *et al.* (2015)
misc plant properties	Converter, arrayed	Greenhouse model - other plant properties	See Table 9-26.	-	Anderson *et al.* (2015), nutritionvalue.org
incineration reactants per kg dry waste	Converter, arrayed	Physical-chemical systems - Incinerator formulas	1.969	-	Anthony and Hintze (2014)
incineration products per kg dry waste	Converter, arrayed	Physical-chemical systems - Incinerator formulas	See Table 9-27.	-	Anthony and Hintze (2014)
electrolyzer products per kg H2O	Converter, arrayed	Physical-chemical systems - electrolyzer formulas	See Table 9-28.	-	n.a.
sabatier reactants per kg CO2	Converter, arrayed	Physical-chemical systems - Sabatier reactor formulas	0.18322	-	n.a.
sabatier products per kg CO2	Converter, arrayed	Physical-chemical systems - Sabatier reactor formulas	See Table 9-29.	-	n.a.

3.11   Model Validation

Greenhouse model

The greenhouse model has been verified against the original MEC. Therefore the values shown in Table 3-16 have been used to calculate the crop growth rates for each of the nine implemented crop species. Table 3-17 shows the crop growth graph for peanut of the original MEC model in the left column and the graph in the right column generated by the author's model. One can see that the greenhouse model accurately reproduces the original MEC val-

ues. The model graph has a smoother look, because more values per time step are being calculated than in the original MEC model.

The model has also been validated for the other eight crops. The graphs of the described model all matches those of the MEC model, but only the peanut graphs are shown here.

Table 3-16: Input values for the MEC model validation according to Jones *et al.* (2002).

Crop	H [h]	PPF [µmol/(m²*s)]	CO2 [ppm]	light/dark temperature [°C]	plants per m²
Dry Bean	12	600	1200	26/22	7
Lettuce	16	300	1200	23/23	19.2
Peanut	12	600	1200	26/22	7
Potato	12	655	1200	20/16	6.4
Rice	12	1200	1200	29/21	200
Soybean	12	800	1200	26/22	35
Sweet Potato	18	600	1200	28/22	6.3
Tomato	12	500	1200	26/22	6.3
Wheat	20	1400	1200	23/23	720

Table 3-17: Comparing the output of the original model and its implementation in Stella.

Crop growth rates according to Jones *et al.* (2002)	Crop growth rates of the described Stella model
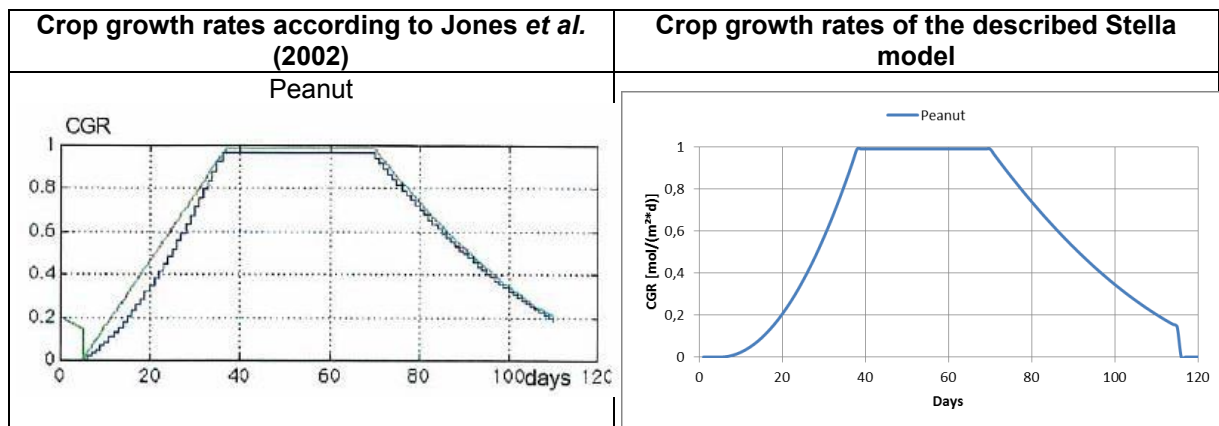
Model closure

The model has flows at certain spots which do not connect to another model part but rather end in a sink or start from a source outside the model border. This is the case, for example, for the oxygen consumption and carbon dioxide production by the crew inside the gases layer module. It is therefore important to check the model closure with respect to the fundamental elements carbon, oxygen and hydrogen which make up all the material in the model. A closed model does not lose or gain any carbon, oxygen or hydrogen throughout the whole simulation. A few additional model building blocks have been added to the model to perform the necessary calculations, which are described in the following paragraphs.

In principle one has to sum up all the carbon, oxygen and hydrogen contained in the whole system and calculate the sums every time step to see whether they change or not. Table 3-18 shows the different stocks of the model that contain carbon, oxygen and hydrogen. For compounds of multiple elements such as carbon dioxide, water and food the respective molecular ratios of the elements need to be taken into account for the calculations.

The model closure has been validated in a simulation similar to the one described in Chapter 4.3. This simulation uses all model parts and calculates the life support system behavior of a

Mars surface habitat which includes a greenhouse and a crew of six for mission duration of 500 days.

Table 3-19 shows the results of the model closure validation simulation. In general one can see that the model generates additional elements when performing the calculations. Carbon and hydrogen are almost in balance with only small surpluses between the values at mission start and mission end. Oxygen shows a higher surplus at mission end compared to the other two elements. Since the other two elements are almost in balance the larger surplus of oxygen might be related to a minor imbalance in the calculation of the respiratory quotient of the crew. This could result in a minor imbalance between consumed oxygen and produced carbon dioxide by the crew. The calculation of the respiratory quotient however looks plausible and no error could be identified.

Table 3-18: Model stocks that contain carbon, oxygen and hydrogen.

Carbon (C)	Oxygen (O)	Hydrogen (H)
CO Storage	CO Storage	
CH4 Storage		CH4 Storage
CO2 Storage	CO2 Storage	
CO2 in Habitat	CO2 in Habitat	
CO2 in Greenhouse	CO2 in Greenhouse	
	O2 Storage	
	O2 in Habitat	
	O2 in Greenhouse	
		H2 Storage
	Potable Water Storage in Greenhouse	Potable Water Storage in Greenhouse
	Potable Water Storage in Habitat	Potable Water Storage in Habitat
	Wastewater Storage	Wastewater Storage
	Water Accumulated in Harvested Edible Biomass	Water Accumulated in Harvested Edible Biomass
	Water Accumulated in Harvested Inedible Biomass	Water Accumulated in Harvested Inedible Biomass
	Water in Greenhouse Atmosphere	Water in Greenhouse Atmosphere
	Water in Habitat Atmosphere	Water in Habitat Atmosphere
	Water Accumulated in Living Plant Biomass	Water Accumulated in Living Plant Biomass
	Water in Crew	Water in Crew
Resupply Food Storage	Resupply Food Storage	Resupply Food Storage
Crew Metabolic Solids	Crew Metabolic Solids	Crew Metabolic Solids
Misc Solids Storage	Misc Solids Storage	Misc Solids Storage
Solid Waste Storage in Habitat	Solid Waste Storage in Habitat	Solid Waste Storage in Habitat
Inedible Dry Biomass in Plants	Inedible Dry Biomass in Plants	Inedible Dry Biomass in Plants
Edible Dry Biomass in Plants	Edible Dry Biomass in Plants	Edible Dry Biomass in Plants
Crop Food Storage	Crop Food Storage	Crop Food Storage
Harvested Inedible Dry Biomass	Harvested Inedible Dry Biomass	Harvested Inedible Dry Biomass
Harvested Edible Dry Biomass	Harvested Edible Dry Biomass	Harvested Edible Dry Biomass

In general the model has a high degree of closure with a small daily deviation of 0.0282 kg/d (carbon, oxygen and hydrogen combined). When comparing this deviation to the total amount of carbon, oxygen and hydrogen contained in the model stocks, the model gains $2.379*10^{-4}$ % of its original total mass per day. The deviations are fairly constant throughout the whole simulation duration and consequently add up over time. The total model closure

calculated after 500 simulation days is 99.881 %. This value is good enough for the simulations envisioned for this thesis.

Table 3-19: Results of the model closure validation.

	Carbon (C)	Oxygen (O)	Hydrogen (H)
Amount at the start of the simulation [kg]	2574.323	8450.524	812.180
Amount at the end of the simulation [kg]	2574.352	8464.552	812.183
Difference [kg]	+0.029	+14.048	+0.003
Difference [%]	$+1.127*10^{-3}$	$+1.662*10^{-1}$	$+3.694*10^{-4}$
Deviation [kg/d]	$+5.80*10^{-5}$	$+2.81*10^{-2}$	$+6.00*10^{-6}$

4 Simulations

4.1 Outline

The following subchapters describe in detail the simulations performed for this dissertation. All simulations use the model described in the previous chapter, if not stated otherwise. Four simulation cases have been investigated for this dissertation. Figure 4-1 shows the four cases and their corresponding subchapters. Chapter 4.2 describes the simulations performed to understand the behavior of the MEC crop model and the effects of varying input parameters. The result of this chapter is the determination of nominal input parameters and hence nominal output values of the crop model. The second simulation case is about a Mars surface habitat life support system architecture which is based on reference documents, Chapter 4.3. First the behavior of the system under nominal operation has been investigated and then a number of sensitivity and perturbation analyses have been performed in order to gain a better understanding of the overall system behavior and its strength and weaknesses. One result of these simulations is the large impact of the greenhouse production schedule and the greenhouse startup phase on the various mass flows. Consequently, a number of simulations have been executed to further investigate the greenhouse startup phase and production schedule. These simulations are described in Chapter 4.5. The final simulation case is about a habitat with a full nutrition greenhouse, Chapter 4.4. These simulations are used to study the life support system behavior of a habitat with a high independency from resupply missions.

The following four subchapters describe independent analysis and simulations performed on certain aspects of a hybrid life support system. The different simulation cases however always incorporate findings and improvements from previous simulations and subchapters, as indicated by the arrows in Figure 4-1.
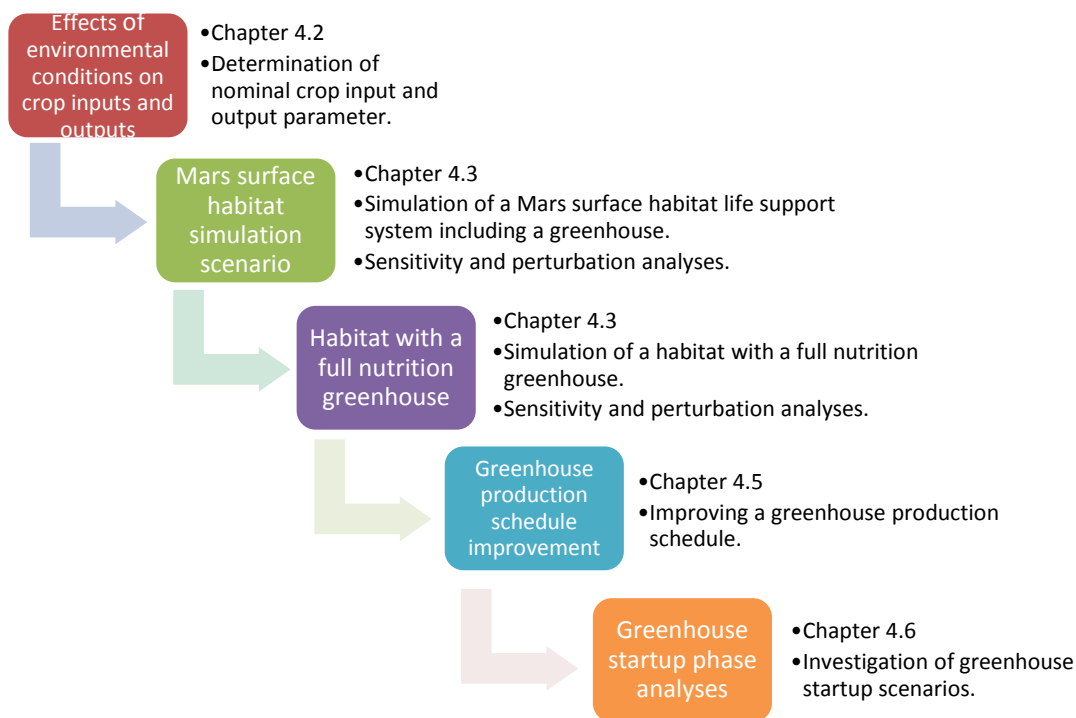
Figure 4-1: Overview of the subchapter structure of Chapter 4.

4.2 Effects of Environmental Conditions on Crop Inputs and Outputs

4.2.1 Description

Greenhouses play a central role in hybrid life support systems. The input and output mass flows of a greenhouse designed to produce a significant amount of food for the crew are larger than those of the crew itself. The productivity of the plants inside the greenhouse strongly depends on the environmental conditions. Studying the effects of different environmental conditions on the inputs and outputs of the greenhouse are therefore essential. The simulations explained in this chapter are only using the greenhouse model as described in Chapter 3.8. All nine available crops are investigated.

A number of parameters are defined as constants for the simulations:

- The cultivation area is set to 1 m² for each crop species.
- The photoperiod H is set to the nominal value H0 for each crop species.
- The relative humidity (RH) inside the greenhouse is set to 0.75.
- The temperature during illumination (Tlight) is set to the nominal value for each crop species.
- The growth cycles of all crop species include a germination period of five days at the beginning of the growth cycle.

The light intensity (PPF) and the CO_2 concentration are varied within the limits of each crop species as defined in Table 3-9. The variations of these two parameters strongly affect the greenhouse model inputs and outputs as shown in the following subchapters.

The CO_2 level has been varied for all crop species in four steps (330, 700, 1000 and 1300 ppm) within the boundaries of the model. The boundaries for the variable PPF are different for the nine crop species. Therefore, each crop species has different intervals of PPF assigned for the simulations, see Table 4-1.

Table 4-1: Simulation intervals for all nine crop species.

Crop species	CO2 level simulation intervals in ppm	PPF simulation intervals in µmol/(m²*s)
Dry bean	330; 700; 1000; 1300	200; 400; 600; 800; 1000
Lettuce	330; 700; 1000; 1300	200; 300; 400; 500
Peanut	330; 700; 1000; 1300	200; 400; 600; 800; 1000
Rice	330; 700; 1000; 1300	200; 400; 600; 800; 1000; 1500; 2000
Soybean	330; 700; 1000; 1300	200; 400; 600; 800; 1000
Sweet Potato	330; 700; 1000; 1300	200; 400; 600; 800; 1000
Tomato	330; 700; 1000; 1300	200; 400; 600; 800; 1000
Wheat	330; 700; 1000; 1300	200; 400; 600; 800; 1000; 1500; 2000
White Potato	330; 700; 1000; 1300	200; 400; 600; 800; 1000

4.2.2 Effects on DCG, DOP, TCB and Water Accumulation Rate

The daily oxygen production (DOP), the total crop biomass (TCB) and the water accumulation rate are all functions of the daily carbon gain (DCG). While all of the mentioned variables are simulated for each variable combination, only the graphs of the daily carbon gain are shown in the following. All effects of variations in PPF and CO_2 explained on the daily carbon gain also apply for the daily oxygen production, total crop biomass and water accumulation rate of the different crop species.

The graphs in Figure 4-2 to Figure 4-6 show the daily carbon gain for each crop species for all combinations of CO_2 and PPF. In general one can say that an increase in CO_2 or PPF leads to a higher daily carbon gain. However, the increase is not linear and with higher values of CO_2 and PPF the increase levels off indicating the approach to the maximum production capacity. The effect of increased CO_2 alone while keeping the PPF constant is relatively low compared to the effects of increased PPF for a constant CO_2 level. This indicates that the more limiting factor to a high daily carbon gain is the light energy provided to the plants. However, the combination of the highest allowed PPF and the highest allowed CO_2 usually achieves the highest daily carbon gain.

Lettuce has the lowest daily carbon gain of all nine crop species, which results from the relatively small size of the plants and therefore their smaller total production capacity compared to the other eight species. Furthermore, the upper limit for the PPF with 500 µmol/(m²*s) is much lower than for the other plants. Dry bean, lettuce, tomato, white potato, peanut and soybean all have their highest daily carbon gain values between 6.5 and 11 g/(m²*d), while sweet potato has a highest daily carbon gain of around 20 g/(m²*d). Rice and wheat have an even higher upper limit of daily carbon gain of 27 and 35 g/(m²*d) respectively, because of the higher limit for the PPF input of 2000 µmol/(m²*s).

In general an increase of CO_2 from 1000 to 1300 ppm for a defined PPF level is very small or almost non-existent, e.g. lettuce daily carbon gain from 6.37 to 6.48 g/(m²*d). This corresponds very well with the typically assumed CO_2 level for closed environment agriculture of 1000 ppm.

White potato, peanut and soybean show a different behavior for high PPF (600; 800; 1000) then the other crop species. Their increase in daily carbon gain from 600 to 800 µmol/(m²*s) is very small and from 800 to 1000 µmol/(m²*s) almost negligible. This indicates that those three plant species have already approached their maximum production capacity at medium light intensities.

The consequences of the findings in the daily carbon gain outputs for varying CO_2 and PPF levels are evaluated and explained in Chapter 4.2.5.
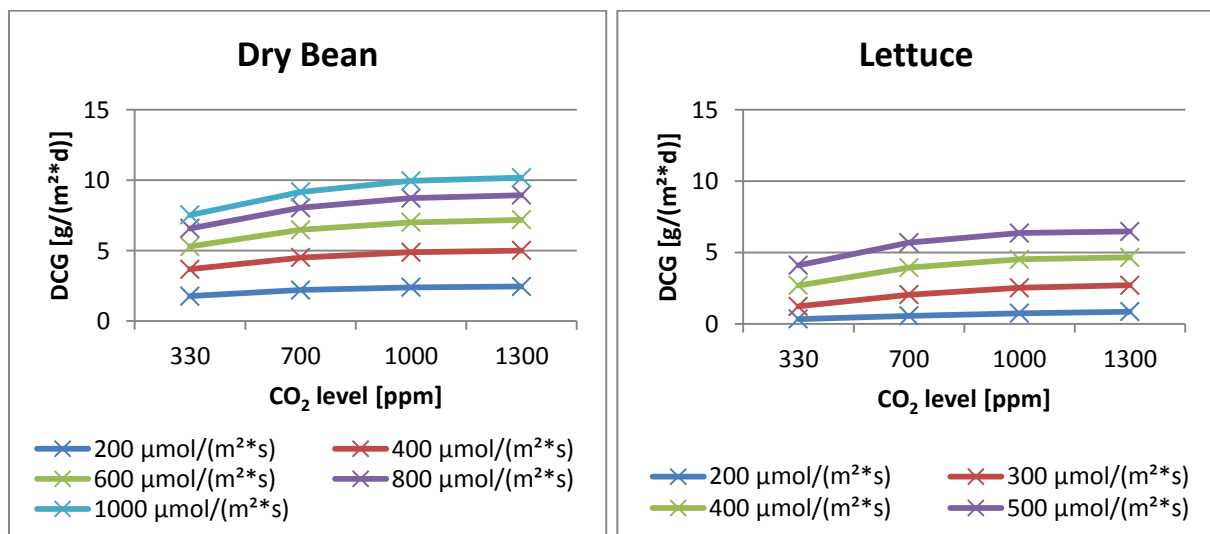
Figure 4-2: Dry Bean and Lettuce daily carbon gain (DCG) average over one growth cycle (including germination) for different PPF [µmol/(m²*s)] and CO_2 [ppm] values.
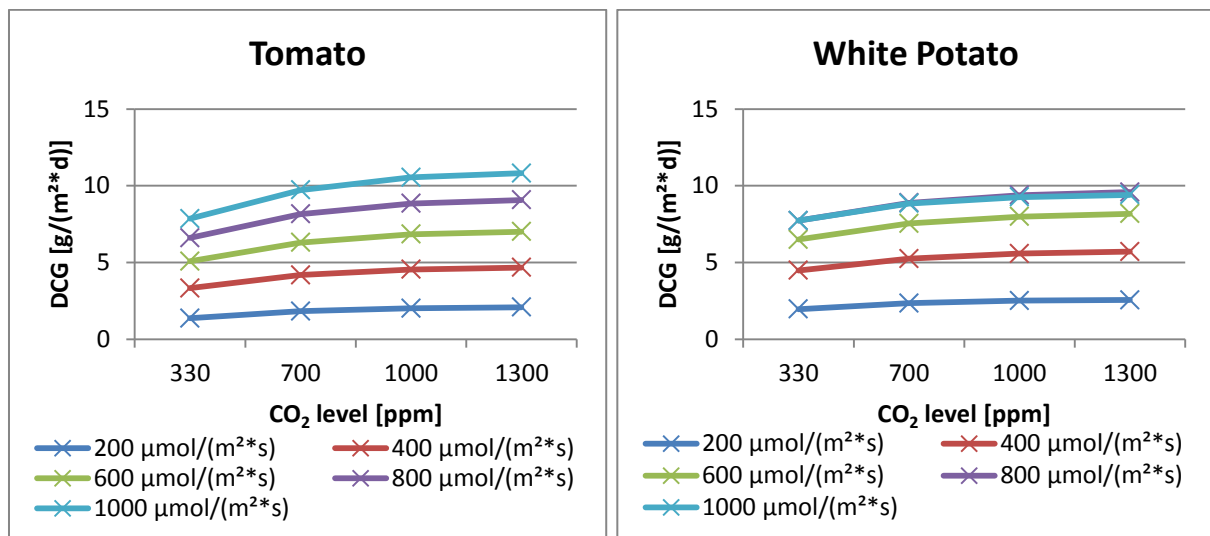
Figure 4-3: Tomato and White Potato daily carbon gain (DCG) average over one growth cycle (including germination) for different PPF [µmol/(m²*s)] and CO$_2$ [ppm] values.
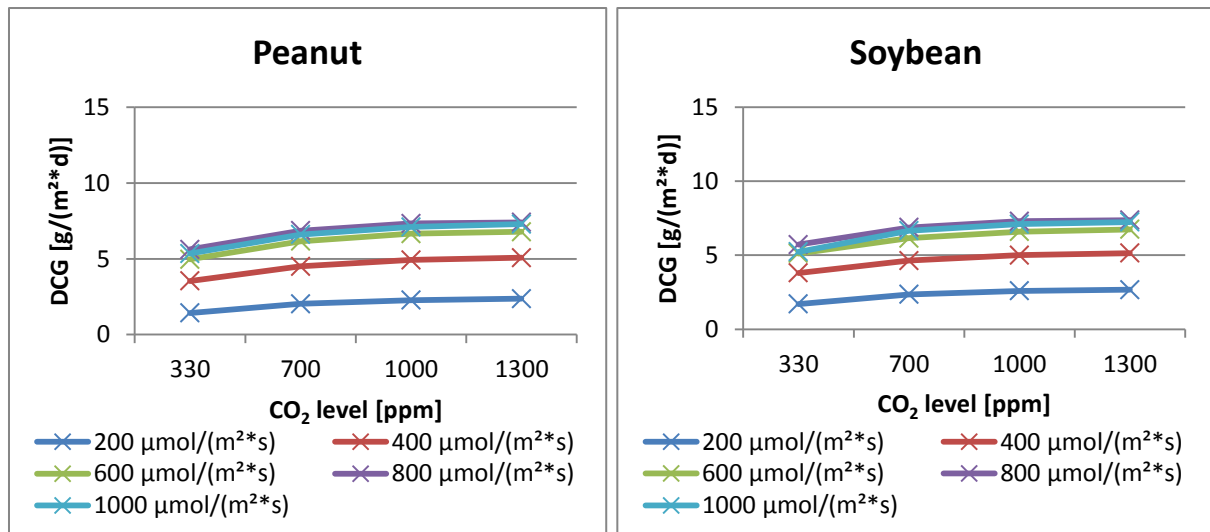
Figure 4-4: Peanut and Soybean daily carbon gain (DCG) average over one growth cycle (including germination) for different PPF [µmol/(m²*s)] and CO$_2$ [ppm] values.
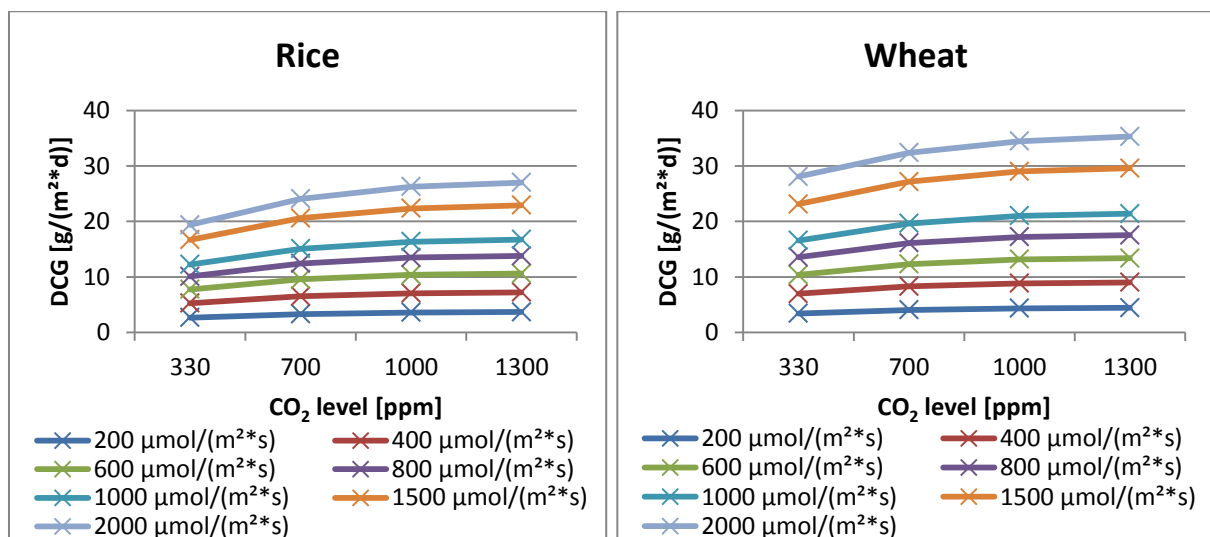
Figure 4-5: Rice and Wheat daily carbon gain (DCG) average over one growth cycle (including germination) for different PPF [µmol/(m²*s)] and CO$_2$ [ppm] values.
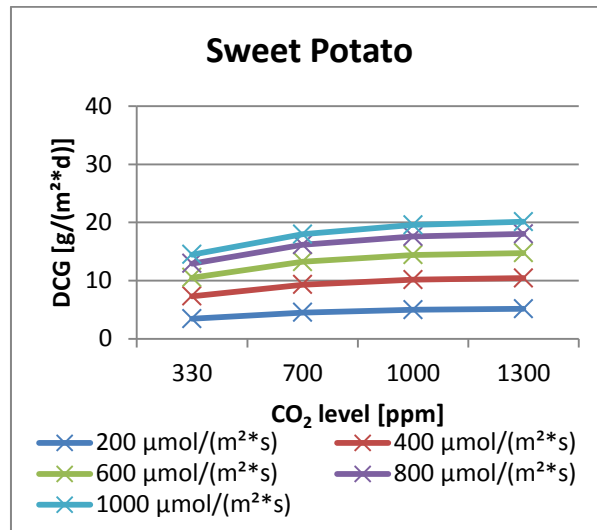
Figure 4-6: Sweet Potato daily carbon gain (DCG) average over one growth cycle (including germination) for different PPF [μmol/(m²*s)] and CO₂ [ppm] values.

4.2.3 Effects on DTR

The daily transpiration rate (DTR) is not a function of daily carbon gain, but a function of PPF/CO₂. Consequently, the daily transpiration rate graphs (Figure 4-7 to Figure 4-11) decline with increasing PPF and CO₂ levels. Similar to the daily carbon gain behavior, dry bean, lettuce, tomato, white potato, peanut and soybean form the groups of crops having a much lower daily transpiration rate than sweet potato, rice and wheat. Also similar to the daily carbon gain calculations, the daily transpiration rate values for white potato, peanut and soybean at high PPF levels show almost now difference between 600, 800 and 1000 μmol/(m²*s).

The consequences of the findings in the daily transpiration rate outputs for varying CO₂ and PPF levels are evaluated and explained in Chapter 4.2.5.
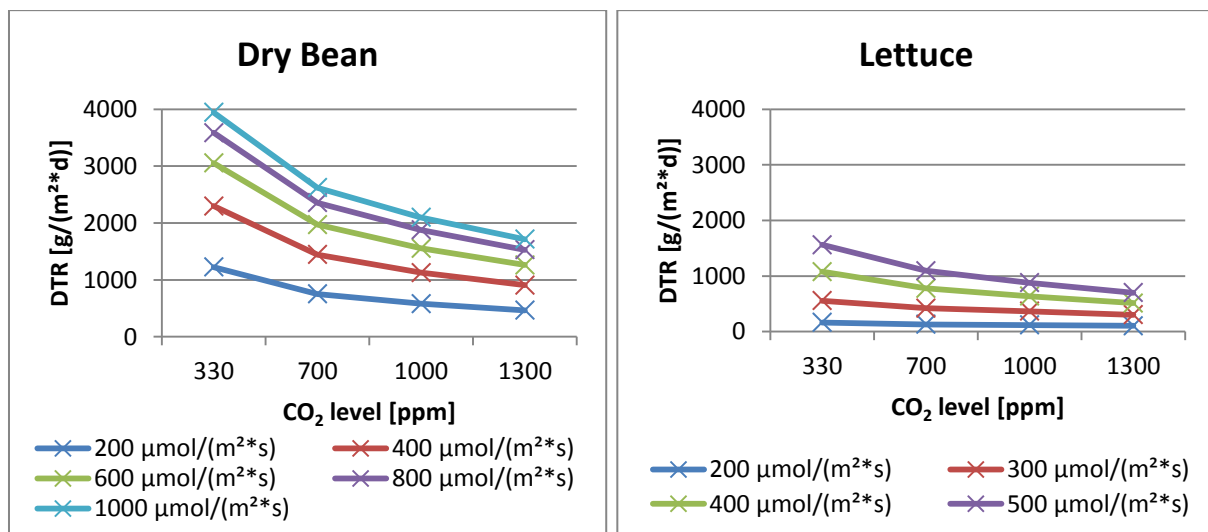
Figure 4-7: Dry Bean and Lettuce daily transpiration rate (DTR) average over one growth cycle (including germination) for different PPF [μmol/(m²*s)] and CO₂ [ppm] values.
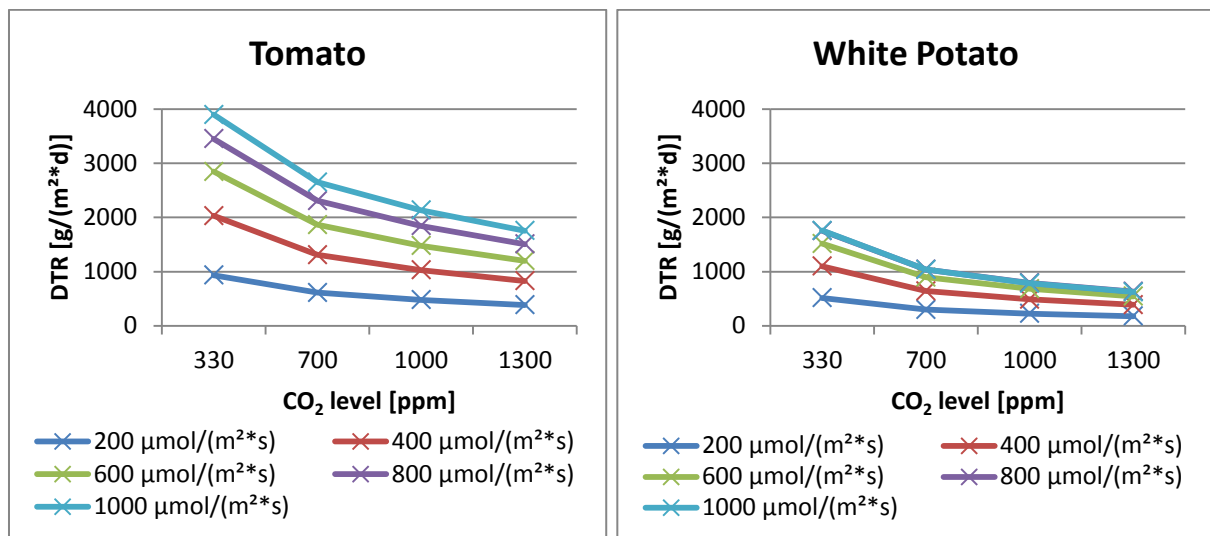
Figure 4-8: Tomato and White Potato daily transpiration rate (DTR) average over one growth cycle (including germination) for different PPF [μmol/(m²*s)] and CO₂ [ppm] values.
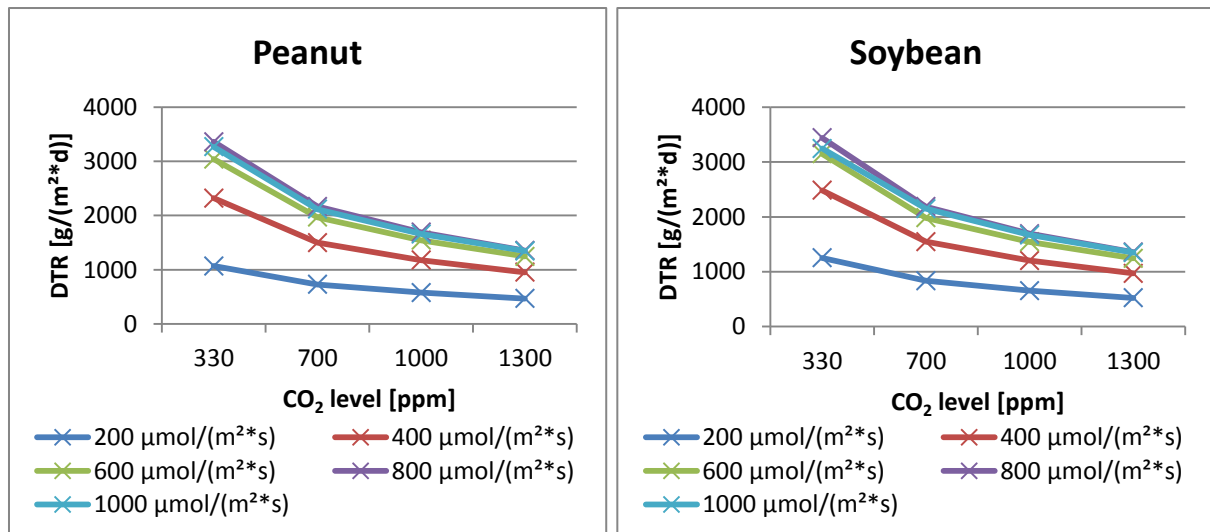
Figure 4-9: Peanut and Soybean daily transpiration rate (DTR) average over one growth cycle (including germination) for different PPF [μmol/(m²*s)] and CO₂ [ppm] values.
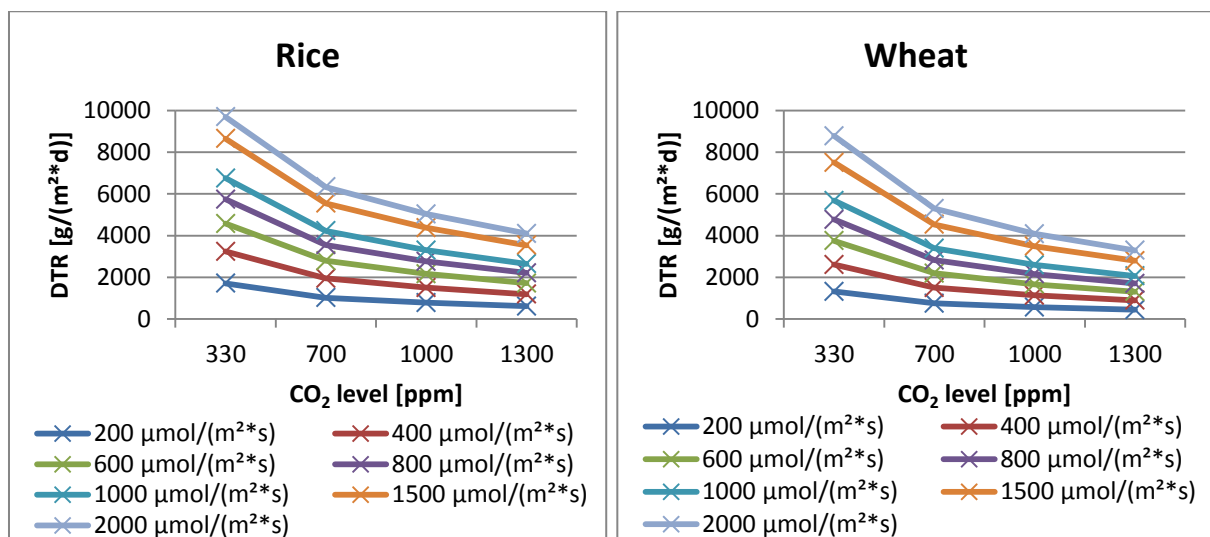
Figure 4-10: Rice and Wheat daily transpiration rate (DTR) average over one growth cycle (including germination) for different PPF [μmol/(m²*s)] and CO₂ [ppm] values.
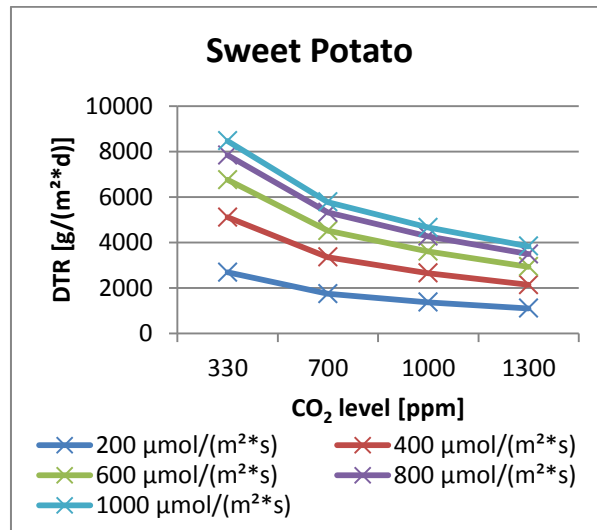
Figure 4-11: Sweet Potato daily transpiration rate (DTR) average over one growth cycle (including germination) for different PPF [μmol/(m²*s)] and CO₂ [ppm] values.

4.2.4 Determining Nominal CO₂ and PPF Values

The investigations of the two previous subchapters are used to determine a nominal value for the CO_2 and PPF level for the following simulations. The determination of the CO_2 level is relatively straightforward. As described before 1000 ppm is usually assumed as the nominal value for the CO_2 level of closed environment agriculture and consequently also defined as nominal value for the following simulations. While the model allows a higher level of up to 1300 ppm for all crop species, the increase in production from 1000 to 1300 ppm is rather small.

The determination of the nominal PPF level is more complicated and is performed for each crop species individually. Achieving high values of PPF is usually done with electrical illumination. Consequently an increase in PPF always means an increase in electrical energy demand of the greenhouse and therefore more launch mass for the energy supply system. However, an increase in delivered light energy means higher productivity per square meter and therefore a smaller greenhouse to produce the same amount of biomass. A smaller greenhouse means less launch mass and volume.

A trade-off of this kind is best done using the Equivalent System Mass (ESM) approach. The ESM is an evaluation tool for life support systems and is used to determine which of several system options with the same performance has the lowest launch mass for a defined mission. For the evaluation different performance values such as volume (V), power demand (P), cooling demand (C) and crew time (CT) are converted by multiplying with mission specific constants (V_{eq}, P_{eq}, C_{eq}, CT_{eq}) to a mass value and added to the actual system mass (M) to form the ESM value (see equation 4-1). The crew time calculation also includes the mission duration (D) (Levri *et al.*, 2003).

$$ESM = M + V * V_{eq} + P * P_{eq} + C * C_{eq} + CT * D * CT_{eq} \qquad (4\text{-}1)$$

The following analysis assumes a Mars surface mission as defined in Anderson *et al.* (2015) with the conversion parameters shown in Table 4-2. The values for the conversion parameters are taken from NASA's Baseline Values and Assumptions Document (BVAD), a com-

monly used collection of reference values for designing and planning human space flight mission Anderson *et al.* (2015).

Table 4-2: Mars surface mission ESM mass penalties (Anderson *et al.*, 2015).

V_{eq} [kg/m³]	P_{eq} [kg/kW]	C_{eq} [kg/kW]	CT_{eq} [kg/h]
215.5	87.0	146.0	0.465

Anderson *et al.* (2015) also provides ESM values per cultivation area for plant growth chambers, see Table 4-3.

Table 4-3: ESM values for plant growth chambers based on the BVAD (Anderson *et al.*, 2015).

Mass (M) [kg/m²]	Volume (V) [m³/m²]	Power (P) [kW/m²]	Cooling (C) [kW/m²]	Crew time (CT) [h/(m²*y)]
101.5	1.03	2.6	2.6	13.1

The thermal control value equals the power demand value. The power demand value consists of two components, an electrical illumination value (2.175 kW/m², assuming 1000 µmol/(m²*s)) and a value for the remaining equipment of the plant growth chamber (0.44 kW/m²). While the latter is adequate and is also used for the following analysis, the value for electrical illumination is outdated, because it is based on high-pressure sodium lamps. The rapidly evolving development of plant growth LED lamps results in a much lower power demand per square meter.

Equation 4-2 is used to determine the power demand per square meter for LED lamps (P_{LED}) for different illumination levels (PPF). Therefore the PPF value is converted to Watts per square meter and multiplied by the efficiency of converting electrical energy to light energy within PAR of the LED lamps (ρ_{PAR-e}).

$$P_{LED} = PPF * 0.22 \, (W * s)/\mu mol * \rho_{PAR-e} \tag{4-2}$$

Table 4-4 shows power demand values for plant growth LED lamps assuming a conversion efficiency of 0.35 which is well in the limits of current LED technology. Compared to the power demand value of 2.175 kW/m² for high-pressure sodium lamps at 1000 µmol/(m²*s), the value for LED lamps (0.629 kW/m²) is less than one third for the same light intensity.

Table 4-4: Power demand per square meter of LED lamps for different PPF level.

PPF [µmol/(m²*s)]	P_{LED} [kW/m²]
200	0.126
400	0.251
600	0.377
800	0.503
1000	0.629
1500	0.943
2000	1.257

The new power demand value P as a function of PPF is therefore calculated as the following:

$$P(PPF) = P_{LED}(PPF) + 0.44 \, kW/m^2 \tag{4-3}$$

With these assumptions equation 4-1 is modified to an ESM equation (equation 4-4) for the trade-off analysis between light intensity and greenhouse size to determine a nominal PPF

value for each crop species. Equation 4-4 calculates an ESM value per produced biomass as function of PPF:

$$\frac{ESM}{biomass}(PPF) = \left(M + V * V_{eq} + P(PPF) * P_{eq} + P(PPF) * C_{eq} + CT * D * CT_{eq}\right) * A(PPF) \quad (4\text{-}4)$$

The value A in equation 4-4 represents the cultivation area required to produce 1 kg of biomass. This value is crop specific and a function of PPF and can be determined from the DCG values mentioned before. The value D is usually the mission duration. However, for the following analysis this value represents the life cycle of each crop.

Table 4-5 shows as an example the calculation results for dry bean. One can see that when the PPF doubles, the power demand (P) also doubles because P has a linear dependency on PPF. The cultivation area (A) however has a non-linear dependency on PPF. The ESM values power and cooling are a function of PPF and A whereas the ESM values for mass, volume and crew time are a function of A alone. As a summary one can say that the positive effect of a reduced cultivation area (caused by an increased PPF) on the total ESM is greater than the negative effect of an increased power demand.

Table 4-5: Exemplary ESM calculation values for dry bean (D=68 d; CO_2= 1000 ppm).

PPF [μmol/(m²*s)]	P(PPF) [W/m²]	A(PPF) [m²]	ESM (power + cooling) [kg/kg_biomass]	ESM (mass + volume + crew time) [kg/kg_biomass]	ESM total [kg/kg_biomass]
200	125,71	2,73	359,27	884,74	**1244,01**
400	251,43	1,34	215,40	434,01	**649,41**
600	377,14	0,93	177,51	302,64	**480,15**
800	502,86	0,75	164,82	243,53	**408,35**
1000	628,57	0,66	163,86	213,63	**377,49**

Figure 4-12 and Figure 4-13 show the total ESM values as a function of PPF for all nine crop species of the MEC at a CO_2 level of 1000 ppm. The positive effect of an increased PPF is visible for all crops. White potato, peanut and sweet potato show a different behavior than the other plants because their lowest total ESM is not at the highest PPF value like for the other six crop species. This is caused by their production behavior which levels off faster to the maximum value as for the other plants.
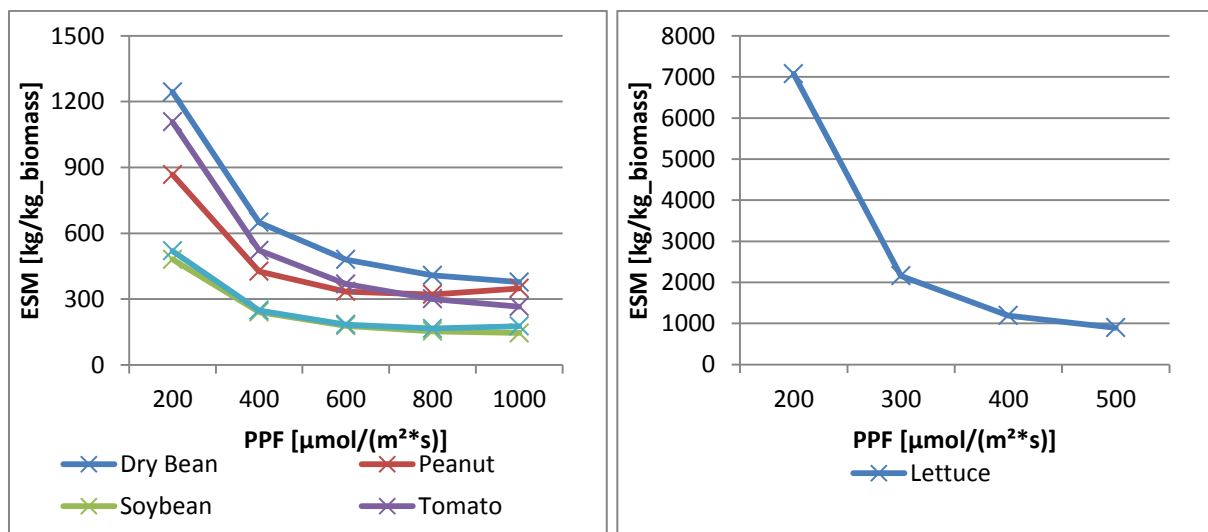
Figure 4-12: Total ESM values for dry bean, peanut, soybean, tomato, white potato and lettuce.
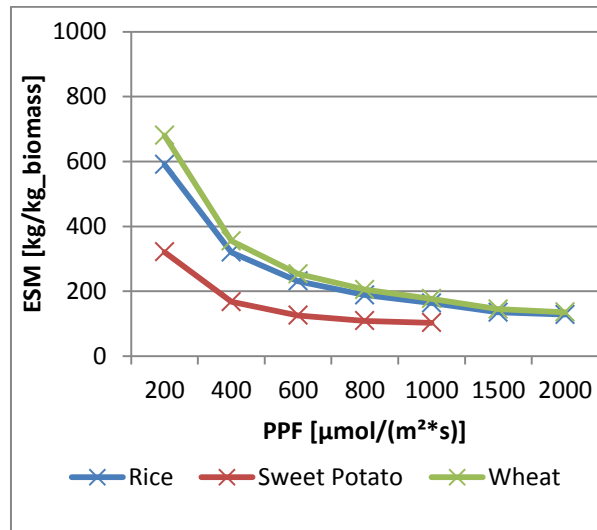
Figure 4-13: Total ESM values for rice, sweet potato and wheat.

One should note that the ESM total values shown here should not be used for plant selection evaluation. It is assumed here that all crops have the same structural mass and volume requirement per square meter. In a space greenhouse the structure of the different plant compartments will be adapted to the morphology and size of the crop cultivated. This would lead to different structure mass and volume penalty for each crop species. The crew time for tending plants is also different for each crop species (e.g. lower for lettuce, higher for tomato). However, these crop specific values for mass, volume penalty and crew time penalty are not available in current literature. With the current values, small plants (e.g. lettuce) have a much higher total ESM value than tall plants.

Although the total ESM values for all crop species are based on the same mass, volume and crew time values and therefore not ideal, the general trend of a lower total ESM with higher PPF remains the same. Using the results of the analysis, the nominal PPF levels for each crop species have been determined, see Table 4-6.

The nominal PPF level for lettuce is set to 300 µmol/(m²*s), although high PPF levels have a lower total ESM. At high PPF levels lettuce produces more biomass which reduces the ESM value. Nevertheless, experiments of the author with lettuce have shown that a PPF higher than 300 µmol/(m²*s) often results in thicker and harder leaves. The leaves also taste more bitter than usual, which is not desirable for a space greenhouse.

For peanut, sweet potato and white potato, the nominal PPF level is 800 µmol/(m²*s), because all three plants have their lowest total ESM at that value. The nominal PPF level for dry bean, soybean and tomato is also 800 µmol/(m²*s), although these plants have a slightly lower total ESM at 1000 µmol/(m²*s).

Wheat and rice have an allowed maximum PPF of 2000 µmol/(m²*s), which is also the value of their lowest total ESM. Providing more than 1000 µmol/(m²*s) in closed environment agriculture is possible, but rather challenging from a technical point of view. Therefore, 1000 µmol/(m²*s) is selected for the nominal PPF level of rice and wheat. In case large cultivation areas are dedicated to rice and wheat during the following simulations there is still the option to increase their PPF levels for sensitivity analyses.

Table 4-6: Nominal CO_2 and PPF levels selected for following simulation cases.

Crop species	Nominal CO_2 level [ppm]	Nominal PPF level [µmol/(m²*s)]
Dry bean	1000	800
Lettuce	1000	300
Peanut	1000	800
Rice	1000	1000
Soybean	1000	800
Sweet potato	1000	800
Tomato	1000	800
Wheat	1000	1000
White potato	1000	800

4.2.5 Summary of Nominal Production Values

The average values of daily carbon gain (DCG), daily oxygen production (DOP), total crop biomass (TCB), H_2O accumulation rate, daily transpiration rate (DTR) and total edible biomass of one growth cycle and crop specific nominal CO_2 and PPF levels are shown in Table 4-7. These values are the baseline for the following simulations.

Table 4-7: Average DCG, DOP, TCB, H_2O accumulation rate, DTR and total edible biomass of one growth cycle for crop specific nominal CO_2 and PPF levels.

Crop species	DCG [g/(m²*d)]	DOP [g/(m²*d)]	TCB [g/(m²*d)]	H_2O accumulation rate [g/(m²*d)]	DTR [g/(m²*d)]	Total edible biomass [kg/m²]
Dry Bean	8.72	25.56	19.38	111.49	1877.06	0.469
Lettuce	2.54	7.30	6.34	117.30	366.64	0.207
Peanut	7.32	23.22	14.65	92.86	1689.92	0.499
Rice	16.36	47.07	37.18	249.17	3303.94	0.881
Soybean	7.29	22.53	15.85	84.56	1694.20	0.587
Sweet potato	17.61	47.84	40.01	155.16	4271.91	3.899
Tomato	8.85	25.70	21.07	251.09	1844.22	0.777
Wheat	21.01	59.88	47.74	262.19	2596.24	1.243
White potato	9.39	25.51	22.90	117.44	792.95	2.531

4.3 Mars Surface Habitat Simulation Scenario

4.3.1 Description

The model setup for this simulation scenario represents a Mars surface habitat architecture. The mission architecture and therefore the simulation inputs are partially based on NASA's Human Exploration of Mars Design Reference Architecture 5.0 (DRA 5.0) (Drake, 2009).

The simulation scenario incorporates a Mars surface habitat with a hybrid life support system consisting of physical-chemical life support technologies as well as a greenhouse for plant cultivation. Figure 4-14 shows the life support architecture in the conventional way, indicating mass flows between the different subsystems, the crew and the plants.

The simulation inputs defined for this simulation scenario are explained in detail in the following subchapter.
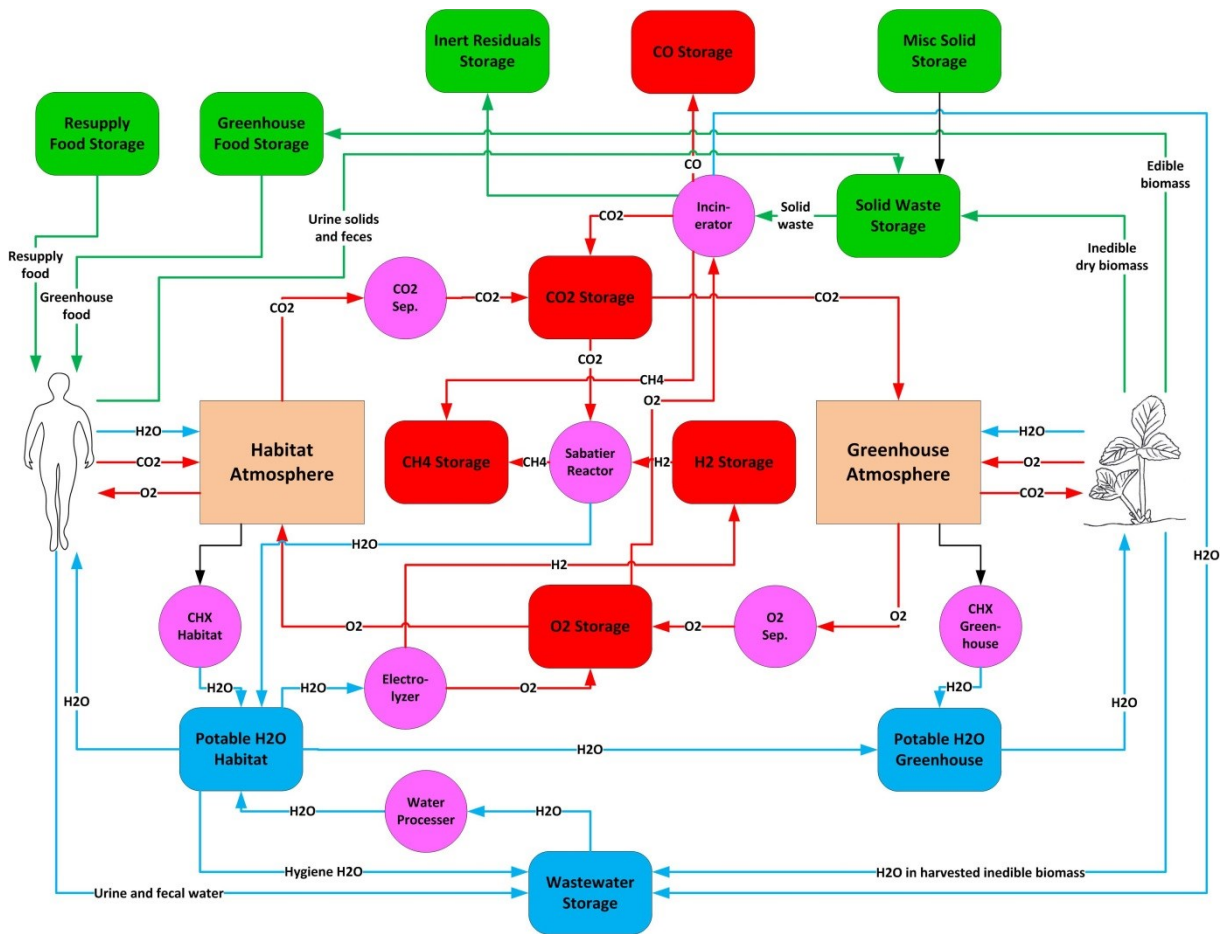
Figure 4-14: Life support system architecture for the Mars surface habitat simulation scenario. Physical-chemical systems are in purple, liquid mass flows in blue, gaseous mass flows in red and solid mass flows in green.

4.3.2   Initial Simulation Inputs

4.3.2.1 Root Model Setup

The simulation run specifications are set in the root model. The run specs include the start and stop time of the simulation, the simulation step interval (DT) and the time unit. Further-more certain simulation options such as the integration method and the simulation speed need to be set.

Table 4-8 shows a screenshot of the Run Specs set for this simulation scenario. The simula-tion runs from 0 to 500 days, which represents the length of a Mars surface stay for a con-junction class mission (long-stay mission) according to Drake (2009). The value for DT is set to 1/128 which means that 128 calculation steps are performed per time step. The DT is ra-ther small which increases the simulation time, because more calculations are performed. This small value is necessary because of the large number of feedback loops that are pre-sent in the developed model and because of the way Stella Professional is performing the calculations. More calculation steps also mean smoother results.

As integration method Euler's method is selected. While the 4th order Runge-Kutta Method and the Cycle Time method would lead to more precise results they cannot deal well with all the IF-THEN-ELSE conditions implemented in the model.

Table 4-8: Root model setup (Run Specs) for the Mars surface habitat simulation.

Run Specs	Value/Option	
Start Time	0	
Stop Time	500	
DT	1/128	fractional on
Time Units	d	
Sim Speed	Semi-Fast	
Pause Interval	off	
Integration Method	Euler	
Pause before computing flows or converters	on	
Keep all variable results	on	

4.3.2.2 Gases Layer Inputs

Seven inputs need to be set in the Gases Layer module. The input variables are shown in Table 4-9. The stocks O2 in Habitat, O2 in Greenhouse, CO2 in Greenhouse, CO2 in Habitat, CO Storage, CH4 Storage and H2 Storage stocks are empty at the start of the simulation and therefore set to zero kilograms.

Table 4-9: Gases Layer simulation inputs.

Variable Name	Variable Type	Value	Unit
O2 in Habitat	Stock	0	kg
O2 in Greenhouse	Stock	0	kg
CO2 in Greenhouse	Stock	0	kg
CO2 in Habitat	Stock	0	kg
O2 Storage	Stock	600	kg
CO2 Storage	Stock	50	kg
habitat pressurized volume	Converter	900	m³
greenhouse pressurized volume	Converter	885.874	m³
CO Storage	Stock	0	kg
CH4 Storage	Stock	0	kg
H2 Storage	Stock	0	kg

The initial values of the O2 Storage and the CO2 storage stocks are determined by the amount of oxygen respectively carbon dioxide required to pressurize the habitat and the greenhouse to the desired partial pressure. Furthermore the two stocks have an additional amount of gases to supply the crew and the plants in the greenhouse until the life support system reaches a steady-state of production. Equation 5-1 and 5-2 show how to determine the input values for the two stocks. The values for the two stocks shown in Table 4-9 were determined using the equations and the partial pressure, total pressure and volume inputs defined in this and the following subchapters.

$$O2\ Storage = \frac{p_{O2_{habitat}}}{p_{total_{habitat}}} * V_{habitat} * \rho_{O2}(p_{total\_habitat}) +$$

$$\frac{p_{O2_{greenhouse}}}{p_{total_{greenhouse}}} * V_{greenhouse} * \rho_{O2}(p_{total\_greenhouse}) +$$

$$m_{O2\_start} \tag{5-1}$$

$$CO2\ Storage = \frac{p_{CO2_{greenhouse}}}{p_{total_{greenhouse}}} * V_{greenhouse} * \rho_{CO2}(p_{total\_greenhouse}) + m_{CO2\_start} \tag{5-2}$$

The values for the habitat and greenhouse pressurized volume converters are important, because the atmosphere volume acts as a buffer for the gas exchange of humans and plants. A larger pressurized volume has a larger buffer capacity, but also means more structural mass for the habitat and the greenhouse. For the determination of the habitat pressurized volume, the volume of past and present spacecraft are compared to each other and the crew size in Table 4-10. A stay of 500 days on the surface of Mars might require a habitat of the size of the ISS. Therefore the pressurized volume of the habitat in this simulation scenario is set to 150 m³ per person, which leads to a total pressurized volume of the habitat of 900 m³ for a crew of six.

Table 4-10: Pressurized volume of past and present spacecraft designed for long-stay missions.

	ISS	Skylab	Mir
Crew size	6 (7)*	3	3
Total pressurized volume [m³]	932	358	~350
Volume per CM [m³/CM]	155.3 (133.1)*	119.3	116.7

*ISS is designed for 7, but currently operated with 6 crew members.

The pressurized volume of the greenhouse depends mainly on the cultivation area, which in turns depends on the amount of plants to be cultivated. Table 4-11 shows cultivation area and volume of different space greenhouse test facilities. Due to the lack of operational space greenhouse only those values can be used to assess a feasible value for the greenhouse pressurized volume converter. A value of 3 m³ per square meter of cultivation area seems to be a good assumption for this simulation scenario. Consequently the pressurized volume of the greenhouse is 885.874 m³ for a total cultivation area of 299.098 m² as defined in Chapter 4.3.2.6.

Table 4-11: Cultivation area and volume of different terrestrial greenhouse test facilities.

	Bios-3	BPC	EDEN ISS	BIO-Plex
Plant cultivation area [m²]	39 (63)*	20	12.5	82.4
Plant cultivation volume [m³]	158 (237)*	113	32	187.8
Volume per cultivation area [m³/m²]	4.05 (3.77)*	5.65	2.56	2.28

*Bios-3 has been operated with two and three phytotron active, which leads to two different values.

4.3.2.3 Liquids Layer Inputs

The inputs needed to be defined in the liquids layer module are the initial water storage of the habitat, the crew and the greenhouse as well as two variables which define the water storage limits inside the greenhouse. Table 4-12 shows the input values of the liquids layer module. The stocks Water in Habitat Atmosphere and Water in Greenhouse Atmosphere have an initial value of zero kilograms. They are initially filled during the first time step with water equal to match the relative humidity requirements. The stocks Water Accumulated in Living Plant Biomass, Water Accumulated in Harvested Edible Biomass and Water Accumulated in Harvested Inedible Biomass have an initial value of zero kilograms because there are no living plants and no harvested biomass at the start of the simulation. The stock Wastewater Storage also has an initial value of zero kilograms.

The Potable Water Storage in Habitat stock is the primary supply of water at the beginning of the simulation. The amount of water in the stock at simulation start needs to be large enough to make up the water bound in the plants of the greenhouse and the demands of the crew. The Water Reservoir in Crew stock can be calculated with the values for body water content mentioned in Chapter 4.7.6 (62.5% of total body weight for men, 52.5% for women). The po-

table Water Storage in Greenhouse stock requires a small amount of water at the start of the simulation in order to humidify the atmosphere inside the greenhouse to the desired level. The upper and the lower limit of the potable water storage in greenhouse can be defined at will, but should make up at least the maximum total daily transpiration rate of all plants cultivated.

Table 4-12: Liquids Layer simulation inputs.

Variable Name	Variable Type	Value	Unit
Water in Habitat Atmosphere	Stock	0	kg
Water in Greenhouse Atmosphere	Stock	0	kg
Water Accumulated in Living Plant Biomass	Stock, arrayed	0	kg
Water Accumulated in Harvested Edible Biomass	Stock	0	kg
Water Accumulated in Harvested Inedible Biomass	Stock	0	kg
Wastewater Storage	Stock	0	kg
Potable Water Storage in Habitat	Stock	3500	kg
Water Reservoir in Crew	Stock, arrayed	50.0 (men), 31.5 (women)	kg
Potable Water Storage in Greenhouse	Stock	50	kg
potable water storage in greenhouse lower limit	Converter	200	kg
potable water storage in greenhouse nominal limit	Converter	350	kg

4.3.2.4 Solids Layer Inputs

The Liquids Layer module inputs define the variables concerning Resupply Food stock, greenhouse food diet, biomass, harvest events and the misc solids stock. The stocks Crop Food Storage, Harvested Edible Dry Biomass, Edible Dry Biomass in Plants per compartment per cycle, Inedible Dry Biomass in plants per compartment per cycle, Harvested Inedible Dry Biomass and Solid Waste Storage in Habitat are initially set to zero kilograms, see Table 4-13.

The Misc Solids Storage stock is filled with miscellaneous items used by the crew (e.g. wipes, cloths, gloves). The stock is initially filled at simulation start and continuously declines over the mission duration. The misc solids storage has to provide enough material for the complete mission. This value can be calculated with formula 5-3.

$$Misc_{Solid_{Storage_{initial\ value}}} =$$

$$mission_{duration} * CM * CM\_misc\_solid\_waste\_production \qquad (5\text{-}3)$$

With a mission duration of 500 days, a crew of six and a CM misc solid waste production of 1.93 kg/(CM*d), see chapter 4.3.2.5, the value shown in Table 4-13 is defined for this simulation scenario.

Table 4-13: Solids Layer simulation inputs.

Variable Name	Variable Type	Value	Unit
Crop Food Storage	Stock, arrayed	0	kg
Harvested Edible Dry Biomass	Stock, arrayed	0	kg
Edible Dry Biomass in Plants per compartment per cycle	Stock, arrayed	0	kg
Inedible Dry Biomass in Plants per compartment per cycle	Stock, arrayed	0	kg
Harvested Inedible Dry Biomass	Stock	0	kg
Solid Waste Storage in Habitat	Stock	0	kg
Resupply Food Storage	Stock, arrayed	1000	kg
greenhouse diet composition per astronaut	Converter, arrayed	Table 4-14 for values.	kg/d
harvest events	Converter, arrayed	Dependent on the production schedule of the greenhouse model.	-
Misc Solids Storage	Stock	6000	kg
Crew Metabolic Solids	Stock	350	kg

Table 4-14: Greenhouse diet per astronaut in kilograms dry mass per day.

	astronaut 1	astronaut 2	astronaut 3	astronaut 4	astronaut 5	astronaut 6
Dry Bean	0.01926	0.01926	0.01926	0.01926	0.01926	0.01926
Lettuce	0.01274	0.01274	0.01274	0.01274	0.01274	0.01274
Peanut	0.0271872	0.0271872	0.0271872	0.0271872	0.0271872	0.0271872
Rice	0.018832	0.018832	0.018832	0.018832	0.018832	0.018832
Soybean	0.2106	0.2106	0.2106	0.2106	0.2106	0.2106
Sweet Potato	0.022272	0.022272	0.022272	0.022272	0.022272	0.022272
Tomato	0.017124	0.017124	0.017124	0.017124	0.017124	0.017124
Wheat	0.084744	0.084744	0.084744	0.084744	0.084744	0.084744
White Potato	0.02094	0.02094	0.02094	0.02094	0.02094	0.02094

The greenhouse diet composition per astronaut converter defines the amount of crop edible biomass each astronaut consumes per day assuming there is biomass available. This varia-

ble also defines the size of the greenhouse as it is explained in Chapter 4.3.2.6. The greenhouse diet for this simulation scenario is inspired by the 'All ELS Crops' diet described in Anderson *et al.* (2015). The diet is composed of a variety of crops in order to maintain nutritional integrity, but does not fulfill the energy requirements of the crew because the diet delivers only around 1580 kcal per day. Consequently, additional resupply food is necessary. Table 4-14 shows the diet composition established in the model. The original diet by Anderson *et al.* (2015) also lists small amounts carrot, green onion, radish and spinach. These crops however are not available in the implemented greenhouse model. Therefore the amount of lettuce has been increased for this simulation compared to the original diet in order to make up for the missing crops.

The Resupply Food Storage stock is initially filled with food brought from Earth. The resupply food is consumed by the crew to fill the remaining kilocalorie demand after eating the greenhouse produce. There is no resupply implemented besides at simulation start. Consequently, the stock content declines over time depending on how much the greenhouse produces. The initial value of the Resupply Food Storage stock is set to 1000 kg, see Table 4-13. The amount of resupply food is given in kilograms dry mass.

The harvest events arrayed converter defines the days in the simulation on which the different compartments of the greenhouse are harvested. The harvest events depend on the crop grown in the compartments and on the production schedule of the greenhouse model, which is explained in Chapter 4.3.2.6. For this simulation scenario the crops are always harvested at the end of their defined growth period.

The Crew Metabolic Solids stock is filled initially with 350 kg and declines over time as it is emptied into the Solid Waste Storage Stock depending on the crew activity level. As described in Chapter 3.6.5 this stock is installed in order to calculate the mass balance of the model.

4.3.2.5 Crew Model Inputs

The crew model inputs define the crew composition and certain characteristics of each crew member. Furthermore, the crew mission profiles (the combination of crew days) needs to be defined for each crew member. For this simulation scenario each crew member does have five BVAD work days followed by two BVAD weekend days. All crew members execute their week days and weekend days simultaneously. The crew consists of six crew member, which is equal to what is suggested by DRA 5.0 (Drake, 2009). There are three male and three female crew member. The values are shown in Table 4-15.

The CM hygiene water demand and CM misc solid waste production value are defined according to Anderson *et al.* (2015). Three values for solid waste production are listed. Comparing data from space shuttle flights an average value of 1.39 kg/(CM*d) is defined. For the ISS the assumption is 1.69 kg/(CM*d) and for a Mars surface habitat the assumption is 1.93 kg/(CM*d). For this simulation scenario the value for the Mars surface habitat, which is also the highest value, is taken.

Table 4-15: Crew Model simulation inputs.

Variable Name	Variable Type	Value	Unit	Reference
CM parameters	Converter, arrayed	See Table 4-16 for values	-	-
CM mission profiles	Converter, arrayed	5 BVAD week day + 2 BVAD week-end day. Repeating.	-	-
CM hygiene H2O demand	Converter	5.16	kg/ (people*d)	(Anderson *et al.*, 2015)
CM misc solid waste production	Converter	1.93	kg/ (people*d)	(Anderson *et al.*, 2015)

Table 4-16: CM parameters arrayed converter simulation scenario input.

	Active	Height	Weight	Sex	Age
astronaut 1	1	1.8	80	10	40
astronaut 2	1	1.8	80	10	40
astronaut 3	1	1.8	80	10	40
astronaut 4	1	1.6	60	20	40
astronaut 5	1	1.6	60	20	40
astronaut 6	1	1.6	60	20	40

4.3.2.6 Greenhouse Model Inputs

The greenhouse model requires only two inputs, the plant production schedule and the compartment cultivation area, see Table 4-17.

Table 4-17: Greenhouse Model simulation inputs.

Variable Name	Variable Type	Value	Unit
scheduler	Converter, arrayed	See Table 4-18 for exemplary values.	-
compartment cultivation area	Converter, arrayed	See Table 4-19 for values.	m²

The scheduler arrayed converter requires the crop species, the seed date, the light intensity PPF and the photoperiod H as input for each compartment and cycle. Table 4-18 shows the inputs for compartment 1 as an example. The values for PPF should be defined as explained in Chapter 4.2.4 and the values for H equal to the nominal value of H as defined in Chapter 3.8. The first column (t cycle start) defines the point in time when the plant seedlings are moved into the greenhouse compartments.

Table 4-18: Scheduler arrayed converter input example for compartment 1.

No.	t cycle start	crop compartment	PPF compartment	H compartment
1	4	1	800	12
2	69	1	800	12
3	134	1	800	12
4	199	1	800	12
5	264	1	800	12
6	329	1	800	12
7	394	1	800	12
8	459	1	800	12
9	0	0	0	0
10	0	0	0	0

The greenhouse is one of the two main consumers and producers, the crew being the other one. Consequently, the timing of the different production cycles for each compartment is of high importance in order to sustain balanced mass flows in the life support system. The so called plant production schedule defines in general at which points in time which plants are grown. Defining a plant production schedule is a complicated task. For this simulation scenario a rather primitive production schedule is defined as initial input. Figure 4-15 shows this production schedule.

It is assumed, that all plants are sown on simulation start (t=0). After a germination period of five days, all plants are transferred to their compartments inside the greenhouse. The first growth cycles of all compartments start at the same time and the next cycle starts immediately after the previous one. Note that no special attention to the timing of the different cycles, in order to balance the production rate of the greenhouse, is being paid at this point. At the end of the mission the production of the greenhouse levels out to zero, because no new plants are sown if the plants of the last growth cycle cannot be harvested within the mission duration.

The current model allows for ten compartments and ten cycles per compartment. For lettuce with a very short growth cycle ten growth cycles are not enough to guarantee a continuous production in one compartment over the whole mission duration. Therefore lettuce is cultivated in two compartments (compartment 2 and compartment 10). When the tenth cycle in compartment 2 ends the first cycle in compartment 10 starts, see Figure 4-15.
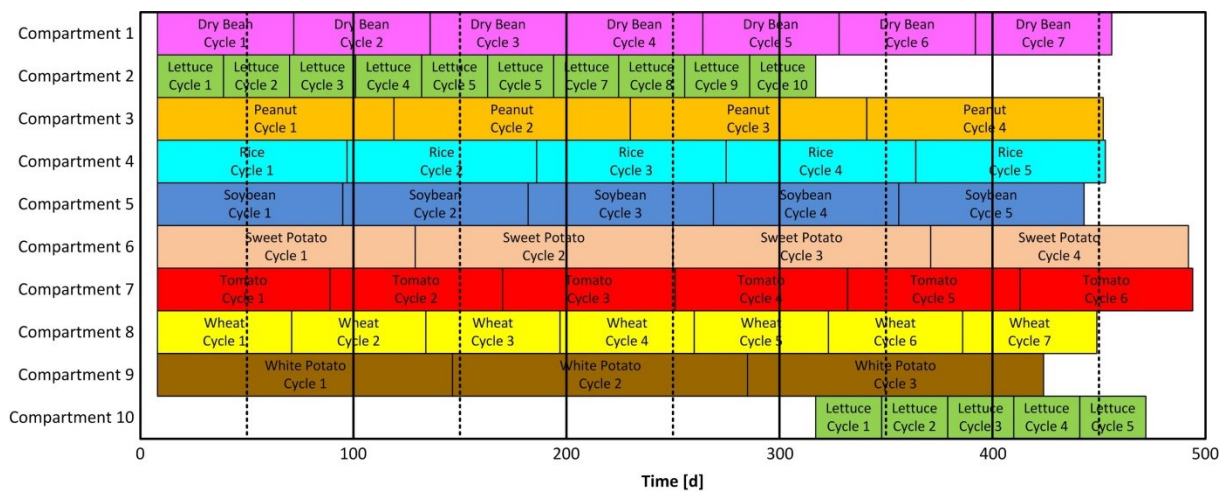
Figure 4-15: Initial greenhouse model plant production schedule input.

The cultivation area per compartment is adjusted in order to provide the greenhouse diet as defined in Chapter 4.3.2.4. The values in square meters for each compartment are shown in Table 4-19. Compartment 6 with 175.8 m² has the largest cultivation area of the greenhouse. This compartment is used to grow Soybeans which make up a large portion of the greenhouse diet.

Table 4-19: Cultivation area per compartment in square meters.

1	2	3	4	5	6	7	8	9	10
15.169	11.420	31.410	10.413	175.800	3.205	9.119	25.252	5.890	11.420

4.3.2.7 Physical-Chemical Systems Inputs

The inputs for the Physical-Chemical Systems module are shown in Table 4-20. The values for these variables depend to a large degree on the inputs of the other modules. Once all other inputs are defined, an iterative process is required to define the capacities for the different physical-chemical technologies. The threshold values for the different storage stocks, which are used to control the activity of the physical-chemical systems, need to be found out the same way.

Table 4-20: Physical-chemical systems simulation inputs.

Variable Name	Variable Type	Value	Unit
incinerator capacity	Converter	20	kg/d
solid waste storage lower threshold	Converter	50	kg
O2 storage upper threshold	Converter	200	kg
CO2 storage lower threshold	Converter	50	kg
electrolyzer capacity	Converter	12	kg/d
O2 storage lower threshold	Converter	50	kg
Sabatier capacity	Converter	7	kg/d
CO2 storage upper threshold	Converter	100	kg
H2 storage lower threshold	Converter	10	kg
habitat CHX capacity	Converter	10	kg/d
greenhouse CHX capacity	Converter	1000	kg/d
VPCAR capacity	Converter	75	kg/d
potable water storage habitat lower threshold	Converter	100	kg
wastewater storage upper threshold	Converter	50	kg
wastewater storage lower threshold	Converter	0	kg
O2 separator capacity	Converter	15	kg/d
CO2 separator capacity	Converter	20	kg/d
inedible biomass processor capacity per crop	Converter	5	kg/d
harvested inedible biomass storage upper threshold	Converter	50	kg

4.3.3 Simulation Results for Nominal Operation

4.3.3.1 Overview of results for nominal operation

For the first simulation of the Mars surface habitat scenario, the model was run with the simulation inputs defined in Chapter 4.3.2 to simulate the nominal operation of the life support system. Nominal operation in this case means:

- All crew members survived the mission in good shape.
- The stocks for potable water, oxygen, carbon dioxide and food stayed within ranges to sustain all crew members.
- No system failures or other perturbations have been included.

The model validation method explained in Chapter 3.11 was executed again with the parameter setting for the nominal operation simulation. The results show that the system closure is equal to the results of the model validation. Consequently the results which are explained in the following chapters are valid within the capabilities of the model.

4.3.3.2 Gases Layer behavior for nominal operation

The behavior of the Gases Layer module for the nominal operation scenario of the Mars surface habitat life support system architecture gives valuable insight in the mass flows of oxygen and carbon dioxide. Furthermore the production and consumption of hydrogen, carbon monoxide and methane caused by the physical-chemical systems is shown.

The oxygen concentration in the atmosphere of the habitat and the greenhouse is constant at 21 % of the pressurized volume, see Figure 4-16. This behavior is caused by the strict control of the oxygen flows, which are implemented in the model to assure crew survival. There is a step on mission day 1 in the graphs shown in Figure 4-16. This step is caused by the initial fill-up of the habitat and greenhouse atmosphere from the oxygen storage stock.
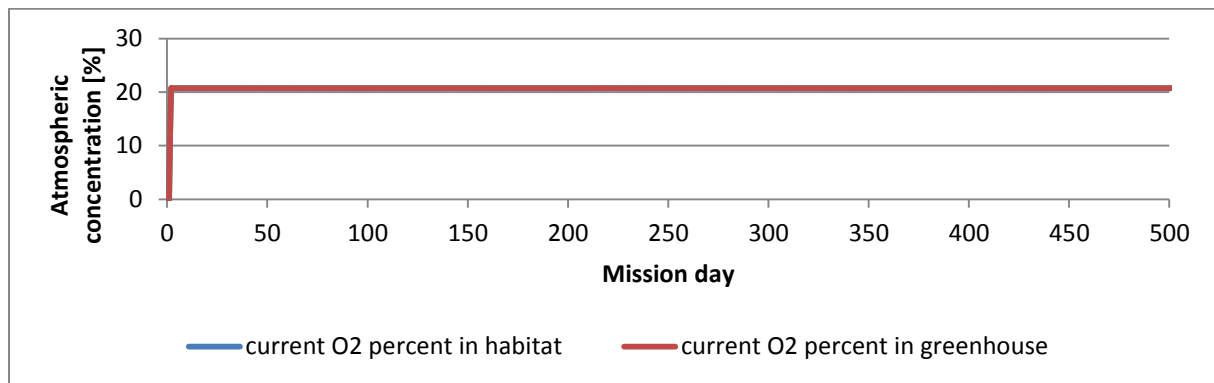
Figure 4-16: Atmospheric concentration of oxygen inside the habitat and the greenhouse under nominal operation.

The concentration of carbon dioxide inside the greenhouse, see Figure 4-17, also has a strict control to assure that the concentration does not fluctuate too much in order to provide a controlled environment for the plants. The concentration of carbon dioxide in the greenhouse atmosphere is constant at the desired value of 1000 ppm throughout the whole simulation. There is also a step on mission day 1 in the graph for the greenhouse carbon dioxide, which is caused by the initial fill up from the carbon dioxide storage stock.

While the concentration inside the greenhouse is strictly controlled, the carbon dioxide in the habitat can fluctuate. Normally the greenhouse takes up the carbon dioxide produced by the crew inside the habitat to keep the concentration inside the habitat at the nominal level of 4000 ppm. In case the greenhouse cannot take up all the carbon dioxide produced, the physical-chemical systems take over the carbon dioxide reduction once the upper threshold of 7000 ppm is reached. This behavior can be seen in Figure 4-17. At the start and at the end of the mission when the greenhouse is not at full capacity the carbon dioxide in the habitat rises to the upper threshold and is kept at this level by the physical-chemical systems.

There are however two more spikes in the habitat carbon dioxide concentration, one around day 180 and one around day 267.These spikes indicate a low carbon dioxide uptake capability of the greenhouse. The production schedule, see Figure 4-15, causes this behavior. The spikes are in line with the harvest of the soybean compartment which has the largest cultivation area and therefore the largest carbon dioxide uptake. At the second spike between day 256 and day 279, six out of nine active compartments are harvested in a span of two and a half weeks. Only the compartments with the peanut, sweet potato and tomato plants still have plants and the tomato and sweet potato plants are only one and a half weeks old and

not yet at full carbon dioxide uptake capability. The described behavior is the evidence of the influence of the production schedule on the balance of the life support mass flows.
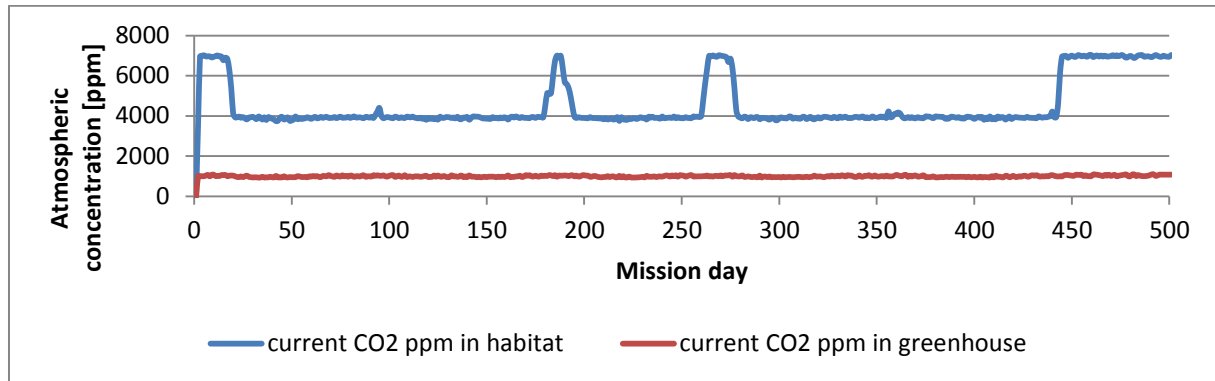
Figure 4-17: Atmospheric concentration of carbon dioxide inside the habitat and the greenhouse under nominal operation.

The spikes in concentration of carbon dioxide inside the habitat atmosphere are caused by an imbalance between production by the crew and consumption by the greenhouse. The rates of production and consumption of carbon dioxide are shown in Figure 4-18. Whenever the carbon dioxide in the habitat raises above the nominal level the consumption of carbon dioxide by the greenhouse is lower than the production by the crew.

While the crop's consumption of carbon dioxide varies depending on the production cycle, the production from the crew members is fairly constant. The cycles in the production graph of the crew in Figure 4-18 is caused by the weekly cycle of the crew activity (five days normal activity followed by two days with reduced activity). There is also a small step in the crew production curve around day 90 which is caused by a change in the ratio of food consumed from the resupply stock and food from the greenhouse. The resupply food has a higher respiratory quotient than the greenhouse food. Consequently in the first 90 days when the crew relies on resupply food the carbon dioxide production is slightly higher than during the rest of the mission when greenhouse food is consumed.

A graph for the oxygen production respectively consumption is not shown here, because there is a direct dependency to the carbon dioxide consumption respectively production.
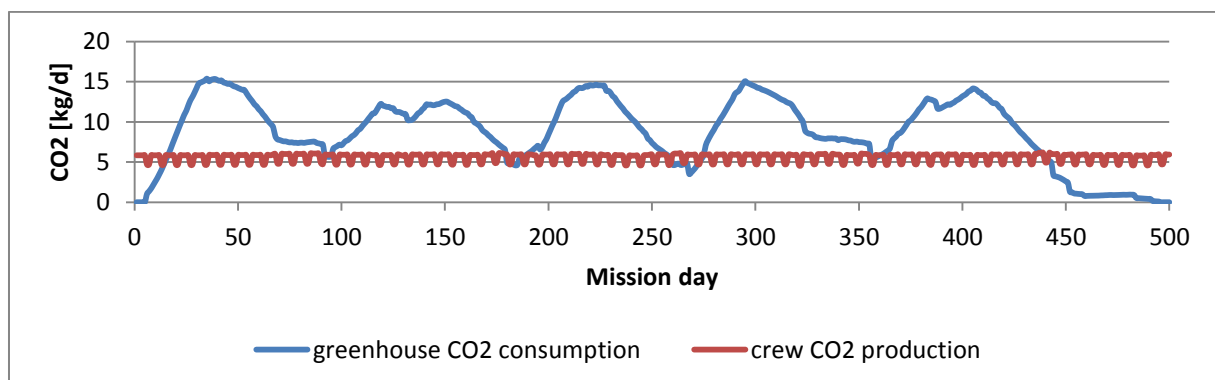
Figure 4-18: Greenhouse carbon dioxide consumption and crew carbon dioxide production under nominal operation.

The other two stocks involved in the oxygen and carbon dioxide loops besides the habitat and the greenhouse are the storage stocks. The behavior of these for the simulation under

nominal operation is shown in Figure 4-19. The oxygen storage stock has a steep decline on mission day 1 caused by the initial fill up of the habitat and greenhouse atmosphere.

During the first 23 days the amount of carbon dioxide in the storage stock slightly rises and the amount of oxygen decreases slightly. From day 23 until day 81 the behavior changes in the opposite direction. The amount of oxygen rises and the amount of stored carbon dioxide falls slightly. This behavior is caused by the growth rates of the plants and therefore by their carbon dioxide uptake and oxygen production. At the beginning the capacity of the greenhouse to contribute to the life support system is small but rises fast until the first harvest of compartments with a large amount of plants around day 81.

Due to the harvest events around day 81 there is a large amount of inedible biomass stored and there is also excess oxygen in the oxygen storage. Those are conditions under which the incinerator and the inedible biomass processor start to recycle the solid waste products. Consequently the carbon dioxide storage is constantly at its upper threshold, because consumed carbon dioxide is replenished immediately by the two systems. Since the carbon dioxide storage is at the upper threshold, excess oxygen accumulates over time in the oxygen storage. The behavior of the incinerator and the inedible biomass processor is described further in Chapter 4.3.3.5.

The last phase of the mission from day 450 onwards is characterized by the declining greenhouse capacity. The excess carbon dioxide produced by the crewmembers and their demand in oxygen is now exchanged with the storage stocks. The oxygen storage stock declines and the carbon dioxide storage stock rises.
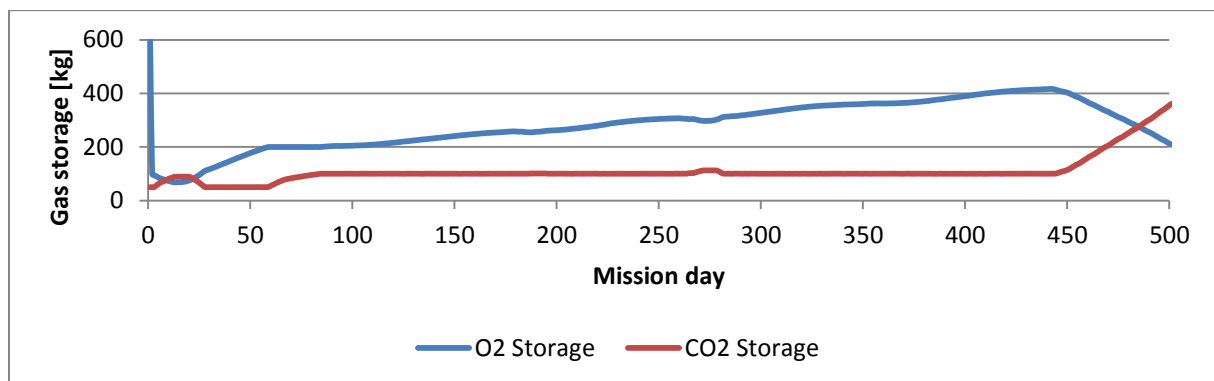
Figure 4-19: Amount of oxygen respectively carbon dioxide in the storage stocks under nominal operation.

The last components of the Gases Layer module to be discussed are the storage stocks for carbon monoxide, methane and hydrogen. The behavior of the three stocks is shown in Figure 4-20. As mentioned before, around day 40 the incinerator starts the recycling of solid waste products. Since the incinerator produces carbon monoxide and methane as by-products, the amount of gas stored in the storage stocks slowly rises. Note that all the methane is produced by the incinerator, because the Sabatier reactor is not active throughout the whole simulation (see Chapter 4.3.3.5). The same is true for the electrolyzer which also not active and therefore the hydrogen storage stock remains zero all the time.
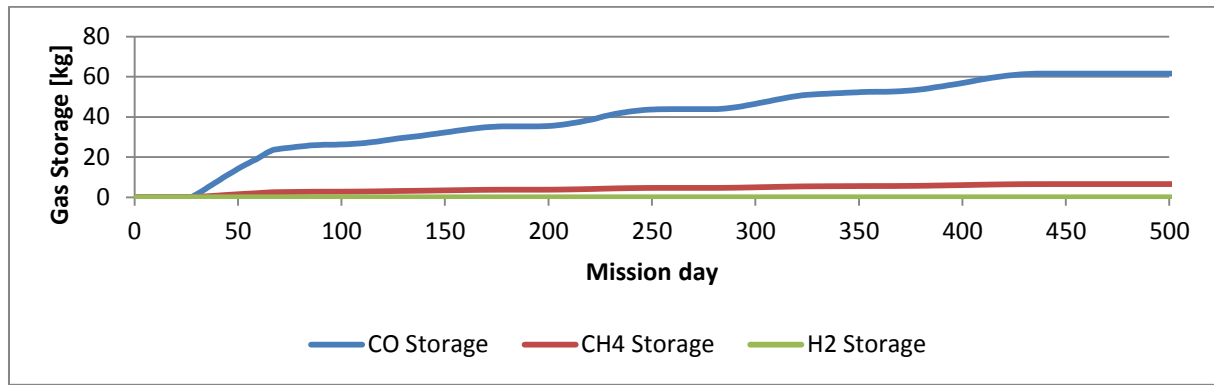
Figure 4-20: Amount of carbon monoxide, methane and hydrogen gas in their respective storage stocks under nominal operation.

4.3.3.3 Liquids Layer behavior for nominal operation

The Liquids Layer module calculates all water stocks and flows of the life support system. Of particular importance are the potable water storage in the habitat, the potable water storage in the greenhouse, the wastewater storage and the water accumulated in the living plant biomass. Their behavior during the simulation is shown in Figure 4-21. The graphs for the water contained in the body of the crew members, the habitat atmosphere and the greenhouse atmosphere are not shown here, because these stocks are kept constant by strict control parameter throughout the whole mission.

The potable water storage in habitat stock has a step on day 1, because the stock is used to initially fill up the habitat atmosphere with humidity and the potable water storage in greenhouse stock, see Figure 4-21. Between day 1 and day 14 is a slight increase in potable water in the habitat caused by the water recovery from the habitat atmosphere and the crew wastewater recycling. From day 14 until day 67 a steep decrease of the amount of water in the habitat potable water storage can be observed. This is caused by the potable water demand from the greenhouse potable water storage which is in turn caused by the water accumulating in the growing amount of living plant biomass. Consequently there is a transfer from the potable water storage in the habitat to the living plant biomass.

The water accumulating in the living plant biomass is transferred upon harvest to the wastewater storage stock. The step in accumulated water at day 67 and day 81 indicate harvest events of a large amount of plants. The wastewater is recovered by the VPCAR and directed back into the potable water storage of the habitat. For more information on the VPCAR activity see Chapter 4.3.3.5.

Figure 4-21 also provides evidence of the long-term water cycles in the life support system of the simulated Mars surface habitat. There is a constant cycle of water coming from the potable water storage in the habitat, going to the potable water storage in the greenhouse and from there into the living plant biomass and from there into the wastewater storage upon harvest and back into the potable water storage of the habitat after recycling.
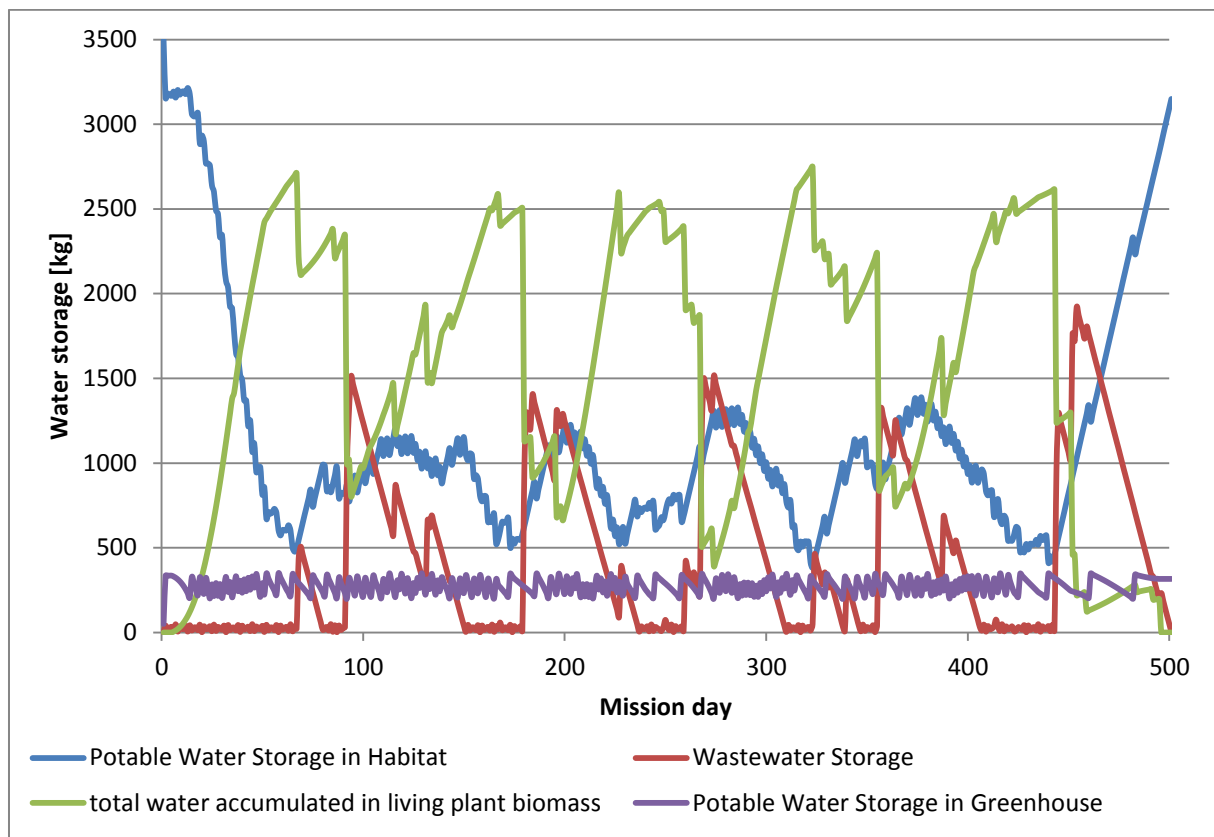
Figure 4-21: Behavior of the four main water stocks in the Liquids Layer module under nominal operation.

The wastewater recycling by the VPCAR plays an important role in the life support system's water cycle. The VPCAR recycles wastewater coming from four different sources: the water accumulated in the inedible biomass, the water produced by the incinerator, the water produced by the inedible biomass processor and the wastewater produced by the crew. In total the VPCAR has to recycle roughly 35000 kilograms of wastewater throughout the mission. Figure 4-22 shows the ratio of the four wastewater sources. The crew wastewater and the water accumulated in the inedible biomass make up around 98% of the wastewater production.

While the production of wastewater by harvesting and drying inedible biomass is also evident in Figure 4-21, the crew wastewater production cannot be observed directly in these graphs. This is caused by the difference in total production of the crew and the recycling capacity of the VPCAR. The wastewater production by the crew members is fairly constant at 40 kg/d throughout the mission. Since the VPCAR capacity of 75 kg/d is significantly higher than the crew wastewater production, the effect of the latter on the wastewater storage cannot be seen in Figure 4-21.
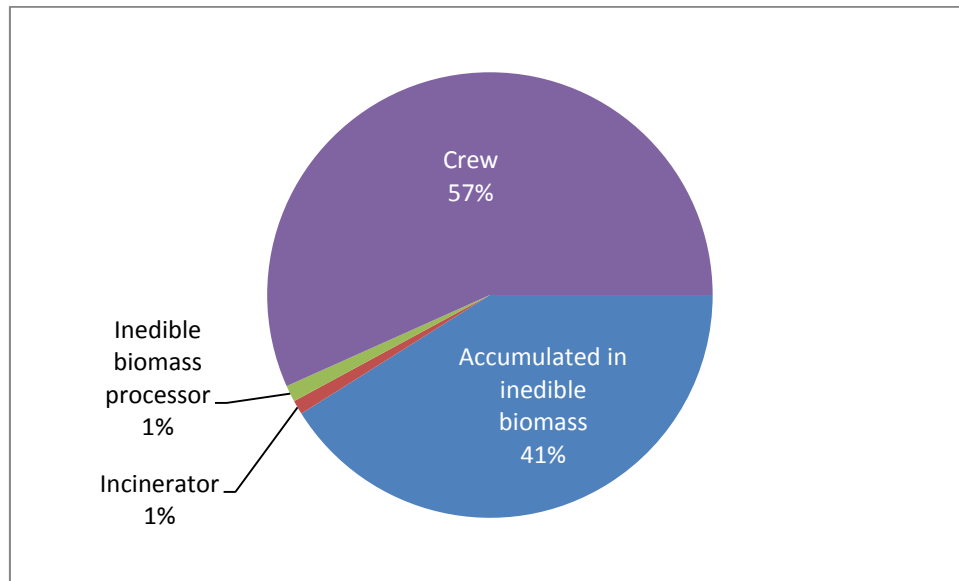
Figure 4-22: Ratio of the total wastewater production over the whole simulation duration under nominal operation.

4.3.3.4 Solids Layer behavior for nominal operation

The Solids Layer module calculates the values for the plant biomass inside the greenhouse, the two food storage stocks (resupply and greenhouse food) and the two solid waste stocks for crew waste and harvested inedible biomass. The previous two chapters already mentioned the influence of the greenhouse production schedule on certain mass flows of the life support system. The graphs shown in Figure 4-23 can explain most of the observed behavior. The figure shows the accumulated curves of the dry biomass contained in the living plants.

Since the oxygen production and carbon dioxide consumption of the crops is correlated to their size, which means their biomass, the greenhouse graph shown in Figure 4-18 follows the cycle of the crop biomass shown in Figure 4-23.

There is a long-term oscillation with a period of around 97 days in Figure 4-23. This oscillation is caused by compartment five which contains the soybean plants. Since soybean makes up most of the greenhouse diet (Chapter 4.3.2.5) and therefore requires the largest cultivation area (Chapter 4.3.2.6), the growth cycle of this compartment has the strongest impact on the dry biomass in living plants graph. The soybean oscillation is then overlapped by the growth cycles of the other crops, which causes the smaller spikes in the dry biomass graph.

The impact of the living plants is dampened to some degree by the life support architecture itself mainly by the different storage stocks for gases and liquids. Whether the plant production schedule and the cultivation area allocated to each compartment in this simulation scenario is reliable and resilient to off-nominal conditions is discussed in Chapter 4.3.3.6 and investigated in Chapter 4.3.4.2.
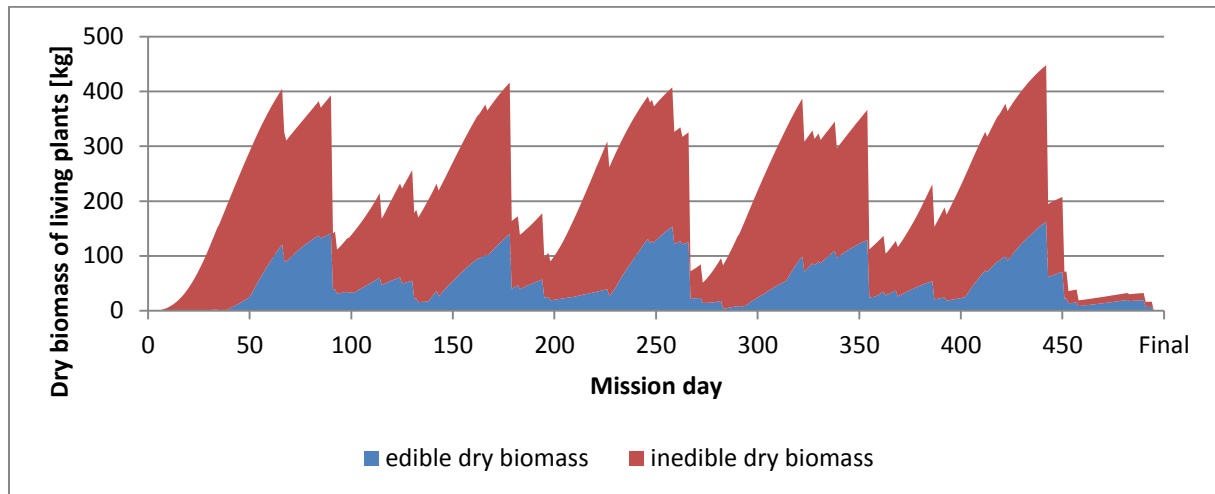
Figure 4-23: Dry biomass accumulated in living plants inside the greenhouse under nominal operation.

The food consumed by the crew is a mix of resupply food brought from Earth and the food grown in the greenhouse, as mentioned in previous chapters. Figure 4-24 shows the consumption rates of resupply food and greenhouse of the whole crew. The small oscillations observed in the resupply food curve are caused by the weekly cycle of the crew activity (five days of normal activity followed by two days of reduced activity). At the start of the mission the crew relies solely on the resupply food until the first crops are harvested around day 40, day 65 and day 95. From day 95 onwards the greenhouse produces constantly enough food to contribute more to the overall food consumption than the resupply food. There is however four interruptions in the greenhouse food consumption graph. Those are most likely caused by depleting the food stock of a certain crop before the next harvest event. The resupply food storage is able to compensate for the missing greenhouse food.
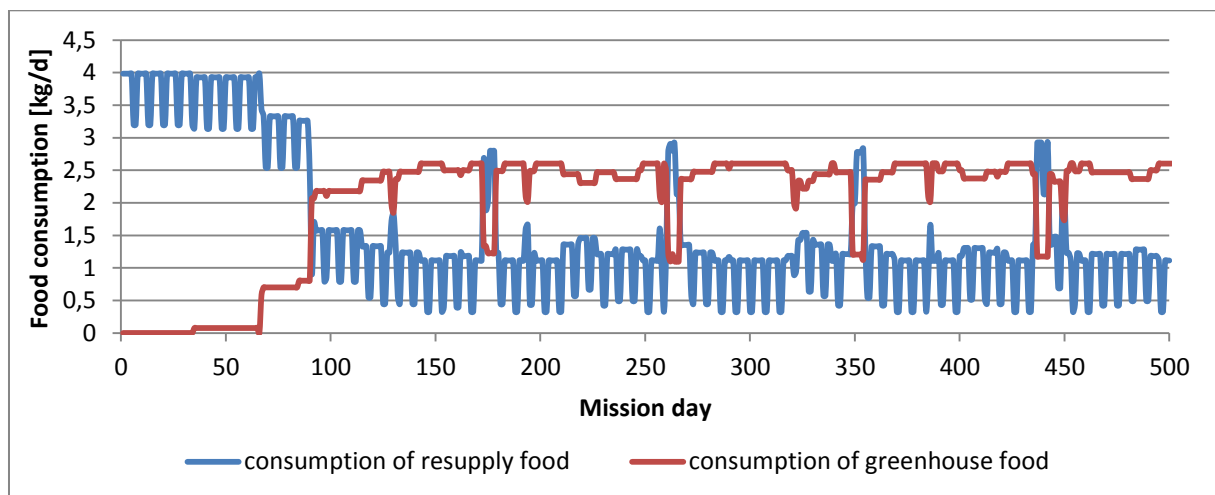
Figure 4-24: Crew food consumption from resupply storage or greenhouse food storage under nominal operation.

Figure 4-25 shows the amount of food present in the resupply storage and the greenhouse storage stocks over the mission duration. The resupply food storage steadily declines, because it is only initially filled at mission start and because there is no scheduled resupply mission in this simulation scenario. The resupply food storage however declines more in the early days of the mission when the crop food starts to provide most of the food. From there

one the resupply food storage stock depletes slower. The crop food storage oscillates in correlation to the greenhouse production schedule mentioned earlier.
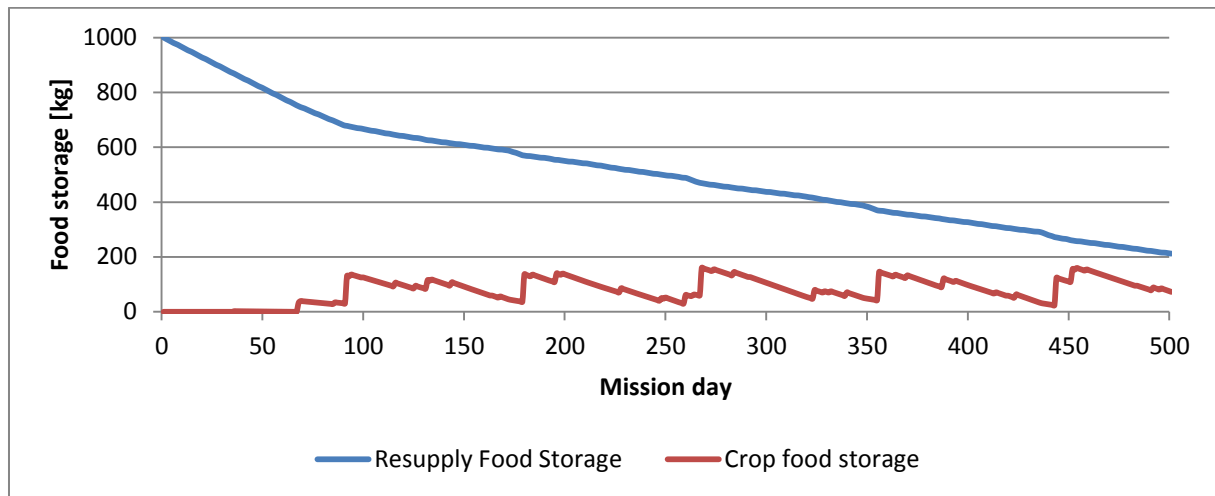
Figure 4-25: Amount food in the resupply storage and the crop food storage under nominal operation.

The crew and the greenhouse produce a large amount of solid waste products over the course of the mission. The graphs for the corresponding storage stocks are shown in Figure 4-26. The solid waste storage in habitat stock value constantly increases due to the waste production by the crew of roughly 12.5 kg/d. The incinerator is in theory capable of processing the produced waste products. The carbon dioxide storage at the upper threshold however prevents the system from recycling more waste. The harvested inedible dry biomass also increases over time out of the same reason. The activity of both systems is described in Chapter 4.3.3.5.
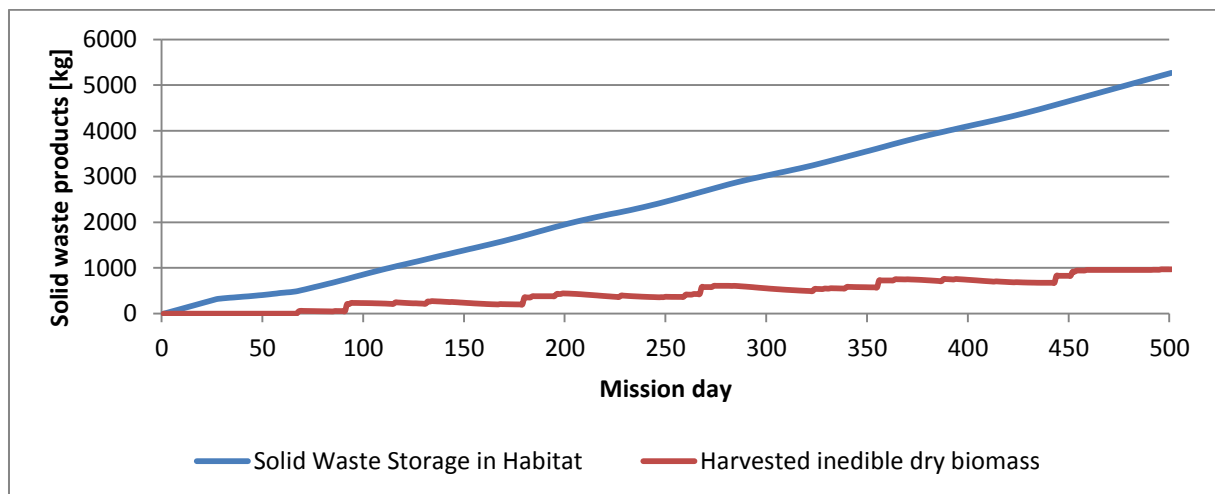
Figure 4-26: Behavior of the solid waste storage and the harvested inedible dry biomass storage under nominal operation.

4.3.3.5 Physical-chemical systems behavior for nominal operation

The physical-chemical systems implemented in the model take over major roles in the life support system architecture. These systems are however not constantly active, but their activity is controlled by different parameter as described in Chapter 3.9.

Chapter 4.3.3.3 already mentioned the importance of the VPCAR water recycling system. This fact is also evident from Figure 4-27. The VPCAR is active on 453 out of the 500 mission days in order to transform wastewater into potable water for the crew and the plants.
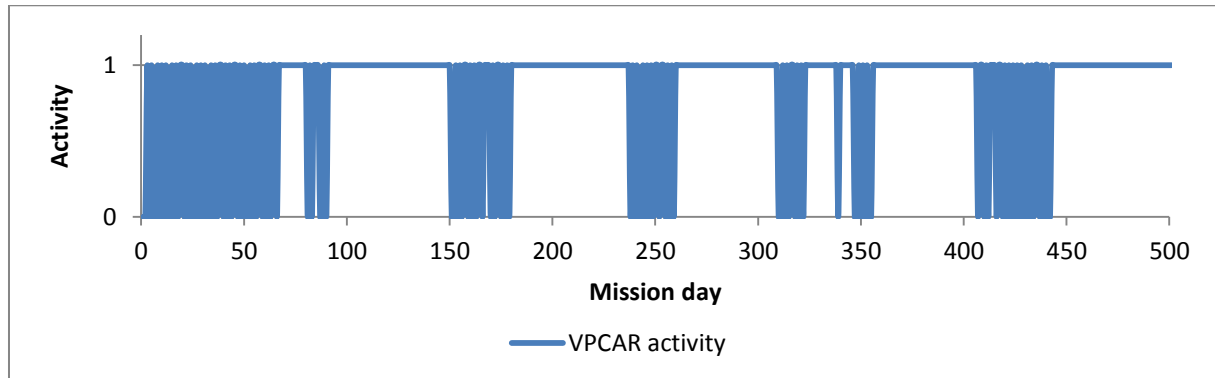
Figure 4-27: VPCAR activity under nominal operation (active=1; inactive=0).

As mentioned in Chapter 4.3.3.4 the activity of the incinerator and the inedible biomass processor is restricted by the carbon dioxide storage upper threshold. Figure 4-28 and Figure 4-29 prove that fact. While there are still enough solid waste products to be processed (see Figure 4-26), both systems are only working in short intervals and are only active on roughly 110 days throughout the mission.
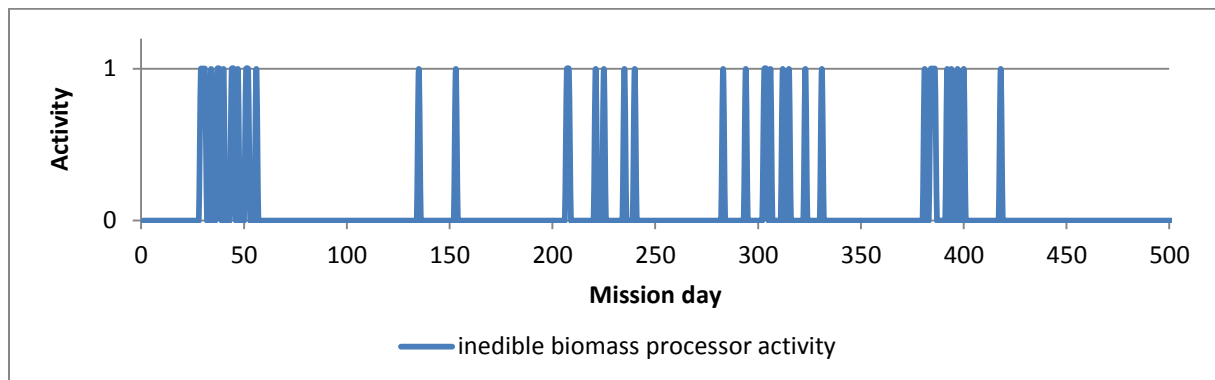
Figure 4-28: Inedible biomass processor activity under nominal operation (active=1; inactive=0).
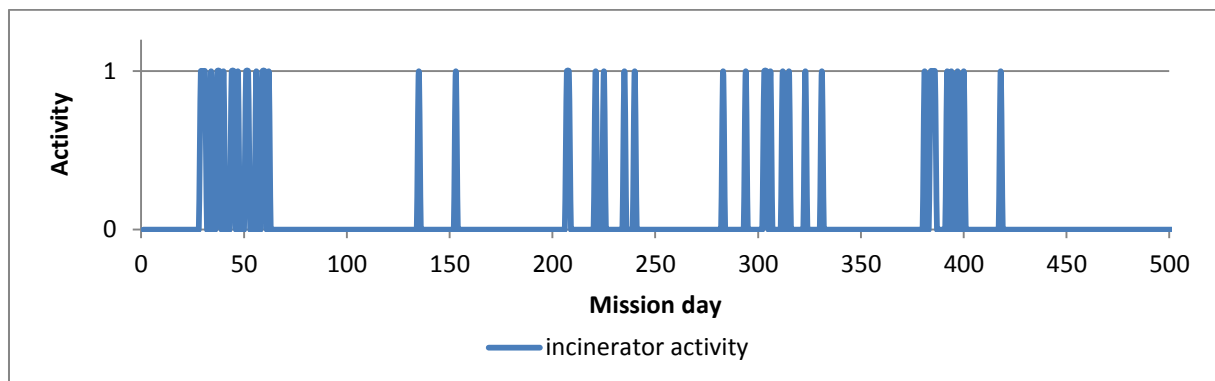
Figure 4-29: Incinerator activity under nominal operation (active=1; inactive=0).

The electrolyzer and the Sabatier reactor are implemented as backup systems in the model. That is done by having the thresholds for the systems activation at thresholds which should not be reached under nominal operation. Consequently the activity of both systems during this simulation scenario is always zero, see Figure 4-30.
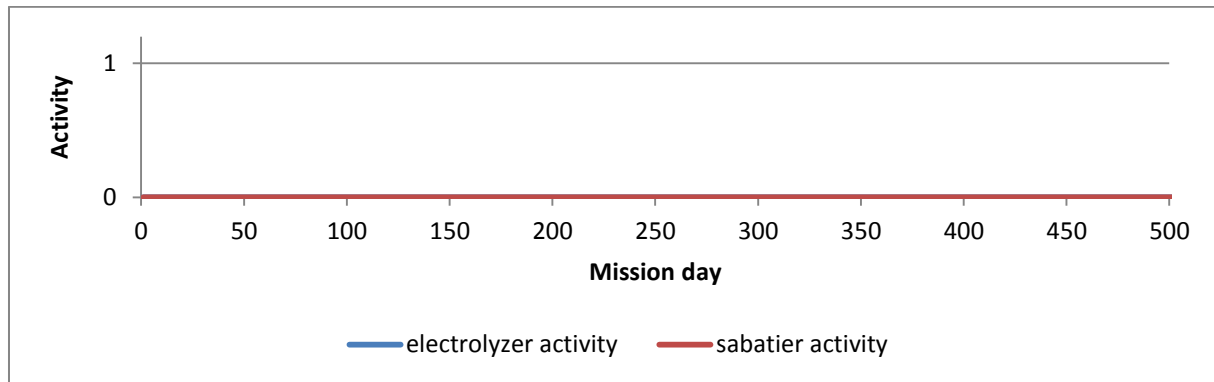
Figure 4-30: Activity of the electrolyzer and the Sabatier reactor under nominal operation (active=1; inactive=0).

4.3.3.6 Discussion of results for nominal operation

The previous subchapters described the results for the simulation under nominal operation conditions of the Mars surface habitat. The crew is sustained throughout the whole mission duration. Nevertheless some system behavior that could lead to a fatal mission end could already be identified from the results of this simulation run.

The startup phase of the greenhouse is a critical period of the whole mission, which is already described in the second chapter of this dissertation (see Chapter 2.4). The startup of the greenhouse results in large mass redistributions within the life support system. The greenhouse acts as a resource sink for the first roughly 90-100 days with the used simulation inputs. After that period the simulated hybrid life support system has a cyclic behavior.

This behavior is caused by the implemented (relatively simple) production schedule. Always when the capability of the greenhouse to consume carbon dioxide and produce oxygen is limited due to the production schedule, the survival of the crew is at risk. A perturbation e.g. a system failure during that period could lead to a lethal mission end.

The simulation results show a minimum in available potable water of 29 kilograms on day 229. This amount of water is less than the tolerable minimum for a crew of six with an average potable water demand of around 48 kg/d (includes around 31 kg/d hygiene water) and a greenhouse full of plants. The minimum in potable water is not caused by a general lack of available water. There are 870 kilograms of unprocessed wastewater stored inside the wastewater storage. The control parameters and the capacity of the VPCAR water recycling system seem to be of high importance for the modelled system architecture to avoid shortages in potable water.

Over the whole mission the life support system has accumulated around 5200 kg of solid waste and around 920 kg of unprocessed harvested inedible biomass. The incinerator and the inedible biomass processor are not able to recycle more solid material as mentioned before.

It is also evident from this simulation that the end of the mission when the greenhouse performance declines might be critical situation if system failures happen during that period.

4.3.4 Sensitivity Analyses

4.3.4.1 VPCAR capacity

The previous chapter described how that the potable water storage in the habitat reached a critical minimum on day 229. A sensitivity analysis of the VPCAR capacity has been performed in order to avoid this situation. The value for the VPCAR capacity converter has been set to nine different values from 60 to 100 kg/d. All other simulation inputs have not been changed. Figure 4-31 shows the results of the analysis. For the first 66 days when the VPCAR only has to process the wastewater production caused by the crew and small amounts from the incinerator there is no difference between the nine graphs, because the capacity values are all greater than the total wastewater production. That the overall cyclic behavior of the potable water in habitat storage is not affected by the value of the VPCAR capacity converter is also evident from Figure 4-31, because all graphs follow the same cycle. The cyclic behavior is caused by the greenhouse production schedule as mentioned earlier.
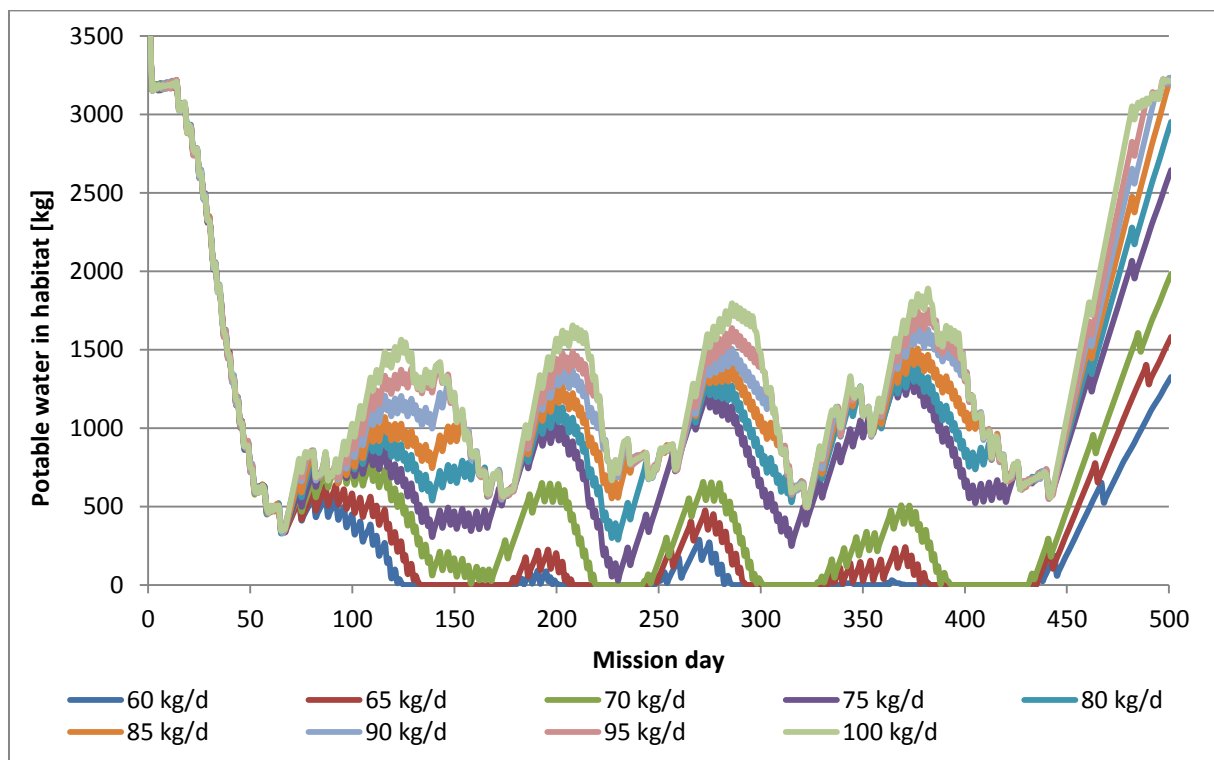
Figure 4-31: Potable water in habitat storage over mission duration for different VPCAR capacity values.

A VPCAR capacity of less than 75 kg/d always leads to shortages in potable water and therefore to mission critical situations. Although in such a situation the hygiene water demand would be reduced to zero in order to save potable water, that effort would not be enough to guarantee the survival of the crew because of the high water demand of the greenhouse. Reducing the potable water transfer to the greenhouse in this situation might save the crew's short term survival but would lead to reduced working capacity of the greenhouse and therefore to problematic situations in the long-term.

Chapter 4.3.3.3 already described the minimum of remaining potable water of 29 kilograms on day 229 for a VPCAR capacity of 75 kg/d. A higher capacity leads to a higher value of the potable water minimum as is shown in Table 4-21. One can also see that an increase in the

VPCAR capacity by 5 kg/d to 80 kg/d leads to a ten times higher potable water minimum of 290 kilograms on day 229. Another increase of the capacity from 80 to 85 kg/d almost doubles the remaining potable water on day 229. In order to increase system resilience the capacity of the VPCAR should be increased to 85 kg/d.

Table 4-21: Potable water minimum for different VPCAR capacities on mission day 229.

VPCAR capacity [kg/d]	75	80	85	90	95	100
Potable water in habitat minimum [kg]	29	290	557	686	708	713

4.3.4.2 Daily carbon gain and edible biomass fraction

The daily carbon gain (DCG) of a plant defines a series of other model parameters. Among these are the crop growth rate, the carbon dioxide consumption, the oxygen production and the water accumulating in the plant. Consequently a variation in the DCG value affects the life support system behavior at multiple spots. These variations can happen in a real space greenhouse even under controlled environmental conditions. A sensitivity analysis has been performed in order to understand the effects of a variation in the DCG. The DCG has been varied in steps of 5% from 90 to 110 % of the nominal value. This sensitivity analysis already includes the new value for the VPACR capacity of 85 kg/d.

The response of the system architecture to different values of DCG is best explained by looking at the oxygen storage stock, the potable water in habitat stock and the resupply food stock. The results of the sensitivity analysis are shown in Figure 4-32, Figure 4-33 and Figure 4-34. The purple line in all three figures represents normal DCG values for the grown crops. The red and the green lines symbolize an under performance of the crops by 10% respectively 5%. The teal and the blue lines show the results for an increased DCG by 5% respectively 10%. Larger deviations from the normal DCG values were not investigated.

The amount of oxygen in the oxygen storage stock is generally larger for higher DCG values (see Figure 4-32), because a higher DCG value means increased metabolism of the crop. Consequently more carbon dioxide is consumed and more oxygen produced. Higher DCG values also result in more biomass grown by the plants. More biomass means more water is accumulated inside the plants. This causes a higher demand of potable water by the habitat and therefore the amount of water inside the potable water in habitat stock is lower for higher DCG values, see Figure 4-33. For a DCG 10% higher than nominal throughout the whole mission, the potable water in habitat stock reaches critical minimums of remaining water several times. This can be compensated by a larger initial amount of potable water or by an increase in the VPCAR capacity, as was explained before.

Since the edible biomass fraction of the crop biomass has been kept constant for this analysis, less total biomass means less edible biomass. Consequently the demand of resupply food is higher for low DCG value as the lack of crop food is compensated by the resupply food. The initial value of the resupply food storage stock was set with a relatively small margin for the simulation under nominal condition. An underperformance of the crops represented by a lower than normal DCG value leads to a shortage of resupply food at the end of the mission, see Figure 4-34.
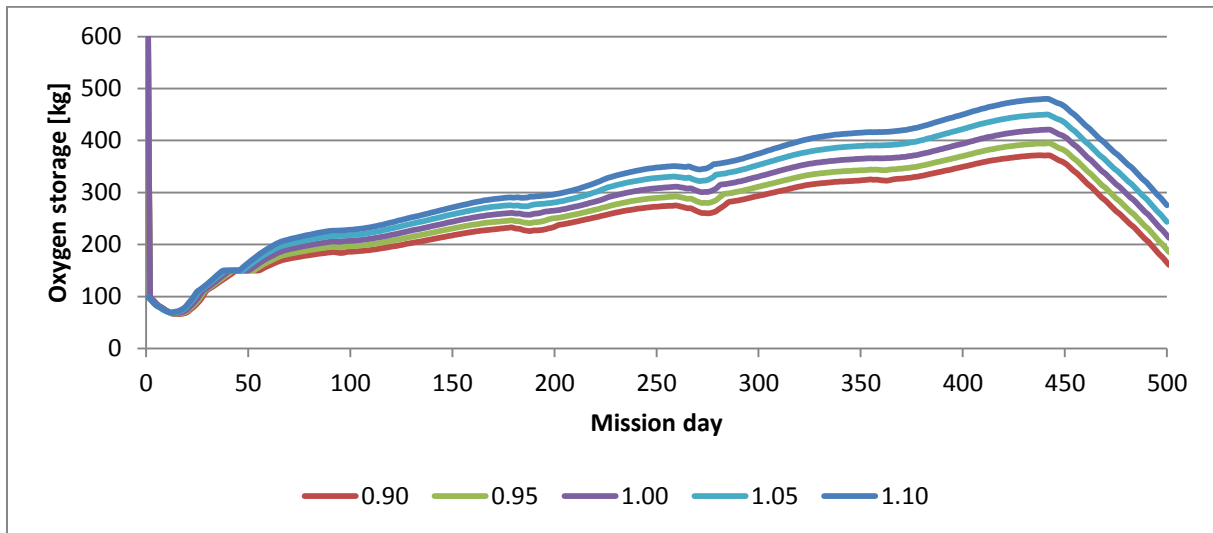
Figure 4-32: Oxygen storage stock for different factors of DCG.
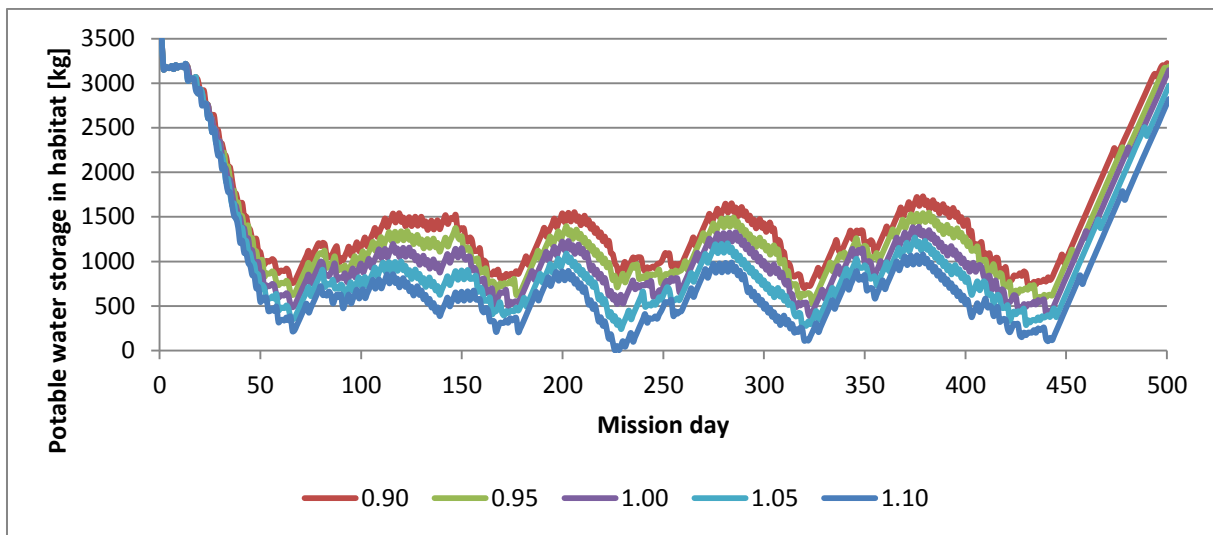
Figure 4-33: Potable water storage in habitat for different factors of DCG.
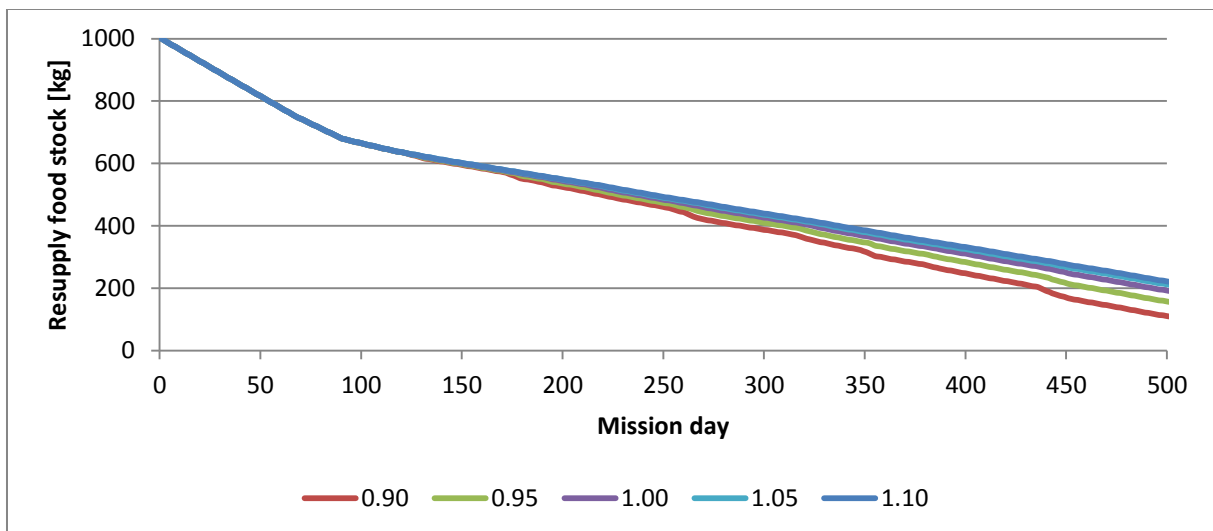
Figure 4-34: Resupply food stock for different factors of DCG.

Another important factor for crop performance is the edible fraction of the total biomass (XFRT) grown by a specific crop which is defined as a constant in the MEC plant model (see

Chapter 3.8). In a real greenhouse however plants might produce more inedible biomass (roots, leaves, etc.) and less edible biomass than expected. This was investigated in another sensitivity analysis for which XFRT was modified in the same way as the DCG. A factor was applied to the calculation of the edible biomass by modifying XFRT in steps of 5% from 90% to 110%.

The main effect of a variation of XFRT is on the produced edible biomass. There are also effects on the water balance and the inedible biomass production but those are minor. As mentioned before, the resupply storage stock makes up the remaining kilocalorie demand which cannot be fulfilled by the greenhouse diet. Consequently for lower values of XFRT the demand for resupply food is higher, which leads to food shortages at the end of the mission as shown in Figure 4-35. Again these shortages can be avoided by having a higher amount of resupply food at mission start.
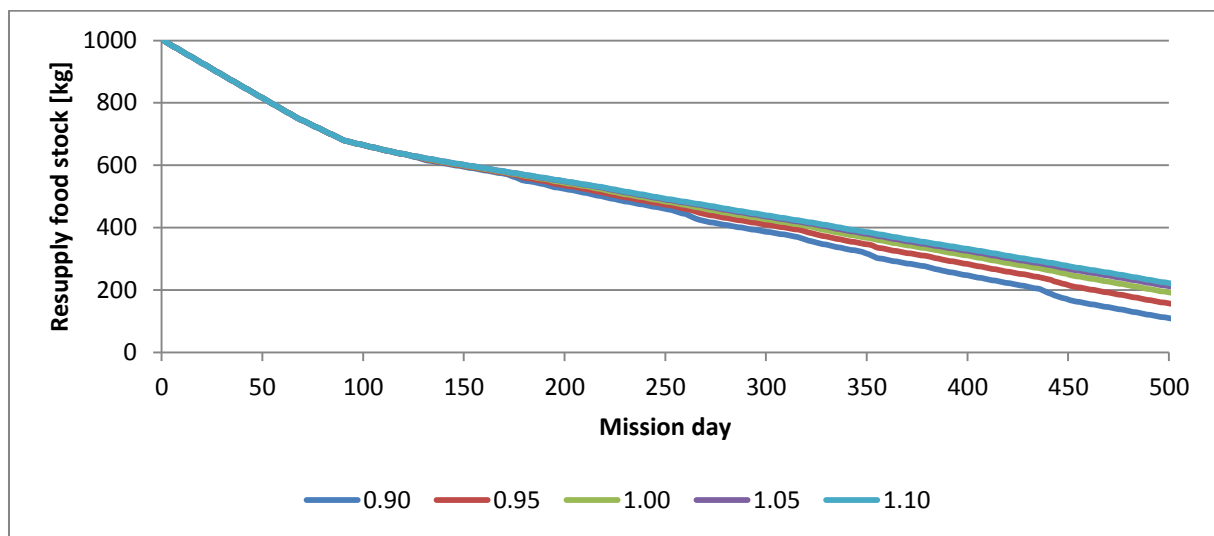
Figure 4-35: Resupply food stock for different factors of XFRT.

4.3.4.3 Habitat and greenhouse pressurized volume

The habitat and the greenhouse pressurized volume act as a buffer for the gas and humidity exchange of humans and plants with their environment. A larger pressurized volume in this case offers more buffer capability than a smaller volume. The value for the habitat volume defined for the simulation under nominal operation is rather big for an early Mars surface habitat. The greenhouse volume is based on a comparison of systems that were built and operated.

The results of a sensitivity analysis could not verify the hypothesis of an effect of the pressurized volume on the life support system behavior. The oxygen and the carbon dioxide concentrations inside the habitat and the greenhouse are not depending on the pressurized volume converters during nominal operation. This might be caused by the strict control parameters for the atmospheric concentrations of oxygen and carbon dioxide. There is however still the possibility that the pressurized volume values are of importance during off-nominal conditions in order to act as buffer.

4.3.5 Perturbation Analyses

All perturbation analyses include the new values for the VPCAR capacity converter of 85 kg/d and for the initial resupply food storage stock of 1000 kg. These values were determined in the previous chapter. All other simulation inputs remain at the values listed in Chapter 4.3.2

4.3.5.1 System failure

A failure of one component of a life support system is always a mission critical moment. Normally all life support systems have redundant components or backup systems that should take over in that case. Nevertheless an analysis has been performed to investigate a number of system failures. Each failure is defined by the duration and the time it occurs.

The previous chapters identified the VPCAR as a focal point within the modelled life support system. A failure of the VPCAR therefore can have a large impact on the mission success. Perturbation analyses have been run for two different time points of the mission. The first one is during the start-up phase of the greenhouse where the VPCAR mainly deals with the crew wastewater. A VPCAR system failure has been implemented on day 30. Simulations were performed with duration of 5 days and 15 days. The results are shown in Figure 4-36. Since there is still a lot of potable water left in the storage the 5 days and 15 days, failures have no significant impact. The amount of water declines faster than during the nominal operation scenario, but there are still around 280 liters left at the minimum. Failure duration of 15 days without repair or replacement of the VPCAR is relatively unlikely, but nevertheless the analysis shows that a VPCAR failure during the greenhouse start-up is not critical.
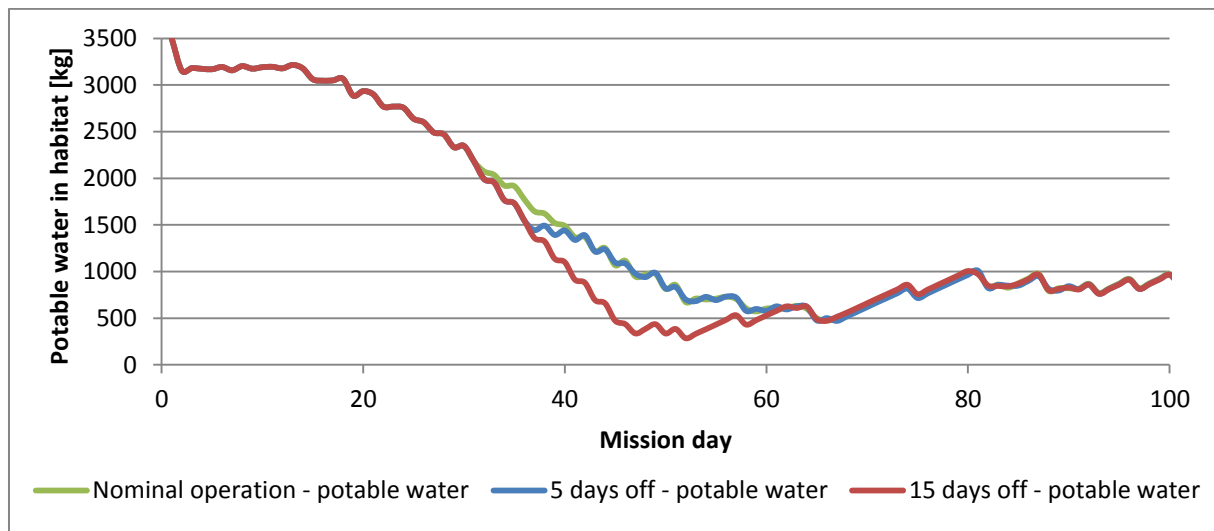
Figure 4-36: Potable water in habitat storage during VPCAR failure starting on day 30. Only the first 100 days of the simulation are shown here, because there is not difference in the graphs beyond day 100.

A critical moment during the mission with respect to a VPCAR failure is when the potable water storage stock is already very low because a lot of water is bound in living plants. This situation occurs around day 180. On day 179 a lot of plants are harvested and consequently the amount of water inside the wastewater storage is high. The newly sown plants require a lot of water from day 180 on. Figure 4-37 shows the results for a VPCAR failure on day 179 with duration of 5 days and 10 days compared to nominal operation. For both failure scenarios there is no immediate effect of the failure. The potable water storage declines as ex-

pected. The effects of the failure however continue to influence the amount of potable water up to day 260. This is caused by the fact that the plants are accumulating a lot of water in the time frame investigated. The VPCAR capacity cannot recycle enough water to provide potable water for the crew and the greenhouse. The 5 day failure scenario reaches its minimum of remaining water on day 227 with less than 5 kg water left in the stock. For the 10 day failure scenario the potable water stock in the habitat is already completely depleted on day 219.

There are means that the crew can take in the case of a VPCAR failure that lasts several days in order to decrease the impact of the failure. The crew can reduce the hygiene water to the bare minimum and could save around 30 kg/d of potable water. Furthermore, the crew could also reduce the illumination level inside the greenhouse to slow down the growth of the plants and therefore their water demand. This countermeasure however would lead to changes in the production schedule of the greenhouse and could cause issues later in the mission.
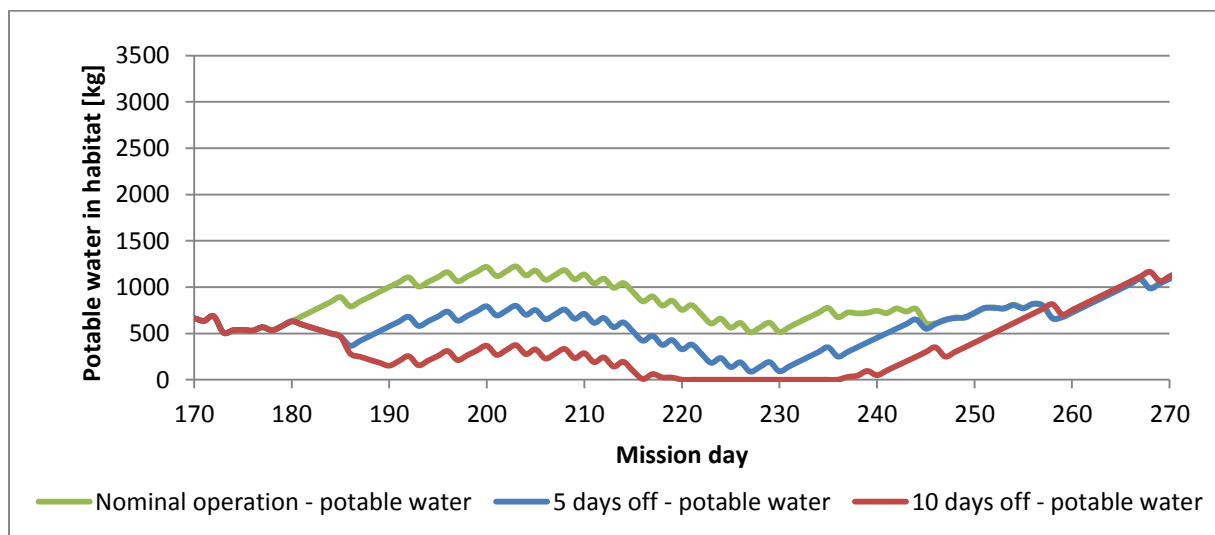
Figure 4-37: Potable water in habitat storage during VPCAR failure starting on day 179. Only the time period of importance for the analysis is shown here.

Failures of the CHX systems inside the habitat and the greenhouse have not been simulated. Such a failure would cause issues with the humidity in the atmosphere within a few hours of the failure which is smaller than he time step of the used model setup. This is especially the case for the greenhouse with the high transpiration rates of the plants.

Due to the architecture of the life support system with two separated atmospheres (habitat and greenhouse), failures of the carbon dioxide ad oxygen separator systems would cause trouble with the concentrations of the two gases within a few hours. The effects can only be seen with a time resolution in the range of hours. Since the shortest time step implemented in the model is one day, failures of the two gas separator cannot be investigated with the current model setup.

A failure of the incinerator and the edible biomass processor is especially critical during the start-up phase of the greenhouse. The initial amount of carbon dioxide in the storage stock is only enough to compensate such a failure during the first 60 days of the mission for around 5 days. Later in the mission when the carbon dioxide storage stock is filled up to its upper

threshold the amount of stored gas is enough to supply the greenhouse for 15-20 days of failure of the solid waste processors.

The failure of greenhouse systems such as the illumination or the nutrient delivery subsystem cannot be simulated by the model. There is however the possibility to investigate different scenarios of crop failure which would be the result of a long duration subsystem failure in the greenhouse, which are described in the next subchapter.

4.3.5.2 Greenhouse failure

A failure of the greenhouse can be caused by the failure of subsystems, by energy shortages or by mistreating the crops. Furthermore the plants can become infected by fungi or viruses, although that should theoretically never happen in a space greenhouse. Nevertheless a greenhouse failure could cause the death of plants and therefore lead to a mission critical scenario where the greenhouse cannot contribute to the life support system as planned. A greenhouse failure can affect only one compartment or multiple compartments or even the whole greenhouse at once. This chapter describes the results of perturbation analyses performed in order to investigate greenhouse failures.

The failure of one or multiple compartments is introduced by harvesting the plants before reaching the desired harvest date. The edible and inedible biomass accumulated within the plants until that point is directed to the respective harvested biomass stocks. Immediately after the failure occurs new plants are sown in order to bring the greenhouse back to its full production capacity.

The impact of the failure depends on the time when the failure occurs with respect to the mission duration and also on the time during the growth cycle of the plant. Therefore failures have been introduced at different time steps to investigate the effects. The analyses focus on failures in the soybean compartment which has the largest cultivation area of all compartments and on a complete greenhouse failure.

Figure 4-38 shows the greenhouse oxygen production graphs for simulated failures of the soybean compartment on day 14, day 47 and day 223 compared to the production during nominal operation. Overall one can say that all four graphs show a similar behavior, but with shifted peaks for the failure scenarios. The failure on day 14 has only a minimal effect on the production graph because the failure appears so early in the soybean growth cycle (14 days after sowing). The failures on day 47 and day 223 occur in the middle of the growth cycle of the soybean plants and both scenarios show a larger impact on the production graph than the failure on day 14. What is most evident is that the production peaks are offset to nominal operation. The last harvest for the day 47 and day 223 scenario is closer to the mission end, which results in more oxygen production at the end of the mission.

All failure scenarios of the soybean compartment still produce the same amount of edible biomass over the whole mission duration, because the cultivation area and the number of harvests are not influenced by the failures. Nevertheless the crew consumes more resupply food in the failure scenarios compared to the nominal operation. This is caused by the shifted harvests combined with the fixed mission duration of 500 days which leads to the effect, that the crew is not able to completely consume the edible biomass of the last soybean harvest. The missing food energy is compensated by the resupply food. The crew consumes roughly 18

kg (day 14 scenario), 79 kg (day 47 scenario) and 72 kg (day 223 scenario) more resupply food compared to nominal operation.

The additional demand of resupply food can be supplied by the initial amount food brought from Earth so that the crew does not need to starve. The simulations of the soybean compartment failures do not show shortages in water or oxygen. The implemented life support architecture with its buffer capacities dampens the effects of the failures greatly. In all three failure scenarios there was no need to turn on either the electrolyzer or the Sabatier reactor.

Another set of failure simulations has been performed. This time the failure affects the whole greenhouse and consequently the production schedule is interrupted. Failures have been introduced at day 0, day 50 and day 200 with different down times which means that the greenhouse is offline for a certain number of days following the failure event.

Figure 4-39 shows the oxygen production results of the greenhouse failure simulations to explain the effects. A complete greenhouse failure always results in a breakdown of the oxygen production to zero. After the failure event new plants are sown and transferred into the greenhouse. The oxygen production of the greenhouse increases with the plant growth and then follows the same pattern as the nominal operation graph, but shifted in time.
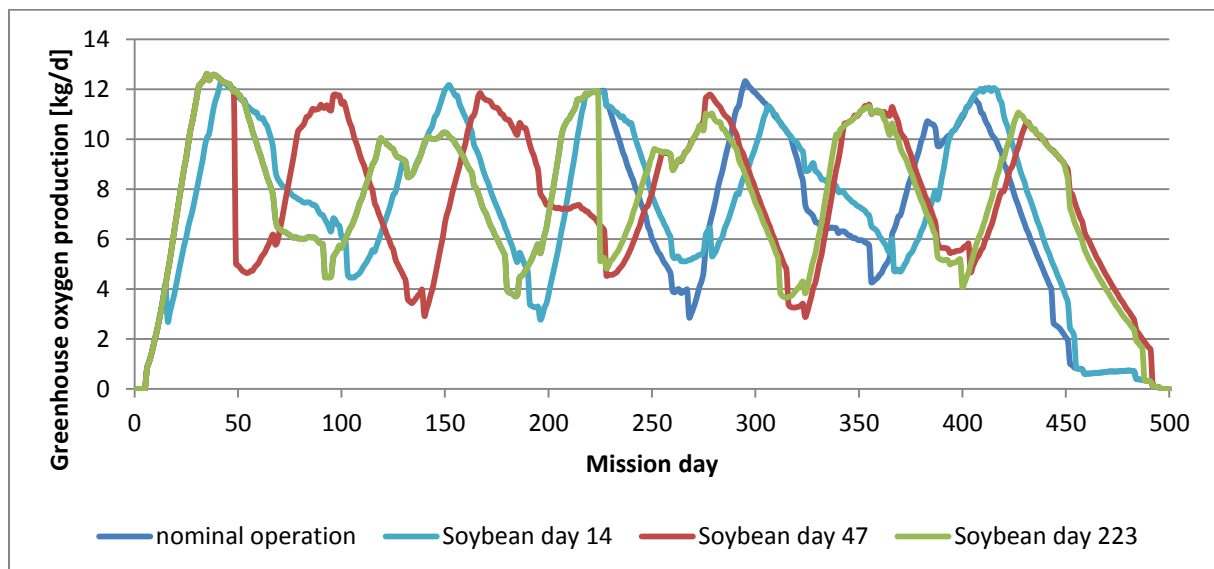
Figure 4-38: Greenhouse oxygen production for a complete failure of the soybean compartment on day 14, day 47 and day 223 compared to nominal operation.

The oxygen production graphs alone are not enough to show the impact of a complete greenhouse failure. Figure 4-40 shows the oxygen storage stock values throughout the mission for the different complete failure scenarios. One can see that the scenario with a greenhouse failure on day 0 with a down time of 30 days causes the oxygen storage stock to be depleted until the lower threshold of 50 kg is reached. Once this point is reached the electrolyzer starts operating to assure the survival of the crew. The electrolyzer needs to be operated for the whole duration of the greenhouse down time (30 days) and is only shut down once the greenhouse again produces enough oxygen.
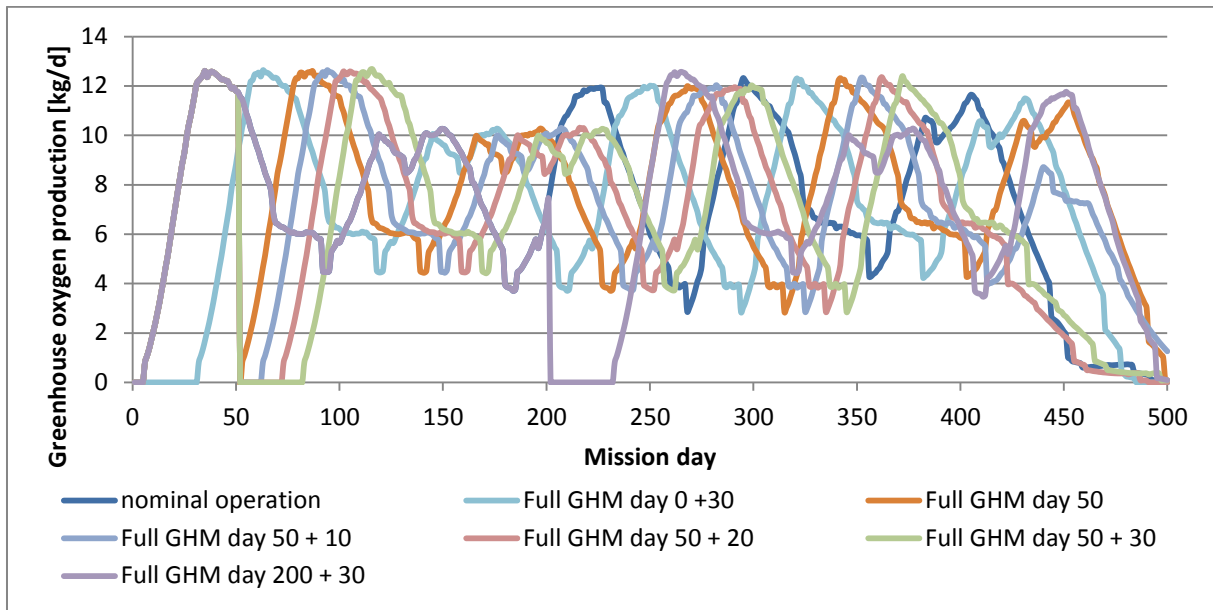
Figure 4-39: Greenhouse oxygen production for a complete greenhouse module (GHM) failure at different mission days and for different down times compared to nominal operation.

The failure scenarios on day 50 occur in the middle of the greenhouse startup phase. There has been only one lettuce harvest so far. No other plants have been harvested before the failure event occurs. One can see in Figure 4-40 that the surplus oxygen produced by the plants until day 50 has already built up a considerable amount of stored oxygen. Greenhouse down times of around less than 25 days for a failure on day 50 do not cause the oxygen storage stock to reach its lower threshold. When the down time is longer than around 25 days (e.g. the day 50 + 30 graph) the lower threshold is reached and the electrolyzer starts producing oxygen for the crew.

Since there is a general increase of stored oxygen over time, a complete greenhouse failure occurring later in the mission (e.g. on day 200) does not lead to a critical situation. Not even 30 days of down time following a failure event on day 200 requires the activation of the electrolyzer.
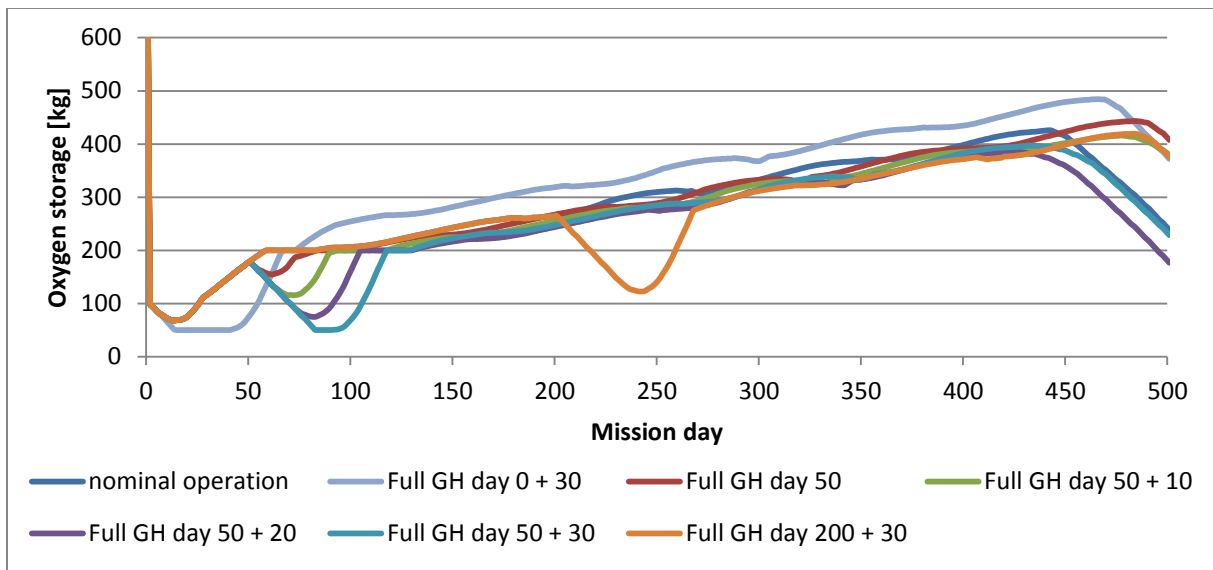
Figure 4-40: Oxygen storage for a complete greenhouse module (GHM) failure at different mission days and for different down times compared to nominal operation.

All complete failure greenhouse failure scenarios still produce the same amount of plant based food over the duration of the mission. Nevertheless similar to the soybean failure scenarios the crew consumes more resupply food, because the harvests are shifted closer to the mission end when the crew cannot consume all the harvested food before departure. The increase in resupply food consumption ranges from 80 kg (day 0 + 30 scenario) up to 190 kg (day 50 + 30 scenario). Again the initial food stock brought from Earth, as defined in 4.3.2, is enough to sustain the crew without starvation.

4.3.6 Summary of Results for a 500 day Mars Surface Habitat Mission

The simulations and analyses for a 500 day Mars surface habitat mission improve the understanding of a hybrid life support system behavior under different situations. The investigations show the importance of a reliable water recycling system (e.g. VPCAR) in order to guarantee that there are no water shortages throughout the mission. The condensing heat exchanger systems are of similar importance especially to recover the large amount of water transpired every day by the plants in the greenhouse. There is surplus oxygen accumulating over the course of the mission, because the resupply food and misc solid equipment consumed are subsequently transformed first into mostly carbon dioxide which is than transformed by the plants into oxygen. Dry solid waste and dry inedible biomass is also accumulating throughout the mission, because there was no need for additional carbon dioxide. The different perturbation analyses have shown the need for an electrolyzer and a Sabatier reactor as backup systems in order for the crew to survive critical situations. The initial amount of resupply food is 1000 kg. Of this amount 350 kg are not consumed under nominal operational conditions and act as buffer for contingencies. The simulations of the previous subchapters also revealed the large impact of the greenhouse production schedule on the overall life support system behavior. The perturbation analyses showed that the early days of the mission, the greenhouse startup phase, are a critical phase of the mission.

4.4 Habitat with a Full Nutrition Greenhouse

4.4.1 Description

The simulations under nominal operation described in Chapter 4.3 use a greenhouse that is able to provide roughly 1900 kcal per day per crewmember. The nominal daily demand per crewmember however is roughly 3000 kcal for men and 2300 kcal for women. The simulations described in the following subchapters utilize a full nutrition greenhouse to understand the life support behavior of such a configuration. Full nutrition in this case means that more than 95% of the kilocalories are provided by the greenhouse. However, there is still the need for resupply food to supply the crew during phases of low production, such as the greenhouse startup phase. A full nutrition greenhouse needs to produce more food than the nominal setup and has therefore more cultivation area. The average kilocalorie production of the greenhouse needs to be increased from around 11400 kcal per day to roughly 15900 kcal per day which is an increase of around 40 %.

4.4.2 Simulation Inputs

The life support system architecture, as described in 4.3.1, has not been changed for the following simulation. The simulation inputs however need to be adapted to the new scenario.

4.4.2.1 Root Model Setup

The root model setup for the full nutrition greenhouse simulations is equal to the setup for the nominal operation described in Chapter 4.3.2.1.

4.4.2.2 Gases Layer Inputs

The Gases Layer inputs for the full nutrition greenhouse are shown in Table 4-9. Compared to Chapter 4.3.2.2, the greenhouse pressurized volume is larger because of the increase in cultivation area for a full nutrition greenhouse.

Table 4-22: Gases Layer simulation inputs.

Variable Name	Variable Type	Value	Unit
O2 in Habitat	Stock	0	kg
O2 in Greenhouse	Stock	0	kg
CO2 in Greenhouse	Stock	0	kg
CO2 in Habitat	Stock	0	kg
O2 Storage	Stock	600	kg
CO2 Storage	Stock	50	kg
habitat pressurized volume	Converter	900	m³
greenhouse pressurized volume	Converter	1108.5	m³
CO Storage	Stock	0	kg
CH4 Storage	Stock	0	kg
H2 Storage	Stock	0	kg

4.4.2.3 Liquids Layer Inputs

The increase in cultivation area and the related increase of plants inside the greenhouse require an increase of the initial value of the potable water storage in habitat stock. Compared to Chapter 4.3.2.3 the value is increased to 5000 kg. All liquids layer inputs for the full nutrition greenhouse simulations are shown in Table 4-12.

Table 4-23: Liquids Layer simulation inputs.

Variable Name	Variable Type	Value	Unit
Water in Habitat Atmosphere	Stock	0	kg
Water in Greenhouse Atmosphere	Stock	0	kg
Water Accumulated in Living Plant Biomass	Stock, arrayed	0	kg
Water Accumulated in Harvested Edible Biomass	Stock	0	kg
Water Accumulated in Harvested Inedible Biomass	Stock	0	kg
Wastewater Storage	Stock	0	kg
Potable Water Storage in Habitat	Stock	5000	kg
Water Reservoir in Crew	Stock, arrayed	50.0 (men), 31.5 (women)	kg
Potable Water Storage in Greenhouse	Stock	50	kg
potable water storage in greenhouse lower limit	Converter	200	kg
potable water storage in greenhouse nominal limit	Converter	350	kg

4.4.2.4 Solids Layer Inputs

The astronauts in the full nutrition greenhouse simulations consume more greenhouse food compared to the simulations under nominal operation (Chapter 4.3). The new values for the greenhouse diet array are shown in Figure 4-41. Since the greenhouse contributes much more to the diet in the full nutrition greenhouse scenario, the initial amount of resupply food is reduced to 600 kg. All Solids Layer Inputs are shown in Table 4-13.

Table 4-24: Solids Layer simulation inputs.

Variable Name	Variable Type	Value	Unit
Crop Food Storage	Stock, arrayed	0	kg
Harvested Edible Dry Biomass	Stock, arrayed	0	kg
Edible Dry Biomass in Plants per compartment per cycle	Stock, arrayed	0	kg
Inedible Dry Biomass in Plants per compartment per cycle	Stock, arrayed	0	kg
Harvested Inedible Dry Biomass	Stock	0	kg
Solid Waste Storage in Habitat	Stock	0	kg
Resupply Food Storage	Stock, arrayed	600	kg
greenhouse diet composition per astronaut	Converter, arrayed	See Figure 4-41 for values.	kg/d
harvest events	Converter, arrayed	Dependent on the production schedule of the greenhouse model.	-
Misc Solids Storage	Stock	6000	kg
Crew Metabolic Solids	Stock	350	kg

	astronaut 1	astronaut 2	astronaut 3	astronaut 4	astronaut 5	astronaut 6
Dry Bean	0.02	0.02	0.02	0.01	0.01	0.01
Lettuce	0.02	0.02	0.02	0.015	0.015	0.015
Peanut	0.05	0.05	0.05	0.035	0.035	0.035
Rice	0.04	0.04	0.04	0.03	0.03	0.03
Soybean	0.2106	0.2106	0.2106	0.17	0.17	0.17
Sweet Potato	0.05	0.05	0.05	0.035	0.035	0.035
Tomato	0.02	0.02	0.02	0.015	0.015	0.015
Wheat	0.2	0.2	0.2	0.15	0.15	0.15
White Potato	0.1	0.1	0.1	0.075	0.075	0.075

Figure 4-41: Greenhouse diet per astronaut in kilograms dry mass per day for a full nutrition greenhouse.

4.4.2.5 Crew Model Inputs

The crew model inputs for the full nutrition greenhouse simulations are equal to the setup for the nominal operation described in Chapter 4.3.2.5.

4.4.2.6 Greenhouse Model Inputs

The greenhouse production plan for the full nutrition greenhouse is the same as the one shown in Figure 4-15 in Chapter 4.3.2.6. The cultivation area of the different compartments had to be increased significantly in order to produce enough crop food for a diet almost fully

based on greenhouse produce. The cultivation area values for the full nutrition greenhouse simulations are shown in Table 4-25.

Table 4-25: Cultivation area per compartment in square meters.

1	2	3	4	5	6	7	8	9	10
12	16	55	21	166	8	11	51.5	29	16

4.4.2.7 Physical-Chemical Systems Inputs

Table 4-20 shows the input values for the physical-chemical systems module. The only value that had to be changed compared to Chapter 0 is the VPCAR capacity. The VPCAR capacity is increased from 85 kg/d to 100 kg/d in order to be able to process more wastewater generated through plant biomass recycling. Furthermore, the greenhouse CHX had to be increased to 1500 kg/d to adjust to the increase in transpiration water produced by the greenhouse.

Table 4-26: PC Systems simulation inputs.

Variable Name	Variable Type	Value	Unit
incinerator capacity	Converter	20	kg/d
solid waste storage lower threshold	Converter	50	kg
O2 storage upper threshold	Converter	150	kg
CO2 storage lower threshold	Converter	50	kg
electrolyzer capacity	Converter	12	kg/d
O2 storage lower threshold	Converter	50	kg
Sabatier capacity	Converter	7	kg/d
CO2 storage upper threshold	Converter	100	kg
H2 storage lower threshold	Converter	10	kg
habitat CHX capacity	Converter	10	kg/d
greenhouse CHX capacity	Converter	1500	kg/d
VPCAR capacity	Converter	100	kg/d
potable water storage habitat lower threshold	Converter	100	kg
wastewater storage upper threshold	Converter	50	kg
wastewater storage lower threshold	Converter	0	kg
O2 separator capacity	Converter	18	kg/d
CO2 separator capacity	Converter	20	kg/d
inedible biomass processor capacity per crop	Converter	5	kg/d
harvested inedible biomass storage upper threshold	Converter	50	kg

4.4.3 Full Nutrition Greenhouse Simulation Results

4.4.3.1 Overview of results for the full nutrition greenhouse

For the simulation of the habitat with a full nutrition greenhouse scenario the model was run with the simulation inputs defined in Chapter 4.4.2 to simulate the operation of the life support system. The following conditions have been achieved:

- All crew members survived the mission in good shape.
- The stocks for potable water, oxygen, carbon dioxide and food stayed within ranges to sustain all crew members.

- No system failures or other perturbations have been included.

The model validation method explained in Chapter 3.11 was executed again with the parameter setting of for the full nutrition greenhouse simulation. The results show that the system closure is equal to the results of the model validation. Consequently the results which are explained in the following subchapters are valid within the capabilities of the model.

4.4.3.2 Gases Layer behavior for the full nutrition greenhouse

The full nutrition greenhouse simulation scenario incorporates the same production schedule as it is used for the nominal operation simulation described in Chapter 4.3. Consequently, the oxygen production graph for the full nutrition greenhouse simulation shows the same pattern as the graph of the nominal operation, see Figure 4-42. However, since the full nutrition greenhouse has a larger cultivation area and therefore contains more plants, the oxygen production is larger. Even at times of less oxygen production (e.g. around day 270), the greenhouse produces more oxygen than the crew requires.
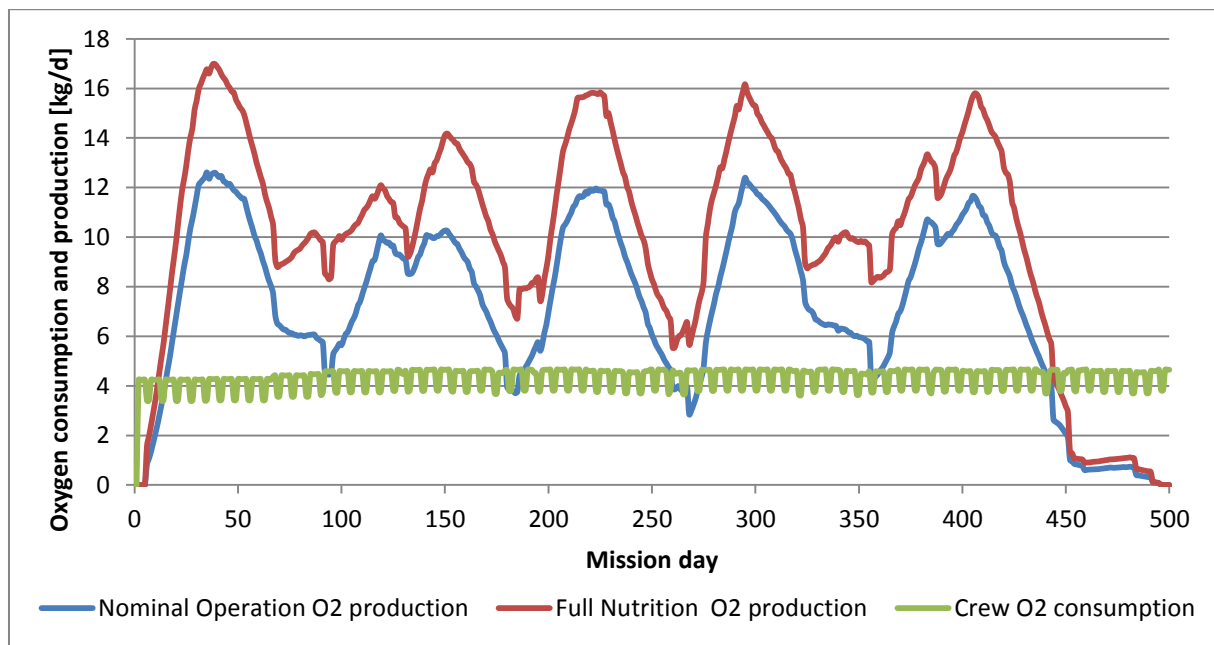
Figure 4-42: Greenhouse oxygen production for nominal operation (blue graph) and for the full nutrition greenhouse (red graph) compared to the crew oxygen consumption (green graph).

4.4.3.3 Liquids Layer behavior for the full nutrition greenhouse

The behavior of the water storage stocks for the full nutrition greenhouse simulation is shown in Figure 4-43. As mentioned before the initial value of the potable water storage in habitat stock was increased to 5000 kg in order to have enough water available for the enlarged greenhouse. The VPCAR capacity was also increased. Both adjustments together ensure that there is enough potable water, including a safety margin, throughout the whole mission.
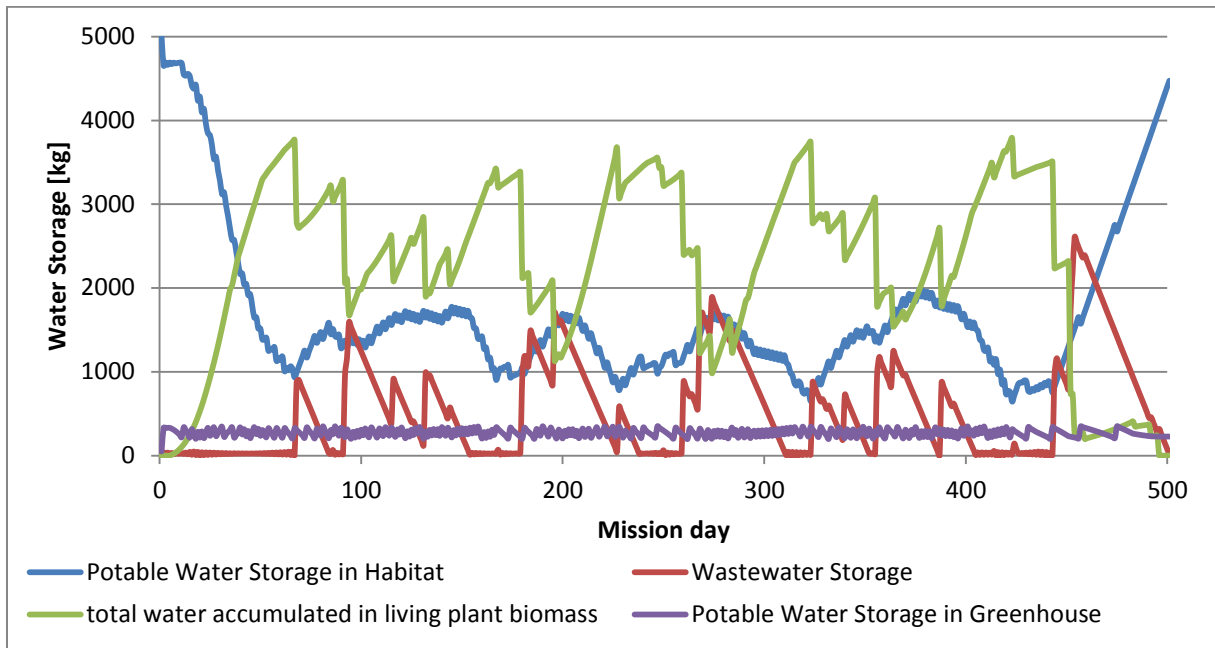
Figure 4-43: Water storages during the simulation of the full nutrition greenhouse scenario.

4.4.3.4 Solids Layer behavior for full nutrition greenhouse

The food consumption during the mission with a full nutrition greenhouse is shown in Figure 4-44. During the greenhouse startup phase the crew needs to rely on some resupply food. From day 143 on the greenhouse is able supply the majority of the food that the crew requires. While the crew consumes around 350 kg during the greenhouse startup phase, the consumption of resupply food between day 143 and day 500 is only roughly 13.5 kg, which is on average around 0.037 kg/d for the whole crew. This behavior is also visible in Figure 4-45 (red graph). The total resupply food consumption is, as expected, much less compared to the nominal operation scenario described in Chapter 4.3. While the crew consumes roughly 800 kg of resupply food under nominal operation, the consumption with a full nutrition greenhouse is only around 365 kg.
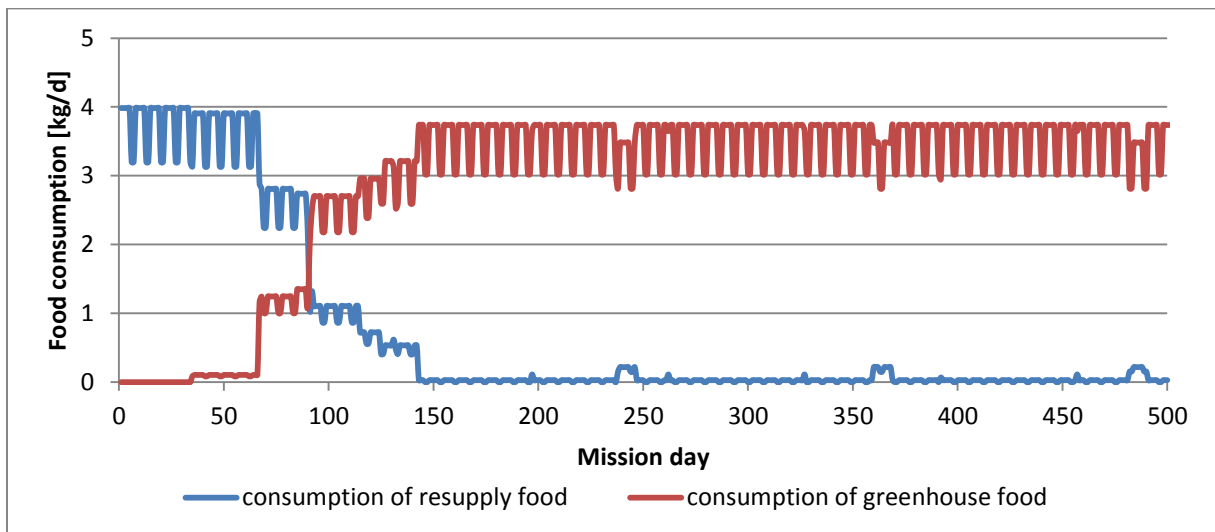
Figure 4-44: Resupply food and greenhouse food consumption for the full nutrition greenhouse scenario.
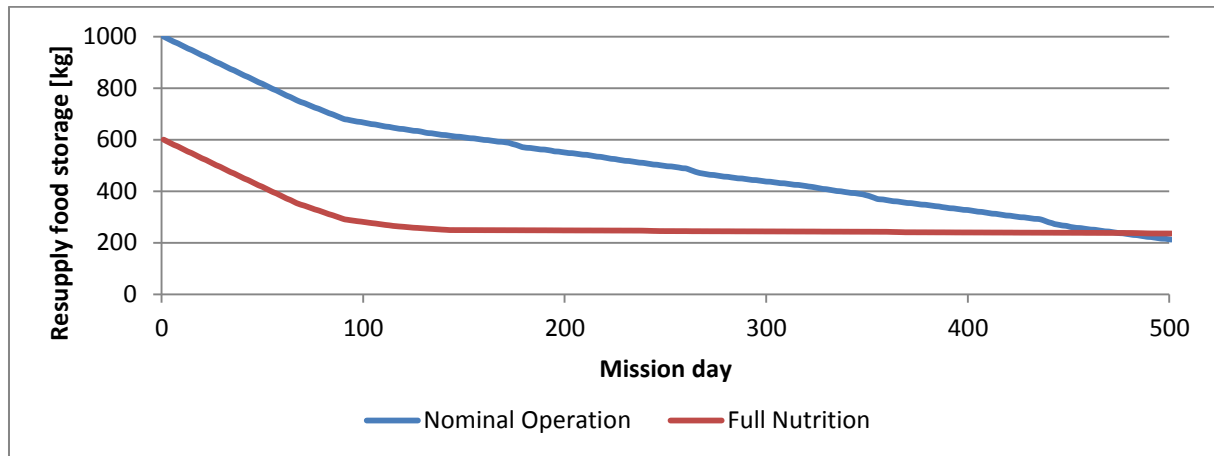
Figure 4-45: Resupply food storage behavior for the nominal operation scenario (blue graph) compared to the full nutrition greenhouse scenario (red graph).

4.4.3.5 Physical-Chemical Systems behavior for the full nutrition greenhouse

The capacity of the VPCAR water recycling system and the greenhouse CHX had to be increased for the full nutrition greenhouse, as mentioned before. The higher carbon dioxide demand of the full nutrition greenhouse causes more activity of the incinerator and the inedible biomass processor compared to the simulations under nominal operation. Otherwise there are no differences between the full nutrition greenhouse scenario and the nominal operation scenario of Chapter 4.3.

4.4.3.6 Discussion of results for the full nutrition greenhouse

The previous subchapters described the results for the simulation of a Mars surface habitat containing a full nutrition greenhouse. A few adjustments had to be made compared to the nominal operation scenario of Chapter 4.3 in order to make the life support system work as desired. The initial amount of potable water had to be increased significantly from 3500 kg to 5000 kg, while the amount of resupply food could be reduced from 1000 kg to 600 kg. The VPCAR capacity had to be increased from 85 to 100 kg/d and the greenhouse CHX capacity from 1000 to 1500 kg/d.

The crew is sustained throughout the whole mission duration. The behavior of the life support system with a full nutrition greenhouse is very similar to the nominal operation scenario. The behavior of the life support system is defined by the implemented plant production schedule, as mentioned in previous chapters. How a hybrid life support system with a full nutrition greenhouse responses to certain perturbations is described in the following chapter.

4.4.4   Sensitivity Analyses

4.4.4.1 VPCAR capacity

A sensitivity analysis of the VPCAR capacity for the full nutrition greenhouse scenario has been performed. As mentioned before, the VPCAR capacity has been increased for the full nutrition greenhouse scenario compared to the nominal operation scenario. The results are shown in Figure 4-46. The graphs show that a VPCAR capacity of more than 90 kg/d is sufficient for the full nutrition greenhouse scenario to always have enough potable water left in the storage, including a safety margin.
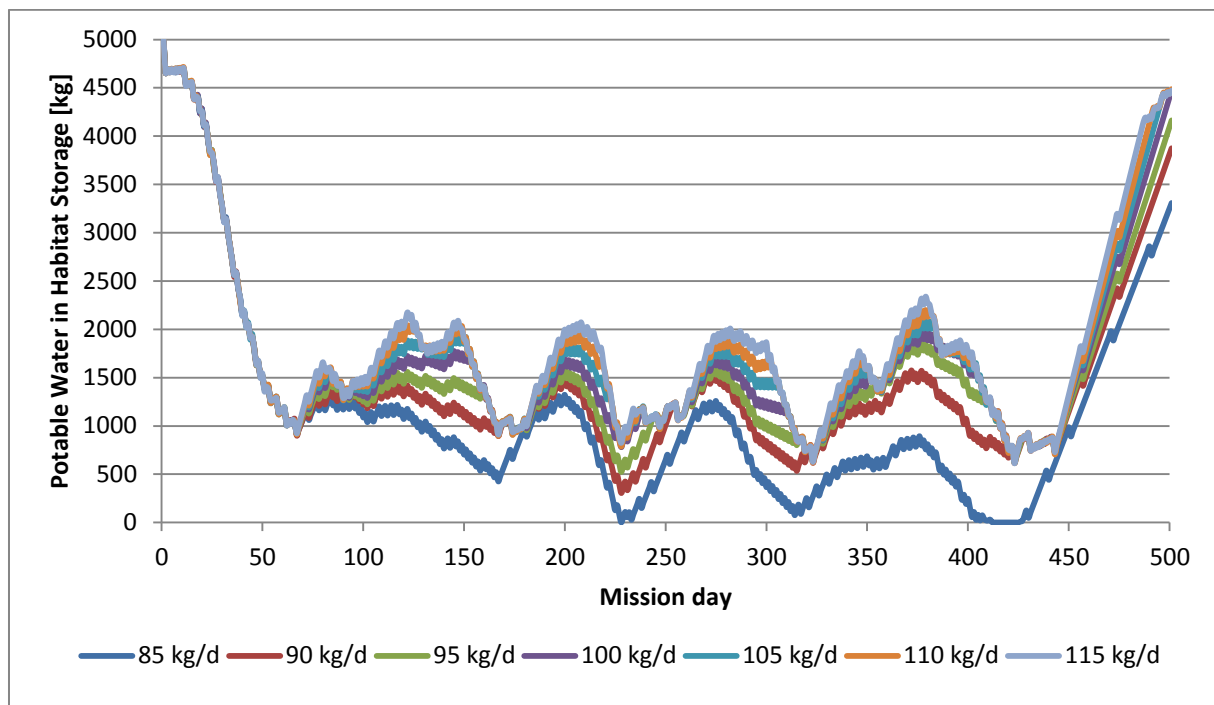
Figure 4-46: Potable water storage in habitat behavior for a full nutrition greenhouse and different VPCAR capacity values.

4.4.4.2 Daily carbon gain and edible biomass fraction

The daily carbon gain (DCG) has been varied for this sensitivity analysis from 0.90 to 1.10 times the nominal value in the same way as in the investigation for the nominal greenhouse operation in Chapter 4.3.4.2. A higher DCG values represents a faster crop growth and a larger plant at harvest. Consequently higher DCG values lead to more produced oxygen over the course of the mission. The behavior of the oxygen storage stock during the full nutrition greenhouse simulation is similar to the simulation under nominal operation. The same is valid for the potable water storage stock. Here a higher DCG leads to more potable water demand by the greenhouse and to lower potable water minimums during the mission similar to the results of the nominal operation simulation described in Chapter 4.3.4.2. Therefore no graphs for the oxygen storage stock and the potable water in habitat storage stock are shown here.

Figure 4-47 shows the graphs of the resupply food storage stock for different values of DCG. One can see that a DCG greater than 1.00 is not beneficial, because the full nutrition green-house already produces enough food for the crew under nominal conditions. A DCG value smaller than 1.00 results in a higher demand of resupply food. For a DCG value of 0.90, meaning that the full nutrition greenhouse only produces 90 % of the expected food, the crew requires around 150 kg more resupply food than normal. This is 25 % of the initial resupply food stock.

As already mentioned in Chapter 4.3.4.2, the value XFRT (edible biomass fraction) only affects the ratio of inedible to edible biomass generated by the plants. Figure 4-48 shows the analysis results for varying XFRT of the resupply food stock. When comparing Figure 4-47 and Figure 4-48, one can see that the variation of DCG and XFRT has the same effect on the behavior of the resupply food stock.
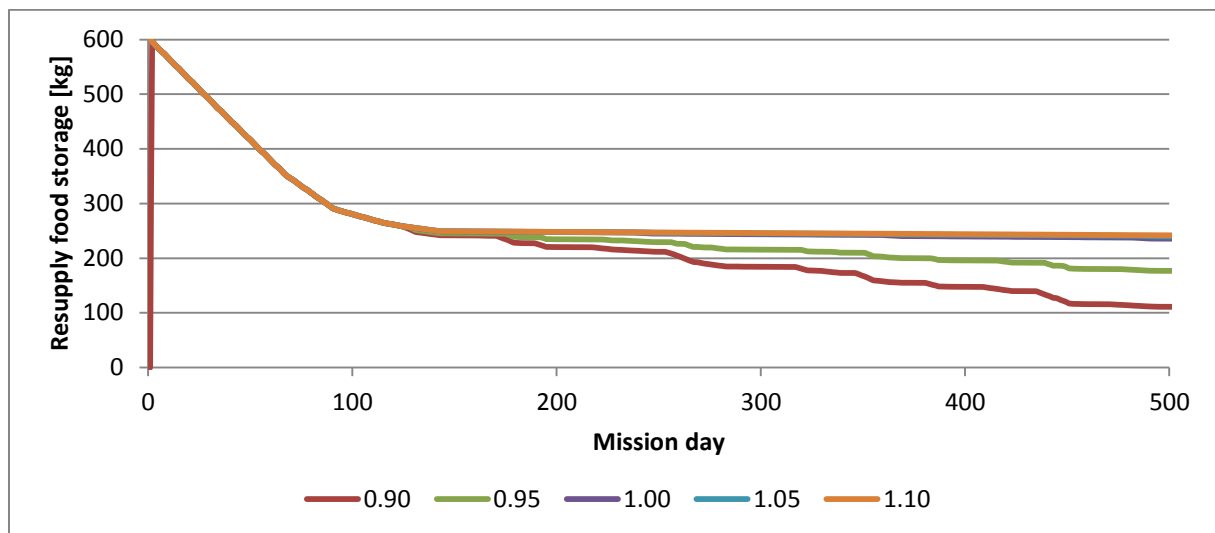
Figure 4-47: Resupply food storage for a full nutrition greenhouse and different factors of DCG.
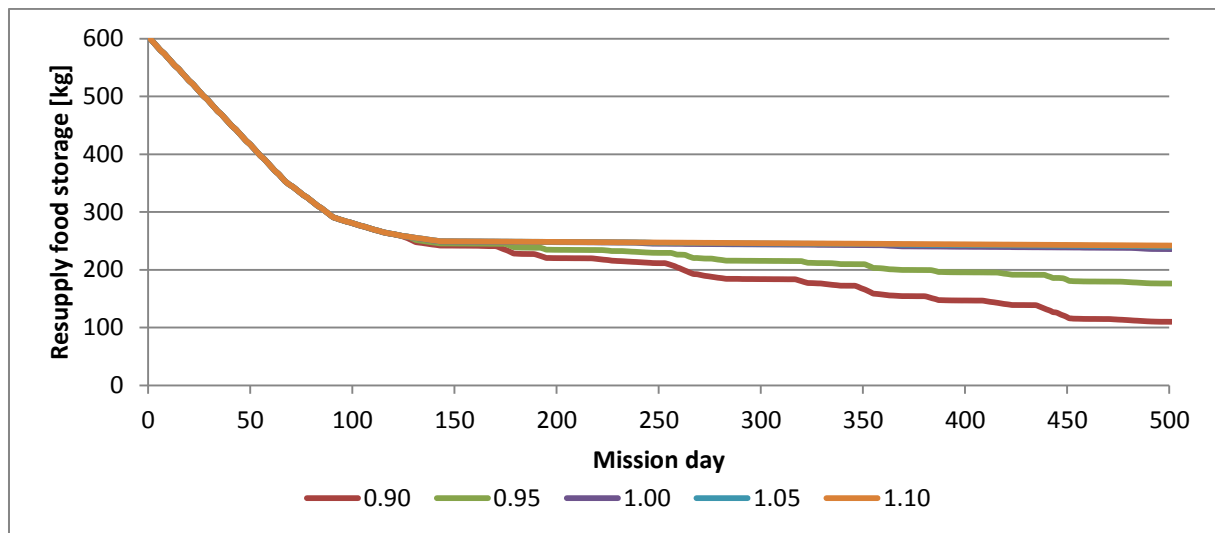
Figure 4-48: Resupply food storage for a full nutrition greenhouse and different factors of XFRT.

4.4.5 Perturbation Analyses

4.4.5.1 VPCAR system failure

The VPCAR system failure analysis for the full nutrition greenhouse scenario has been performed in the same way as for the nominal operation scenario (see Chapter 4.3.5.1). Figure 4-49 shows the behavior of the potable water in habitat stock for a VPCAR failure on day 30 and a defined amount of non-operational days. The exact same perturbation analysis has been performed for the simulations under nominal operation.

The full nutrition greenhouse setup however is more robust, because the overall amount of water is larger and therefore provides more buffer capability. The failure would have last more than 25 days to result in a critical mission end. Whereas for the nominal operation this is already the case for failure duration of around 17 days (see Figure 4-36 for comparison). Figure 4-49 also shows that the life support system is able to recover from a VPCAR system failure once the system has been repaired. The longer the period of non-operational days the longer is the time recovery period. A 5 day failure requires only a few days recovery period. A

15 day failure period starting on day 30 already requires a recovery period of 27 days and the scenario with 25 non-operational days only recovers normal operational behavior after 127 days.

For the second VPCAR failure scenario under nominal operation day 179 was chosen, because this point during the mission is critical. This is however not true for the full nutrition greenhouse scenario. Here VPCAR failures on day 179 do not have a large effect on the system behavior. The full nutrition greenhouse scenario has a critical point around day 200, when a high productive phase of the greenhouse begins and the potable water storage is rather low. Figure 4-50 shows the results of a VPCAR failure on day 200 and two different options for the amount of non-operational days following the failure. It is clear that already a period of 5 non-operational days of the water recycling system leads to a dangerously low amount of potable water on day 227. A period of 10 non-operational days results in water shortages and a critical mission outcome.
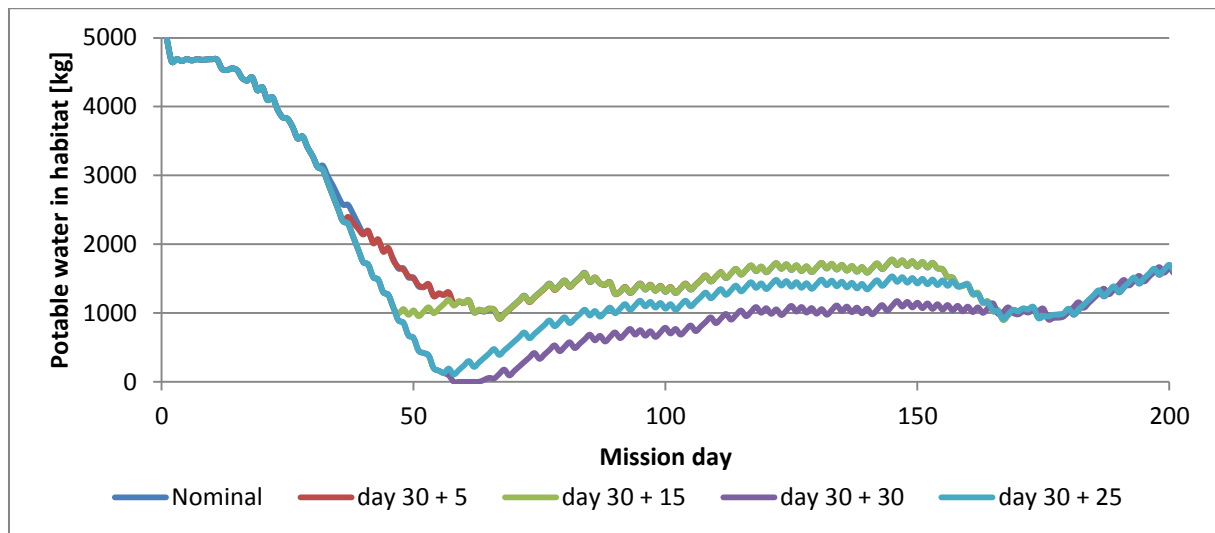
Figure 4-49: Potable water in habitat for a full nutrition greenhouse and VPCAR failures on day 30 for different amounts of non-operational days (graphs only shown for the first 100 days).
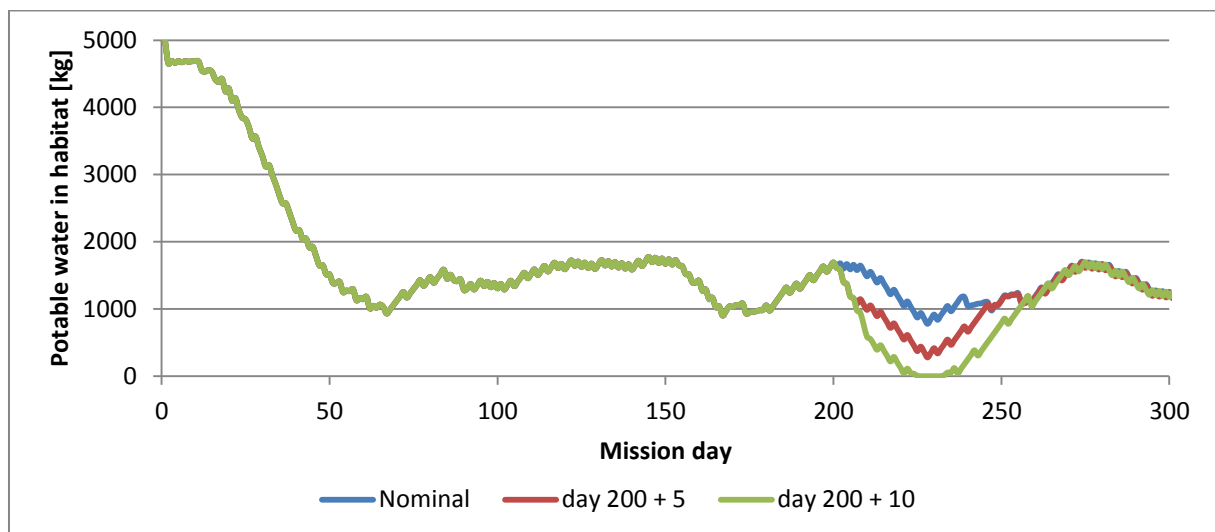
Figure 4-50: Potable water in habitat for a full nutrition greenhouse and VPCAR failures on day 200 for different amounts of non-operational days (graphs only shown for the first 300 days).

As with the perturbation analysis under nominal operation (Chapter 4.3.5.1), no active countermeasures have been implemented. An active countermeasure could be for example a reduction of hygiene water consumption.

4.4.5.2 Greenhouse failure

Only full greenhouse failures are simulated for the full nutrition greenhouse scenario. Therefore, the failures occur on the same days and with the same amount of non-operational days as for the perturbation analysis under nominal operation (see Chapter 4.3.5.2). The greenhouse production goes down after a failure. Similar to the simulation under nominal operation, the activation of the electrolyzer and the Sabatier reactor is required in order to sustain the oxygen supply for the crew.

In the full nutrition greenhouse scenario the crew relies largely on greenhouse food and has less resupply food available than in the nominal operation scenario. Figure 4-51 shows the values of the resupply food storage for different full greenhouse failure scenarios. All full greenhouse failure scenarios require significantly more resupply food, see Table 4-27. When the failure occurs on day 50 and the greenhouse is not operational for 30 days after the failure, the resupply food storage is completely depleted around day 200. A few days later the greenhouse is again able to supply the majority of the food. However since the resupply food storage is depleted, the crew would have a deficit in kilocalorie supply of around 5 % per day until the end of the mission. An additional greenhouse failure after day 200 would lead to the starvation of the crew.

Table 4-27: Resupply food consumption (in kg) for a full nutrition greenhouse and different greenhouse failure scenarios.

nominal	day 30 + 0	day 50 + 0	day 50 + 10	day 50 + 20	day 50 + 30	day 200 + 30
364.3	459.8	506.6	543.9	581.3	600	546.2
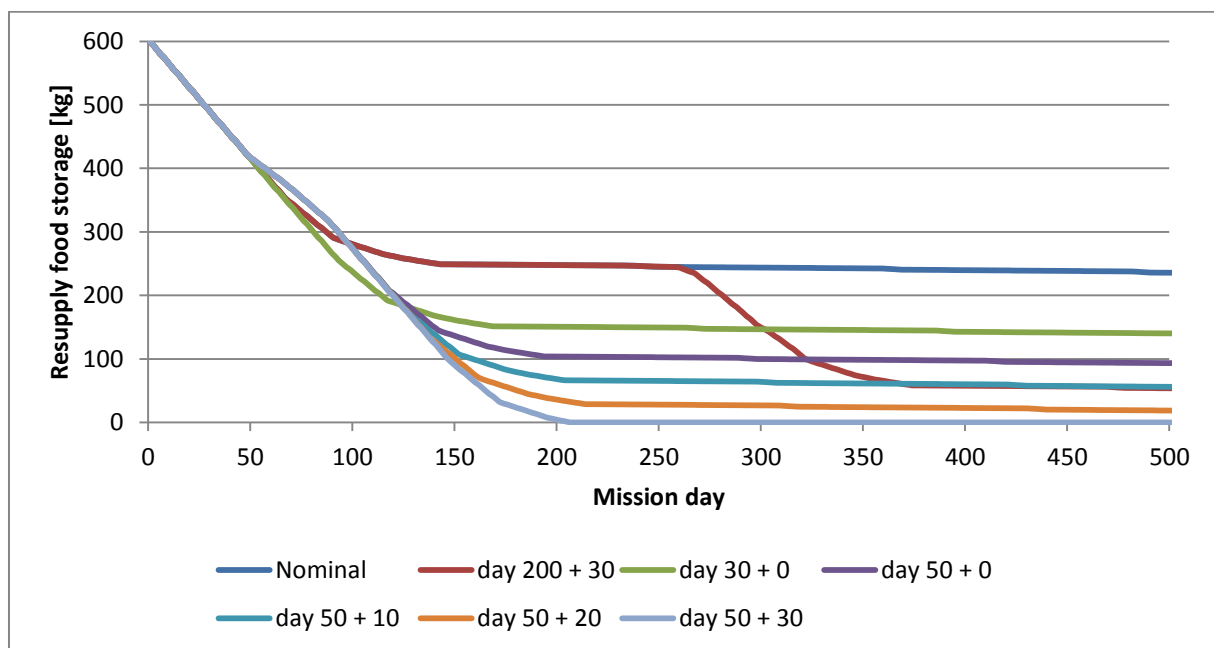
Figure 4-51: Resupply food storage for a full nutrition greenhouse and different full greenhouse failure scenarios.

4.4.6 Summary of Results for a Full Nutrition Greenhouse Scenario

For the full nutrition greenhouse scenario the cultivation area inside the greenhouse has been significantly increased in order to supply more food to the crew. The scenario requires a larger amount of potable water at mission start than the nominal operation scenario in order to sustain the increased amount plants. Furthermore, the VPCAR capacity had to be increased in order to handle the larger amounts of wastewater produced by the greenhouse.

The behavior of the oxygen and carbon dioxide mass flows with a full nutrition greenhouse is equal to the scenario described in Chapter 4.3. The only difference being a higher activity of the incinerator and the inedible biomass processor in order to produce additional carbon dioxide. The various water streams also look very similar between the two scenarios with the exception that there are 1500 kg more water in the system for the full nutrition greenhouse.

The main difference between the nominal greenhouse of Chapter 4.3 and the full nutrition greenhouse of this chapter is in the behavior of the different food and biomass cycles. Since the full nutrition greenhouse produces nearly all the food the crew requires, the resupply food demand is much lower compared to the simulation scenario of Chapter 4.3.

The sensitivity and perturbation analysis performed with the full nutrition greenhouse show no significant difference to results acquired during the simulation with the greenhouse of Chapter 4.3.

4.5 Greenhouse Production Schedule Improvement

One result of the previous simulations is the large effect the greenhouse production schedule has on the overall life support system behavior. The simulation described in this chapter serves as an example how to optimize a greenhouse production schedule. For the analysis the simulation input and results of Chapter 4.3 are used as reference.

There are moments in the simulation under nominal condition when the oxygen production by the greenhouse is lower than the demand by the crew (around day 180 and 270 in Figure 4-52). One goal of improving the production schedule is to avoid such moments, because these are potentially critical situations when perturbations occur at the same time. Furthermore, the oxygen production of the greenhouse greatly varies over the course of the mission. The maximum is at around 12.5 kg/d while the minimum is at around 3.0 kg/d (excluding the beginning and the end of the mission).

The large cultivation area (175.8 m²) of compartment 6 containing the soybean plants which is roughly 59 % of the total greenhouse cultivation area greatly dominates the overall system behavior. Therefore the first step to smoothing the production curve is to split the soybean cultivation area over two compartments with their growth cycles offset by half of the growth duration. Furthermore, the growth cycles of the wheat, peanut and white potato compartments have been shifted slightly to further smooth the production curve. The improved production schedule is shown in Figure 4-53 compared to the initial production schedule shown in Figure 4-15.
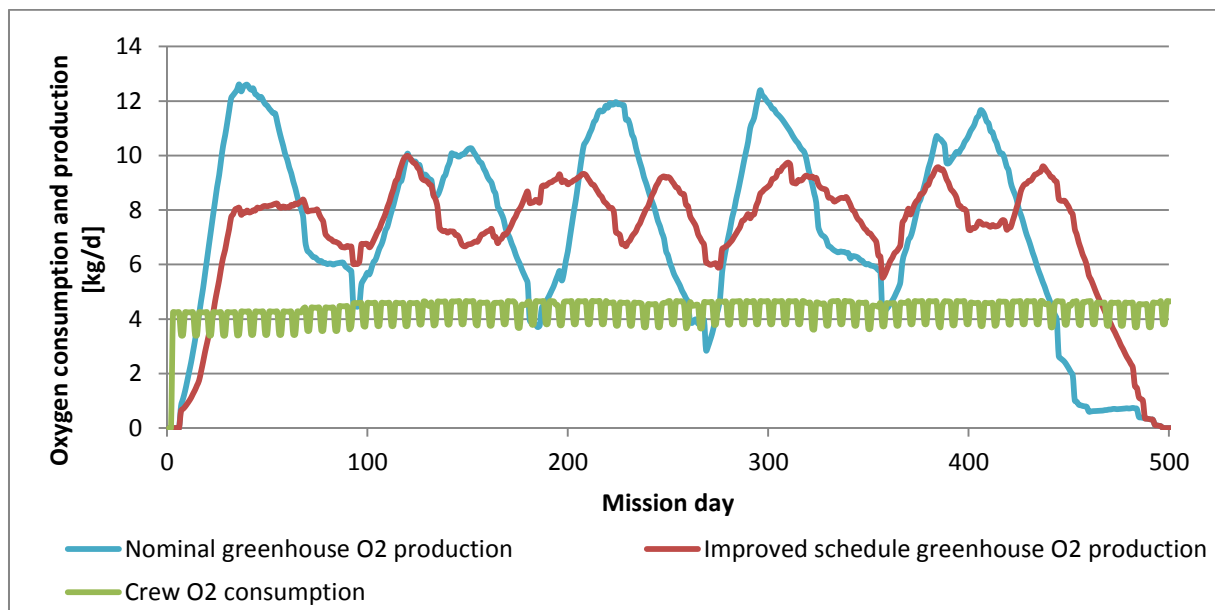
Figure 4-52: Crew oxygen demand (green curve) and greenhouse oxygen production under nominal operation (light blue curve) and greenhouse oxygen production with an improved schedule (red curve).
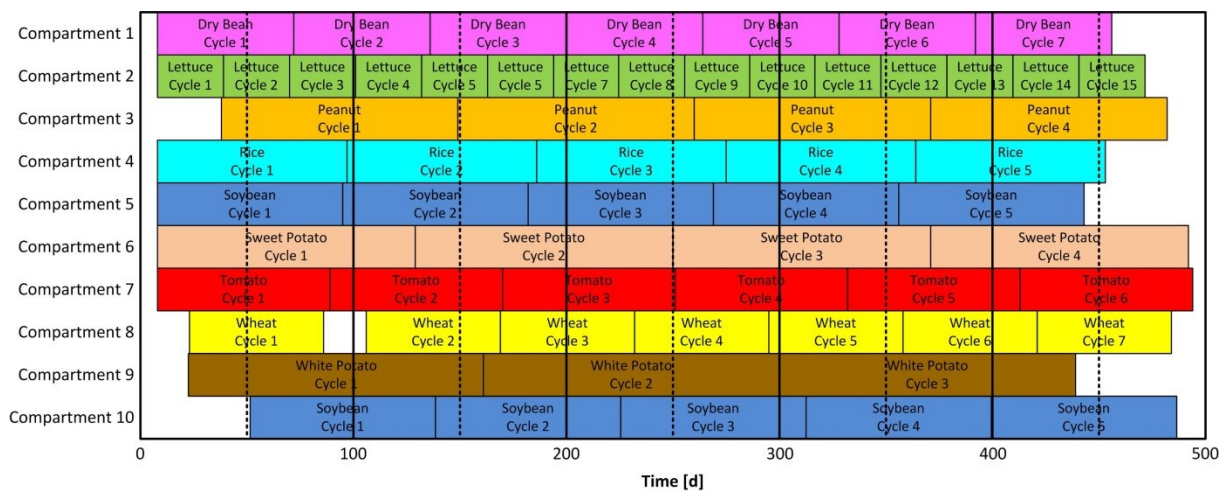
Figure 4-53: Improved greenhouse production schedule.

The resulting oxygen production curve is shown Figure 4-52 as red line. The production is always greater than the demand of the crew (except at the beginning and the end of the mission). The oxygen production with the improved production schedule varies between 5.8 kg/d and 10 kg/d which is an improvement to the old schedule. Due to the shifted growth cycles the greenhouse oxygen production at the end of the mission is lasting longer.

It should be noted, that the total greenhouse food production is equal for both production schedules. However, the shifted growth cycles in the scenario with the improved schedule cause later harvests for the modified compartments. Since the last harvests of the wheat, soybean, white potato and peanut compartments are now closer to the end of the mission, the crew is consuming less edible biomass compared to the original schedule. This results in an increased demand of resupply food for the improved schedule. The difference is 35 kg. This effect is almost negligible compared to a better overall greenhouse production distribution, which increases the life support systems resilience.

There are almost infinite possibilities to setup and optimize a greenhouse production schedule. The schedule always needs to be adjusted and optimized for the given mission scenario and production requirements. Consequently the above described improvements to the production schedule should be seen as an example. In general one can say that with an increasing number of compartments the production curve can be better smoothed, but this increases the complexity and effort to operate the greenhouse.

4.6 Greenhouse Startup Phase Analyses

A critical phase for a hybrid life support system is the startup of a greenhouse. The startup phase here means the period from the seeding of the first plants until the greenhouse reaches its production equilibrium. The production of a greenhouse is never going to be constant, but after some time the production rates stay in a certain range. This is meant with equilibrium here. The time until equilibrium depends on the chosen crop species and on the production schedule. For the following descriptions the startup phase is defined by longest growth cycle of the implemented crop, which is white potato with 142 days.

Four different startup scenarios have been defined, see Figure 4-54. The scenarios are clustered depending on when the greenhouse starts operation with respect to the arrival of the crew. In the post-arrival of crew startup scenarios the greenhouse is turned on after the crew has arrived at the habitat. The pre-arrival of crew scenarios require an autonomous or remote-controlled greenhouse startup, because the crew has not yet arrived at the habitat. There are two variations for both categories. The seeding together option means, that the plants of all compartments are sown together at the same time. The seeding shifted option has a distinct production schedule with the plants of each compartment being sown at a specific time.

The post-arrival - seeding together scenario is equal to the mission scenario under nominal operation, which is described in detail in Chapter 4.3. The post-arrival - seeding shifted simulation case is equal to the simulation performed in the production schedule improvement, see Chapter 4.5.
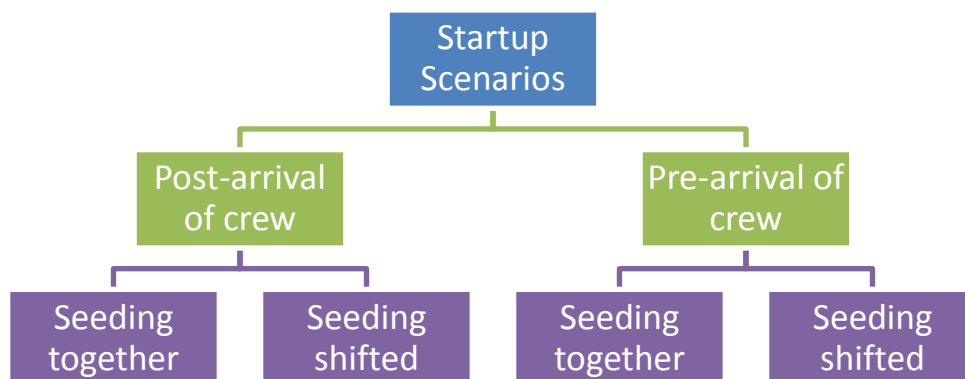
Figure 4-54: Overview of simulated startup scenarios.

Figure 4-55 and Figure 4-56 show an overview of the production schedules for the four different greenhouse startup scenarios. In these graphs a mission day smaller than zero is used for the time prior to crew arrival, which happens on day zero. In the post-arrival - seeding together scenario all plants are sown on day zero and after a germination period of four days transferred to the greenhouse. The post-arrival - seeding shifted production schedule

incorporates adjustments to smoothen the greenhouse production over the mission duration. Therefore the large soybean compartment has been divided into two smaller compartments with half of the original cultivation area. The two soybean compartments are also offset by 43 days.

The pre-arrival - seeding together scenario has a scheduled seeding for all compartments on day -142. The day is chosen because of the growth cycle of white potato of 142 days, which is the longest among the implemented crop species. This means that in this scenario the whole startup phase of the greenhouse takes place prior to the arrival of the crew.

For the pre-arrival - seeding shifted simulation case the seeding of the plants is shifted in a way that all compartments can be harvested for the first time on day one. Consequently, the crew can rely on greenhouse food from the first day of their surface mission in both pre-arrival scenarios.

Figure 4-55: Greenhouse production schedules for the two post-arrival startup scenarios. From top to bottom: Post-arrival - seeding together, post-arrival - seeding shifted.

For the pre-arrival startup scenarios the life support system is not balanced, because the human component is missing. This means, that the plants in the greenhouse are the main consumers and producers of resources. The greenhouse is a large carbon dioxide sink during the startup phase. Without having the crew producing carbon dioxide for the plants, all the necessary carbon dioxide needs to be provided to the greenhouse from other sources (e.g. imported from Earth or generated in-situ). There are also no solid waste products and almost no inedible biomass to be processed into carbon dioxide that early in the mission. Figure 4-57 shows graphs of the carbon dioxide storage behavior for all four startup scenarios. While the post-arrival scenarios can cope with an initial carbon dioxide amount of 50 kg, the pre-arrival scenarios require 700 kg and 800 kg respectively.

The longer overall production time of the greenhouse and the absence of crew in the first 142 days of the mission cause a significant higher overall produced oxygen amount for the pre-arrival scenarios, see Figure 4-58. The excess oxygen produced in the phase prior to the arrival of the crew could be used to fill up the atmosphere of the habitat to the desired oxygen concentration. This could greatly reduce the amount of oxygen to be imported for the habitat.

Figure 4-56: Greenhouse production schedules for the two pre-arrival startup scenarios. From top to bottom: Pre-arrival - seeding together, pre-arrival - seeding shifted.
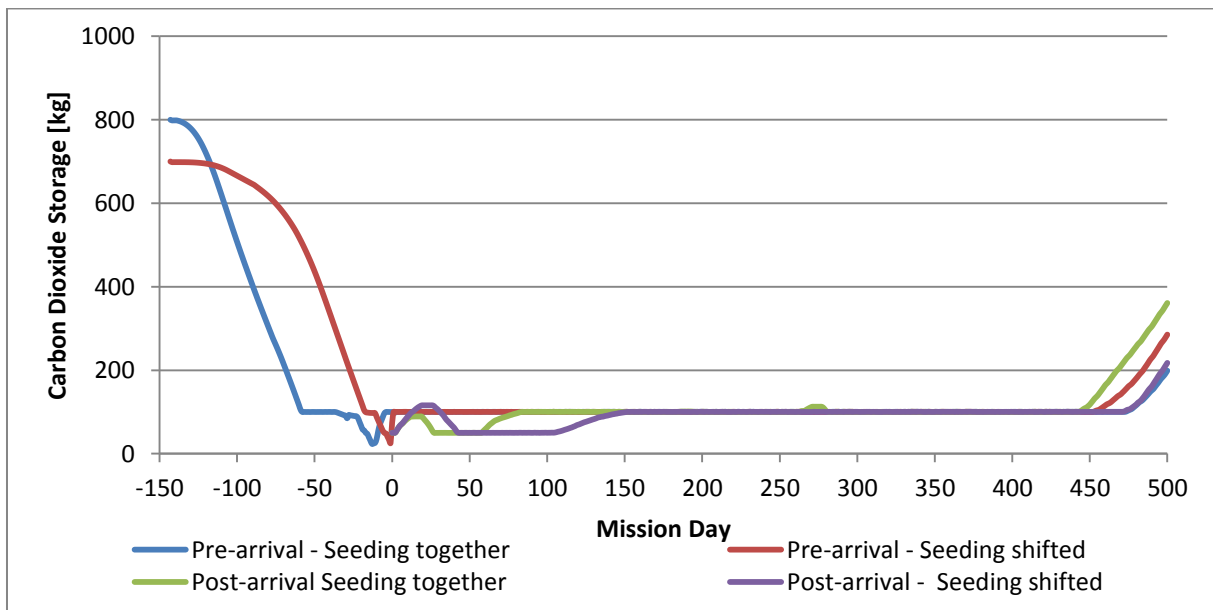
Figure 4-57: Carbon dioxide storage for different startup scenarios.
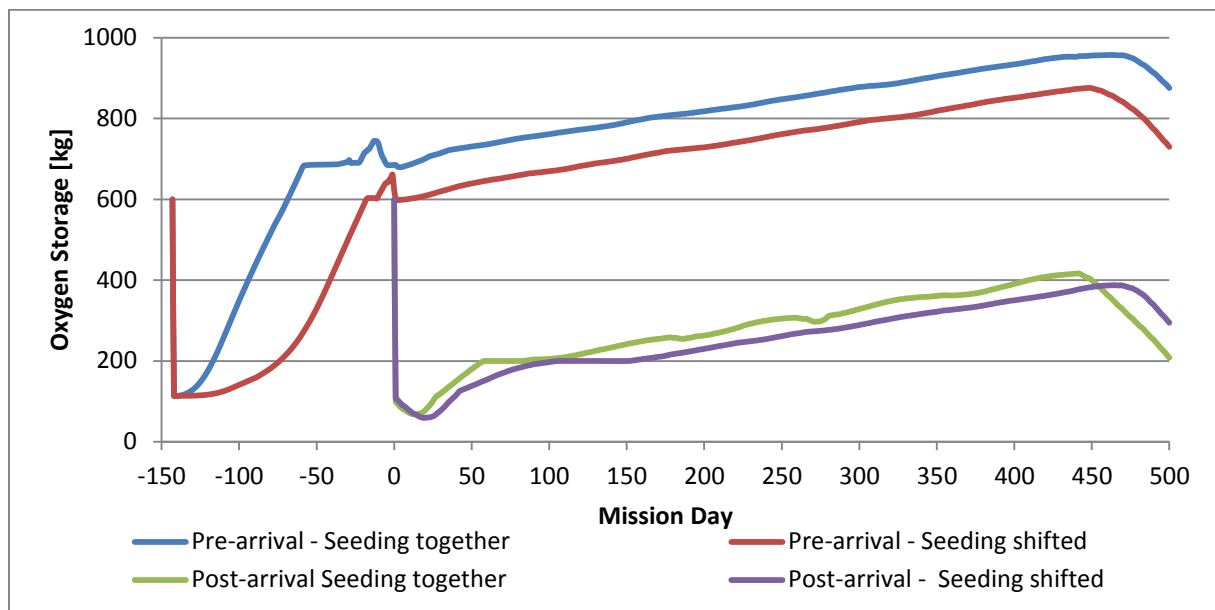
Figure 4-58: Oxygen storage for different startup scenarios.

The different production schedules lead to a different amount of produced plant food and therefore to a different amount of resupply food demand. Table 4-28 shows the resupply food consumption for all four greenhouse startup scenarios. The pre-arrival scenarios require less resupply food, due to their overall higher production caused by additional growth cycles. Furthermore, the crew is able to rely on greenhouse food from the first day on and therefore requires much less resupply food. The disadvantage of the pre-arrival startup scenarios is the need for sophisticated automation for the setup of the greenhouse, the seeding and the harvest of plants.

Table 4-28: Resupply food consumption in kilograms for different startup scenarios.

Pre-arrival		Post-arrival	
Seeding together	Seeding shifted	Seeding together	Seeding shifted
482	554	788	822

Graphs for the behavior of the water cycle and the activity of the physical-chemical systems are not shown here, because the behavior of these is only slightly affected by the startup scenario.

5 Experiment

The research performed during the development of the simulation model revealed that basically all available life support models do not incorporate a loop to generate or recycle plant nutrients. This can be explained by the rather small amounts of nutrients that are required for plant cultivation during short missions. Nutrients can also easily be stored and transported in their crystalline form. Nevertheless, producing nutrients for plant cultivation in-situ is a necessary step forward to a more sustainable life support system for a permanently occupied planetary base. An experiment on growing crops with a nutrient solution derived from human urine has therefore been performed for this dissertation in order to improve the basic knowledge in that field. Furthermore the plant cultivation experiments also helped the author to better understand the biological und technical challenges involved in growing plants in a closed environment. This experience improved the modelling and simulation efforts described earlier in this thesis.

5.1   Background and Purpose

In commercial greenhouses the nutrient solutions are usually prepared by mixing crystalline and/or liquid fertilizers with water. This procedure guarantees an optimal supply of all required minerals in the correct amount. Adapting this procedure for a space greenhouse is not trivial. Either the nutrient salts have to be supplied from Earth or produced in-situ at the location of the space greenhouse. The first might work for plant growth chambers and small greenhouses and short mission durations, but is inconvenient for large greenhouses and long mission durations. The production of nutrient salts in-situ is only possible if the minerals are present and easily accessible at the location of the greenhouse. Nevertheless, this process is work and energy intensive.

DLR's C.R.O.P. (Combined Regenerative Organic Food Production) project investigates the production of plant nutrient solution out of biological waste produced by the crew and the greenhouse itself in order to recycle valuable nutrients. The goal of C.R.O.P. is to develop a bio-regenerative life support system that combines biological waste (e.g. food residuals, urine, plant material) treatment with soilless plant cultivation.

The waste treatment system is under development at the DLR Institute of Aerospace Medicine in Cologne, Germany and the plant cultivation tests are done at the DLR Institute of Space Systems in Bremen, Germany. The experiments conducted for this thesis are part of the latter.

The C.R.O.P. waste management system is a water-based microbiological treatment system or filter. Each C.R.O.P. filter consists of a large plastic tube loosely filled with pumice, see Figure 5-1. The pumice is infused with a bacteria culture from soil and filled with water. The recycling material (e.g. urine) is put in at the top of the filter. A pump ensures that the liquid which leaves the filter at the bottom is brought back up to the top of the filter and therefore allows recirculation of the liquid. After a certain time most of the waste put into the filter is degraded by the microorganisms. The microbiological culture inside the C.R.O.P. filter is subject to natural evolution and consequently can adapt itself to the waste that is put into the filter (Bornemann *et al.*, 2015).
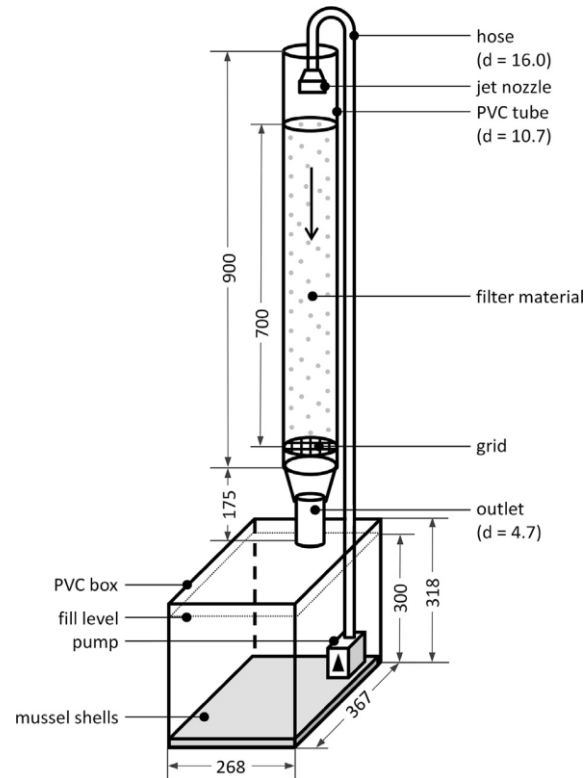
Figure 5-1: Schematic representation of a filter unit. Dimensions given as internal dimensions [mm]; d =diameter (Bornemann *et al.*, 2015).

The purpose of the experiment described in this thesis is the evaluation of the nutrient solution generated by the C.R.O.P. waste treatment system by processing artificial urine. The artificial urine is made up according to Feng and Wu (2006). The experiment compares the C.R.O.P. nutrient solution with a reference nutrient solution known as Half-Strength Hoagland Solution (Hoagland and Arnon, 1950). This solution is commonly used as a baseline for soilless plant cultivation. For the crop used in the experiments, Micro-Tina super dwarf tomato (Scott *et al.*, 2000) were selected, because of the small size suitable for small plant growth chambers in space.

The human body uses urine to get rid of certain substances which are currently not needed or are generally not welcome within the body. Consequently, urine contains minerals in high concentration which has to be taken into account during recycling. The salt concentrations in urine are strongly affected by the food und liquids the person consumed. The artificial urine used for the experiments reflects a typical composition.

The experiment objectives are:

- Can plants grow and thrive with the C.R.O.P. nutrient solution?
- How do the plants perform compared to a reference nutrient solution?
- Does a tuned version of the C.R.O.P. nutrient solution performs better than the normal one?

5.2　Hardware and Software

5.2.1　Overview

All experiments were conducted in four self-build growth chambers (GC), see Figure 5-2. The chamber structure is built out of aluminum profiles. The wall elements are compressed hard plastic with a white coating. Each chamber is 1.0 m wide, 0.5 m deep and 1.0 m high. This results in a cultivation area of 0.5 m² and a volume of 0.5 m³ per chamber.

There is a high-power LED lamp with customizable spectrum in each chamber, see also Chapter 5.2.2. The left two chambers (GC 1 and GC 2) and the right two chambers (GC 3 and 4) share the same nutrient solution tank. More information on the nutrient delivery system and the nutrient solutions used can be found in Chapter 5.2.3. On the backside of each chamber is a circulation fan and the connections to the centralized atmosphere management system of the laboratory, see also Chapter 5.2.4. All four chambers are connected to a stand-alone control and data acquisition system based on a Programmable Logic Controller (PLC), which is mounted on the right wall of the experiment setup. This system is explained in Chapter 5.2.5.
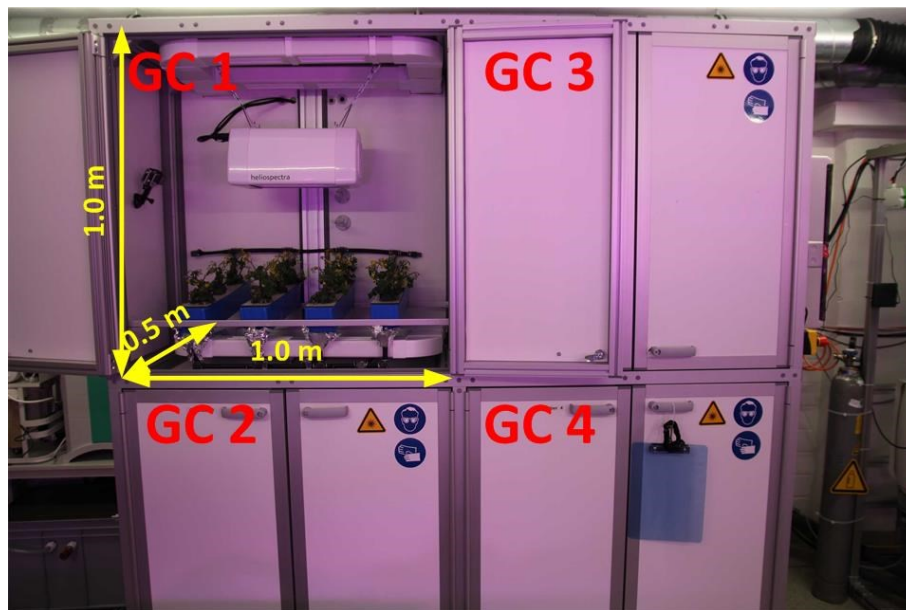
Figure 5-2: Overview of GC 1-4 hardware setup.

5.2.2　Illumination System

The illumination system consists of one LX601 C-plate lamp of the Swedish company Heliospectra AB, see Figure 5-3. The lamp is design to illuminate an area of 1.2 x 1.2 m² at a distance of 0.5 m and is air-cooled. The LX601 has 240 LEDs of four different wavelengths: blue LEDs (450 nm), red LEDs (660), far-red LEDs (735 nm) and white LEDs (5700 K). Each of the wavelengths can be controlled separately. When the lamp is set to 100 % for the full spectrum it has a photon flux of 862-1011 µmol/s and a power demand of 630 W.

All lamps are connected via Ethernet to the network of the EDEN laboratory and accessible through the central control computer. The LX601 is a stand-alone lamp and does only require network access to change the lamp settings. Heliospectra provides a browser-based control system for their lamps. The intensity of each wavelength can be controlled in increments

from 0-1000 which correspond to 0-100 % intensity. The control system also allows implementing a light schedule, which means that the lamp can be programmed with a number of daily repeating illumination sequences. Furthermore, the control system measures and displays the temperature of the LED circuit plate.

Figure 5-3: Heliospectra LX-601 LED lamp.

5.2.3 Nutrient Delivery System

The nutrient delivery system consists of two 80 L plastic tanks each containing a submersible aquarium pump capable of pumping water up to two meters height. One tank supplies the left two chambers (GC1-2) and one tank supplies the right two chambers (GC3-4) through a system of pipes and manual valves, as shown in Figure 5-4. The supply line of each chamber is then split into smaller pipes feeding the plants. The number of growth channels and the number of plants per channel can be adapted for different plants and different experiments.
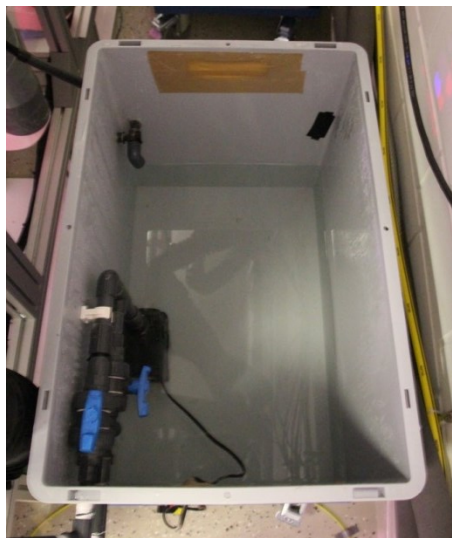
Figure 5-4: GC 3-4 nutrient solution tank including pump.

The current setup consists of four growth channels per chamber each holding three plants. The small pipes end in three drippers, one for each plant, and are commercially available gardening components. The growth channels itself are made out of plastic and can be outfitted with different lids. They are mounted inside the chamber with a small inclination towards the doors to allow water flow towards the return water collection tube. This tube transports the nutrient solution back towards the supply tank. The complete layout of the fluid lines is

shown in Figure 5-5. The growth channels are large enough to contain the 80 x 80 x 60 mm Rockwool blocks in which the plants are growing.
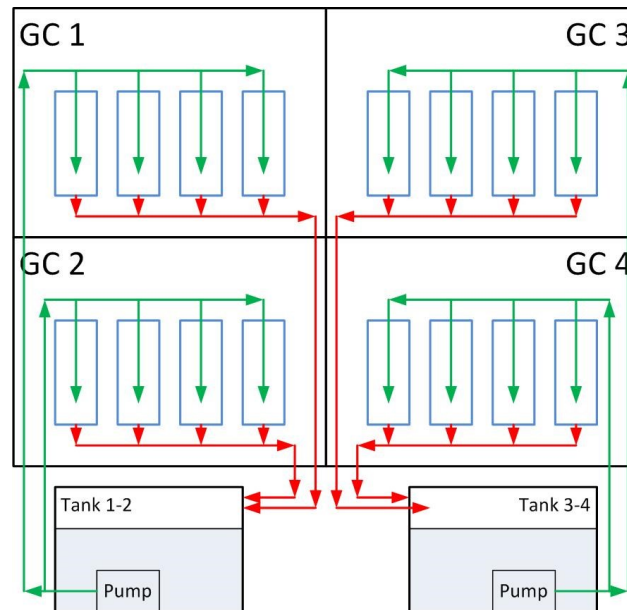
Figure 5-5: NDS schematic. A pump in each tank supplies nutrient solution (green lines) to the growth channels (blue boxes). Excess fluids return to the tanks (red lines).

5.2.4 Atmosphere Management System

The atmosphere management system of GC1-4 consists of two parts: circulation fans and the centralized system of the EDEN laboratory. Both parts are connected to air inlet and outlet tubes inside the different chambers. Figure 5-6 shows how the different parts of the atmosphere management system are connected to each other.
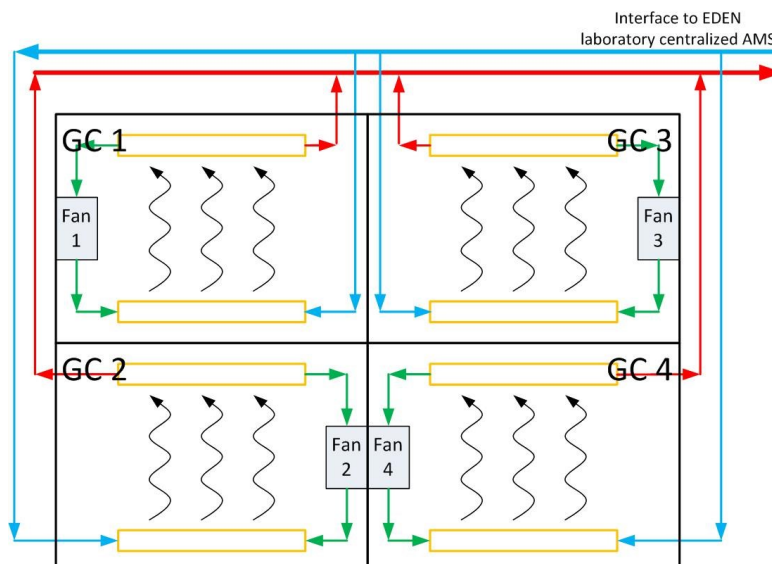
Figure 5-6: AMS schematic. Fan 1-4 are used to circulate air (green lines). Additionally GC 1-4 are connected to the EDEN laboratory centralized AMS to receive cool air (blue lines) and to get rid of warm air (red lines). Orange boxes symbolize the air distribution channels inside each chamber.

The circulation fans are of the type InlineVent RR EC 125 of the company Helios and mounted on the backside of the chambers, as shown in Figure 5-7, with a maximum air flow rate of 610 m³/h and are controllable with a 0-10 VDC input. Their purpose is to guarantee a proper

air mixture inside the chambers. Within GC 1 and GC 3 sensors for temperature, relative humidity and carbon dioxide concentration are placed and the data is collected every minute and saved on a flash drive.
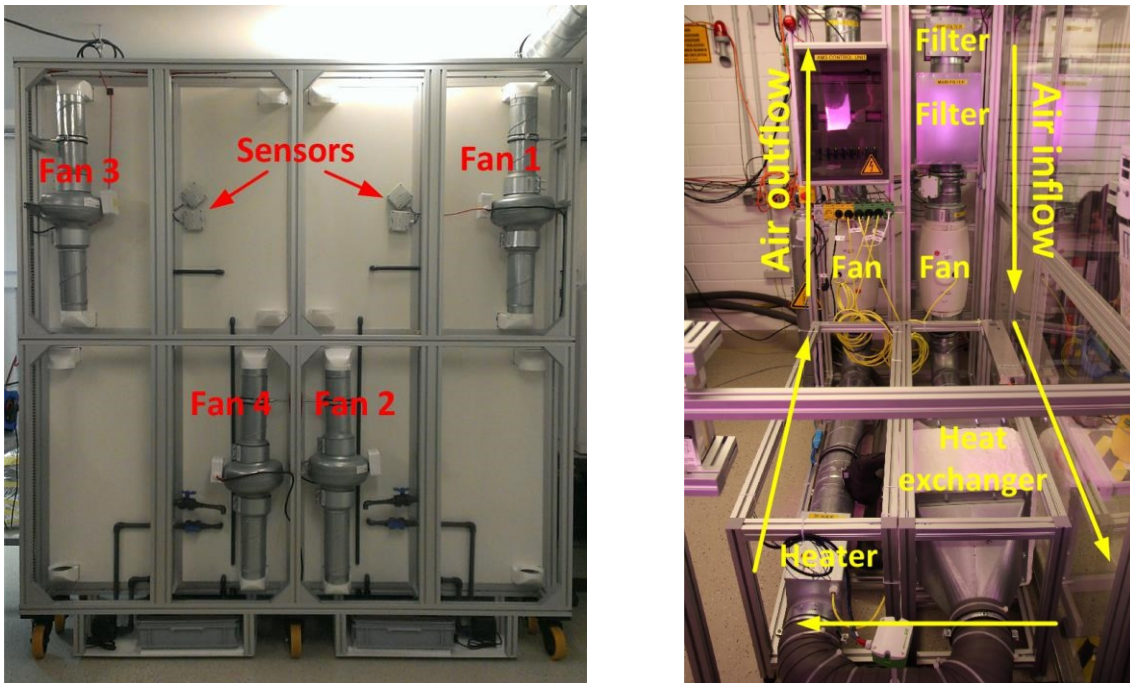
Figure 5-7: Backside of GC 1-4 (left image); EDEN laboratory centralized atmosphere management system (right image).

The purpose of the centralized system, shown in Figure 5-7, is the conditioning of the air flow itself. Therefore, fans, a heat exchanger to cool the air and reduce humidity, a heater and a carbon dioxide injection system are built into the air stream. This system is controlled by a modular National Instrument CompactDAQ and programmed by the Software LabView running. Depending on the experiment and therefore the sensor inputs, the centralized atmosphere management system can be programmed to optimize the conditions in one of the nine chambers in the laboratory.

5.2.5 Control and Data Acquisition Hardware

The control and data acquisition hardware encompasses the power distribution to all components of the chambers, a programmable logic controller (PLC) including a graphical user interface and a number of sensors. Figure 5-8 shows the power and control box of the growth chambers. This box distributes the 230 VAC supply line (bottom row) via relays and circuit breakers (middle row) to the consumers and houses a 24 VDC supply, the PLC and its extension module (top row). The PLC is programmed using the software package CoDeSyS. The software allows programming the PLC, its extension module and the graphical user interface.

The system is supplied from a single 230 VAC standard socket, this is wired through an emergency stop button and then connected to a distribution network. The 24 VDC supply module is responsible for transforming the 230 VAC to 24 VDC required by the PLC and the sensors. The two 24 VDC outputs of the module are used to supply two further distribution networks. The first supplies power to the PLC and its extension module whilst the second supplies power to the four sensors in chambers one and three.

Each of the nine consumers being supplied with 230 VAC from the distribution network has its own circuit breaker. Whilst the main function of a circuit breaker is to protect the equipment they are also used as switches to allow the user to manually control the outputs if required e.g. if a pump has failed it could be turned off and removed without having to stop or modify the program.
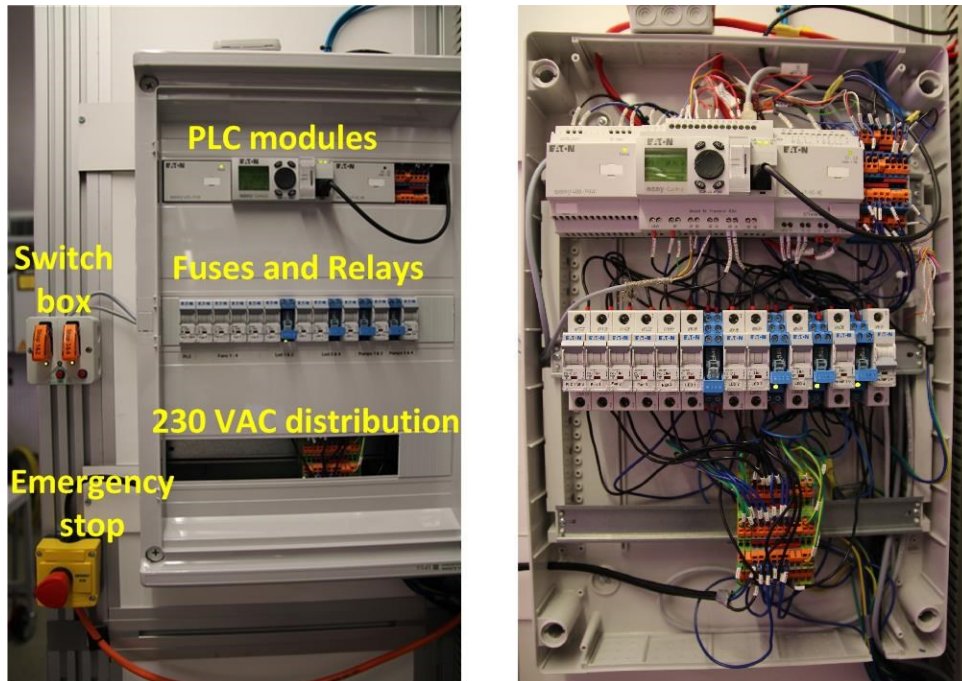
Figure 5-8: Experiment power box and control and data acquisition system.

5.3   Test Growth Cycle

5.3.1 Description and General Appearance

A test growth cycle with Micro-Tina super dwarf tomatoes was performed in 2015 in order to test the experiment hardware and procedures. No C.R.O.P. nutrient solution was used in the test growth cycle. The Micro-Tina No.1 growth cycle started with the seeding on October 30th 2015 and ended in March 2016, see Figure 5-9. In total 55 seeds were placed in the germination greenhouse and 54 of them germinated and developed sprouts over the next days. End of November the 48 best seedlings were placed in GC1-4.
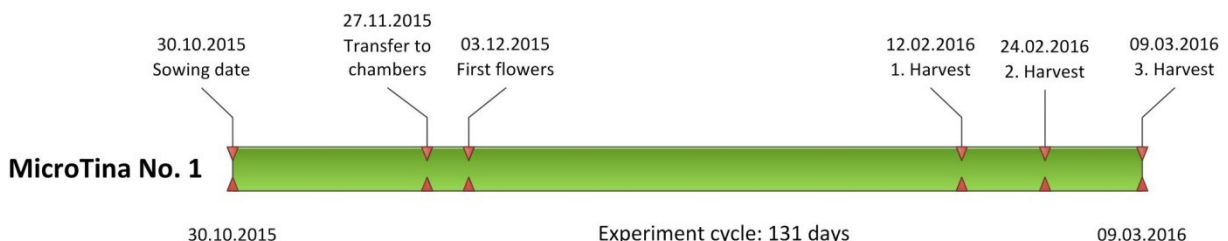
Figure 5-9: Micro-Tina No. 1 experiment timeline.

During the early weeks the plants grew well and developed the first flowers around December 10th and the first fruits during the Christmas 2015 (see Figure 5-10). Figure 5-11 shows the plants after transferring them into the growth chambers and while carrying ripe fruits.

Figure 5-10: First flowers on the 10.12.2015 (left side) and first fruits on the 04.01.2016 (right side).

Figure 5-11: Micro-Tina plants in GC1 after transferring from germination greenhouse in early November 2015 (left side) and carrying ripe fruits in February 2016 (right side).

While the plants continued growing, the shoots were getting longer and longer. The tallest plant was around 35 cm high. When more and more fruits were developed, the branches began to drop and hang over the growth channels. The reason for the shoot elongation was the relatively low light intensity of the LED lamps installed during the test trials. Furthermore, during the Micro-Tina No.1 trial the lamps in three of the four chambers partly failed. The installed lamps consisted of three independently powered panels. In three chambers one panel per lamp broke during the trial.

5.3.2 Atmosphere Data

Atmosphere data during the Micro-Tina No.1 trial have been measured in 30 second intervals with the sensors in GC 1 and GC 3. The values of both chambers are almost equal that is why only the values of GC 1 are shown in the following. The atmosphere in GC 2 and GC 4 is not actively monitored, but a number of measurements with a handheld have shown that the atmosphere is equal to the ones measured in GC 1 and GC 3. Table 5-1 shows the average values for temperature and relative humidity in GC 1 for the photoperiod (16 h per day) and the dark period (8 h per day).

Table 5-1: Micro-Tina No.1 trial average temperature and relative humidity values.

	Photoperiod temperature	Dark period temperature	Photoperiod relative humidity	Dark period relative humidity
Average	23.5 °C	17.2 °C	42.5 %	63.1%

5.3.3 Nutrient Solution Data

EC and pH of the nutrient solution in both tanks have been measured regularly during the Micro-Tina No.1 trial. Usually the measured pH was always above the set point when measured and had to be lowered, while the EC value was more constant. At the start of the growth cycle the EC was kept at 1.0 and was increased to 1.7 after two weeks.

5.3.4 Harvest Data

Three times the ripe fruits on the tomato plants have been harvested. Table 5-2 gives an overview about the harvests. In total 642 fruits with a total fresh weight of almost 2 kg could be harvested. The average diameter and average fresh weight per fruit was highest at the first harvest, because small fruits were not harvested to allow them to get bigger. However, during the last harvest all red fruits have been removed from the plant, including also the very small ones.

Table 5-2: Harvest key values.

Harvest date	Number of fruits	Average diameter per fruit	Average fresh weight per fruit	Total fresh weight
12.02.2016	45	18.44 mm	3.52 g	158.3 g
24.02.2016	317	17.38 mm	3.21 g	1016.4 g
09.03.2016	280	16.33 mm	2.76 g	774.0 g
TOTAL	642	16.99 mm	3.04 g	1948.7 g

Figure 5-12 shows the number of fruits with a certain diameter for all three harvests. The columns of the harvests add up so that the height shown represents the total number per diameter. This figure also shows the high amount of small fruits (relative to the first two harvests) for the harvest of March 09th 2016. Figure 5-13 illustrates the amount of fruits within a certain fresh weight range.
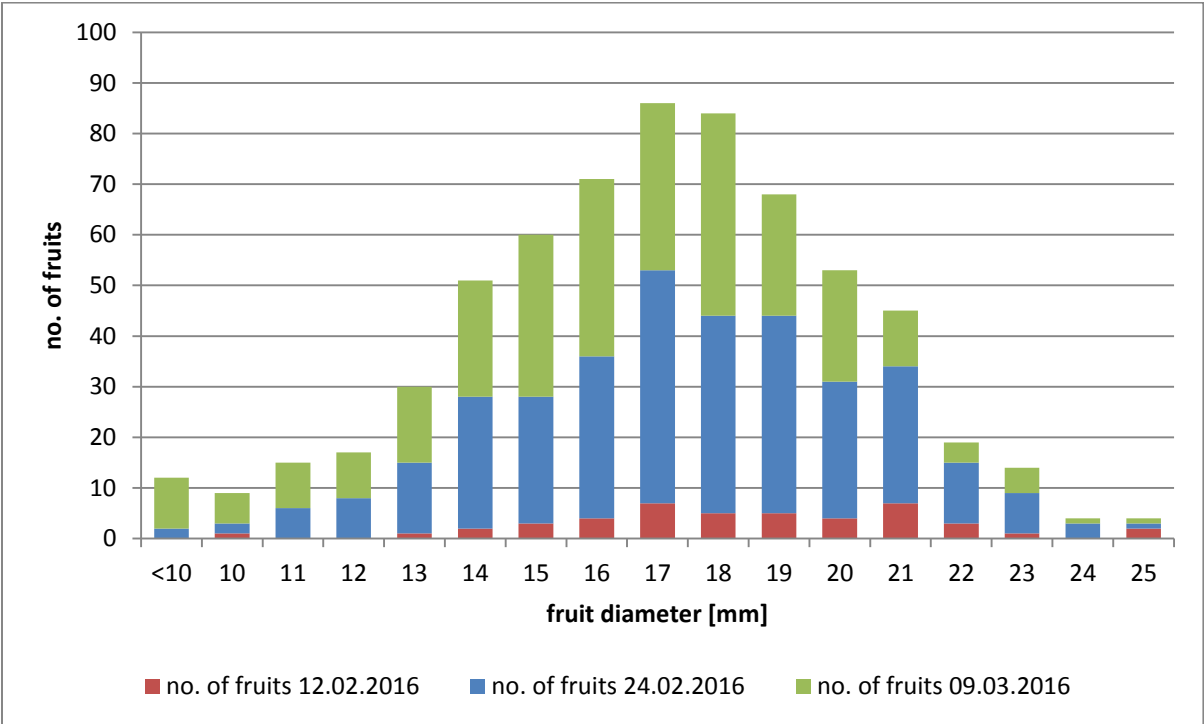
Figure 5-12: Number of fruits per harvest and with a certain diameter.
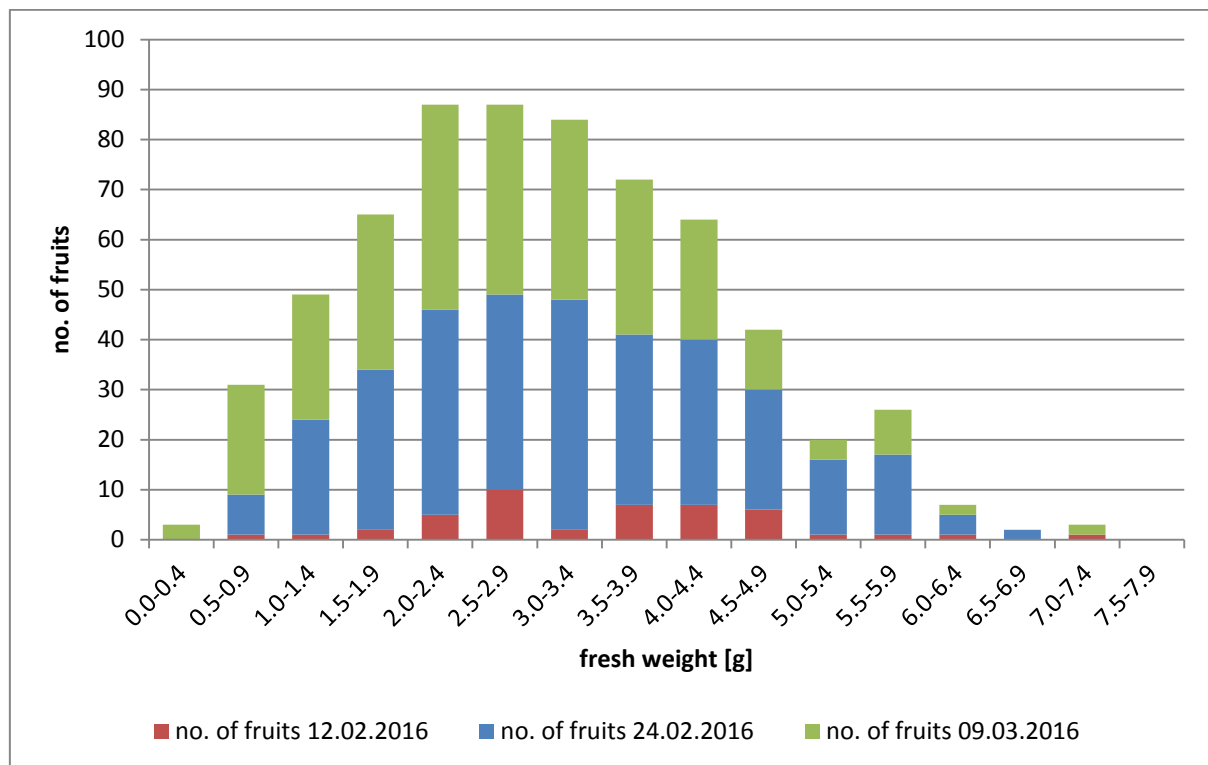
Figure 5-13: Number of fruits per harvest with a certain fresh weight.

A sample of 30 fruits was put aside from the harvest on March 9th 2016 for the determination of the dry mass content of the fruits. Those fruits were dried in an oven at 70°C for one week. The weight before and after the drying process were measured. The dry weight of the fruits was 8.53 % of the fresh weight, on average.

5.3.5 Conclusions for Experiment

The test growth cycle was very useful for the preparation of the experiment. The growth chambers could be tested intensively over a long period of time. A number of weaknesses of the growth chambers and procedures could be identified and corrected. All LED lamps of the illumination system were exchanged after the test cycle with new and qualitatively better lamps (Heliospectra LX-601). They also allow the customization of the light spectrum, see Chapter 5.2.2. The early design of the nutrient delivery system's fluid lines leaked frequently. Especially the return pipes from the growth channels back to the nutrient solution tanks caused trouble and were rebuild.

The atmosphere management system of the growth chambers proved to be very robust. However, GC1-4 are only four out of nine chambers in use inside the EDEN laboratory. Since all of them are connected to the same centralized air conditioning system, they influence the climate of each other. Although the influence is rather small, one can see them in the data. Another influence is caused by the environment of the laboratory itself. GC1-4 are not hermetically sealed and therefore interact with the atmosphere inside the cultivation area of the laboratory. Here the varying carbon dioxide concentration mostly caused by working personnel affects the growth chamber atmosphere. Although the carbon dioxide concentration rarely falls below 450 ppm, it can go up to 3000 ppm due to human activity. The experiment procedures (e.g. manual data acquisition, nutrient solution maintenance) were tested

and adjusted during the test growth cycle. The final procedures are described in the next chapter.

5.4 Experiment Procedures

5.4.1 Nutrient Solution Preparation

5.4.1.1 Half-Strength Hoagland Solution

The makeup of a Half-Strength Hoagland solution is a three step process:

Step 1: Make up six different stock solutions á 1 L,
Step 2: Mix stock solutions to make up a bulk solution,
Step 3: Dilute bulk solution with deionized water and fill into nutrient tanks.

Step 1: Make up six different stock solutions

All ingredients for the stock solutions are available in crystalline form. For each stock solution a 1 L glass bottle is first filled half with deionized water. Afterwards the correct amount of powder is weighted and added to the dedicated bottle. Lastly the bottle is filled up to 1 L with deionized water. Table 5-3 shows the ingredients for each stock solution.

Table 5-3: Composition of stock solutions.

Stock solution number	Fertilizer	Formula	Amount for 1 L
1	Potassium Nitrate	KNO_3	101.102 g
2	Ammonium Dihydrogen Phosphate	$NH_4H_2PO_4$	115.024 g
3	Magnesium Sulfate Heptahydrate	$MgSO_4\text{-}7H_2O$	246.471 g
4	Calcium Nitrate	$Ca(NO_3)_2\text{-}4H_2O$	236.145 g
5	Boric acid	H_3BO_3	1.430 g
	Manganese(II) Chloride Tetrahydrate	$MnCl_2\text{-}4H_2O$	0.905 g
	Zinc Sulfate Heptahydrate	$ZnSO_4\text{-}7H_2O$	0.110 g
	Copper(II) Sulfate Pentahydrate	$CuSO_4\text{-}5H_2O$	0.040 g
	Molybdic Acid	H_2MoO_4	0.010 g
6	Sodium Iron EDTA	$C_{10}H_{12}FeN_2NaO_8$	16.435 g

Step 2: Make up bulk solution

The bulk solutions for the experiment are mixed and stored in 4 L plastic bottles. The concentration of nutrients in the bulk solution is set so that one 4 L bottle can be used to make up 50 L of nutrient solution. Firstly the empty bottle is filled with roughly 1 L of deionized water. Afterwards the stock solutions are added one by one according to the volumes listed in Table 5-4. Lastly the bottle is filled up with deionized water until it contains 4 L of solution.

Table 5-4: Ingredients of bulk solution (4 L for 50 L).

No.	Stock solution name	Volume
1	KNO_3	150 mL
2	$NH_4H_2PO_4$	25 mL
3	$MgSO_4\text{-}7H_2O$	50 mL
4	$Ca(NO_3)_2\text{-}4H_2O$	100 mL
5	Micronutrients	50 mL
6	Iron Chelate	50 mL

Step 3: Fill nutrient tanks

The initial fill of a nutrient starts by filling it with 35 L of deionized water. Afterwards the bulk solution is added carefully to the tank until the desired electrolytic conductivity (EC) is achieved. For example, if an EC of 1.7 is required for the plants, roughly 3.75 L of bulk solution need to be added. The last step is to measure and adjust the pH level to the desired level.

Table 5-5 shows the nutrient concentration of a 4 liter half-strength Hoagland bulk solution used in the experiment. The values are also used as a reference point for the evaluation of the C.R.O.P. nutrient solutions explained in the following two sub chapters.

Table 5-5: Average nutrient concentration in mg/L in the half-strength Hoagland solution.

Substance	K+	Ca2+	Mg2+	Cl-	NO3-	SO4-	NH4+	PO4-	Na+
half-strength Hoagland	1466	1002	304	4	5425	1203	106	594	13

5.4.1.2 C.R.O.P. pure nutrient solution

The original C.R.O.P. pure nutrient solution as produced by the biological waste treatment units is very rich in nitrate, ammonium, sodium and chloride (see Table 5-6). For better comparison to the Hoagland reference nutrient solution, the original C.R.O.P. pure solution is diluted with deionized water. A mixture of 1.5 L original C.R.O.P. pure solution and 2.5 L deionized water brings the concentration of nitrate close to the reference values. As evident from Table 5-6 the diluted C.R.O.P. pure solution is lacking potassium, magnesium and sulfate, but still has a much higher concentration of sodium, chloride and ammonium.

The diluted C.R.O.P. pure solution is used directly without any other treatment as a nutrient solution during the experiments described in the following chapters.

Table 5-6: Average nutrient concentration in mg/L in the original and diluted C.R.O.P. pure nutrient solution.

Substance	K+	Ca2+	Mg2+	Cl-	NO3-	SO4-	NH4+	PO4-	Na+
Pure original	1145	2182	99	3610	18137	1079	1928	992	1723
Pure diluted	459	1048	46	1168	5853	433	733	459	669

5.4.1.3 C.R.O.P. tuned nutrient solution

The idea behind the C.R.O.P. tuned nutrient solution is to improve the nutrient composition of the solution by adding certain minerals up to the point where the concentration is similar to the half-strength Hoagland solution. Consequently, potassium, magnesium, sulfate and sometimes also calcium need to be added to the C.R.O.P. pure solution. The nutrient concentrations in the original C.R.O.P. pure solution vary between supply batches. An ion-chromatography measurement is always required to determine the exact concentrations of the produced batch.

An excel sheet is used to calculate the deficit of the C.R.O.P. pure solution compared to the reference half-strength Hoagland solution. Since the nutrient minerals always come as a pair of a cation and an anion, determining the acceptable amount of added minerals is challeng-

ing. One has to be careful not to increase the already high values of some nutrients such as nitrate.

For the C.R.O.P. tuned nutrient solution used in the experiments the following mineral combinations were used:

- Potassium dihydrogen phosphate KH_2PO_4
- Magnesium sulfate heptahydrate $MgSO_4\text{-}7H_2O$
- Calcium nitrate tetrahydrate $Ca(NO_3)_2\text{-}4H_2O$

Potassium phosphate and magnesium sulfate needed to be added to all used batches of original C.R.O.P. pure solution. For those batches 1.5 L of original C.R.O.P. pure solution was mixed with 2.5 L of deionized water and the additional minerals. A few batches had a low calcium concentration (up to 50 % less) than normal. This is most likely caused due to aging of the nutrient solution due to long storage times. The batches which need additional calcium were diluted to 1 L original C.R.O.P. solution and 3 L deionized water. Afterwards calcium nitrate was added. Due to the higher dilution this batches required more amount of potassium phosphate and magnesium sulfate to be added. However, the final concentrations of all C.R.O.P. tuned solutions were very similar.

Table 5-7: Average nutrient concentration in mg/L in the C.R.O.P. tuned nutrient solution.

Substance	K+	Ca2+	Mg2+	Cl-	NO3-	SO4-	NH4+	PO4-	Na+
Tuned	879	1213	315	1080	6176	1434	650	1782	621

5.4.1.4 Nutrient solution comparison

This chapter describes the differences between the three nutrient solutions explained in the previous subchapters. Figure 5-14 shows a diagram and a table with the nutrient concentrations for all three solutions.

The most significant difference between the three solutions is the high concentrations of sodium and chloride in the two C.R.O.P. nutrient solutions. As described before, this is the result of using urine as the base product. The microorganisms in the filter units do not reduce the amounts of sodium chloride present in the urine of a human on an average diet. The half-strength Hoagland solution on the other side has basically no sodium chloride, because it is not desired to have for plant cultivation. Sodium cations are competing with potassium cations in root uptake and chloride anions are competing with the uptake of nitrate. Both effects are associated with impeding plant development and reduced yield.

The concentrations of calcium and nitrate are in the same range for all three nutrient solutions. Ammonium is more present in the C.R.O.P. solution. This is again a result of the microorganism culture in the filter units and the use of urine as the base material. The magnesium and sulfate concentrations are much lower in the C.R.O.P. pure solution than in the two others. The C.R.O.P. tuned solution has similar values compared to the half-strength Hoagland solution, due to the added magnesium sulfate.

Problematic is the lack of potassium in the original C.R.O.P. pure solution. Increasing the potassium concentration in the C.R.O.P. tuned solution to the same level as the reference solution was not possible without increasing the concentration of anions beyond the level of the reference solution. A trade between too low concentrations of potassium and too high con-

centrations of phosphate was made. Which leads to the C.R.O.P. tuned solution having only two third of the potassium of the reference solution but still twice as much as the C.R.O.P. pure solution. However, due to the addition of potassium phosphate the concentration of phosphate in the C.R.O.P. tuned solution is around three times as high as in the half-strength Hoagland solution. The effects of the different nutrient concentrations on the plant development and yield are the main objective of the experiments described within this thesis.

5.4.2 Plant Seeding, Germination and Transfer to Growth Chambers

The Micro-Tina seeds are placed in 20 x 20 x 40 mm^3 Rockwool blocks. The blocks have to be watered before. The Rockwool blocks containing the seeds are then placed in a simple germination greenhouse, which is then filled a few millimeters of tap water. The germination greenhouses are placed under LED lamps within the EDEN laboratory. The described procedure is also shown in Figure 5-15.

	K+	Ca2+	Mg2+	Cl-	NO3-	SO4-	NH4+	PO4-	Na+
C.R.O.P. pure diluted	459	1048	46	1168	5853	433	733	459	669
C.R.O.P. tuned	879	1213	315	1080	6176	1434	650	1782	621
1/2 Strength Hoagland	1466	1002	304	4	5425	1203	106	594	13
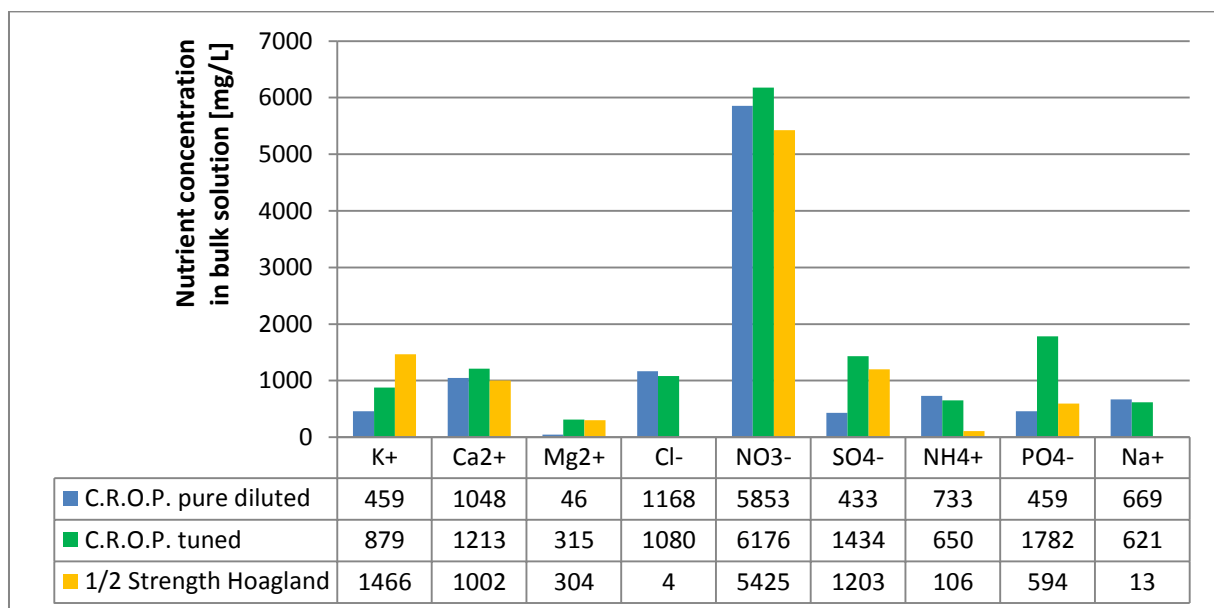
Figure 5-14: Comparison of the nutrient concentrations in all three solutions.

Once the seeds are germinated and the plants have developed their first leaves, which take one week under good conditions, they are transferred into the growth chambers. The small Rockwool blocks are put into larger blocks (75 x 75 x 65 mm^3). The larger blocks also need to be watered and rinsed before use to remove residuals of the production process. The blocks containing the seedlings are then placed into the growth channels. Afterwards the channels are closed with a lid and integrated into the chambers, see Figure 5-16.
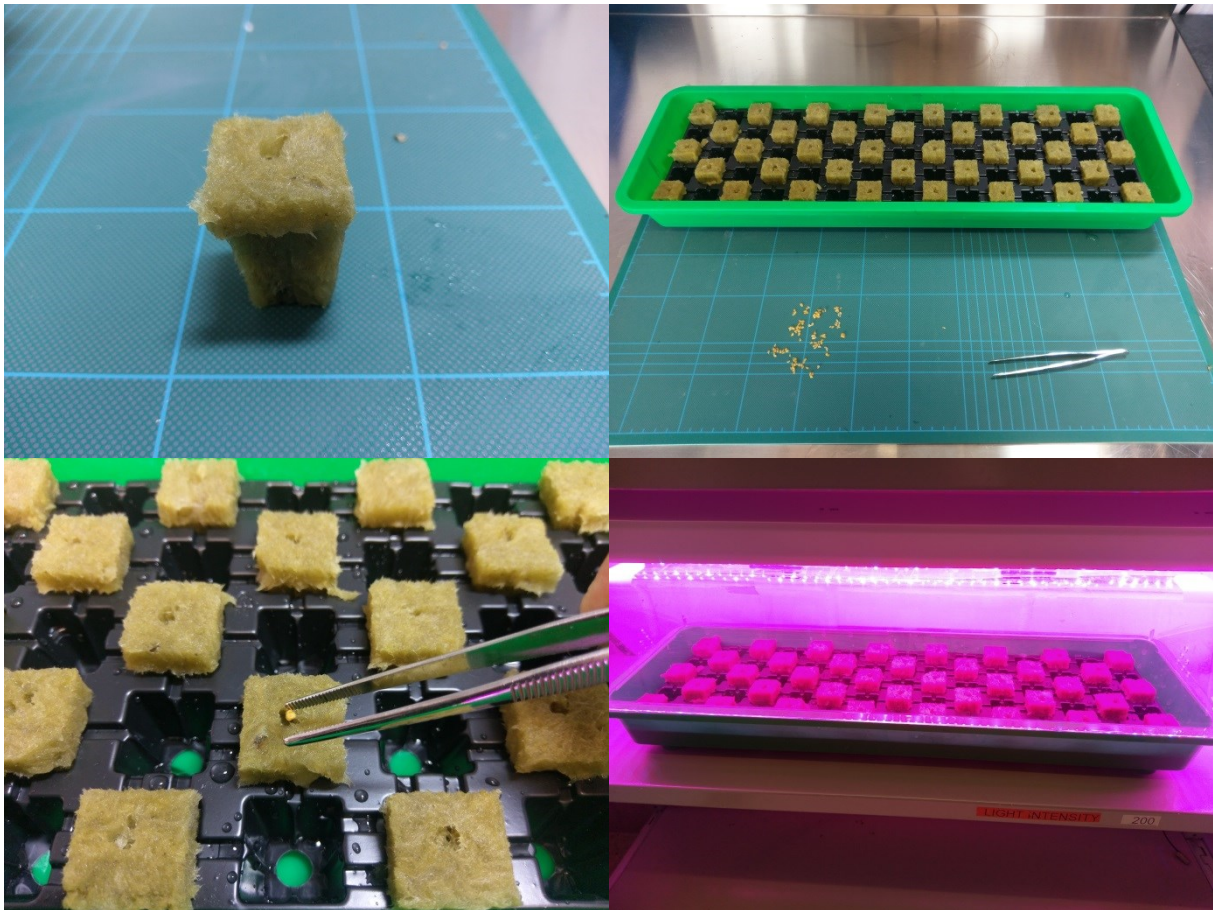
Figure 5-15: Plant seeding and germination. Top left: Rockwool block for germination. Top right: Germination greenhouse tray. Bottom left: Seed put into a Rockwool block. Bottom right: Closed germination greenhouse under LED growth lamps.

Figure 5-16: Micro-Tina seedling after transferring from the germination greenhouse into the growth chamber.

5.4.3 Experiment Maintenance

A weekly schedule (see Table 5-8) for the plant and chamber maintenance was developed and then performed throughout the experiments. All tasks had to be scheduled on the work-days of a week.

Table 5-8: Plant and chamber maintenance weekly schedule.

Task	Monday	Tuesday	Wednesday	Thursday	Friday	Saturday	Sunday
Measure EC, pH and water level in both tanks	X		X		X		
Adjust EC, pH and water level in both tanks	X		X		X		
Ion-selective measurement in both tanks	X		X		X		
Visual inspection of plants and hardware (e.g. leaks, malfunctions)	X		X		X		
Hi-res photos with Canon camera	X		X		X		
Count flowers/fruits	X						
Measure plant height	X						

5.4.4 Plant Harvesting

During the harvest period of the experiment, the ripe fruits are removed from the plants roughly every two weeks. Ripe fruits can be identified by their red color and withered fruit leaves (small leaves where the fruit is attached to the branch). Furthermore, the ripe fruit can be pulled from the plant easily. When force needs to be applied to remove the fruit, the fruit is not fully ripe.

For each harvested fruit the fresh weight and diameter are immediately determined after harvest. The values are documented on a per plant basis, so that the total values per plant can be identified. The harvested fruits are then dried in an oven at 70 °C for at least 3 days and weighted afterwards to find out the dry weight of the fruits. After the last harvest of each experiment run the plants are cut off directly above the Rockwool block and then dried as well to measure the dry weight of the shoot zone. The dry weight measurements can then be used to determine the efficiency of each plant.

5.4.5 Chamber Cleaning

After each growth cycle the chambers need to be cleaned thoroughly to avoid spreading of potential microorganisms to the plants of the next growth cycle. Therefore, the growth channels, lids, tanks and most of the piping are disintegrated from the chambers. All of the components are first washed with hot water, dried and then sanitized with a special anti-microbial cleaning agent. The inner surfaces of the growth chambers and the door handles are cleaned with a moist wipe containing an anti-microbial agent. If there is any residual plant material (e.g. dried leaves) in the chamber, it is removed.

Once all growth chamber parts are cleaned and sanitized they are integrated again in the growth chambers. Fresh deionized water is filled in the tanks and flushed through the piping

for at least a full day. Afterwards the water is dumped and the growth chambers are ready for the next growth cycle.

5.5 Experiment Set Points

5.5.1 Illumination System

The LED lamps were set to a photoperiod of 16 hours per day. The photoperiod started at 08:00 each day and lasted until 23:59, from 00:00 until 07:59 the lamps were off. All lamps go on simultaneously and followed the same cycle. The distance between the bottom of the lamps and the top of the growth channels was around 315 mm and the distance between lamp and the top of the plant canopy around 200 mm. Figure 5-17 shows the PAR intensity for each plant location within the chamber. The plants in growth channels one and four received significantly less light than the plants in the middle. This is caused by the short distance between the plant canopy and the lamp. The lamp is also not centered within the chamber, so that the lamps at the backside of the chamber received more light. The difference in the distribution of the light was very similar among all four chambers.
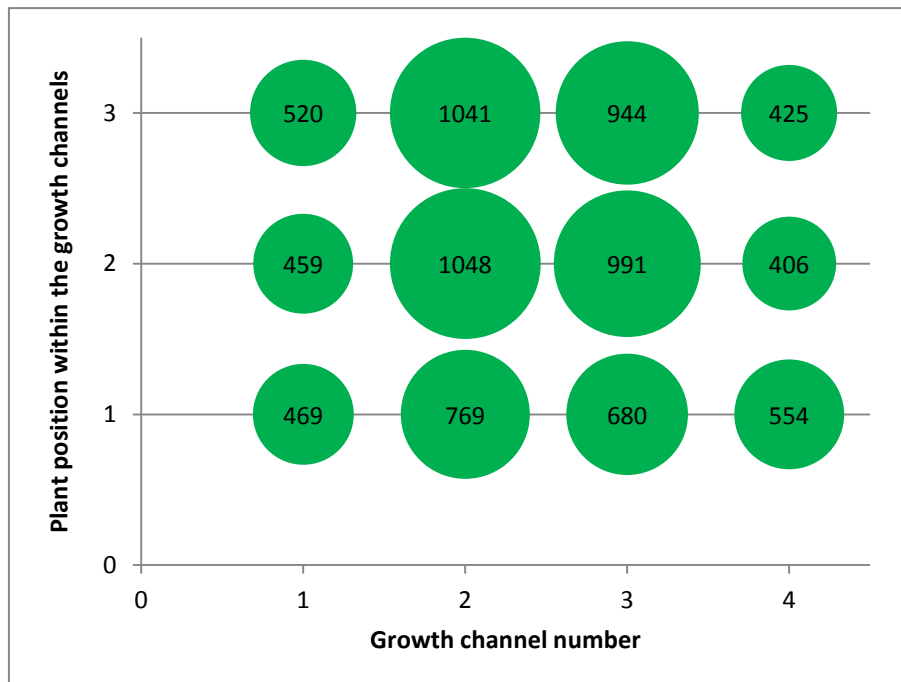
Figure 5-17: PAR light intensity in μmol/(m²*s) per plant position within one of the growth chambers.

5.5.2 Nutrient Delivery System

The parameters of the nutrient delivery system are pH and EC of the nutrient solution, the supply interval and the supply duration. Table 5-9 shows the experiment set points for the nutrient delivery system. Both nutrient supply cycles were set to the same parameters, the pumps went on at the same time. The EC value of the nutrient solution was set to 1.0 for the first two weeks, when the plants are still small. For the rest of the growth cycle the EC value was increased to 2.0.

Table 5-9: Summary of nutrient delivery system set points.

pH value	EC value	Time between supply intervals	Supply duration
6.1	1.0/2.0	15 minutes	1 minute

5.5.3 Atmosphere Management System

The ability to control the atmosphere inside the growth chambers was rather limited. The circulation fans of GC1-4 were set to 40 % of their maximum capacity of 610 m³/h. The temperature and relative humidity of the air could be actively controlled, because they were affected by the air stream coming from the centralized air conditioning of the laboratory. However, the sensors inside the cambers allowed monitoring of the temperature and the relative humidity as well as the carbon dioxide concentration. Table 5-10 shows typical average values during the experiment runs.

Table 5-10: Average temperature and relative humidity values during the experiment runs.

	Photoperiod temperature	Darkperiod temperature	Photoperiod relative humidity	Darkperiod relative humidity	Carbon dioxide concentration
Average	24.6 °C	17.9 °C	44.7 %	65.3 %	600 ppm*

*with the lowest concentration being around 400 ppm and the highest spike around 2300 ppm

5.6 Experiment Results and Evaluation

5.6.1 Overview of Experiment Growth Cycles

The following chapter describe in detail the three experiment growth cycles conducted for this thesis. Table 5-11 summarizes the growth cycles showing the date, name of the experiment, grown crop and the nutrient solutions used for each cycle.

Table 5-11: Overview of experiment growth cycles.

Date	Experiment name	Crop	Nutrient solutions
Mar. - July 2016	Micro-Tina No. 2	48x Micro-Tina super dwarf tomato	GC1-2 with 1/2 strength Hoagland solution. GC3-4 with C.R.O.P. pure solution.
July - Dec. 2016	Micro-Tina No. 3	48x Micro-Tina super dwarf tomato	GC1-2 with C.R.O.P. pure solution. GC3-4 with C.R.O.P. tuned solution.
Dec. 2016 - May 2017	Micro-Tina No. 4	48x Micro-Tina super dwarf tomato	GC1-2 with C.R.O.P. pure solution. GC3-4 with C.R.O.P. tuned solution.

5.6.2 Micro-Tina No. 2 Description

The Micro-Tina No. 2 experiment started after the test growth cycle (Micro-Tina No. 1). The plants were sown on March the 9th 2016 and the experiment was terminated on the 26th of July 2016, see Figure 5-18. In total 73 seeds were planted. Of those seeds, 13 were taken from fruits harvested during the Micro-Tina No. 1 growth cycle. On March the 18th, 48 seedlings were transferred into the growth chambers. GC 1-2 were supplied with a half-strength Hoagland nutrient solution, while GC3-4 were supplied with the pure version of the C.R.O.P. nutrient solution.

The plants grew well and developed the first flowers around April 18th. No differences between the plants fed by the different nutrient solutions could be observed during the first months of the experiment cycle. However, after the first harvest differences between the plants in GC1-2 and GC3-4 became more and more visible. While the plants fed with the Hoagland solution in GC1-2 remained strong and healthy, the plants fed with the C.R.O.P. pure solution stopped developing new leaves and new flowers. The remaining leaves started to wither. After the second harvest, the first plants in GC3-4 died.
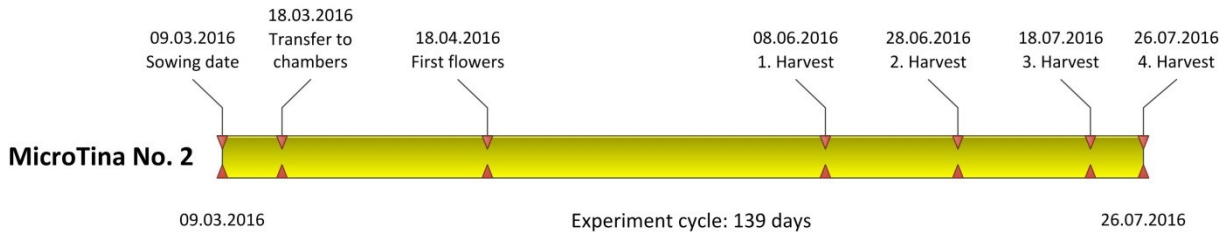
Figure 5-18: Micro-Tina No. 2 experiment timeline.

5.6.3 Micro-Tina No. 3 Description

The second experiment run and the third in total, Micro-Tina No. 3, started in July 2016 and went on for around five months until end of December 2016. The transfer from the germination boxes to the plant growth chambers happened ten days later than scheduled due to technical issues with the plant growth chambers. Consequently, the seedlings were significantly larger when transferred. The plants in chambers GC 1-2 were supplied with the C.R.O.P. pure nutrient solution, while the plants in GC 3-4 were fed with the C.R.O.P. tuned nutrient solution.

One plant in GC 1 died within days after the transfer. All other plants grew well and developed flowers and fruits. No differences in the appearance of the plants fed with both nutrient solutions have been visible during the growth cycle. All plants appeared healthy and strong after around 135 days into the experiment run. This fact and the approaching Christmas holidays let to the decision to leave the plants in the chambers for another two weeks, which led to an additional harvest during that experiment run.
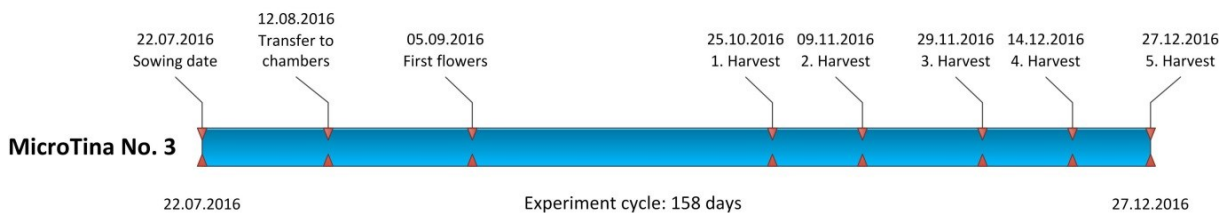
Figure 5-19: Micro-Tina No. 3 experiment timeline.

5.6.4 Micro-Tina No. 4 Description

The Micro-Tina No. 4 experiment run began immediately after the previous run at the end of 2016. After 16 days the seedlings were transferred from the germination boxes to the plant growth chambers. All plants developed flowers in early February 2017. The first harvest was performed at the end of March 2017.

All plants grew well and developed flowers and fruits. No differences in the appearance of the plants fed with both nutrient solutions have been visible during the growth cycle. All plants appeared healthy and strong throughout the whole experiment.
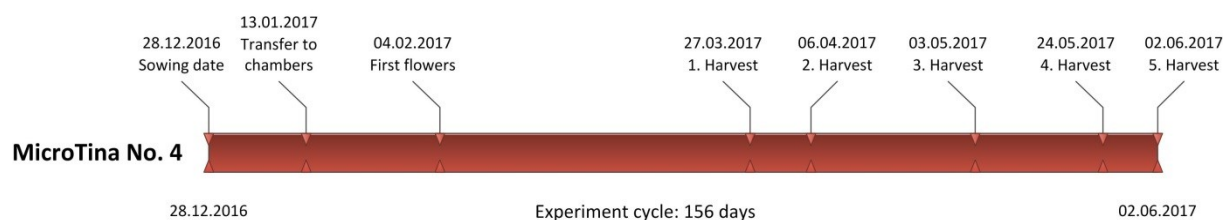
Figure 5-20: Micro-Tina No. 4 experiment timeline.

5.6.5 Timing of First Flowers and First Harvest

There is no significant difference in the timing of the first flowers and first harvest between the three experiment runs. Figure 5-21 shows an overview of the timing of the three experiment runs. The first flowers appeared on day 40, 45 and 39 after sowing for the experiment runs No. 2, No. 3 and No. 4. The first ripe fruits were harvested on day 91, day 95 and day 90 respectively. The plants of the MicroTina No. 3 experiment run took a few days longer to develop the first flowers and consequently the first harvest was delayed as well. This was most likely caused by the delayed transfer from the germination greenhouse into the plant growth chambers due to technical issues with the experiment hardware.
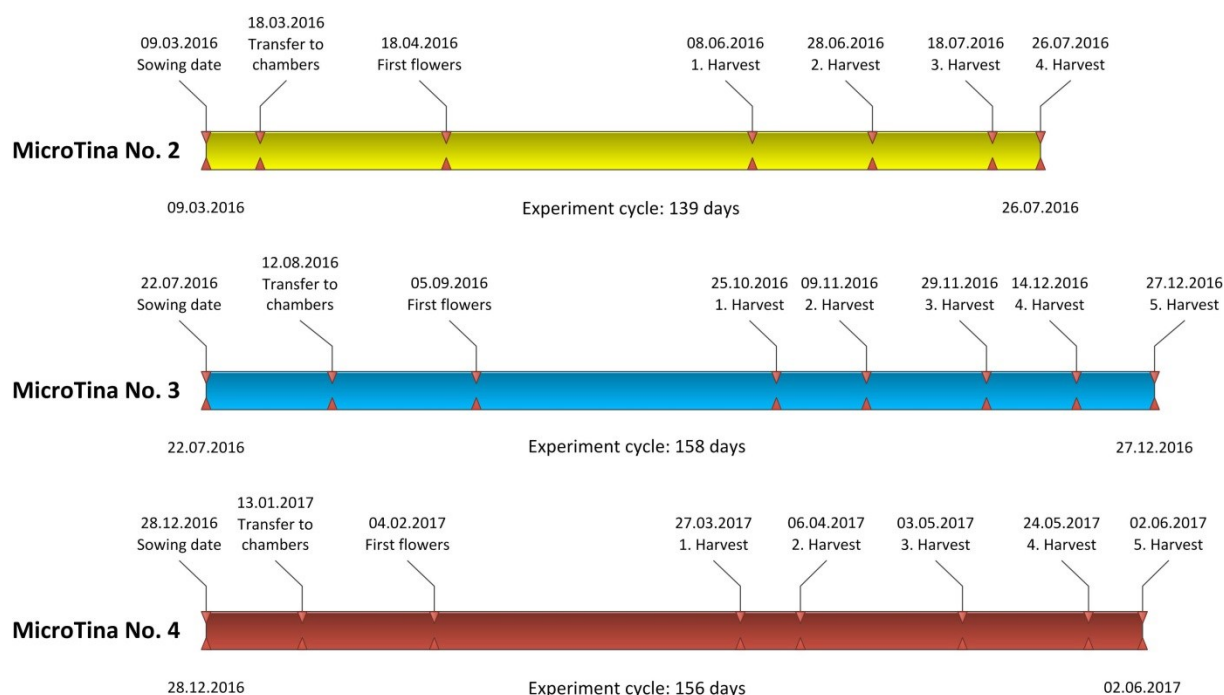
Figure 5-21: Overview of the timing of all three experiment runs.

5.6.6 Harvest Data

Upon each harvest the number of fruits per plant, the fresh weight (FW) of each fruit and the fruit dry weight (DW) per plant have been determined. Additionally the DW (without roots) of each plant has been measured at the end of each experiment run. The DW of the roots could not be determined, because most roots were contained inside the growth substrate. The combined total production results of all experiment runs are shown in Table 5-12.

The plants supplied with the half-strength Hoagland solution clearly outperform the plants cultivated with the C.R.O.P. solutions. This result was to some degree anticipated, because the C.R.O.P. solutions have significant deficits and imbalances in their nutrient compositions,

as explained in Chapter 5.4.1.4. Each plant grown with the half-strength Hoagland solution produced more fruits than the plants grown with the other nutrient solutions. The half-strength Hoagland plants also produced more fruit fresh weight and had a higher harvest index. Harvest index in this case means the ratio of edible dry biomass to inedible dry biomass.

The results of the two C.R.O.P. solutions show similarities in the average fruit fresh weight per plant. There are however differences in the average number of fruits and in the average size of the fruits. The plants grown with the C.R.O.P. pure solution produced more fruits but with less average fruit fresh weight than the plants cultivated with the C.R.O.P. tuned nutrient solution.

The C.R.O.P. tuned plants show the highest total growth rate of dry biomass of all three solutions, even slightly higher than the half-strength Hoagland plants. The harvest index values indicate that the C.R.O.P. tuned plants produced more leaves and other inedible biomass than the plants cultivated with the other solutions. Consequently, the C.R.O.P. tuned plants have the lowest harvest index. This is most likely caused by an imbalance in the nutrient solution mainly the deficit in potassium which tomato plants require to grow fruits.

Table 5-12: Summary of experiment harvest data for the reference half-strength Hoagland solution and the two C.R.O.P. solutions. Green marked cells indicate highest value per row.

	1/2 strength Hoagland*	C.R.O.P. pure**	C.R.O.P. tuned**
Average fruits per plant	60.79	53.49	48.81
Average fruit FW [g]	2.30	2.22	2.43
Average fruit FW per plant [g]	140.01	118.57	118.53
Fruit FW [g/m²]	3360.20	2786.31	2844.75
Fruit FW [g/(m²*d)]	24.17	17.75	18.12
Total plant DW [g/(m²*d)]	4.96	4.28	5.05
Harvest index [%]	56.89	48.07	38.48

* Average values of one growth cycle with 24 plants in total

** Average values for two growth cycles with 48 plants in total

As mentioned before in Chapter 5.5.1, the individual plants inside the growth chambers received different light intensities due to the setup of the chambers and the characteristics of the LED lamps. No significant difference in the production values between the 12 plant positions is visible in the harvest data.

5.6.7   Ion Concentrations in Leaves

Leaves grown by the plants of the MicroTina No. 4 experiment run were analyzed in order to determine the ion concentrations in the biomass. Leaves of plants grown with the half-strength Hoagland solution could not be analyzed. As mentioned previously the plants grown with the C.R.O.P. nutrient solutions showed withering and dropping of leaves during the

growth, which was not observed with the plants grown with the half-strength Hoagland solution. Dropped and fresh leaves were analyzed to compare the nutrient concentration in both. The dropped leaves were already dried, while the fresh leaves were cut from the plants and then dried. Figure 5-22 shows the results of the analysis.

The leave material of plants grown by both C.R.O.P. nutrient solutions show high contents of sodium cations and chloride anions caused by the high concentration in the nutrient solutions. The main difference between dropped and fresh leaves is the higher concentration of potassium and nitrate ions in dropped leaves. One can therefore assume that the withering and dropping of leaves is caused by the relatively high concentrations of nitrate or by an imbalance of the ions in the nutrient solutions. Figure 5-22 also shows the higher concentrations of potassium, calcium, magnesium, phosphate and sulfate in the leaf material of plants grown with the C.R.O.P. tuned nutrient solution as expected due to the higher concentrations of these elements in the solution.

	Na+	NH4+	K+	Ca2-	Mg2+	Cl-	NO3-	PO4-	SO4-
C.R.O.P. pure - dropped	107	63	278	391	14	187	225	112	188
C.R.O.P. pure - fresh	102	54	248	368	19	193	188	85	167
C.R.O.P. tuned - dropped	102	54	387	414	41	198	332	137	211
C.R.O.P. tuned - fresh	123	59	316	442	60	207	234	133	246
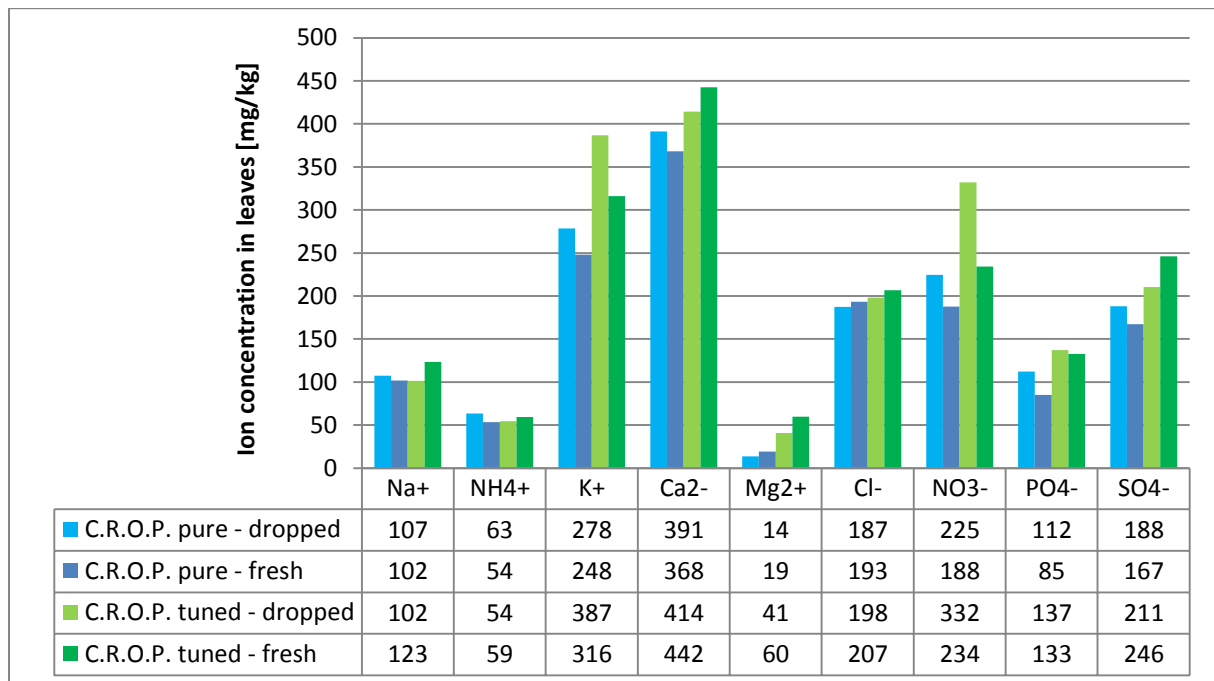
Figure 5-22: Ion concentrations in dropped and fresh leaves for both C.R.O.P. nutrient solutions.

5.6.8   Ion Concentrations in Fruits

Fruits of the last harvest of the MicroTina No. 4 experiment run were analyzed in order to determine the ion concentrations in the biomass. Fruits of plants grown with the half-strength Hoagland solution could not be analyzed. The results are shown in Figure 5-23. The high concentration of nitrate in the nutrient solutions is not carried on into the fruit material. The nitrate concentration is in line with results obtained by other researchers (Zamrik, 2013; Simion *et al.*, 2008). The main difference between the two C.R.O.P. solutions is observed in the concentration of phosphate. The fruits grown with the C.R.O.P. tuned solution have more than double the amount of phosphate in the biomass, which is associated with the higher concentration of phosphate in the nutrient solution (see Chapter 5.4.1.4). The tomatoes of both C.R.O.P. nutrient solutions show high concentrations of sodium chloride as a result of the high concentration of both elements in the nutrient solution.

	Na+	NH4+	K+	Ca2-	Mg2+	Cl-	NO3-	PO4-	SO4-
■ C.R.O.P. pure	161	82	1054	80	69	366	142	140	190
■ C.R.O.P. tuned	129	99	958	64	72	346	139	312	172
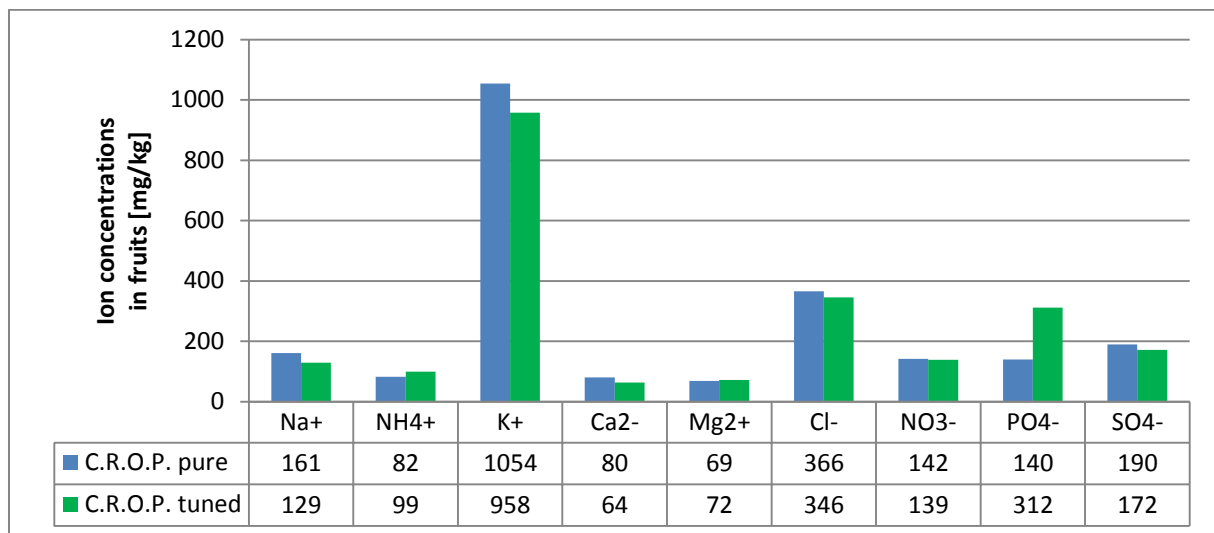
Figure 5-23: Ion concentrations in harvested fruits for both C.R.O.P. nutrient solutions.

5.7 Implications for the Life Support Model

The experiments with the C.R.O.P. filters and the cultivation of plants with the urine-derived nutrient concentrate are in an early research and development stage. Nevertheless, there are already some implications for the hybrid life support system architecture and the corresponding modelling of the system. Figure 5-24 shows the adapted system architecture with an integrated C.R.O.P. filter for urine in orange. The implementation of the C.R.O.P. filter results in a redirection of the crew metabolic solids mass flow from the crew to the C.R.O.P. filter instead of to the solid waste storage. The urine and fecal water mass flow is now going from the crew to the C.R.O.P. filter instead of going to the wastewater storage. These adaptations reduce the burden on the water processor. The product nutrient concentrate from the C.R.O.P. filter is directed to the nutrient solution tank. Here the nutrient concentrate is mixed with potable water and, when necessary, with crystalline fertilizer in order to make up a plant nutrient solution with the desired nutrient concentration and pH value.

The liquids layer of the life support system model as described in Chapter 3 needs to be modified in order to implement a C.R.O.P. filter for urine treatment. An additional stock for the C.R.O.P. filter reservoir needs to be added to the model in order to represent the liquid present in the filter tubes. The urine wastewater and fecal wastewater flows are now ending in that stock instead of going to the wastewater storage stock. The urine C.R.O.P. filter reservoir stock is connected to the greenhouse part of the liquids layer by a new flow which represents the transfer of the urine-derived nutrient concentrate from the filter units to the greenhouse. This flow depends on the amount of nutrient solution present in the greenhouse, the amount of liquid inside the C.R.O.P. filter, the nutrient concentration and pH value of the nutrient solution in the greenhouse and on the C.R.O.P. filter capacity. All these new elements and the corresponding interdependencies are shown in Figure 5-25. For comparison, the original version of the liquids layer is shown in Figure 3-27.
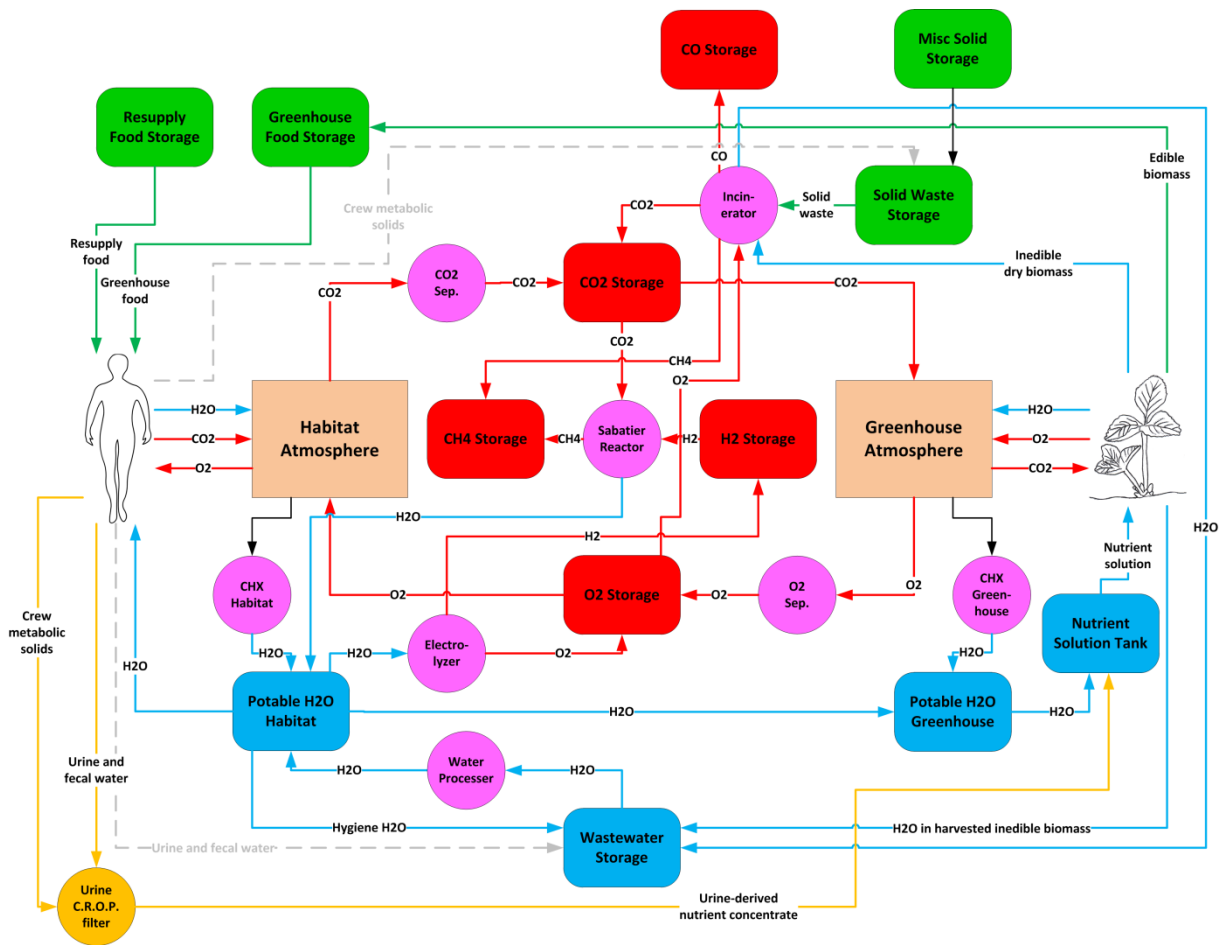
Figure 5-24: Hybrid life support system architecture with integrated C.R.O.P. filters for urine and fecal water and for inedible biomass recycling (orange elements). Grey dashed lines indicate obsolete mass flows compared to the original configuration.

Although, Figure 5-25 shows how the C.R.O.P. filter can be integrated into the existing model, the underlying formulas still need to be derived and implemented. Some of the required values still need to be determined by additional experiments, as described in Chapter 6.3.2. before a C.R.O.P. filter can be integrated into the existing life support model.
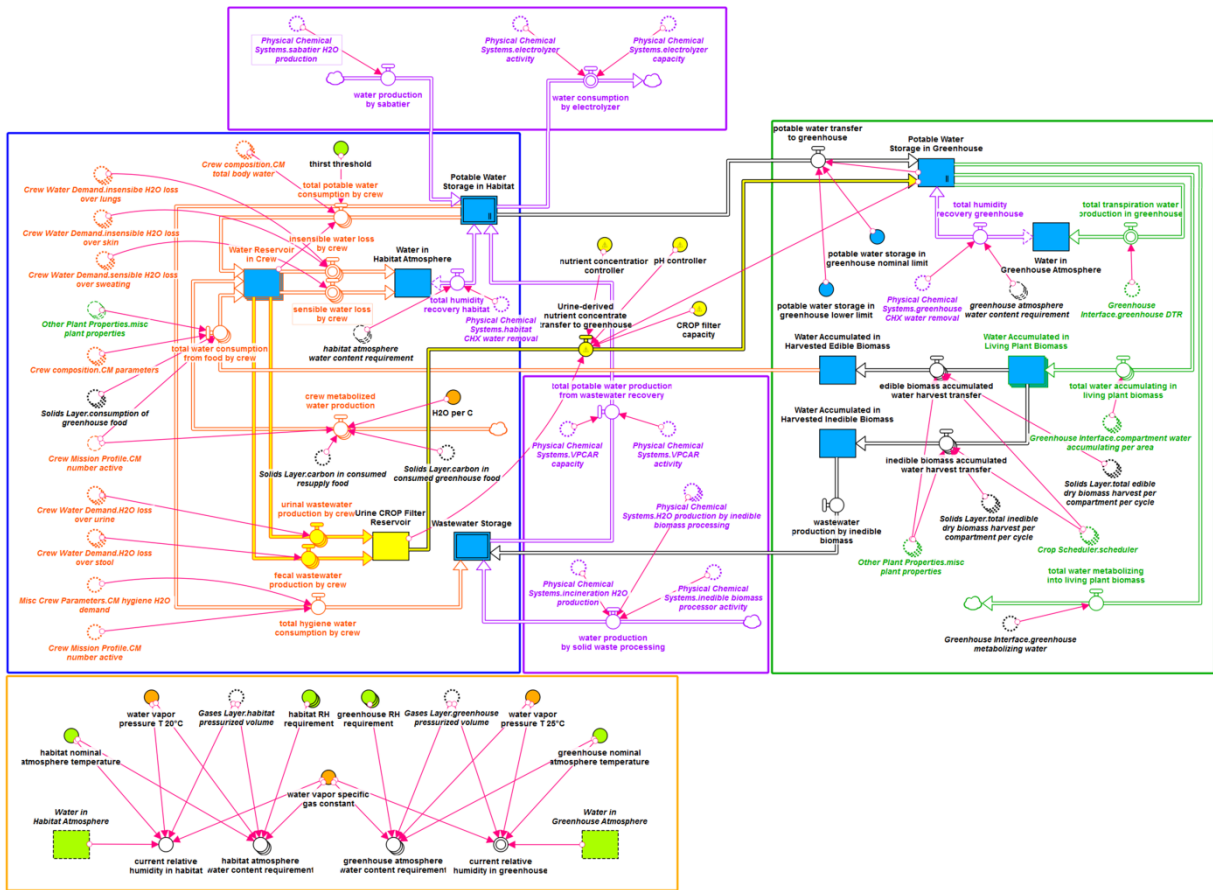
Figure 5-25: Modified liquids layer setup in Stella with implemented C.R.O.P. filter for urine treatment. New or modified elements are colored in yellow.

6 Conclusion

6.1 Summary

This thesis addressed questions associated with the combination of biological systems (especially space greenhouses) with physical-chemical life support technologies. These so called hybrid life support systems are often discussed options for near term human space exploration missions to Moon, Mars and beyond.

Knowledge about the dynamic behavior of hybrid life support systems under different nominal and off-nominal conditions is important for any space mission using such systems. Building and operating a test facility which is capable of testing a full-scale hybrid life support system is complex and expensive. The next best option is modelling and simulation.

Although there have been many other life support models in the past and some are still under development by various research groups, no model was suitable for the investigation of the thesis' research objectives. As a conclusion, a new life support model was developed to specifically examine the behavior of hybrid life support systems.

The model consists of six modules which are all interconnected to each. The backbone of the model is setup in three layers: the gases layer, the liquids layer and the solids layer. These layers calculate the matter exchange between the habitat, the crew model module, the greenhouse model module and the physical-chemical technologies module.

The crew model contains formulas that can simulate the crew metabolic inputs and outputs depending on the activity level. Each crew member can have an individual schedule assigned to him. The individual schedules are setup by the implemented crew scheduler, which combines activities to certain mission days and then mission days to full mission profiles.

The greenhouse model is based on the Modified Energy Cascade (MEC) model which is frequently used to simulate space greenhouses. The MEC is able to calculate plant inputs and outputs based on environmental conditions in a certain range. The original MEC model was enhanced by a water accumulator to also calculate the water accumulated in plant material during growth.

The physical-chemical technologies module contains formulas for certain life support technologies namely for an incinerator, an electrolyzer, a Sabatier reactor, condensing heat exchanger, a Vapor Phase Catalytic Ammonia Removal (VPCAR) water recycling system, an oxygen separator, a carbon dioxide separator and an inedible biomass processor.

In this thesis, a number of simulations have been executed with the developed life support model. First only the greenhouse model has been used to determine the nominal environmental conditions for each crop species. The setup for the first full model simulation represents a Mars surface habitat mission of 500 days duration under nominal conditions. With this simulation the general behavior of the modelled hybrid life support system has been determined and minor adjustments to the starting conditions have been made. Afterwards a number of sensitivity and perturbation analyses have been executed in order to better understand the behavior of the system under off-nominal conditions such as system or crop failures. The simulations have shown that the modelled life support system can recover from some off-nominal situations. In general one can say that the greenhouse has the largest impact on the overall behavior of the system compared to its other components.

The simulations with nominal and off-nominal conditions have been executed again with a significantly larger greenhouse (~95 % of daily calorie demand supplied by greenhouse produce). Furthermore additional simulations have been performed in order to optimize the greenhouse production schedule and in order to analyze different greenhouse startup scenarios.

Another component of this thesis was an experiment on cultivating plants with a urine-derived nutrient solution. The nutrient solution is produced by a microbiological filter. The microbiome inside the filter breaks down the components of human urine to mineral compounds which can be fed to plants. A number of experiments in cultivating super dwarf tomatoes with the urine-derived nutrient solution have been executed. The experiment results show that plants do grow when fed with the urine-derived nutrient solution. The plants developed flowers and also tomato fruits. However, the overall harvest was significantly lower compared to the reference nutrient solution. Nevertheless the experiments have shown the applicability of microbiological filters to transform human urine into a plant nutrient solution. Further experiments are necessary in order to optimize the whole process before such a filter can be part of a future life support system.

6.2   Discussion

The previous subchapter summarized the thesis work in general. This subchapter is used to compare the results of the work with the research objectives stated in Chapter 1.2 and to interpret the outcome of the work.

6.2.1   Model

The first objective of this thesis was to improve the knowledge and understanding of the behavior of hybrid life support systems, mainly the combination of space greenhouses with physical-chemical technologies. A life support model was assumed to be the best way to perform this kind of analyses. Although many life support models exist, no model suitable for the task could be found. Consequently, a new life support model has been developed for this thesis.

The developed model consists of a habitat model (represented by a gases layer, a liquids layer and a solids layer), **a crew model, a greenhouse model and models for different physical-chemical technologies**.

The three layers of the habitat model act as backbone of the over model. The layers manage the exchange of matter and information between the other components of the model and calculate the related mass flows.

The **crew model is a responsive input and output model**. The crew can be defined by the number of crew members and their gender, age and weight. A crew scheduler allows the user of the model to schedule different activities for each crew member to specific crew member days and these days to a mission profile. The crew model then calculates the different crew member inputs and outputs based on the activity level of each day.

There are more sophisticated human models available for space life support system simulations than the one developed for this thesis. In order to reduce simulation times and complexity of the model, only an input and output model was established.

The **greenhouse model is based on the Modified Energy Cascade (MEC) plant model**. The cultivation of nine different crop species can be simulated and there inputs and outputs calculated. The calculations are sensitive to a range of environmental conditions. The greenhouse model has a crop scheduler which allows the user of the model to setup a specific greenhouse production schedule (e.g. seeding, harvest dates, growth cycles). The model can simulate a greenhouse of up to ten different compartments with different environmental settings (e.g. light intensity, carbon dioxide concentration).

Since **the greenhouse model utilizes the MEC plant model it also inherits its weaknesses**. The MEC plant model can only be used to simulate plant development for a very specific range of environmental conditions. Outside these boundaries the simulation results are not validated against experimental data. Furthermore there are only formulas for nine plant species mainly high caloric density plants (e.g. wheat, potato, beans). A real space greenhouse would most likely be used to cultivate a more diverse set of plants, but those cannot be simulated with the developed model. The original MEC model lacked formulas for water accumulation in plant tissue and metabolic water consumption during photosynthesis. These formulas have been added to improve the model.

The different implemented **physical-chemical technology models are based on formulas of chemical processes**. This procedure is convenient for achieving mass closure of the overall model, but it comes with the downside that process efficiencies are not yet implemented in the model.

Different parts of the model have been validated. The original MEC plant models are based on experimental data and the model of this thesis accurately reproduces the MEC model. The crew model is based on the well-established Metabolic Equivalent Task (MET) principle. The different activity values have been validated by combining them to a typical week day of an ISS astronaut and calculating the daily kilocalorie demand. The result is very similar to values presented by NASA. As mentioned before the physical-chemical technologies are based on chemical process formulas which are assumed to be accurate.

The **overall model could not be validated against experimental data**, because of the lack of such data for the life support system architecture implemented in the model.

The **mass closure of the model has been proven** by tracking and summing up all hydrogen, oxygen and carbon present in the model during each simulation. **The total model closure calculated after 500 simulation days is 99.881 %**.

The described **model allows the investigator to setup a wide range of input parameters** such as mission duration, habitat size, crew size and composition, greenhouse production schedule etc. for a hybrid life support system. Implementing the input parameters can be partially done via predefined excel tables and partially by modifying the code of the model.

The **model has been setup utilizing the Systems Dynamics approach**, which uses only a few building blocks and a graphical programming language. This makes it easier for new users to understand and use the model. By using the Stella Professional software for the programming of the model the user is provided by **a wide range of investigation options such as built-in sensitivity and perturbation analysis tools**. Simulation results can be easily exported as excel files.

While the developed model is already capable of performing simulations to fulfill the research objectives stated at the beginning of this thesis, there is still room for some improvements. Chapter 6.3.1 discusses ideas for future work on the described life support model.

6.2.2 Simulation

A number of simulations have been performed for this thesis using the described life support system model. The goal of the simulations was to improve the knowledge and understanding of the behavior of hybrid life support systems, mainly the combination of space greenhouses with physical-chemical technologies.

The **first simulation** only utilized the greenhouse model and **had the objective to determine nominal environmental conditions for each crop species.** Therefore different combinations of input parameters, namely light intensity and carbon dioxide concentration, have been simulated for each crop species. The results have been evaluated by using the Equivalent System Mass (ESM) evaluation tool developed by NASA. The results of this evaluation are nominal environmental conditions for the following simulations.

Further **a 500 day Mars surface mission with a crew of six has been simulated** using the all model parts. The mission scenario is based on NASA's Mars Design Reference Architecture 5.0 (DRA 5.0). The life support system architecture utilizes a space greenhouse for food production and an array of physical-chemical technologies for air, water and waste treatment. First the whole mission has been simulated under nominal conditions, which in this case means no internal or external perturbations whatsoever.

The behavior of the life support system is strongly affected by the production schedule of the greenhouse. During the first 100 days of the mission, for example, the greenhouse acts as a large resource sink taking up and binding almost all of the potable water in the system and also a lot of carbon and oxygen. All these elements are used to build up the plant biomass and the water in the plant tissue. From day 100 on the overall behavior of the system is defined by the production cycle of the largest plant compartment (in this case soybean), which leads to a cyclic behavior with a period of around 90 days. This behavior could be compensated by the physical-chemical technologies and the implemented buffers. The simulated hybrid life support system was able to sustain the crew during the whole mission.

The **sensitivity analyses revealed that the stability of the life support system strongly depends on the performance of the water recycling system**. Small changes in the capacity of that system can lead to mission critical situations.

Another sensitivity analysis investigated the effects of crop under- and overperformance. Usually a space greenhouse is designed to produce a certain amount of food, etc. Changes in the environmental or operational conditions can lead to crop underperformance where the greenhouse does not meet the production targets or to crop overperformance where the plants grow better than expected. A crop underperformance usually leads to deficits in the food and oxygen supply and in the carbon dioxide uptake of the greenhouse. These effects can be buffered with contingency food supplies and by the physical-chemical systems. While crop overperformance first seems to be a benefit for the mission, it causes even more trouble than crop underperformance. Crops that grow faster and larger than expected require more resources to sustain that enhanced growth. When these resources are

not carefully managed, the greenhouse can deplete buffer tanks (especially potable water) and cause mission critical events e.g. water shortages.

Further a set of perturbation analyses have been executed. Therefore system and plant failures have been simulated at different times during the mission. **The system with the highest effect on the overall life support system behavior caused by a total failure is the water recycling system.** As mentioned before the system behavior is very sensitive to the performance of the water recycling system. Consequently, a failure of exactly that system almost always leads to mission critical situations. **Plant failures can almost always be compensated by contingency food supplies and by the physical-chemical technologies**. The system can even recover from a complete greenhouse failure assuming that the cause of the failure can be solved and new plants are sown immediately after.

Since the greenhouse has such a large effect on the overall system behavior, **the same 500 day Mars surface mission has been simulated again with a significantly larger greenhouse**. The greenhouse for this simulation is called a full nutrition greenhouse since it is able to provide more than 95 % of the daily calorie demand of the crew. The general behavior of the life support system was very similar to the previous simulation, but the effects of system and greenhouse failures were more severe, as expected.

The simulations with the 500 day Mars surface habitat mission **have shown the sensitivity of the system behavior to the greenhouse production schedule**. Therefore additional simulations have been performed in order to try out improvements to the greenhouse production schedule. The simulation results show that the original greenhouse production schedule can be improved in or to dampen certain spikes in the behavior without sacrificing much of the production capability of the greenhouse.

The greenhouse startup phase, the phase from seeding to the first harvest of the plants with the longest life cycle, **is a critical phase during a mission relying on a hybrid life support system**. Four different greenhouse startup scenarios have been simulated. A greenhouse which is setup with plants prior to the arrival of the crew always performs better than a greenhouse that is started after the arrival of the crew. A greenhouse which uses shifted seeding to avoid spikes in the matter flows produces slightly less food than a greenhouse with a simultaneous seeding (assuming the same cultivation area).

The simulations executed and described in this thesis already revealed a number of interesting facts on the behavior of a hybrid life support system. Ideas for additional simulation cases are described in Chapter 6.3.1.

6.2.3 Experiment

The goal of the experiment was to determine whether a nutrient solution derived from recycled human urine (C.R.O.P. nutrient solution) can be used for plant cultivation in space greenhouses. When taking all three experiments runs into account the following key values can be listed:

- The experiments took more than 2 years to be conducted.
- A total of 144 plants were grown and 143 reached maturity.
- Over 6600 tomato fruits were harvested and analyzed.
- The fruits had a total fresh weight of over 15 kilograms.

The experiment results show that **plants can be grown with the C.R.O.P. nutrient solution**. The tomato plants reached maturity, developed flowers and eventually ripe fruits.

The plants cultivated with the C.R.O.P. showed **signs of imbalances and deficiencies of the nutrient solution**. These are mainly caused by the high concentrations of sodium and chloride ions, but also by high concentrations of nitrate and a lack of potassium, magnesium and calcium. As a result of these issues **the yield was lower for the plants fed with the urine-derived nutrient solution** compared to those fed with the reference solution. Although the average number of fruits was higher than for the plants of the reference solution, but the average fruit size was smaller.

Attempts to tune the C.R.O.P. nutrient solution by adding specific nutrients have not been fully successful. Although the leaves of the plants fed with the C.R.O.P. tuned nutrient solution showed less signs of nutrient deficits and the plant mass was higher, the yield was not significantly improved compared to the normal C.R.O.P. nutrient solution.

The experiments described in this thesis are only the beginning of the research in this field and need to be complemented by additional experiments and further research. Ideas on future work with the C.R.O.P. nutrient solution are described in Chapter 6.3.2.

6.3   Future Work

6.3.1   Model Improvements and Additional Simulations

The developed model is designed to simulate a hybrid life support system consisting of physical-chemical technologies and a space greenhouse. Other biological systems such as microbial water and waste treatment systems and algae bioreactors are not incorporated into the model so far, but could be added later because of the modular structure of the model. The same can be said about the number of physical habitat or spacecraft modules. The current model only has one habitat and one greenhouse module, but typical spacecraft and habitats consist of several modules connected together. More physical models can be added to the model if defined habitat architecture needs to be investigated. Adding more physical modules to the model however would require the implementation of air exchange flows between the modules.

The current model simulates matter flows (e.g. gases, water, food) between its components. The model could be extended by an energy layer to also simulate flows of heat and electrical energy, which are also important aspects of developing a life support system. Stella Professional, the software used to build the model, allows for modelling energy flows and consequently an energy layer can be incorporated into the current model. Implementing an energy layer however would require major changes to the model and corresponding literature research.

For all simulations explained in this dissertation the subsystem efficiency was kept constant throughout the mission. In reality however subsystems and components degrade over time resulting in reduced efficiency. LED lamps for example are known to degrade over a period of several years. Other subsystems might degrade even faster. A mechanism to simulate subsystem degrading could be integrated into the model. This step would increase the complexity of the model and should only be done when it is clear that a certain subsystem degrades significantly within the timeframe of the simulated mission.

The current model uses a fixed life support architecture consisting of a habitat, crew, greenhouse, physical-chemical technologies and certain buffer. All simulations have been performed with this setup and small variations of it. The model has been built this way, because of information found in literature and based on the author's knowledge about life support system architectures. There are however many more architecture options which could be considered for a hybrid life support system (e.g. different physical-chemical technologies, different buffer setup, and additional bio-regenerative technologies). The model allows for some flexibility regarding the life support architecture. Making the model more flexible by implementing additional architecture options is possible but would increase the complexity of the model significantly. This should only be done if different architecture options need to be compared to each other e.g. in the case of trade-off studies.

The biggest limitation in modelling space greenhouses is the restricted amount of plant models suitable for simulating life support system behavior. There are many plant models available in general. However, most of them were developed for traditional agriculture, terrestrial greenhouses or for modeling biological processes. These plant models are usually not suitable for life support simulations where input and output models for different controlled environmental conditions are required. The MEC plant model implemented in the model of this dissertation is the most suitable plant model to be found in literature. However it still has some limitations. First of all the number of available crop species is restricted to nine with most of them being crops with high caloric values. Leafy greens such as lettuce, spinach, herbs, etc. are only represented by a model for lettuce. Fresh vegetables such as tomato, pepper, cucumber, etc. are only represented by a MEC model for tomato. Crops with a valuable composition of nutrients such as red beet, strawberries, cauliflower, etc. are not represented in the MEC model at all. This limitation in crop variety restricts the simulation of space greenhouses to such with low plant diversity.

Adding more crops and more crop varieties to the MEC plant model database would require extensive experiments. Due to the nature of plant growth, those experiments would also require most likely several years of research. Nevertheless that kind of research needs to be done in order to provide life support engineers with a more diverse set of plant models in order to simulate future space greenhouses. The research could be split up between several research institutions in order to utilize more resources and speed up the experiments.

The model described in this dissertation focuses on the matter flows of hydrogen, oxygen, carbon and the different combinations of these elements. While this is sufficient for most of the investigations, a closed loop model should also include the mass flows of other elements. Especially the mass flows of compounds involved in plant nutrition such as nitrate, ammonium, potassium, calcium, magnesium, phosphate, sulfate, sodium and chloride should be simulated over the course of a long mission.

The current model was not setup to be utilized as a ready-to-use tool. Before each simulation a number of settings and parameters (besides the mission requirements) need to be implemented manually in order to guarantee model functionality. However, the model could be extended by a graphical user interface in order to allow other engineers to use the model for their own simulations without the need for familiarization with all model parts. Stella Professional can be upgraded with an additional software package in order to setup such an interface.

6.3.2 Experiments with Recycled Urine

Recycling urine using the C.R.O.P. filter is a promising element for future life support systems and terrestrial applications. The filter produces valuable nutrients from human metabolic waste products. The experiments conducted for this dissertation show the general feasibility of cultivating plants with C.R.O.P. nutrient solutions, but there are still some open research questions.

The experiments have shown certain weaknesses in the nutrient composition of the urine-derived solutions. The high content of sodium and chloride ion is a general problem when working with urine and means to reduce the amount of both ions in the resulting nutrient solutions require more research. Plant development would greatly benefit from a reduced amount of these ions. Another way to reduce the amount of sodium and chloride ions in the final product of the C.R.O.P. is the reduction of both elements in the nutrition of the crew. This seems to be possible in future space missions, because the nutrition of astronauts is already controlled and measured extensively today.

Further experiments with other crop species are highly recommended to prove the acceptability of the urine-derived nutrient solution. Here plant species with a higher demand of nitrogen and lower demand of potassium should be investigated in particular, because these plants might require fewer adjustments to the C.R.O.P. nutrient solution which is rich in nitrogen available as nitrate and relatively poor in potassium.

When it comes to adjusting the C.R.O.P. pure solution to a more suitable nutrient solution, a horticulture expert with experience in plant nutrition is required. Plant nutrition is a very complex topic requiring profound knowledge of chemistry and the underlying plant metabolic processes which are no typical working areas of aerospace engineers. It is therefore recommended to continue the work on tuning the urine-derived nutrient solution in partnership with a horticultural research institute.

During each experiment run with the urine-derived nutrient solution biofilms were forming on top of the growth medium and eventually in the nutrient solution tanks despite the pasteurization of the solution after extraction out of the C.R.O.P. filter. The biofilm seems to have no effect on the development of the plants. Nevertheless the composition of the biofilm should be further investigated by a microbiologist when they also occur in future experiments.

7 References

Allada, R.K., Lange, K. and Anderson, M. (2011), "Dynamic Modeling of Process Technologies for Closed-Loop Water Recovery Systems", paper presented at 42nd International Conference on Environmental Systems, Vail, Colorado.

Alling, A., Nelson, M. and Silverstone, S. (1993), *Life under glass: The inside story of Biosphere 2*, Biosphere Press, Oracle, AZ, U.S.A.

Anderson, M.S., Ewert, M.K., Keener, J.F. and Wagner, S.A. (2015), "Life Support Baseline Values and Assumptions Document", *NASA*, No. NASA/TP-2015–218570.

Anthony, S.M. and Hintze, P.E. (2014), "Trash-to-Gas: Determining the ideal technology for converting space trash into useful products", paper presented at 44th International Conference on Environmental Systems, Tucson, Arizona.

Arai, T., Fanchiang, C., Aoki, H. and Newman, D.J. (2008), "Educational tool for modeling and simulation of a closed regenerative life support system", *Acta Astronautica*, Vol. 63 No. 7-10, pp. 1100–1105.

Averner, M.M. (1981), "An Approach to the Mathematical Modelling of a Controlled Ecological Life Support System", *NASA*, CR-166331.

Aydogan, S., Orcun, S., Blau, G., Pekny, J.F. and Reklaitisa, G.V. (2004), "A Prototype Simulation Based Optimization Approach to Model and Design an Advanced Life Support System", paper presented at 34th International Conference on Environmental Systems, Colorado Springs, Colorado.

Aydogan-Cremaschi, S., Orcun, S., Blau, G., Pekny, J.F. and Reklaitis, G.V. (2009), "A novel approach for life-support-system design for manned space missions", *Acta Astronautica*, Vol. 65 No. 3-4, pp. 330–346.

Babcock, P.S., Auslander, D.M. and Spear, R.C. (1984), "Dynamic considerations for control of closed life support systems", *Advances in Space Research*, Vol. 4 No. 12, pp. 263–270.

Bacskay, A.S. and Knox, J.C. (1989), "System Level Design Analyses for the Space Station Environment Control and Life Support System", paper presented at 19th Intersociety Conference on Environmental Systems, San Diego, California.

Bamsey, M., Berinstain, A., Graham, T., Neron, P., Giroux, R., Braham, S., Ferl, R., Paul, A.-L. and Dixon, M. (2009a), "Developing strategies for automated remote plant production systems: Environmental control and monitoring of the Arthur Clarke Mars Greenhouse in the Canadian High Arctic", *Advances in Space Research*, Vol. 44 No. 12, pp. 1367–1381.

Bamsey, M., Graham, T., Stasiak, M., Berinstain, A., Scott, A., Vuk, T.R. and Dixon, M. (2009b), "Canadian advanced life support capacities and future directions", *Advances in Space Research*, Vol. 44 No. 2, pp. 151–161.

Belakovsky, M.S., Voloshin, O.V. and Morgunov, P.S. (2010), *Mars-500 Project: Step Three: 520-day isolation*.

Berkovich, J.A., Krivobok, N.M., Siniak, J.E., Zaitsev, E.R. and Monakhov, B.N. (1997), "Perspectives of developing a space greenhouse for the International Space Station", in *6th European Symposium on Space Environmental Control Systems, Noordwijk, The Netherlands, 20-22 May*, ESA.

Berkovich, Y., Krivobok, N.M. and Sinyak, Y. (1998), "Project of conveyer-type space greenhouse for cosmonauts' supply with vitamin greenery", *Advances in Space Research*, Vol. 22 No. 10, pp. 1401–1405.

References

Berkovich, Y., Smolyanina, S.O., Krivobok, N.M., Erokhin, A.N., Agureev, A.N. and Shanturin, N.A. (2009), "Vegetable production facility as a part of a closed life support system in a Russian Martian space flight scenario", *Advances in Space Research*, Vol. 44 No. 2, pp. 170–176.

Berkovich, Y.A., Krivobok, N.M., Sinyak, Y., Smolyanina, S.O., Grigoriev, Y., Romanov, S. and Guissenberg, A.S. (2004), "Developing a vitamin greenhouse for the life support system of the international space station and for future interplanetary missions", *Advances in Space Research*, Vol. 34 No. 7, pp. 1552–1557.

Berkovitch, Y.A. (1996), "Instrumentation for plant health and growth in space", *Advances in Space Research*, Vol. 18 No. 4-5, pp. 157–162.

Bingham, G.E., Salisbury, F.B., Campbell, W.F., Carman, J.G., Bubenheim, D.L., Yendler, B., Sytchev, V.N., Berkovitch, Y., Levinskikh, M.A. and Podolsky, I.G. (1996), "The Spacelab-Mir-1 "Greenhouse-2" experiment", *Advances in Space Research*, Vol. 18 No. 4-5, pp. 225–232.

Bingham, G.E., Topham, T.S., Mulholland, J.M. and Podolsky, I.G. (2002), "Lada: The ISS Plant Substrate Microgravity Testbed", paper presented at 32nd International Conference on Environmental Systems, San Antonio, Texas.

Bingham, G.E., Topham, T.S., Taylor, A., Podolsky, I.G., Levinskikh, M.A. and Sychev, V.N. (2003), "Lada: ISS Plant Growth Technology Checkout", paper presented at 33rd International Conference on Environmental Systems, Vancouver, Canada.

Blankenship, R.E. (2010), "Photosynthesis: The light reactions", in Taiz, L. and Zeiger, E. (Eds.), *Plant physiology*, 5th ed, Sinauer Associates, Sunderland, MA.

Bloom, A. (2010), "Mineral Nutrition", in Taiz, L. and Zeiger, E. (Eds.), *Plant physiology*, 5th ed, Sinauer Associates, Sunderland, MA.

Bornemann, G., Waßer, K., Tonat, T., Moeller, R., Bohmeier, M. and Hauslage, J. (2015), "Natural microbial populations in a water-based biowaste management system for space life support", *Life sciences in space research*, Vol. 7, pp. 39–52.

Boscheri, G., Guarnieri, V., Chirico, S., Zabel, P. and Lasseur, C. (2017a), "SCALISS: An European Tool for Automated Scaling of Life Support Systems", paper presented at 47th International Conference on Environmental Systems, Charleston, South Carolina.

Boscheri, G., Guarnieri, V., Locantore, I., Lamantea, M., Lobascio, C., Iacopini, C. and Schubert, D. (2016), "The EDEN ISS Rack-Like Plant Growth Facility", paper presented at 46th International Conference on Environmental Systems, 10-14 July, Vienna, Austria.

Boscheri, G., Lamantea, M.M., Lobascio, C., Volponi, M., Schubert, D. and Zabel, P. (2017b), "Main performance results of the EDEN ISS Rack-Like Plant Growth Facility", paper presented at 47th International Conference on Environmental Systems, 16-20 July, Charleston, South Carolina.

Brinckmann, E. (1999), "Spaceflight opportunities on the ISS for plant research — The ESA perspective", *Advances in Space Research*, Vol. 24 No. 6, pp. 779–788.

Brinckmann, E. (2005), "ESA hardware for plant research on the International Space Station", *Advances in Space Research*, Vol. 36 No. 7, pp. 1162–1166.

Bubenheim, D.L. and Wydeven, T. (1994), "Approaches to resource recovery in Controlled Ecological Life Support Systems", *Advances in space research the official journal of the Committee on Space Research (COSPAR)*, Vol. 14 No. 11, pp. 113–123.

Buchanan, B.B. and Wolosiuk, R.A. (2010), "Photosynthesis: The Carbon reactions", in Taiz, L. and Zeiger, E. (Eds.), *Plant physiology*, 5th ed, Sinauer Associates, Sunderland, MA.

References

Bula, R.J., Tennessen, D.J., Morrow, R.C. and Tibbitts, T.W. (1994), "Light Emitting Diodes as a Plant Lighting Source", in Tibbits, T.W. (Ed.), *International Lighting in Controlled Environments Workshop, University of Wisconsin*, NASA.

Campbell, W.F., Salisbury, F.B., Bugbee, B., Klassen, S., Naegle, E., Strickland, D.T., Bingham, G.E., Levinskikh, M., Iljina, G.M., Veselova, T.D., Sytchev, V.N., Podolsky, I., McManus, W.R., Bubenheim, D.L., Stieber, J. and Jahns, G. (2001), "Comparative floral development of Mir-grown and ethylene-treated, earth-grown Super Dwarf wheat", *Journal of Plant Physiology*, Vol. 158 No. 8, pp. 1051–1060.

Chambliss, J.P., Stambaugh, I.S. and Moore, M. (2016), "Resource Tracking Model Updates and Trade Studies", paper presented at 46th International Conference on Environmental Systems, 10-14 July, Vienna, Austria.

Chambliss, J.P., Stambaugh, I.S., Sargusingh, M., Shull, S. and Moore, M. (2015), "Development of a Water Recovery System Resource Tracking Model", paper presented at 45th International Conference on Environmental Systems, 12-16 July, Bellevue, Washington.

Cowles, J.R., Scheld, H.W., Lemay, R. and Peterson, C. (1984), "Growth and lignification in seedlings exposed to eight days of microgravity", *Annals of Botany*, Vol. 54 No. 3, pp. 33–48.

Cox, P. (1987), "Insensible water loss and its assessment in adult patients: a review", *Acta Anaesthesiologica Scandinavica*, Vol. 31 No. 8, pp. 771–776.

Coyle, R.G. (1977), *Management system dynamics*, Wiley, London, New York.

Crabb, T.M., Morrow, R.C. and Frank, J.G. (2001), "Plant Research Unit – Program Overview", paper presented at 31st International Conference on Environmental Systems, Orlando, Florida.

Cullingford, H.S. (1989), "Development of the CELSS Emulator at NASA JSC", paper presented at 19th Intersociety Conference on Environmental Systems, San Diego, California.

Cusick, A., Killian, M. and Olthoff, C. (2016), "Integrated EVA Thermal Simulations using TherMoS and V-SUIT", paper presented at 46th International Conference on Environmental Systems, 10-14 July, Vienna, Austria.

Czupalla, M. (2012), *The virtual habitat - Integral modeling and dynamic simulation of life support systems,* 1. Aufl., Verl. Dr. Hut, München.

Czupalla, M., Hager, P., Pfeiffer, M., Harder, J. and Dirlich, T. (2009), "An environmentally sensitive dynamic human model for LSS robustness studies with the V-HAB simulation", *Advances in Space Research*, Vol. 44 No. 12, pp. 1413–1427.

Czupalla, M., Zhukov, A., Mecsaci, A., Beck, M. and Deiml, M. (2011), "Dynamic Life Support System Simulations with the Virtual Habitat", paper presented at 41st International Conference on Environmental Systems, 17-21 July, Portland, Oregon.

Czupalla, M., Zhukov, A., Schnaitmann, J., Bickel, T. and Walter, U. (2010), "The Virtual Habitat - A Tool for Dynamic Life SUpport System Simulations", paper presented at 40th International Conference on Environmental Systems, Barcelona, Spain.

Czupalla, M., Zhukov, A., Schnaitmann, J., Olthoff, C., Deiml, M., Plötner, P. and Walter, U. (2015), "The Virtual Habitat – A tool for dynamic life support system simulations", *Advances in Space Research*, Vol. 55 No. 11, pp. 2683–2707.

DaLee, R.C. and Lee, T.C. (1993), "Expert System Based Tool for Advanced Life Support System Optimization - A Mission Analysis Perspective", paper presented at 23rd International Conference on Environmental Systems, Colorado Springs, Colorado.

References

Deaton, M.L. and Winebrake, J.J. (1999), *Dynamic Modeling of Environmental Systems, Modeling Dynamic Systems*, Springer New York, New York, NY.

Detrell, G. and Belz, S. (2017), "ELISSA - a comprehensive software package for ECLSS technology selection, modelling and simulation for human spaceflight missions", paper presented at 47th International Conference on Environmental Systems, Charleston, South Carolina.

Detrell, G., Ganzer, B. and Messerschmid, E. (2011), "Adaptation of the ELISSA Simulation Tool for Reliability Analysis", paper presented at 41st International Conference on Environmental Systems, 17-21 July, Portland, Oregon.

Detrell, G., Messerschmidt, E. and Griful i Ponsati, E. (2016), "ECLSS reliability analysis tool for long duration spaceflight", paper presented at 46th International Conference on Environmental Systems, 10-14 July, Vienna, Austria.

Do, S., Owens, A. and de Weck, O. (2015), "HabNet - An Integrated Habitation and Supportability Architecting and Analysis Environment", paper presented at 45th International Conference on Environmental Systems, 12-16 July, Bellevue, Washington.

Drake, B.G. (2009), *Human Exploration of Mars Design Reference Architecture 5.0*, NASA.

Drysdale, A. (1997), "OCAM-2: A Second Generation Bioregenerative Life Support System Model", paper presented at 27th International Conference on Environmental Systems, Lake Tahoe, Nevada.

Drysdale, A., Thomas, M., Fresa, M. and Wheeler, R. (1992), "OCAM-A CELLS modeling tool: description and results", paper presented at 22nd International Conference on Environmental Systems, Seattle, Washington.

Dueck, T., Kempkes, F., Meinen, E. and Stanghellini, C. (2016), "Choosing crops for cultivation in space", paper presented at 46th International Conference on Environmental Systems, 10-14 July, Vienna, Austria.

Duffie, N.A., Bula, R.J., Morrow, R.C., Quirin, P.E., Macaulay, P.D., Wranovsky, S.R., Vignali, J.C. and Tibbits, T.W. (1994), "Humidity and Temperature Control in the ASTROCULTURE™ Flight Experiment", paper presented at 24th International Conference on Environmental Systems, Friedrichshafen, Germany.

Duffie, N.A., Zhou, W., Morrow, R.C., Bula, R.J., Tibbitts, T.W., Wranovsky, S.R. and Macaulay, P.D. (1995), "Control and Monitoring of Environmental Parameters in the ASTROCULTURE™ Flight Experiment", paper presented at 25th International Conference on Environmental Systems, San Diego, California.

Dussap, C.G. (2003), "REGLISSE - Review of European Ground Laboratories and Infrastructures for Sciences and Support of Exploration", *ESA*, TN3 - Definition of the Ideal Facility for Life Support Issues.

Eckart, P. (1996), *Spaceflight life support and biospherics, Space technology library*, v. 5, Microcosm Press; Kluwer Academic, Torrance, Calif, Dordrecht, Boston.

Ehleringer, J. and Sandquist, D. (2010), "Photosynthesis: Physiological and ecological considerations", in Taiz, L. and Zeiger, E. (Eds.), *Plant physiology*, 5th ed, Sinauer Associates, Sunderland, MA.

Encyclopedia of Safety (2012), "The Memorial Museum of Cosmonautics", available at: http://survincity.com/2012/07/the-memorial-museum-of-cosmonautics/ (accessed 28 May 2014).

Evans, C.A., Robinson, J.A., Tate-Brown, J., Thumm, T., Crespo-Richey, J., Baumann, D. and Rhatigan, J. (2009), *International Space Station Science Research Accomplishments*

During the Assembly Years: An Analysis of Results from 2000-2008 No. NASA/TP-2009-213146-Revision A, NASA, available at:
http://www.nasa.gov/pdf/389388main_ISS%20Science%20Report_20090030907.pdf.

Feng, D.-L. and Wu, Z.-C. (2006), "Culture of Spirulina platensis in human urine for biomass production and O(2) evolution", *Journal of Zhejiang University. Science. B*, Vol. 7 No. 1, pp. 34–37.

Ferral, J., Ganapathi, G.B., Rohatgl, N. and Seshan, P.K. (1995), "Parametric Studies Usind LiSSA for An Extra-Terrestrial Manned Outpost", paper presented at 25th International Conference on Environmental Systems, San Diego, California.

Finn, C.K. (1999), "Dynamic System Modeling of Regenerative Life Support Systems", paper presented at 29th International Conference on Environmental Systems, Denver, Colorado.

Fleischer, D., Ting, K., Hill, M. and Eghbali, G. (1999), "Top Level Modeling of Biomass Production Component of ALSS", paper presented at 29th International Conference on Environmental Systems, Denver, Colorado.

Fleischmann, M., Mittelbach, E. and Schütz, A. (2015), *Alexander Gerst shapes our future on the International Space Station*, DLR.

Floyd, H. (1974), "Student experiments on Skylab", in *Scientific investigations on the Skylab satellite; Conference*, *Meeting Paper Archive*, American Institute of Aeronautics and Astronautics.

Ford, A. (2010), *Modeling the environment,* 2nd ed, Island Press, Washington, DC.

Forehand, L. (2005), "NASA Office of Legislative Affairs Memo: NASA Plans for Plant and Animal Research", available at: http://www.spaceref.ca/news/viewsr.html?pid=17716 (accessed 3 March 2014).

Forrester, J.W. (1961), *Industrial dynamics, System dynamics series*, Pegasus Communications, Waltham, MA.

Forrester, J.W. (1969), *Urban dynamics, System dynamics series*, Pegasus Communications, Waltham, Mass.

Giacomelli, G.A., Patterson, L., Nelkin, J., Sadler, P.D. and Kania, S. (2006), "CEA in Antarctica - Growing vegetables on "the ice"", *Resource: Engineering and technology for sustainable world*, Vol. 13 No. 1, pp. 3–5.

Gierszewski, D. and Olthoff, C. (2016), "Integrated Thermal Simulation of the Space Evaporator Absorber Radiator using TherMoS and V-SUIT", paper presented at 46th International Conference on Environmental Systems, 10-14 July, Vienna, Austria.

Giroux, R., Berinstain, A., Braham, S., Graham, T., Bamsey, M., Boyd, K., Silver, M., Lussier-Desbiens, A., Lee, P., Boucher, M., Cowing, K. and Dixon, M. (2006), "Greenhouses in extreme environments: The Arthur Clarke Mars Greenhouse design and operation overview", *Advances in Space Research*, Vol. 38 No. 6, pp. 1248–1259.

Gitelson, I.I., Lisovsky, G.M. and MacElroy, R.D. (2003), *Manmade closed ecological systems, Earth Space Institute book series*, v. 9, Taylor & Francis, London, New York.

Gitelson, I.I., Terskov, I.A., Kovrov, B.G., Lisovskii, G.M., Okladnikov, Y., Sid'ko, F., Trubachev, I.N., Shilenko, M.P., Alekseev, S.S., Pan'kova, I.M. and Tirranen, L.S. (1989), "Long-term experiments on man's stay in biological life-support system", *Advances in Space Research*, Vol. 9 No. 8, pp. 65–71.

References

Göser, J. and Olthoff, C. (2014), "Results of a Dynamic Liquid Cooling Garment Simulation in V-SUIT", paper presented at 44th International Conference on Environmental Systems, Tucson, Arizona.

Goudarzi, S. and Ting, K.C. (1999), "Top Level Modeling of Crew Component of ALSS", paper presented at 29th International Conference on Environmental Systems, Denver, Colorado.

Graf, J. (2011), "A Cabin Air Separator for EVA Oxygen", paper presented at 41st International Conference on Environmental Systems, 17-21 July, Portland, Oregon.

Gustavino, S.R., Mankamyer, M.M. and Gardner, A.M. (1990), "Computer Simulation of a Regenerative Life Support System for a Lunar Base", paper presented at 20th International Conference on Environmental Systems, Williamsburg, Virginia.

Haeuplik-Meusburger, S., Paterson, C., Schubert, D. and Zabel, P. (2014), "Greenhouses and their humanizing synergies", *Acta Astronautica*, Vol. 96, pp. 138–150.

Haeuplik-Meusburger, S., Peldszus, R. and Holzgethan, V. (2011), "Greenhouse design integration benefits for extended spaceflight", *Acta Astronautica*, Vol. 68 No. 1-2, pp. 85–90.

Halstead, T.W. and Dutcher, F.R. (1984), "Experiments on plants grown in space. Status and prospects.", *Annals of Botany*, Vol. 54 No. 3, pp. 3–18.

Hannon, B.M. and Ruth, M. (1997), *Modeling dynamic biological systems, Modeling Dynamic Systems*, Springer, New York.

Hargrove, J.L. (1998), *Dynamic modeling in the health sciences, Modeling Dynamic Systems*, Springer, New York.

Heathcote, D.G., Brown, C.S., Goins, G.D., Kliss, M., Levine, H., Lomax, P.A., Porter, R.L. and Wheeler, R.M. (1997), "The Plant Research Unit: Long-Term Plant Growth Support for Space Station", in *6th European Symposium on Space Environmental Control Systems, Noordwijk, The Netherlands, 20-22 May*, ESA.

Hellerstein, S. (1993), "Fluid and electrolytes: clinical aspects", *Pediatrics in review / American Academy of Pediatrics*, Vol. 14 No. 3, pp. 103–115.

Hoagland, D.R. and Arnon, D.I. (1950), *The water-culture method for growing plants without soil*, Berkeley, Calif. College of Agriculture, University of California.

Hoehn, A., Chamberlain D. J., Forsyth, S.W., Gifford, K., Hanna, D.S., Horner, M.B., Scovazzo, P., Smith, J., Stodieck, L.S. and Todd, P.W. (1997), "Plant Generic Bioprocessing Apparatus: A plant growth facility for spaceflight biotechnology research", in *6th European Symposium on Space Environmental Control Systems, Noordwijk, The Netherlands, 20-22 May*, ESA.

Hoehn, A., Clawson, J., Heyenga, A.G., Scovazzo, P., Sterrett, K.S., Stodieck, L.S., Todd, P.W. and Kliss, M.H. (1998), "Mass Transport in a Spaceflight Plant Growth Chamber", paper presented at 28th International Conference on Environmental Systems, Danvers, Massachusetts.

Hoff, J.E., Howe, J.M. and Mitchell, C.A. (1982), *Development of selection criteria and their application in evaluation of CELSS candidate species* No. N83-30016 19-54, NASA.

Holbrook, M. (2010), "Water and plant cells", in Taiz, L. and Zeiger, E. (Eds.), *Plant physiology*, 5th ed, Sinauer Associates, Sunderland, MA.

Holliday, M.A. and Segar, W.E. (1957), "The maintenance need for water in parenteral fluid therapy", *Pediatrics*, Vol. 19 No. 5, pp. 823–832.

References

Hummerick, M., Garland, J., Bingham, G., Sychev, V. and Podolsky, I. (2010), "Microbiological analysis of Lada Vegetable Production Units (VPU) to define critical control points and procedures to ensure the safety of space grown vegetables", paper presented at 40th International Conference on Environmental Systems, Barcelona, Spain.

Hummerick, M., Garland, J., Bingham, G., Wheeler, R., Topham, S., Sychev, V. and Podolsky, I. (2011), "A hazard analysis critical control point plan applied to the Lada vegetable production units (VPU) to ensure the safety of space grown vegetables", paper presented at 41st International Conference on Environmental Systems, 17-21 July, Portland, Oregon.

Ivanova, T. (2002), "Greenhouse aboard Mir shows plants can survive in space", *21st Century*, pp. 41–49.

Ivanova, T., Sapunova, S., Dandolov, I., Ivanov, Y., Meleshko, G., Mashinsky, A. and Berkovich, Y. (1994), "'SVET' space greenhouse onboard experiment data received from 'MIR' station and future prospects", *Advances in Space Research*, Vol. 14 No. 11, pp. 343–346.

Ivanova, T.N., Bercovich, Y., Mashinskiy, A.L. and Meleshko, G.I. (1993), "The first "space" vegetables have been grown in the "SVET" greenhouse using controlled environmental conditions", *Acta Astronautica*, Vol. 29 No. 8, pp. 639–644.

Ivanova, T.N., Kostov, P.T., Sapunova, S.M., Dandolov, I.W., Salisbury, F.B., Bingham, G.E., Sytchov, V.N., Levinskikh, M.A., Podolski, I.G., Bubenheim, D.B. and Jahns, G. (1998), "Six-month space greenhouse experiments — A step to creation of future biological life support systems", *Acta Astronautica*, Vol. 42 No. 1-8, pp. 11–23.

Jetté, M., Sidney, K. and Blümchen, G. (1990), "Metabolic equivalents (METS) in exercise testing, exercise prescription, and evaluation of functional capacity", *Clinical Cardiology*, Vol. 13 No. 8, pp. 555–565.

Jones, H. and Cavazzoni, J. (2000), "Top-Level Crop Models for Advanced Life Support Analysis", paper presented at 30th International Conference on Environmental Systems, Toulouse, France.

Jones, H., Cavazzoni, J. and Keas, P. (2002), "Crop Models for Varying Environmental Conditions", paper presented at 32nd International Conference on Environmental Systems, San Antonio, Texas.

Jones, H., Finn, C., Kwauk, X. and Blackwell, C. (2001), "Modeling Separate and Combined Atmospheres in BIO-Plex", paper presented at 31st International Conference on Environmental Systems, Orlando, Florida.

Jones, H.W. (2009), "Planning Dynamic Simulation of Space Life Support", paper presented at 39th International Conference on Environmental Systems, Savannah, Georgia.

Jones, H.W. (2017), "How Should Life Support be Modeled and Simulated?", paper presented at 47th International Conference on Environmental Systems, Charleston, South Carolina.

Kamada, M., Omori, K., Nishitani, K., Hoson, T., Shimazu, T. and Ishioka, N. (2007), "JAXA Space Plant Research on the ISS with European Modular Cultivation System", *Biological Sciences in Space*, Vol. 21 No. 3, pp. 62–66.

Kern, V.D., Bhattacharya, S., Bowman, R.N., Donovan, F.M., Elland, C., Fahlen, T.F., Girten, B., Kirven-Brooks, M., Lagel, K., Meeker, G.B. and Santos, O. (2001), "Life sciences flight hardware development for the International Space Station", *Advances in Space Research*, Vol. 27 No. 5, pp. 1023–1030.

References

Kleinknecht, K.S. and Powers, J.E. (1973), "Skylab Student Project", in Napolitano, L.G., Contensou, P. and Hilton, W.F. (Eds.), *Astronautical Research 1972*, Springer Netherlands, Dordrecht, pp. 309–317.

Kliss, M., Heyenga, A.G., Hoehn, A. and Stodieck, L.S. (2000a), "Recent advances in technologies required for a "Salad Machine"", *Advances in Space Research*, Vol. 26 No. 2, pp. 263–269.

Kliss, M., Heyenga, G., Hoehn, A. and Stodieck, L. (2000b), "Toward the Development of a "Salad Machine"", paper presented at 30th International Conference on Environmental Systems, Toulouse, France.

Kliss, M. and MacElroy, R.D. (1990), "Salad Machine: A Vegetable Production Unit for Long Duration Space Missions", paper presented at 20th International Conference on Environmental Systems, Williamsburg, Virginia.

Knott, W.M. (1992), "The breadboard project: A functioning CELSS plant growth system", *Advances in Space Research*, Vol. 12 No. 5, pp. 45–52.

Kolodney, D., Lange, K.E. and Edeen, M.A. (1991), "Modeling of advanced ECLSS/ARS with ASPEN", paper presented at 21st International Conference on Environmental Systems, San Fransisco, California.

Kortenkamp, D. and Bell, S. (2003), "Simulating Adavanced Life Support Systems for Integrated Controls Research", paper presented at 33rd International Conference on Environmental Systems, Vancouver, Canada.

Kuang, A., Popova, A., Xiao, Y. and Musgrave, M.E. (2000), "Pollination and Embryo Development in Brassica rapa L. in Microgravity", *International Journal of Plant Sciences*, Vol. 161 No. 2, pp. 203–211.

Kurmazenko, E.A., Fomichev, A.A. and Dokunin, I.V. (1992), "Functions simulation model of integrated regenerable life support system", paper presented at 22nd International Conference on Environmental Systems, Seattle, Washington.

Lane, H.W. (2002), "Introduction overview of the report", in Lane, H.W., Sauer, R.L. and Feeback, D.L. (Eds.), *Isolation: NASA experiments in closed-environment living advanced human life support enclosed system final report*, *Science and technology series*, Published for the American Astronautical Society by Univelt, San Diego, Calif.

Lasseur, C., Brunet, J., de Weever, H., Dixon, M., Dussap, G., Godia, F., Leys, N., Mergeay, M. and Van Der Straeten, D. (2010), "MELiSSA: The European Project of Closed Life Support System", *Gravitational and Space Biology*, Vol. 23 No. 2, pp. 3–12.

Lasseur, C., Dixon, M., Dubertret, G., Dussap, G., Godia, F., Gros, J.B., Mergeay, M., Richalet, J. and Verstraete, W. (2000), "MELISSA: 10 years of Research, Results, Status and Perspectives", paper presented at 30th International Conference on Environmental Systems, Toulouse, France.

Lasseur, C., Paillé, C., Lamaze, B., Rebeyre, P., Rodriguez, A., Ordonez, L. and Marty, F. (2005), "MELISSA: Overview of the Project and Perspectives", paper presented at 35th International Conference on Environmental Systems, Rome, Italy.

Lasseur, C.h., Verstraete, W., Gros, J.B., Dubertret, G. and Rogalla, F. (1996), "MELISSA: a potential experiment for a precursor mission to the Moon", *Advances in space research the official journal of the Committee on Space Research (COSPAR)*, Vol. 18 No. 11, pp. 111–117.

Levine, H., Cox, D., Reed, D., Mortenson, T., Shellack, J., Wells, H., Murdoch, T., Regan, M., Albino, S. and Cohen, J. (2009), "The Advanced Biological Research System (ABRS): A

Single Middeck Payload for Conducting Biological Experimentation on the International Space Station", paper presented at 47th AIAA Aerospace Sciences Meeting including The New Horizons Forum and Aerospace Exposition, 5-8 January, Orlando, Florida.

Levri, J.A., Fisher, J.W., Jones, H.W., Drysdale, A.E., Ewert, M.K., Hanford, A.J., Hogan, J.A., Joshi, J.A. and Vaccari, D.A. (2003), "Advanced Life Support Equivalent System Mass Guidelines Document", *NASA*, No. NASA/TM-2003-212278.

Link, B.M., Durst, S.J., Zhou, W. and Stankovic, B. (2003), "Seed-to-seed growth of Arabidopsis Thaliana on the international space station", *Advances in Space Research*, Vol. 31 No. 10, pp. 2237–2243.

MacElroy, R.D. and Averner, M.M. (1978), *Space Ecosynthesis: An approach to the design of closed ecosystems for use in space* No. NASA-TM-78491, NASA.

Manders, E., Bell, S., Biswas, G. and Kortenkamp, D. (2005), "Multi-Scale Modeling of Advanced Life Support Systems", paper presented at 35th International Conference on Environmental Systems, Rome, Italy.

Marino, B.D., Mahato, T.R., Druitt, J.W., Leigh, L., Lin, G., Russell, R.M. and Tubiello, F.N. (1999), "The agricultural biome of Biosphere 2", *Ecological Engineering*, Vol. 13 No. 1-4, pp. 199–234.

Massa, G.D., Newsham, G., Hummerick, M.E., Caro, J.L., Stutte, G.W., Morrow, R.C. and Wheeler, R.M. (2013), "Preliminary species and media selection for the VEGGIE space hardware", *Gravitational and Space Research*, Vol. 1 No. 1, pp. 95–106.

Masuda, T. (2007), "Food supplies for habitation experiments in an Earth-based advanced life support system", *World of Food Science*, Vol. 2.

McArdle, W.D., Katch, F.I. and Katch, V.L. (2014), *Exercise physiology: Nutrition, energy, and human performance,* Eighth edition.

McGlothlin, E.P., Yeh, H.Y. and Lin, C.H. (1999), "Development of the ECLSS Sizing Analysis Tool and ARS Mass Balance Model Using Microsoft Excel", paper presented at 29th International Conference on Environmental Systems, Denver, Colorado.

Meadows, D.H. (1972), *The Limits to growth;: A report for the Club of Rome's project on the predicament of mankind, Potomac Associates books*, Universe Books, New York.

Meadows, D.H. and Wright, D. (2008), *Thinking in systems: A primer*, Chelsea Green Pub., White River Junction, Vt.

Messerschmid, E. and Bertrand, R. (1999), *Space stations: Systems and utilization*, Springer, Berlin, New York.

Mitchell, C.A. (1994), "Bioregenerative life-support systems", *American Journal of Clinical Nutrition*, Vol. 60, pp. 820–824.

Miyajima, H. (2009), "Development of Simulation Tool for Life Support System Design Based on the Interaction model", paper presented at 39th International Conference on Environmental Systems, Savannah, Georgia.

Morrow, R.C., Bula, R.J., Tibbitts, T.W. and Dinauer, W.R. (1994), "The ASTROCULTURE flight experiment series, validating technologies for growing plants in space", *Advances in Space Research*, Vol. 14 No. 11, pp. 29–37.

Morrow, R.C., Dinauer, W.R., Bula, R.J. and Tibbitts, T.W. (1993), "The Astroculture™-1 Flight Experiment: Pressure Control of the WCSAR Porous Tube Nutrient Delivery System", paper presented at 23rd International Conference on Environmental Systems, Colorado Springs, Colorado.

References

Morrow, R.C., Iverson, J.T., Manzke, R.C., Tuominen, L.K. and Neubaer, J.D. (2007), "Education Payload Operation Kit C: A Miniature, Low ESM Hobby Garden for Space-Based Educational Activities", paper presented at 37th International Conference on Environmental Systems, Chicago, Illinois.

Morrow, R.C., Remiker, R.W., Mischnick, M.J., Tuominen, L.K., Lee, M.C. and Crabb, T.M. (2005), "A Low Equivalent System Mass Plant Growth Unit for Space Exploration", paper presented at 35th International Conference on Environmental Systems, Rome, Italy.

Musgrave, M.E. and Kuang, A. (2003), "Plant Reproductive Development during Spaceflight", in *Developmental Biology Research in Space*, *Advances in Space Biology and Medicine*, Vol. 9, Elsevier, pp. 1–23.

Musgrave, M.E., Kuang, A. and Porterfield, D.M. (1997), "Plant reproduction in spaceflight environments", *Gravit Space Biol Bull.*, Vol. 10 No. 2, pp. 83–90.

NASA (1998), "NASA Advanced life support program memorandum".

NASA (2014), "Portable Astroculture Chamber (PASC)", available at: http://www.nasa.gov/mission_pages/station/research/experiments/372.html (accessed 5 February 2014).

NASA Kennedy Space Center (2015), "Veggies in Space: Astronauts Sample Freshly Grown Lettuce", available at: https://www.youtube.com/watch?v=D_723qwjULM (accessed 11 August 2015).

Nitta, K. (1999), "Basic design concept of Closed Ecology Experiment Facilities", *Advances in Space Research*, Vol. 24 No. 3, pp. 343–350.

Nitta, K. (2005), "The Mini-Earth facility and present status of habitation experiment program", *Advances in Space Research*, Vol. 35 No. 9, pp. 1531–1538.

Olthoff, C. (2017), "Validation of the Virtual Spacesuit Using Apollo 15 Data", paper presented at 47th International Conference on Environmental Systems, Charleston, South Carolina.

Olthoff, C., Schnaitmann, J., Bender, F., Koch, V. and Weber, J. (2015), "Development Status of the Thermal Layer of the Dynamic Life Support System Simulation V-HAB", paper presented at 45th International Conference on Environmental Systems, 12-16 July, Bellevue, Washington.

Olthoff, C., Schnaitmann, J. and Zhukov, A. (2014), "Development Status of the Dynamic Life Support System Simulation V-HAB", paper presented at 44th International Conference on Environmental Systems, Tucson, Arizona.

Osburg, J., Bertrand, R. and Messerschmid, E. (1998), "MELISSA - A Graphical Environment for Life-Support Systems Simulation", paper presented at 28th International Conference on Environmental Systems, Danvers, Massachusetts.

Patterson, R.L., Giacomelli, G.A., Kacira, M., Sadler, P.D. and Wheeler, R.M. (2012), "Description, operation and production of the South Pole Food Growth Chamber", *Acta Horticulturae*, No. 952, pp. 589–596.

Patterson, R.L., Giacomelli, G.A. and Sadler, P.D. (2008), "Resource and production model for the South Pole Food Growth Chamber", paper presented at 38th International Conference on Environmental Systems, San Francisco, California.

Paul, A.-L., Amalfitano, C.E. and Ferl, R.J. (2012), "Plant growth strategies are remodeled by spaceflight", *BMC Plant Biology*, Vol. 12 No. 1, p. 232.

Paul, A.-L., Wheeler, R.M., Levine, H.G. and Ferl, R.J. (2013a), "Fundamental Plant Biology Enabled by The Space Shuttle", *American Journal of Botany*, Vol. 100 No. 1, pp. 226–234.

Paul, A.-L., Zupanska, A.K., Schultz, E.R. and Ferl, R.J. (2013b), "Organ-specific remodeling of the Arabidopsis transcriptome in response to spaceflight", *BMC Plant Biology*, Vol. 13 No. 1, p. 112.

Pérez Vara, R., Mannu, S., Pin, O. and Müller, R. (2003), "Overview of European Applications of EcosimPro to ECLSS, CELASS and ATCS", paper presented at 33rd International Conference on Environmental Systems, Vancouver, Canada.

Pilgrim, A.J. and Johnson, S.P. (1962), *Investigation of selected higher plants as ags exchange mechanisms for closed ecological systems* No. AD0296950 (accessed http://oai.dtic.mil/oai/oai?verb=getRecord&metadataPrefix=html&identifier=AD0296950).

Porterfield, D.M., Neichitailo, G.S., Mashinski, A.L. and Musgrave, M.E. (2003), "Spaceflight hardware for conducting plant growth experiments in space: The early years 1960–2000", *Advances in Space Research*, Vol. 31 No. 1, pp. 183–193.

Poulet, L., Schubert, D., Zeidler, C. and Maiwald, V. (2013), *Technical note 104.1 - Greenhouse module requirements document*, DLR, Bremen, Germany.

Preu, P. and Braun, M. (2014), "German SIMBOX on Chinese mission Shenzhou-8: Europe's first bilateral cooperation utilizing China's Shenzhou programme", *Acta Astronautica*, Vol. 94 No. 2, pp. 584–591.

Pütz, D. (2017), "Analysis of the Impacts the Humidity Released by ACLS has on Other Systems and Crew Time Using V-HAB", paper presented at 47th International Conference on Environmental Systems, Charleston, South Carolina.

Pütz, D., Olthoff, C., Ewert, M.K. and Anderson, M.S. (2016), "Assessment of the Impacts of ACLS on the ISS Life Support System usind Dynamic Simulations in V-HAB", paper presented at 46th International Conference on Environmental Systems, 10-14 July, Vienna, Austria.

Rehrer, N.J. and Burke, L.M. (1996), "Sweat losses during various sports", *Australian Journal of Nutrition & Dietetics*, Vol. 53, pp. 13–16.

Robinson, W.A. (2001), *Modeling Dynamic Climate Systems, Modeling Dynamic Systems*, Springer New York, New York, NY.

Rodriguez, L.F., Jiang, H., Bell, S. and Kortenkamp, D. (2007), "Testing Heuristic Tools for Life Support Sytem Analysis", paper presented at 37th International Conference on Environmental Systems, Chicago, Illinois.

Rodriguez, L.F., Kang, S. and Ting, K.C. (2003), "Top-level modeling of an als system utilizing object-oriented techniques", *Advances in Space Research*, Vol. 31 No. 7, pp. 1811–1822.

Ross, C.W. (1992a), "Mineral Nutrition", in Salisbury, F.B. and Ross, C.W. (Eds.), *Plant physiology*, 4th ed, Wadsworth Pub. Co., Belmont, Calif.

Ross, C.W. (1992b), "Photosynthesis: Chloroplasts and light", in Salisbury, F.B. and Ross, C.W. (Eds.), *Plant physiology*, 4th ed, Wadsworth Pub. Co., Belmont, Calif.

Rudokas, M.R., Cantwell, E.R., Robinson, P.I. and Shenk, T.W. (1989), "DAWN (Design Assistant Workstation) for advanced physical-chemical life support systems", paper presented at 19th Intersociety Conference on Environmental Systems, San Diego, California.

References

Rueda, A., Avezuela, R., Cobas, P. and Pérez-Vara, R. (2010), "New features of EcosimPro 4.6 for the modeling and simulation of ECLSSs and LHPs", paper presented at 40th International Conference on Environmental Systems, Barcelona, Spain.

Rummel, J.D. and Volk, T. (1987), "A modular BLSS simulation model", *Advances in Space Research*, Vol. 7 No. 4, pp. 59–67.

Ruth, M. and Hannon, B.M. (2012), *Modeling dynamic economic systems, Modeling Dynamic Systems,* 2nd ed, Springer, New York.

Sadler, P., Giacomelli, G., Furfaro, R., Patterson, R. and Kacira, M. (2009), "Prototype BLSS Lunar Greenhouse", paper presented at 39th International Conference on Environmental Systems, Savannah, Georgia.

Sadler, P., Patterson, R., Boscheri, G., Kacira, M., Furfaro, R., Lobascio, C., Lamantea, M., Pirolli, M., Rossignoli, S., Grizzaffi, L., DePascale, S. and Giacomelli, G. (2011), "Bio-regenerative Life Support Systems for Space Surface Applications", paper presented at 41st International Conference on Environmental Systems, 17-21 July, Portland, Oregon.

Sager, J.C. and Mc Farlane, J.C. (1997), "Radiation", in Langhans, R.W. and Tibbitts, T.W. (Eds.), *Plant Growth Chamber Handbook*, Iowa State University of Science and Technology.

Salisbury, F.B. (1992a), "Growth and Development", in Salisbury, F.B. and Ross, C.W. (Eds.), *Plant physiology*, 4th ed, Wadsworth Pub. Co., Belmont, Calif.

Salisbury, F.B. (1992b), "Growth responses to temperature", in Salisbury, F.B. and Ross, C.W. (Eds.), *Plant physiology*, 4th ed, Wadsworth Pub. Co., Belmont, Calif.

Salisbury, F.B. (1992c), "Photosynthesis: Environmental and agricultural aspects", in Salisbury, F.B. and Ross, C.W. (Eds.), *Plant physiology*, 4th ed, Wadsworth Pub. Co., Belmont, Calif.

Salisbury, F.B., Campbell, W.F., Carman, J.G., Bingham, G.E., Bubenheim, D.L., Yendler, B., Sytchev, V., Levinskikh, M.A., Ivanova, I., Chernova, L. and Podolsky, I. (2003), "Plant growth during the greenhouse II experiment on the Mir orbital station", *Advances in Space Research*, Vol. 31 No. 1, pp. 221–227.

Salisbury, F.B. and Clark, M.A. (1996), "Choosing plants to be grown in a Controlled Environment Life Support System (CELSS) based upon attractive vegetarian diets", *Life Support Biosphere Science*, Vol. 2, pp. 169–179.

Salisbury, F.B., Gitelson, I.I. and Lisovsky, G.M. (1997), "Bios-3: Siberian experiments in bioregenerative life support", *Bioscience*, Vol. 47 No. 9, pp. 575–585.

Schnaitmann, J. and Olthoff, C. (2017), "Validation and Use Cases for the new Thermal Layer of the V-HAB Crew Model", paper presented at 47th International Conference on Environmental Systems, Charleston, South Carolina.

Schnaitmann, J., Portner, B., Haber, R. and Sakurai, M. (2015), "Using V-HAB to Model and Simulate Air Revitalization System Technologies Developed at JAXA", paper presented at 45th International Conference on Environmental Systems, 12-16 July, Bellevue, Washington.

Schnaitmann, J. and Weber, J.P. (2016), "A New Human Thermal Model for the Dynamic Life Support System Simulation V-HAB", paper presented at 46th International Conference on Environmental Systems, 10-14 July, Vienna, Austria.

Schubert, D., Quantius, D., Hauslage, J., Glasgow, L., Schröder, F. and Dorn, M. (2011), "Advanced Greenhouse Modules for use within Planetary Habitats", paper presented at 41st International Conference on Environmental Systems, 17-21 July, Portland, Oregon.

References

Schubert, F.H., Wynveen, R.A. and Quattrone, P.D. (1984), "Advanced regenerative environmental control and life support systems: air and water regeneration", *Advances in space research the official journal of the Committee on Space Research (COSPAR)*, Vol. 4 No. 12, pp. 279–288.

Schwartzkopf, S.H. and Cobb, M.N. (1990), "A Software Toolkit for Life Support System Simulation Modelling", paper presented at 20th International Conference on Environmental Systems, Williamsburg, Virginia.

Scott, J.W., Harbaugh, B.K. and Baldwin, E.A. (2000), "'Micro-Tina' and 'Micro-Gemma' Miniature Dwarf Tomatoes", *HortScience*, Vol. 35 No. 4, pp. 774–775.

Seshan, P.K., Ferral, J. and Rohatgl, N. (1989), "Human Life Support During Interplanetary Travel and Domicile Part I: System Approach", paper presented at 19th Intersociety Conference on Environmental Systems, San Diego, California.

Seshan, P.K., Ferral, J. and Rohatgl, N. (1991), "Human Life Support During Interplanetary Travel and Domicile - Part II: Generic Modular Flor Schematic Modeling", paper presented at 21st International Conference on Environmental Systems, San Fransisco, California.

Simion, V., Champeanu, G., Vasile, G. and Artimon, M. (2008), "Nitrate and nitrite accumulation in tomatoes and derived products", *Roumanian Biotechnological Letters*, Vol. 13 No. 4, pp. 3785–3790.

Solheim, B. (2009), "3D information from 2D images recorded in the European Modular Cultivation System on the ISS", *Advances in Space Research*, Vol. 44 No. 12, pp. 1382–1391.

Spaceref (2012), "NASA KSC Award: Payload Integration and Operational Support Services Advanced Plant Habitat", available at: http://www.spaceref.com/news/viewsr.html?pid=40076 (accessed 1 February 2014).

Stadler, J.J. and Brideau, L.D. (2004), "Human Factors and Maintainability in the Plant Research Unit (PRU)", paper presented at 34th International Conference on Environmental Systems, Colorado Springs, Colorado.

Stadler, J.J., Brideau, L.D., Emmerich, J.C. and Varma, N.N. (2004), "Integrating Reliability Principles in the Design of the Plant Research Unit (PRU)", paper presented at 34th International Conference on Environmental Systems, Colorado Springs, Colorado.

Stahr, J.D., Auslander, D.M., Spear, R.C. and Young, G.E. (1982), "An Approach to the Preliminary Evaluation of Closed Ecological Life Support System (CELSS) Scenarios and Control Strategies", *NASA*, Vol. 166368.

Stromberg, J. (2014), "NASA is about to harvest lettuce on the International Space Station", available at: http://www.vox.com/2014/6/3/5772628/nasa-is-about-to-harvest-lettuce-on-the-international-space-station (accessed 4 June 2014).

Stutte, G., Wheeler, R., Morrow, R. and Newsham, G. (2011a), "Concept for Sustained Plant Production on ISS Using VEGGIE Capillary Mat Rooting System", paper presented at 41st International Conference on Environmental Systems, 17-21 July, Portland, Oregon.

Stutte, G., Wheeler, R., Morrow, R. and Newsham, G. (2011b), "Operational Evaluation of VEGGIE Food Production System in the Habitat Demonstration Unit", paper presented at 41st International Conference on Environmental Systems, 17-21 July, Portland, Oregon.

Stutte, G.W., Monje, O., Goins, G.D. and Tripathy, B.C. (2005), "Microgravity effects on thylakoid, single leaf, and whole canopy photosynthesis of dwarf wheat", *Planta*, Vol. 223 No. 1, pp. 46–56.

References

Suzuki, S., Tazawa, R., Uchida, T. and Sirko, R.J. (1994), "Regenerative Life Support Systems: Modeling, Analysis and Laboratory Development", paper presented at 24th International Conference on Environmental Systems, Friedrichshafen, Germany.

Sychev, V.N., Levinskikh, M.A., Gostimsky, S.A., Bingham, G.E. and Podolsky, I.G. (2007), "Spaceflight effects on consecutive generations of peas grown onboard the Russian segment of the International Space Station", *Acta Astronautica*, Vol. 60 No. 4-7, pp. 426–432.

Sysoeva, M.I., Markovskaya, E.F. and Shibaeva, T.G. (2010), "Plants under Continuous Light: A Review", *Plant Stress*, Vol. 4, pp. 5–17.

Taiz, L. and Zeiger, E. (Eds.) (2010), *Plant physiology,* 5th ed, Sinauer Associates, Sunderland, MA.

Tako, Y., Tsuga, S., Tani, T., Arai, R., Komatsubara, O. and Shinohara, M. (2008), "One-week habitation of two humans in an airtight facility with two goats and 23 crops – Analysis of carbon, oxygen, and water circulation", *Advances in Space Research*, Vol. 41 No. 5, pp. 714–724.

Tibbits, T.W. and Alford, D.K. (1982), *Controlled ecological life support system: Use of higher plants* No. NASA-CP-2231, NASA.

Turner, M., Lomax, P., Kelly, A., Porter, R., Cobb, M. and Heathcote, D. (1995), "Development of the Plant Research Unit for Use on Space Station", paper presented at 25th International Conference on Environmental Systems, San Diego, California.

Velez-Ramirez, A.I., van Ieperen, W., Vreugdenhil, D. and Millenaar, F.F. (2011), "Plants under continuous light", *Trends in Plant Science*, Vol. 16 No. 6, pp. 310–318.

Villareal, J. and Tri, T. (2001), "Bioregenerative Planetary Life Support Systems Test Complex (BIO-Plex): Progress to Date", paper presented at 31st International Conference on Environmental Systems, Orlando, Florida.

Volk, T., Bugbee, B. and Wheeler, R. (1995), "An approach to crop modeling with the energy cascade", *Life Support and Biosphere Science*, Vol. 1, pp. 119–127.

Vrakking, V., Bamsey, M., Zabel, P., Zeidler, C., Schubert, D. and Romberg, O. (2017), "Service Section Design of the EDEN ISS Project", paper presented at 47th International Conference on Environmental Systems, 16-20 July, Charleston, South Carolina.

Waters, G.C., Olabi, A., Hunter, J.B., Dixon, M. and Lasseur, C. (2002), "Bioregenerative food system cost based on optimized menus for advanced life support", *Life Support Biosphere Science*, Vol. 8 No. 3-4, pp. 199–210.

Weber, J. and Schnaitmann, J. (2016), "A New Human Thermal Model for the Dynamic Life Support System Simulation V-HAB", paper presented at 46th International Conference on Environmental Systems, 10-14 July, Vienna, Austria.

Wheeler, R.M. (2004a), "Horticulture for Mars", *Acta Horticulturae (ISHS)*, Vol. 642, pp. 201–215.

Wheeler, R.M. (2004b), "Horticulture for Mars", *Acta Horticulturae (ISHS)*, Vol. 642, pp. 201–215.

Wheeler, R.M. (2012), "NASA advanced life support technology testing and development", paper presented at Agrospace Conference, May, Sperlonga, Italy.

Wheeler, R.M., Mackowiak, C.L., Stutte, G.W., Sager, J.C., Yorio, N.C., Ruffe, L.M., Fortson, R.E., Dreschel, T.W., Knott, W.M. and Corey, K.A. (1996), "NASA's biomass production chamber: A testbed for bioregenerative life support studies", *Advances in Space Research*, Vol. 18 No. 4-5, pp. 215–224.

Wheeler, R.M., Sager, J.C., Prince, R.P., Knott, W.M., Mackowiak, C.L., Stutte, G.W., Yorio, N.C., Ruffe, L.M., Peterson, B.V., Goins, G.D., Hinkle, C.R. and Berry, W.L. (2003), *Crop Production for Advanced Life Support Systems: Observations From the Kennedy* No. NASA/TM-2003-211184, NASA.

Wieland, P.O. (1994), *Designing for human presence in space: An introduction to environmental control and life support systems*, NASA.

Williams, D.R. (2002), "Isolation and integrated testing: An introduction to the Lunar-Mars life support test project", in Lane, H.W., Sauer, R.L. and Feeback, D.L. (Eds.), *Isolation: NASA experiments in closed-environment living advanced human life support enclosed system final report*, *Science and technology series*, Published for the American Astronautical Society by Univelt, San Diego, Calif.

Wydeven, T. (1988), "A survey of some regenerative physico-chemical life support technology", *NASA*, No. TM 101004.

Yano, S., Kasahara, H., Masuda, D., Tanigaki, F., Shimazu, T., Suzuki, H., Karahara, I., Soga, K., Hoson, T., Tayama, I., Tsuchiya, Y. and Kamisaka, S. (2013), "Improvements in and actual performance of the Plant Experiment Unit onboard Kibo, the Japanese experiment module on the international space station", *Advances in Space Research*, Vol. 51 No. 5, pp. 780–788.

Yeh, H., Brown, C., Anderson, M., Ewert, M.K. and Jeng, F. (2009), "ALSSAT Development Status", paper presented at 39th International Conference on Environmental Systems, Savannah, Georgia.

Yeh, H., Brown, C., Jeng, F., Lin, C. and Ewert, M.K. (2004), "ALSSAT Development Status and its Applications in Trade Studies", paper presented at 34th International Conference on Environmental Systems, Colorado Springs, Colorado.

Yeh, H., Jeng, F., Brown, C., Lin, C. and Ewert, M.K. (2001), "Advanced Life Support Sizing Analysis Tool (ALSSAT) Using Microsoft® Excel", paper presented at 31st International Conference on Environmental Systems, Orlando, Florida.

Zabel, P., Bamsey, M., Schubert, D. and Tajmar, M. (2016a), "Review and analysis of over 40 years of space plant growth systems", *Life sciences in space research*, Vol. 10, pp. 1–16.

Zabel, P., Bamsey, M., Zeidler, C., Vrakking, V., Johannes, B.-W., Rettberg, P., Schubert, D., Romberg, O., Imhof, B., Davenport, R., Hoheneder, W., Waclavicek, R., Gilbert, C., Hogle, M., Battistelli, A., Stefanoni, W., Moscatello, S., Proietti, S., Santi, G., Nazzaro, F., Fratianni, F., Coppola, R., Dixon, M., Stasiak, M., Kohlberg, E., Mengedoht, D., Bucchieri, L., Mazzoleni, E., Fetter, V., Hummel, T., Boscheri, G., Massobrio, F., Lamantea, M., Lobascio, C., Petrini, A., Adami, M., Bonzano, G., Fiore, L., Dueck, T., Stanghellini, C., Bochenek, G., Gilley, A., McKeon-Bennett, M., Stutte, G., Larkin, T., Moane, S., Murray, P., Downey, P., Fortezza, R. and Ceriello, A. (2015), "Introducing EDEN ISS - A European project on advacing plant cultivation technologies and operations", paper presented at 45th International Conference on Environmental Systems, 12-16 July, Bellevue, Washington.

Zabel, P., Bamsey, M., Zeidler, C., Vrakking, V., Schubert, D. and Romberg, O. (2017), "Future Exploration Greenhouse Design of the EDEN ISS Project", paper presented at 47th International Conference on Environmental Systems, 16-20 July, Charleston, South Carolina.

References

Zabel, P., Bamsey, M., Zeidler, C., Vrakking, V., Schubert, D., Romberg, O., Boscheri, G. and Dueck, T. (2016b), "The preliminary design of the EDEN ISS Mobile Test Facility - An Antarctic greenhouse", paper presented at 46th International Conference on Environmental Systems, 10-14 July, Vienna, Austria.

Zamrik, M.A. (2013), "Determination of nitrate and nitrite contents in tomato and processed tomato products in Syrian market", *Int. J. Pharm. Sci. Rev. Res.*, Vol. 19 No. 1, pp. 1–5.

Zhou, W. (2005), "Advanced ASTROCULTURE™ Plant Growth Unit: Capabilities and Performances", paper presented at 35th International Conference on Environmental Systems, Rome, Italy.

Zhou, W., Duffie, N.A. and Mookherjee, B. (2000), "Performance of the ASTROCULTURE™ Plant Growth Unit (ASC-8) During the STS-95 Mission", paper presented at 30th International Conference on Environmental Systems, Toulouse, France.

Zhou, W., Durst, S.J., Demars, M., Stankovic, B., Link, B.M., Tellez, G., Meyers, R.A., Sandstrom, P.W. and Abba, J.R. (2002), "Performance of the Advanced ASTROCULTURE™ Plant Growth Unit During ISS-6A/7A Mission", paper presented at 32nd International Conference on Environmental Systems, San Antonio, Texas.

8 Appendix A - Past and Present Life Support Modelling Efforts

The following table shows past and presents life support modelling and simulation efforts. The table is based on the extensive literature review done by Jones (2017). The model developed in this dissertation is not part of the list.

#	Reference(s)	Location/	Name	Notes
1	(Averner, 1981)	NASA ARC		Plants
2	(Stahr *et al.*, 1982; Babcock *et al.*, 1984)	UC Berkeley NSCORT		Plants, control strategies, failures
3	(Rummel and Volk, 1987)	NASA ARC	BLSS model	Bio-regenerative life support
4	(Cullingford, 1989)	NASA JPL	CELSS emulator	Plants
5	(Rudokas *et al.*, 1989)	NASA ARC	DAWN	Physical-chemical life support, expert systems
6	(Bacskay and Knox, 1989)	NASA MFSC		ISS air system
7	(Seshan *et al.*, 1989; Ferral *et al.*, 1995; Seshan *et al.*, 1991)	NASA JPL	LISSA	Mass, power, open loop versus regenerative
8	(Schwartzkopf and Cobb, 1990)	Lockheed		Life support system design
9	(Gustavino *et al.*, 1990)	McDonnell Douglas		Lunar base
10	(Kolodney *et al.*, 1991)	NASA JSC		Plants and air system
11	(Kurmazenko *et al.*, 1992)	NIICHIMMASH, Moscow	IRLSS model	Regenerable life support
12	(Drysdale *et al.*, 1992; Drysdale, 1997)	NASA KSC	OCAM	Object-oriented CELSS Analysis and Modeling
13	(DaLee and Lee, 1993)	McDonnell Douglas		Expert system ECLSS trade tool
14	(Suzuki *et al.*, 1994)	McDonnell Douglas, SHIMIZU		Model for system analysis
15	(Osburg *et al.*, 1998)	ESA	MELiSSA	Graphical simulation
16	(Finn, 1999; Jones *et al.*, 2001)	NASA ARC		Dynamic models, trade studies
17	(Fleischer *et al.*, 1999; Goudarzi and Ting, 1999; Rodriguez *et al.*, 2003)	Rutgers NSCORT	BPM	Object oriented biomass production simulation
18	(McGlothlin *et al.*, 1999; Yeh *et al.*, 2004; Yeh *et al.*, 2009; Yeh *et al.*, 2001)	NASA JSC	ALSSAT	Static, system sizing, launch mass
19	(Pérez Vara *et al.*, 2003; Rueda *et al.*, 2010)	ESA	EcosimPro	Object oriented, differential equation, multidisciplinary model
20	(Kortenkamp and Bell, 2003; Manders *et al.*, 2005; Rodriguez *et al.*, 2007)	NASA JSC	BioSim	Multi scale continuous-discrete model, controls
21	(Aydogan *et al.*, 2004; Aydogan-Cremaschi *et al.*, 2009)	Purdue NSCORT	SIMOPT	Simulation with deterministic optimization

22	(Arai *et al.*, 2008)	MIT		Educational
23	(Miyajima, 2009)	Tokyo Jogakkan college		Designer-tool interaction
24	(Czupalla *et al.*, 2010; Czupalla *et al.*, 2011; Pütz *et al.*, 2016; Schnaitmann and Weber, 2016)	Technical University of Munich	V-Hab	Dynamic multi-level mission simulation
25*	(Detrell *et al.*, 2016; Detrell and Belz, 2017)	University of Stuttgart	ELISSA	Reliability analysis
26	(Allada *et al.*, 2011)	NASA JSC		Processor simulations
27**	(Boscheri *et al.*, 2017a)	TASI, DLR, Technical University of Munich, EnginSoft (ESA contract)	SCALISS	Scaling of life support systems, static, launch mass
28	(Do *et al.*, 2015)	MIT	HabNet	Habitation, supportability, failures, spares
29	(Chambliss *et al.*, 2015; Chambliss *et al.*, 2016)	NASA JSC		Water tracking model

*An additional reference was added to line 25.

**Line 27 has been updated, because the information in the original reference was not fully correct.

9 Appendix B - Mathematical Model Formulas

The following subchapters display in detail all mathematical formulas implemented in the model described in previous chapters.

For each variable the variable type (e.g. stock, flow), the formula or value and the unit are given in the following tables.

The values given for stock variables indicate the initial value of the stock.

Orange marked variables are constants. Blue marked variables indicate flexible inputs. Those are inputs which are simulation scenario specific. Green marked variables are constant inputs. Those are variables which have a constant value based on literature review, but can be adjusted for a specific simulation scenario when necessary. Variables that are not highlighted indicate calculations.

9.1   Gases Layer Formulas

9.1.1 GL Core Formulas

Variable Name	Variable Type	Formula/value	Unit
O2 Storage	Stock	400 (example)	kg
O2 supply from storage	Flow	IF TIME=STARTTIME THEN habitat_O2_mass_requirement[nominal]/DT ELSE IF O2_transfer_from_greenhouse=0 THEN IF O2_in_Habitat<habitat_O2_mass_requirement[nominal] THEN crew_O2_consumption ELSE 0 ELSE 0	kg/d
O2 in Habitat	Stock	0	kg
O2 transfer from greenhouse	Flow	Physical_Chemical_Systems.O2_separator_activity* Physical_Chemical_Systems.O2_separator_capacity	kg/d
O2 in Greenhouse	Stock	0	kg
O2 transfer to storage	Bi-Flow	IF TIME=STARTTIME THEN greenhouse_O2_mass_requirement[nominal]*(-1)/DT ELSE IF (O2_transfer_from_greenhouse=0 AND O2_in_Greenhouse>greenhouse_O2_mass_requirement[nominal]) THEN Physical_Chemical_Systems.O2_separator_capacity ELSE 0	kg/d
CO2 Storage	Stock	250 (example)	kg
CO2 supply from storage	Flow	IF TIME=STARTTIME THEN greenhouse_CO2_mass_requirement[nominal]/DT ELSE IF CO2_transfer_to_greenhouse=0 THEN IF CO2_in_Greenhouse<greenhouse_CO2_mass_requirement[nominal] THEN greenhouse_CO2_consumption ELSE 0 ELSE 0	kg/d
CO2 in Greenhouse	Stock	0	kg
CO2 transfer to greenhouse	Flow	Physical_Chemical_Systems.CO2_separator_activity* Physical_Chemical_Systems.CO2_separator_capacity	kg/d
CO2 in Habitat	Stock	0	kg
CO2 transfer to storage	Flow	IF (CO2_transfer_to_greenhouse=0 AND CO2_in_Habitat>=habitat_CO2_mass_requirement[maximum]) THEN Physical_Chemical_Systems.CO2_separator_capacity ELSE 0	kg/d

9.1.2 GL Crew Formulas

Variable Name	Variable Type	Formula/value	Unit
habitat O2 partial	Converter,	See Table 9-1 for values.	kPa

pressure requirement	arrayed		
O2 density at 1 atm	Converter	1.331	kg/m^3
habitat nominal pressure	Converter	101.325	kPa
habitat volume per CM	Converter	150 (example)	m^3/people
habitat pressurized volume	Converter	habitat_volume_per_CM*Crew_composition.total_CM_number	m^3
habitat O2 mass requirement	Converter, arrayed	(habitat_O2_partial_pressure_requirement[min_nom_max]/habitat_nominal_pressure)*(habitat_pressurized_volume*O2_density_at_1_atm)	kg
crew O2 consumption	Flow	Solids_Layer.carbon_in_consumed_food*C_to_CO2_mass_converter/O2_to_CO2_mass_converter/Solids_Layer.RQ	kg/d
crew CO2 production	Flow	Solids_Layer.carbon_in_consumed_food*C_to_CO2_mass_converter	kg/d
O2 to CO2 mass converter	Converter	44.0095/31.9988	-
CO2 density at 1 atm	Converter	1.842	kg/m^3
habitat CO2 partial pressure requirement	Converter, arrayed	See Table 9-1 for values.	kPa
habitat CO2 mass requirement	Converter, arrayed	(habitat_CO2_partial_pressure_requirement[min_nom_max]/habitat_nominal_pressure)*(habitat_pressurized_volume*CO2_density_at_1_atm)	kg

Table 9-1: Habitat partial pressure requirements.

	Oxygen	Carbon dioxide
minimum	18	0.031
nominal	21	0.4
maximum	23.1	0.71

9.1.3 GL Greenhouse Formulas

Variable Name	Variable Type	Formula/value	Unit
greenhouse O2 partial pressure requirement	Converter, arrayed	See Table 9-2 for values.	kPa
greenhouse volume per cultivation area	Converter	3 (example)	m^3/m^2
greenhouse pressurized volume	Converter	SUM(Greenhouse_Interface.compartment_cultivation_area[*, *])*greenhouse_volume_per_cultivation_area	m^3
greenhouse nominal pressure	Converter	101.325	kPa
greenhouse O2 mass requirement	Converter, arrayed	(greenhouse_O2_partial_pressure_requirement[min_nom_max]/greenhouse_nominal_pressure)*(greenhouse_pressurized_volume*O2_density_at_1_atm)	kg
greenhouse O2 production	Flow	Greenhouse_Interface.greenhouse_DOP	kg/d
C to CO2 mass converter	Converter	44.0095/12.0107	1
greenhouse CO2 consumption	Flow	C_to_CO2_mass_converter*Greenhouse_Interface.greenhouse_DCG	kg/d
greenhouse CO2	Converter,	See Table 9-2 for values.	kPa

partial pressure requirement	arrayed		
greenhouse CO2 mass requirement	Converter, arrayed	(greenhouse_CO2_partial_pressure_requirement[min_nom_max]/greenhouse_nominal_pressure)*(greenhouse_pressurized_volume*CO2_density_at_1_atm)	kg

Table 9-2: Greenhouse partial pressure requirements.

	Oxygen	Carbon dioxide
minimum	18	0.060795
nominal	21	0.101325
maximum	23.1	0.141855

9.1.4 GL Physical-Chemical Systems Formulas

Variable Name	Variable Type	Formula/value	Unit
O2 consumption by PC systems	Flow	Physical_Chemical_Systems.incineration_O2_consumption+SUM(Physical_Chemical_Systems.O2_consumption_by_inedible_biomass_processing[*])	kg/d
O2 production by PC systems	Flow	Physical_Chemical_Systems.electrolyzer_O2_production	kg/d
CO2 production by PC systems	Flow	Physical_Chemical_Systems.incineration_CO2_production+SUM(Physical_Chemical_Systems.CO2_production_by_inedible_biomass_processing[*])	kg/d
CO2 consumption by PC systems	Flow	IF Physical_Chemical_Systems.sabatier_activity=1 THEN Physical_Chemical_Systems.sabatier_capacity ELSE 0	kg/d
CO Storage	Stock	0	kg
CO production by PC systems	Flow	Physical_Chemical_Systems.incineration_CO_production	kg/d
CH4 Storage	Stock	0	kg
CH4 production by PC systems	Flow	Physical_Chemical_Systems.incineration_CH4_production+Physical_Chemical_Systems.sabatier_CH4_production	kg/d
H2 Storage	Stock	0	kg
H2 production by PC systems	Flow	Physical_Chemical_Systems.electrolyzer_H2_production	kg/d
H2 consumption by PC systems	Flow	Physical_Chemical_Systems.sabatier_H2_consumption	kg/d

9.1.5 GL Atmospheric Composition Conversions Formulas

Variable Name	Variable Type	Formula/value	Unit
umolmol unit converter	Converter	1	umol/mol
current O2 volume in habitat	Converter	O2_in_Habitat/O2_density_at_1_atm	m^3
current O2 percent in habitat	Converter	current_O2_volume_in_habitat/habitat_pressurized_volume*100	1
current CO2 volume in habitat	Converter	CO2_in_Habitat/CO2_density_at_1_atm	m^3
current CO2 ppm in habitat	Converter	current_CO2_volume_in_habitat/habitat_pressurized_volume*10^6*umolmol_unit_converter	umol/mol
current O2 volume in greenhouse	Converter	O2_in_Greenhouse/O2_density_at_1_atm	m^3
current O2 percent	Converter	cur-	1

Variable Name	Variable Type	Formula/value	Unit
in greenhouse		rent_O2_volume_in_greenhouse/greenhouse_pressurized_volume*100	
current CO2 volume in greenhouse	Converter	(CO2_in_Greenhouse/CO2_density_at_1_atm)	m^3
current CO2 ppm in greenhouse	Converter	(current_CO2_volume_in_greenhouse/ greenhouse_pressurized_volume)* 10^6*umolmol_unit_converter	umol/mol

9.2 Liquids Layer Formulas

9.2.1 LL Crew Formulas

Variable Name	Variable Type	Formula/value	Unit
Potable Water Storage in Habitat	Stock	1000 (example)	kg
thirst threshold	Converter	0.005	-
total potable water consumption by crew	Flow, arrayed	IF(Water_Reservoir_in_Crew[astronaut]<((1-thirst_threshold)*Crew_composition.CM_total_body_water[astronaut])) THEN ((Crew_composition.CM_total_body_water-Water_Reservoir_in_Crew)/DT) ELSE 0	kg/d
Water Reservoir in Crew	Stock, arrayed	44 (example)	kg
insensible water loss by crew	Flow, arrayed	Crew_Water_Demand.insensible_H2O_loss_over_skin[astronaut]+ Crew_Water_Demand.insensibe_H2O_loss_over_lungs[astronaut]	kg/d
sensible water loss by crew	Flow, arrayed	Crew_Water_Demand.sensible_H2O_loss_over_sweating[astronaut]	kg/d
Water in Habitat Atmosphere	Stock	0	kg
total humidity recovery habitat	Bi-Flow	IF TIME=STARTTIME THEN (habitat_atmosphere_water_content_requirement[nominal]*(-1))/DT ELSE Physical_Chemical_Systems.habitat_CHX_water_removal	kg/d
total water consumption from food by crew	Flow, arrayed	IF Crew_Mission_Profile.CM_number_active=0 THEN 0 ELSE Crew_composition.CM_parameters[astronaut, Active]* (Solids_Layer.consumption_of_greenhouse_food[Dry_Bean]/ ((1/Other_Plant_Properties.misc_plant_properties[Dry_Bean, Edible_biomass_water_content])-1)+Solids_Layer.consumption_of_greenhouse_food[Lettuce]/((1/Other_Plant_Properties.misc_plant_properties[Lettuce, Edible_biomass_water_content])-1)+Solids_Layer.consumption_of_greenhouse_food[Peanut]/((1/Other_Plant_Properties.misc_plant_properties[Peanut, Edible_biomass_water_content])-1)+Solids_Layer.consumption_of_greenhouse_food[Rice]/((1/Other_Plant_Properties.misc_plant_properties[Rice, Edible_biomass_water_content])-1)+Solids_Layer.consumption_of_greenhouse_food[Soybean]/((1/Other_Plant_Properties.misc_plant_properties[Soybean, Edible_biomass_water_content])-1)+Solids_Layer.consumption_of_greenhouse_food[Sweet_Potato]/((1/Other_Plant_Properties.misc_plant_properties[Sweet_Potato, Edible_biomass_water_content])-1)+Solids_Layer.consumption_of_greenhouse_food[Tomato]/((1/Other_Plant_Properties.misc_plant_properties[Tomato, Edible_biomass_water_content])-1)+Solids_Layer.consumption_of_greenhouse_food[Wheat]/((1/Other_Plant_Properties.misc_plant_properties[Wheat, Edible_biomass_water_content])-	kg/d

Variable Name	Variable Type	Formula/value	Unit
		1)+Solids_Layer.consumption_of_greenhouse_food[White_Potato]/((1/Other_Plant_Properties.misc_plant_properties[White_Potato, Edible_biomass_water_content])-1))/Crew_Mission_Profile.CM_number_active	
urinal wastewater production by crew	Flow, arrayed	Crew_Water_Demand.H2O_loss_over_urine[astronaut]	kg/d
fecal wastewater production by crew	Flow, arrayed	Crew_Water_Demand.H2O_loss_over_stool[astronaut]	kg/d
total hygiene water consumption by crew	Flow	Crew_Mission_Profile.CM_number_active*Misc_Crew_Parameters.CM_hygiene_H2O_demand	kg/d
crew metabolized water production	Flow, arrayed	IF Crew_Mission_Profile.CM_number_active=0 THEN 0 ELSE (Solids_Layer.carbon_in_consumed_greenhouse_food*H2O_per_C+Solids_Layer.carbon_in_consumed_resupply_food*H2O_per_C)/Crew_Mission_Profile.CM_number_active	kg/d
H2O per C	Converter	18.01528/12.0107	-
Wastewater Storage	Stock	0	kg

9.2.2 LL Greenhouse Formulas

Variable Name	Variable Type	Formula/value	Unit
Potable Water Storage in Greenhouse	Stock	100 (example)	kg
potable water transfer to greenhouse	Flow	IF Potable_Water_Storage_in_Greenhouse<potable_water_storage_in_greenhouse_lower_limit THEN (potable_water_storage_in_greenhouse_nominal_limit-Potable_Water_Storage_in_Greenhouse)/DT ELSE 0	kg/d
potable water storage in greenhouse lower limit	Converter	200 (example)	kg
potable water storage in greenhouse nominal limit	Converter	350 (example)	kg
total transpiration water production in greenhouse	Flow	Greenhouse_Interface.greenhouse_DTR	kg/d
Water in Greenhouse Atmosphere	Stock	0	kg
total humidity recovery greenhouse	Bi-Flow	IF TIME=STARTTIME THEN (greenhouse_atmosphere_water_content_requirement[nominal]*(-1))/DT ELSE (Physical_Chemical_Systems.greenhouse_CHX_water_removal)	kg/d
total water accumulating in living plant biomass	Flow, arrayed	Greenhouse_Interface.compartment_water_accumulated_per_area[compartment, cycle]	kg/d
Water Accumulated in Living Plant Biomass	Stock, arrayed	0	kg
edible biomass accumulated water harvest transfer	Flow, arrayed	IF(Crop_Scheduler.scheduler[compartment, cycle, crop_compartment]=0) THEN 0 ELSE Solids_Layer.total_edible_dry_biomass_harvest_per_compartment_per_cycle[compartment, cycle]/((1/Other_Plant_Properties.misc_plant_properties[Crop_Scheduler.scheduler[compartment, cycle, crop_compartment], Edible_biomass_water_content])-1)	kg/d
Water Accumulated	Stock	0	kg

in Harvested Edible Biomass			
inedible biomass accumulated water harvest transfer	Flow, arrayed	IF(Crop_Scheduler.scheduler[compartment, cycle, crop_compartment]=0) THEN 0 ELSE Solids_Layer.total_inedible_dry_biomass_harvest[compartment, cycle]/((1/Other_Plant_Properties.misc_plant_properties[Crop_Scheduler.scheduler[compartment, cycle, crop_compartment], Inedible_biomass_water_content])-1)	kg/d
Water Accumulated in Harvested Inedible Biomass	Stock	0	kg
wastewater production by inedible biomass	Flow	1000	kg/d
total water metabolizing into living plant biomass	Flow	Greenhouse_Interface.greenhouse_metabolizing_water	kg/d

9.2.3 LL Physical-Chemical Systems Formulas

Variable Name	Variable Type	Formula/value	Unit
water production by Sabatier	Flow	Physical_Chemical_Systems.sabatier_H2O_production	kg/d
water consumption by electrolyzer	Flow	Physical_Chemical_Systems.electrolyzer_activity*Physical_Chemical_Systems.electrolyzer_capacity	kg/d
water production by solid waste processing	Flow	Physical_Chemical_Systems.incineration_H2O_production+SUM(Physical_Chemical_Systems.H2O_production_by_inedible_biomass_processing[*])*Physical_Chemical_Systems.inedible_biomass_processor_activity	kg/d
total potable water production from wastewater recovery	Flow	Physical_Chemical_Systems.VPCAR_activity*Physical_Chemical_Systems.VPCAR_capacity	kg/d

9.2.4 LL Humidity Conversions Formulas

Variable Name	Variable Type	Formula/value	Unit
habitat nominal atmosphere temperature	Converter	293	K
water vapor pressure T 20°C	Converter	2338.54	kg/(m*s²)
habitat RH requirement	Converter, arrayed	See Table 9-3 for values.	-
water vapor specific gas constant	Converter	461.51	m²/(s²*K)
current relative humidity in habitat	Converter	Water_in_Habitat_Atmosphere* water_vapor_specific_gas_constant* habitat_nominal_atmosphere_temperature/ (Gases_Layer.habitat_pressurized_volume* water_vapor_pressure_T_20°C)	-
habitat atmosphere water content requirement	Converter, arrayed	Gases_Layer.habitat_pressurized_volume* habitat_RH_requirement[min_nom_max]* water_vapor_pressure_T_20°C/ (water_vapor_specific_gas_constant* habitat_nominal_atmosphere_temperature)	kg

greenhouse RH requirement	Converter, arrayed	See Table 9-3 for values.	-
water vapor pressure T 25°C	Converter	3169	kg/(m*s²)
greenhouse nominal atmosphere temperature	Converter	298	K
greenhouse atmosphere water content requirement	Converter, arrayed	Gases_Layer.greenhouse_pressurized_volume*greenhouse_RH_requirement[min_nom_max]*water_vapor_pressure_T_25°C/(water_vapor_specific_gas_constant*greenhouse_nominal_atmosphere_temperature)	kg
current relative humidity in greenhouse	Converter	Water_in_Greenhouse_Atmosphere*water_vapor_specific_gas_constant*greenhouse_nominal_atmosphere_temperature/(Gases_Layer.greenhouse_pressurized_volume*water_vapor_pressure_T_25°C)	-

Table 9-3: Relative humidity requirements.

	Habitat	Greenhouse
minimum	0.25	0.60
nominal	0.60	0.70
maximum	0.70	0.80

9.3 Solids Layer Formulas

9.3.1 SL Crew Food Formulas

Variable Name	Variable Type	Formula/value	Unit
Crop Food Storage	Stock, arrayed	0	kg
consumption of greenhouse food	Flow, arrayed	IF greenhouse_diet_total_kcal_per_day<Crew_Mission_Profile.total_kcal_consumption THEN greenhouse_diet_composition_total[crop] ELSE Crew_Mission_Profile.total_kcal_consumption/greenhouse_diet_total_kcal_per_day*greenhouse_diet_composition_total[crop]	kg/d
greenhouse diet composition per astronaut	Converter, arrayed	See Table 4-14 for values (example).	kg/d
greenhouse diet composition total	Converter, arrayed	(Crew_Mission_Profile.CM_active[astronaut_1]*greenhouse_diet_composition_per_astronaut[crop, astronaut_1]+ Crew_Mission_Profile.CM_active[astronaut_2]*greenhouse_diet_composition_per_astronaut[crop, astronaut_2]+ Crew_Mission_Profile.CM_active[astronaut_3]*greenhouse_diet_composition_per_astronaut[crop, astronaut_3]+ Crew_Mission_Profile.CM_active[astronaut_4]*greenhouse_diet_composition_per_astronaut[crop, astronaut_4]+ Crew_Mission_Profile.CM_active[astronaut_5]*greenhouse_diet_composition_per_astronaut[crop, astronaut_5]+ Crew_Mission_Profile.CM_active[astronaut_6]*greenhouse_diet_composition_per_astronaut[crop, astronaut_6])/people_unit_converter	kg/d
greenhouse diet total kcal per day	Converter	(greenhouse_diet_composition_total[Dry_Bean]/(1-Other_Plant_Properties.misc_plant_properties[Dry_Bean, Edible_biomass_water_content])* Other_Plant_Properties.misc_plant_properties[Dry_Bean, kcal_per_kg]+ greenhouse_diet_composition_total[Lettuce]/(1-	kcal/d

		Other_Plant_Properties.misc_plant_properties[Lettuce, Edible_biomass_water_content])* Other_Plant_Properties.misc_plant_properties[Lettuce, kcal_per_kg]+ greenhouse_diet_composition_total[Peanut]/(1- Other_Plant_Properties.misc_plant_properties[Peanut, Edible_biomass_water_content])* Other_Plant_Properties.misc_plant_properties[Peanut, kcal_per_kg]+ greenhouse_diet_composition_total[Rice]/(1- Other_Plant_Properties.misc_plant_properties[Rice, Edi- ble_biomass_water_content])* Other_Plant_Properties.misc_plant_properties[Rice, kcal_per_kg]+ greenhouse_diet_composition_total[Soybean]/(1- Other_Plant_Properties.misc_plant_properties[Soybean, Edible_biomass_water_content])* Other_Plant_Properties.misc_plant_properties[Soybean, kcal_per_kg]+ greenhouse_diet_composition_total[Sweet_Potato]/(1- Oth- er_Plant_Properties.misc_plant_properties[Sweet_Potat o, Edible_biomass_water_content])* Oth- er_Plant_Properties.misc_plant_properties[Sweet_Potat o, kcal_per_kg]+ greenhouse_diet_composition_total[Tomato]/(1- Other_Plant_Properties.misc_plant_properties[Tomato, Edible_biomass_water_content])* Other_Plant_Properties.misc_plant_properties[Tomato, kcal_per_kg]+ greenhouse_diet_composition_total[Wheat]/(1- Other_Plant_Properties.misc_plant_properties[Wheat, Edible_biomass_water_content])* Other_Plant_Properties.misc_plant_properties[Wheat, kcal_per_kg]+ greenhouse_diet_composition_total[White_Potato]/(1- Oth- er_Plant_Properties.misc_plant_properties[White_Potato , Edible_biomass_water_content])* Oth- er_Plant_Properties.misc_plant_properties[White_Potato , kcal_per_kg])*kcal_per_kg_unit_converter	
kcal from green- house per day	Converter	(consump- tion_of_greenhouse_food[Dry_Bean]*Other_Plant_Prope rties.misc_plant_properties[Dry_Bean, kcal_per_kg]+ consump- tion_of_greenhouse_food[Lettuce]*Other_Plant_Properti es.misc_plant_properties[Lettuce, kcal_per_kg]+ consump- tion_of_greenhouse_food[Peanut]*Other_Plant_Properti es.misc_plant_properties[Peanut, kcal_per_kg]+ consump- tion_of_greenhouse_food[Rice]*Other_Plant_Properties. misc_plant_properties[Rice, kcal_per_kg]+ consump- tion_of_greenhouse_food[Soybean]*Other_Plant_Proper ties.misc_plant_properties[Soybean, kcal_per_kg]+ consump- tion_of_greenhouse_food[Sweet_Potato]*Other_Plant_P roperties.misc_plant_properties[Sweet_Potato, kcal_per_kg]+ consump- tion_of_greenhouse_food[Tomato]*Other_Plant_Properti es.misc_plant_properties[Tomato, kcal_per_kg]+ consump- tion_of_greenhouse_food[Wheat]*Other_Plant_Propertie	kcal/d

		s.misc_plant_properties[Wheat, kcal_per_kg]+ consumption_of_greenhouse_food[White_Potato]*Other_Plant_Properties.misc_plant_properties[White_Potato, kcal_per_kg])*kcal_per_kg_unit_converter	
kcal per kg unit converter	Converter	1	kcal/kg
resupply food kcal demand	Converter	Crew_Mission_Profile.total_kcal_consumption-kcal_from_greenhouse_per_day	kcal/d
Resupply Food Storage	Stock	100 (example)	kg
consumption of resupply food	Flow	resupply_food_kcal_demand/ energy_content_of_resupply_food	kg/d
energy content of resupply food	Converter	4003.4	kcal/kg
RQ greenhouse food	Converter	IF SUM(consumption_of_greenhouse_food[*])>0 THEN ((1/MEC_Parameters.MEC_parameters[Dry_Bean, OPF]*consumption_of_greenhouse_food[Dry_Bean])+ (1/MEC_Parameters.MEC_parameters[Lettuce, OPF]*consumption_of_greenhouse_food[Lettuce])+ (1/MEC_Parameters.MEC_parameters[Peanut, OPF]*consumption_of_greenhouse_food[Peanut])+ (1/MEC_Parameters.MEC_parameters[Rice, OPF]*consumption_of_greenhouse_food[Rice])+ (1/MEC_Parameters.MEC_parameters[Soybean, OPF]*consumption_of_greenhouse_food[Soybean])+ (1/MEC_Parameters.MEC_parameters[Sweet_Potato, OPF]*consumption_of_greenhouse_food[Sweet_Potato]) + (1/MEC_Parameters.MEC_parameters[Tomato, OPF]*consumption_of_greenhouse_food[Tomato])+ (1/MEC_Parameters.MEC_parameters[Wheat, OPF]*consumption_of_greenhouse_food[Wheat])+ (1/MEC_Parameters.MEC_parameters[White_Potato, OPF]*consumption_of_greenhouse_food[White_Potato])) /SUM(consumption_of_greenhouse_food[*]) ELSE 0	-
RQ resupply food	Converter	1.00	-
RQ	Converter	(RQ_resupply_food*consumption_of_resupply_food+RQ_greenhouse_food*SUM(consumption_of_greenhouse_food[*]))/(consumption_of_resupply_food+SUM(consumption_of_greenhouse_food[*]))	-
carbon in consumed greenhouse food	Converter	consumption_of_greenhouse_food[Dry_Bean]*MEC_Parameters.MEC_parameters[Dry_Bean, BCF]+consumption_of_greenhouse_food[Lettuce]*MEC_Parameters.MEC_parameters[Lettuce, BCF]+consumption_of_greenhouse_food[Peanut]*MEC_Parameters.MEC_parameters[Peanut, BCF]+consumption_of_greenhouse_food[Rice]*MEC_Parameters.MEC_parameters[Rice, BCF]+consumption_of_greenhouse_food[Soybean]*MEC_Parameters.MEC_parameters[Soybean, BCF]+consumption_of_greenhouse_food[Sweet_Potato]*MEC_Parameters.MEC_parameters[Sweet_Potato, BCF]+consumption_of_greenhouse_food[Tomato]*MEC_Parameters.MEC_parameters[Tomato, BCF]+consumption_of_greenhouse_food[Wheat]*MEC_Parameters.MEC_parameters[Wheat, BCF]+consumption_of_greenhouse_food[White_Potato]*MEC_Parameters.MEC_parameters[White_Potato, BCF]	kg/d
carbon in consumed resupply food	Converter	resupply_food_carbon_fraction* consumption_of_resupply_food	kg/d
carbon in consumed food	Converter	carbon_in_consumed_resupply_food+carbon_in_consumed_greenhouse_food	kg/d

resupply food carbon fraction	Converter	0.40001	-

9.3.2 SL Edible Biomass Harvest Formulas

Variable Name	Variable Type	Formula/value	Unit
food production out of edible dry bio-mass	Flow, arrayed	1000	kg/d
Harvested Edible Dry Biomass	Stock, arrayed	0	kg
total edible dry bio-mass harvest per crop	Flow, arrayed	See Table 9-4 for values.	kg/d
Dry Bean edible dry	Converter, arrayed	IF(Crop_Scheduler.scheduler[compartment, cycle, crop_compartment]=1) THEN to-tal_edible_dry_biomass_harvest_per_compartment_per_cycle[compartment, cycle] ELSE 0	kg/d
Lettuce edible dry	Converter, arrayed	IF(Crop_Scheduler.scheduler[compartment, cycle, crop_compartment]=2) THEN to-tal_edible_dry_biomass_harvest_per_compartment_per_cycle[compartment, cycle] ELSE 0	kg/d
Peanut edible dry	Converter, arrayed	IF(Crop_Scheduler.scheduler[compartment, cycle, crop_compartment]=3) THEN to-tal_edible_dry_biomass_harvest_per_compartment_per_cycle[compartment, cycle] ELSE 0	kg/d
Rice edible dry	Converter, arrayed	IF(Crop_Scheduler.scheduler[compartment, cycle, crop_compartment]=4) THEN to-tal_edible_dry_biomass_harvest_per_compartment_per_cycle[compartment, cycle] ELSE 0	kg/d
Soybean edible dry	Converter, arrayed	IF(Crop_Scheduler.scheduler[compartment, cycle, crop_compartment]=5) THEN to-tal_edible_dry_biomass_harvest_per_compartment_per_cycle[compartment, cycle] ELSE 0	kg/d
Sweet Potato edible dry	Converter, arrayed	IF(Crop_Scheduler.scheduler[compartment, cycle, crop_compartment]=6) THEN to-tal_edible_dry_biomass_harvest_per_compartment_per_cycle[compartment, cycle] ELSE 0	kg/d
Tomato edible dry	Converter, arrayed	IF(Crop_Scheduler.scheduler[compartment, cycle, crop_compartment]=7) THEN to-tal_edible_dry_biomass_harvest_per_compartment_per_cycle[compartment, cycle] ELSE 0	kg/d
Wheat edible dry	Converter, arrayed	IF(Crop_Scheduler.scheduler[compartment, cycle, crop_compartment]=8) THEN to-tal_edible_dry_biomass_harvest_per_compartment_per_cycle[compartment, cycle] ELSE 0	kg/d
White Potato edible dry	Converter, arrayed	IF(Crop_Scheduler.scheduler[compartment, cycle, crop_compartment]=9) THEN to-tal_edible_dry_biomass_harvest_per_compartment_per_cycle[compartment, cycle] ELSE 0	kg/d
total edible dry bio-mass harvest per compartment per cycle	Flow, arrayed	har-vest_events[compartment]*Edible_Dry_Biomass_in_Plants_per_compartment_per_cycle[compartment, cycle]/DT	kg/d
Edible Dry Biomass in Plants per com-partment per cycle	Stock, arrayed	0	kg
total edible dry bio-mass production in greenhouse	Flow, arrayed	Green-house_Interface.compartment_TEB_per_cycle[compartment, cycle]	kg/d
harvest events	Converter, arrayed	Input via excel file as list of harvest dates.	1

Table 9-4: Total edible dry biomass harvest per crop arrayed converter values.

Crop	Formula
Dry Bean	SUM(Dry_Bean[*, *])
Lettuce	SUM(Lettuce[*, *])
Peanut	SUM(Peanut[*, *])
Rice	SUM(Rice[*, *])
Soybean	SUM(Soybean[*, *])
Sweet Potato	SUM(Sweet_Potato[*, *])
Tomato	SUM(Tomato[*, *])
Wheat	SUM(Wheat[*, *])
White Potato	SUM(White_Potato[*, *])

9.3.3 SL Inedible Biomass Harvest Formulas

Variable Name	Variable Type	Formula/value	Unit
Inedible Dry Biomass in Plants per compartment per cycle	Stock, arrayed	0	kg
total inedible dry biomass production in greenhouse	Flow, arrayed	Greenhouse_Interface.compartment_TIB_per_cycle[compartment, cycle]	kg/d
total inedible dry biomass harvest per compartment per cycle	Flow, arrayed	harvest_events[compartment]*Inedible_Dry_Biomass_in_Plants_per_compartment_per_cycle[compartment, cycle]/DT	kg/d
Harvested Inedible Dry Biomass	Stock	0	kg
Dry Bean inedible dry	Converter, arrayed	IF(Crop_Scheduler.scheduler[compartment, cycle, crop_compartment]=1) THEN total_inedible_dry_biomass_harvest_per_compartment_per_cycle[compartment, cycle] ELSE 0	kg/d
Lettuce inedible dry	Converter, arrayed	IF(Crop_Scheduler.scheduler[compartment, cycle, crop_compartment]=2) THEN total_inedible_dry_biomass_harvest_per_compartment_per_cycle[compartment, cycle] ELSE 0	kg/d
Peanut inedible dry	Converter, arrayed	IF(Crop_Scheduler.scheduler[compartment, cycle, crop_compartment]=3) THEN total_inedible_dry_biomass_harvest_per_compartment_per_cycle[compartment, cycle] ELSE 0	kg/d
Rice inedible dry	Converter, arrayed	IF(Crop_Scheduler.scheduler[compartment, cycle, crop_compartment]=4) THEN total_inedible_dry_biomass_harvest_per_compartment_per_cycle[compartment, cycle] ELSE 0	kg/d
Soybean inedible dry	Converter, arrayed	IF(Crop_Scheduler.scheduler[compartment, cycle, crop_compartment]=5) THEN total_inedible_dry_biomass_harvest_per_compartment_per_cycle[compartment, cycle] ELSE 0	kg/d
Sweet Potato inedible dry	Converter, arrayed	IF(Crop_Scheduler.scheduler[compartment, cycle, crop_compartment]=6) THEN total_inedible_dry_biomass_harvest_per_compartment_per_cycle[compartment, cycle] ELSE 0	kg/d
Tomato inedible dry	Converter, arrayed	IF(Crop_Scheduler.scheduler[compartment, cycle, crop_compartment]=7) THEN total_inedible_dry_biomass_harvest_per_compartment_per_cycle[compartment, cycle] ELSE 0	kg/d
Wheat inedible dry	Converter, arrayed	IF(Crop_Scheduler.scheduler[compartment, cycle, crop_compartment]=8) THEN total_inedible_dry_biomass_harvest_per_compartment_per_cycle[compartment, cycle] ELSE 0	kg/d
White Potato inedible dry	Converter, arrayed	IF(Crop_Scheduler.scheduler[compartment, cycle, crop_compartment]=9) THEN to-	kg/d

		tal_inedible_dry_biomass_harvest_per_compartment_per_cycle[compartment, cycle] ELSE 0	
total inedible dry biomass harvest per crop	Flow, arrayed	See Table 9-5 for values.	kg/d

Table 9-5: Total inedible dry biomass harvest per crop arrayed converter values.

Crop	Formula
Dry Bean	SUM(Dry_Bean_inedible_dry[*, *])
Lettuce	SUM(Lettuce_inedible_dry [*, *])
Peanut	SUM(Peanut_inedible_dry [*, *])
Rice	SUM(Rice_inedible_dry [*, *])
Soybean	SUM(Soybean_inedible_dry [*, *])
Sweet Potato	SUM(Sweet_Potato_inedible_dry [*, *])
Tomato	SUM(Tomato_inedible_dry [*, *])
Wheat	SUM(Wheat_inedible_dry [*, *])
White Potato	SUM(White_Potato_inedible_dry [*, *])

9.3.4 SL Crew Waste Formulas

Variable Name	Variable Type	Formula/value	Unit
Crew Metabolic Solids	Stock	500 (example)	kg
total fecal solid waste production by crew	Flow	Crew_Solids_Production.total_fecal_solids_production	kg/d
total perspiration solid waste production by crew	Flow	Crew_Solids_Production.total_perspiration_solids_production	kg/d
total urine solid waste production by crew	Flow	Crew_Solids_Production.total_urine_solids_production	kg/d
Misc Solids Storage	Stock	300 (example)	kg
total misc solid waste production by crew	Flow	Crew_Mission_Profile.CM_number_active*Misc_Crew_Parameters.CM_misc_solid_waste_production	kg/d
Solid Waste Storage in Habitat	Stock	0	kg

9.3.5 SL Physical-Chemical Systems Formulas

Variable Name	Variable Type	Formula/value	Unit
total solid waste processing	Flow	Physical_Chemical_Systems.incinerator_capacity*Physical_Chemical_Systems.incinerator_activity	kg/d
inedible biomass processing	Flow	Physical_Chemical_Systems.inedible_biomass_processor_capacity_per_crop*Physical_Chemical_Systems.inedible_biomass_processor_activity	kg/d

9.4 Crew Model Formulas

9.4.1 Activity Database Module Formulas

Variable Name	Variable Type	Formula/value	Unit
activity MET values	Converter, arrayed	See Table 9-6 for values.	MET

Table 9-6: Activity MET values arrayed converter values. All values in MET.

Activity	Value
sleep	0.9
leisure	1.26
eating	1.319
personal hygiene	1.319
science	1.660
communication	1.319
normal maintenance	1.660
repair	4.5
greenhouse maintenance	2.573
training	5.034
emergency	7
ÉVA	10.477
Recreation	1.319

Variable Name	Variable Type	Formula/value	Unit
MET kcal conversion	Converter	0.0175	kcal/(kg*min)/MET

9.4.2 Crew Day Database Module Formulas

Variable Name	Variable Type	Formula/value	Unit
CM day sets	Converter, arrayed	See Table 9-7 for values.	min
per day converter	Converter	1	1/d
CM kcal consumption	Converter, arrayed	per_day_converter*MET_Definitions.MET_kcal_conversion *(Activity_Database.activity_MET_values[sleep, 1]*CM_day_sets[sleep, *Arrayed variable*] +Activity_Database.activity_MET_values[leisure, 1]*CM_day_sets[leisure, *Arrayed variable*] +Activity_Database.activity_MET_values[eating, 1]*CM_day_sets[eating, *Arrayed variable*] +Activity_Database.activity_MET_values[personal_hygiene, 1]*CM_day_sets[personal_hygiene, *Arrayed variable*]+Activity_Database.activity_MET_values[science, 1]*CM_day_sets[science, *Arrayed variable*] +Activity_Database.activity_MET_values[communication, 1]*CM_day_sets[communication, *Arrayed variable*] +Activity_Database.activity_MET_values[normal_maintenance, 1]*CM_day_sets[normal_maintenance, *Arrayed variable*] +Activity_Database.activity_MET_values[repair, 1]*CM_day_sets[repair, *Arrayed variable*] +Activity_Database.activity_MET_values[greenhouse_maintenance, 1]*CM_day_sets[greenhouse_maintenance, *Arrayed variable*] +Activity_Database.activity_MET_values[training,	kcal/(kg*d)

		1]*CM_day_sets[training, *Arrayed variable*] +Activity_Database.activity_MET_values[emergency, 1]*CM_day_sets[emergency, *Arrayed variable*] +Activity_Database.activity_MET_values[EVA, 1]*CM_day_sets[EVA, *Arrayed variable*] +Activity_Database.activity_MET_values[Recreation, 1]*CM_day_sets[Recreation, *Arrayed variable*])	

Table 9-7: CM day sets arrayed converter values. All values in minutes.

Activity	BVAD week day	BVAD weekend day	Nominal day	Emergency day	EVA day
sleep	510	510	510	510	510
leisure	60	60	60	60	60
eating	180	180	180	180	180
personal hygiene	60	60	60	60	60
science	30	0	60	0	60
communication	90	90	90	120	90
normal maintenance	420	180	270	120	120
repair	0	0	0	180	0
greenhouse maintenance	0	0	120	0	0
training	90	0	90	0	0
emergency	0	0	0	60	0
ÉVA	0	0	0	0	180
Recreation	0	360	0	150	180

9.4.3 Crew Composition Module Formulas

Variable Name	Variable Type	Formula/value	Unit
CM parameters	Converter, arrayed	See Table 4-16 for values (example).	-
kg unit converter	Converter	1	kg
CM total body water	Converter, arrayed	IF(CM_parameters[astronaut, Sex]=10) THEN CM_parameters[astronaut, Weight]*0.625*kg_unit_converter ELSE IF(CM_parameters[astronaut, Sex]=20) THEN CM_parameters[astronaut, Weight]*0.525*kg_unit_converter ELSE 0	kg
total CM number	Converter	SUM(CM_parameters[*, Active])*people_unit_converter	people
people unit converter	Converter	1	people

9.4.4 Crew Mission Profile Module Formulas

Variable Name	Variable Type	Formula/value	Unit
CM mission profiles	Converter, arrayed	Input via excel file as list of **CM day sets** per simulation day.	-
kcal consumption per body mass per day	Converter, arrayed	IF CM_mission_profiles=1 THEN Crew_Day_Database.CM_kcal_consumption[BVAD_week_day] ELSE IF CM_mission_profiles=2 THEN Crew_Day_Database.CM_kcal_consumption[BVAD_weekend_day] ELSE IF CM_mission_profiles=3 THEN Crew_Day_Database.CM_kcal_consumption[Nominal_day] ELSE IF CM_mission_profiles=4 THEN Crew_Day_Database.CM_kcal_consumption[Emergency_day] ELSE IF CM_mission_profiles=5 THEN Crew_Day_Database.CM_kcal_consumption[EVA_day] ELSE 0	kcal/(kg*d)
kg unit converter	Converter	1	kg
kcal consumption per day	Converter, arrayed	kcal_consumption_per_body_mass_per_day*Crew_composition.CM_parameters[astronaut,	kcal/d

Variable Name	Variable Type	Formula/value	Unit
		Weight]*kg_unit_converter	
total kcal consumption	Converter	SUM(kcal_consumption_per_day[*])	kcal/d
CM active	Converter, arrayed	IF CM_mission_profiles[astronaut]>0 THEN 1 ELSE 0	people
CM number active	Converter	SUM(CM_active)	people

9.4.5 Crew Water Demand Module Formulas

Variable Name	Variable Type	Formula/value	Unit
insensible H2O loss over skin per kcal	Converter	0.030/100	kg/kcal
insensible H2O loss over lungs per kcal	Converter	0.015/100	kg/kcal
sensible H2O loss over sweating per kcal	Converter	0.010/100	kg/kcal
H2O loss over stool per kcal	Converter	0.005/100	kg/kcal
H2O loss over urine per kcal	Converter	0.050/100	kg/kcal
insensible H2O loss over skin	Converter, arrayed	insensible_H2O_loss_over_skin_per_kcal* Crew_Mission_Profile.kcal_consumption_per_day[astronaut]	kg/d
insensible H2O loss over lungs	Converter, arrayed	insensible_H2O_loss_over_lungs_per_kcal* Crew_Mission_Profile.kcal_consumption_per_day[astronaut]	kg/d
sensible H2O loss over sweating	Converter, arrayed	sensible_H2O_loss_over_sweating_per_kcal* Crew_Mission_Profile.kcal_consumption_per_day[astronaut]	kg/d
H2O loss over stool	Converter, arrayed	H2O_loss_over_stool_per_kcal* Crew_Mission_Profile.kcal_consumption_per_day[astronaut]	kg/d
H2O loss over urine	Converter, arrayed	H2O_loss_over_urine_per_kcal* Crew_Mission_Profile.kcal_consumption_per_day[astronaut]	kg/d

9.4.6 Crew Solids Production Module Formulas

Variable Name	Variable Type	Formula/value	Unit
CM BVAD fecal solid waste production	Converter	0.032	kg/ (people*d)
CM BVAD fecal water production	Converter	0.1	kg/ (people*d)
CM fecal solids production	Converter, arrayed	CM_BVAD_fecal_solid_waste_production/CM_BVAD_fecal_water_production*Crew_Water_Demand.H2O_loss_over_stool[astronaut]	kg/d
total fecal solids production	Converter, summing	SUM(CM_fecal_solids_production[*])	kg/d
CM BVAD urine solid waste	Converter	0.059	kg/ (people*d)
CM BVAD urine water production	Converter	1.6	kg/ (people*d)
CM urine solids production	Converter, arrayed	CM_BVAD_urine_solid_waste/CM_BVAD_urine_water_production* Crew_Water_Demand.H2O_loss_over_urine[astronaut]	kg/d
total urine solids production	Converter, summing	SUM(CM_urine_solids_production[*])	kg/d
CM BVAD perspiration solid waste	Converter	0.018	kg/ (people*d)

CM BVAD respiration and perspiration water production	Converter	1.9	kg/ (people*d)
CM perspiration solids production	Converter, arrayed	CM_BVAD_perspiration_solid_waste/CM_BVAD_respiration_and_perspiration_water_production*(Crew_Water_Demand.insensibe_H2O_loss_over_lungs[astronaut]+Crew_Water_Demand.insensible_H2O_loss_over_skin[astronaut]+Crew_Water_Demand.sensible_H2O_loss_over_sweating[astronaut])	kg/d
total perspiration solids production	Converter, summing	SUM(CM_perspiration_solids_production[*])	kg/d

9.4.7 Misc Crew Parameters Module Formulas

Variable Name	Variable Type	Formula/value	Unit
CM hygiene H2O demand	Converter	5.16 (example)	kg/ (people*d)
CM misc solid waste production	Converter	1.93 (example)	kg/ (people*d)

9.5   Greenhouse Model Formulas

9.5.1 Crop Scheduler Module Formulas

Variable Name	Variable Type	Formula/value	Unit
scheduler	Converter, arrayed	See Table 4-18 for values. Input via Excel file.	-

9.5.2 MEC Parameters Module Formulas

Variable Name	Variable Type	Formula/value	Unit
CQYmax coefficients	Converter, arrayed	See Table 9-8 to Table 9-16 for values.	-
tA coefficients	Converter, arrayed	See Table 9-17 to Table 9-25 for values.	-
MEC parameters	Converter, arrayed	See Figure 9-1 for values.	-
Amax	Converter	0.93	1

Table 9-8: CQYmax coefficients for Dry Bean (Anderson *et al.*, 2015)

	1	2	3	4	5
1	0	0	0	0	0
2	0	4.191*10^-2	-1.238*10^-5	0	0
3	0	5.3852*10^-5	0	-1.544*10^-11	0
4	0	-2.1275*10^-8	0	6.469*10^-15	0
5	0	0	0	0	0

Table 9-9: CQYmax coefficients for Lettuce (Anderson *et al.*, 2015)

	1	2	3	4	5
1	0	0	0	0	0
2	0	4.4763*10^-2	-1.1701*10^-5	0	0
3	0	5.163*10^-5	0	-1.9731*10^-11	0
4	0	-2.075*10^-8	0	8.9265*10^-15	0
5	0	0	0	0	0

Table 9-10: CQYmax coefficients for Peanut (Anderson *et al.*, 2015)

	1	2	3	4	5
1	0	0	0	0	0
2	0	4.1513*10^-2	0	-2.1582*10^-8	0
3	0	5.1157*10^-5	4.0864*10^-8	-1.0468*10^-10	4.8541*10^-14
4	0	-2.0992*10^-8	0	0	0
5	0	0	0	0	3.9259*10^-21

Table 9-11: CQYmax coefficients for Rice (Anderson *et al.*, 2015)

	1	2	3	4	5
1	0	0	0	0	0
2	0	3.6186*10^-2	0	-2.6712*10^-9	0
3	0	6.1457*10^-5	-9.1477*10^-9	0	0
4	0	-2.4322*10^-8	3.889*10^-12	0	0
5	0	0	0	0	0

Table 9-12: CQYmax coefficients for Soybean (Anderson *et al.*, 2015)

	1	2	3	4	5
1	0	0	0	0	0
2	0	4.1513*10^-2	0	-2.1582*10^-8	0
3	0	5.1157*10^-5	4.0864*10^-8	-1.0468*10^-10	4.8541*10^-14
4	0	-2.0992*10^-8	0	0	0
5	0	0	0	0	3.9259*10^-21

Table 9-13: CQYmax coefficients for Sweet Potato (Anderson *et al.*, 2015)

	1	2	3	4	5
1	0	0	0	0	0
2	0	3.9317*10^-2	-1.3836*10^-5	0	0
3	0	5.6741*10^-5	-6.3397*10^-9	-1.3464*10^-11	0
4	0	-2.1797*10^-8	0	7.7362*10^-15	0
5	0	0	0	0	0

Table 9-14: CQYmax coefficients for Tomato (Anderson *et al.*, 2015)

	1	2	3	4	5
1	0	0	0	0	0
2	0	4.0061*10^-2	0	-7.1241*10^-9	0
3	0	5.688*10^-5	-1.182*10^-8	0	0
4	0	-2.2598*10^-8	5.0264*10^-12	0	0
5	0	0	0	0	0

Table 9-15: CQYmax coefficients for Wheat (Anderson *et al.*, 2015)

	1	2	3	4	5
1	0	0	0	0	0
2	0	4.4793*10^-2	-5.1946*10^-6	0	0
3	0	5.1583*10^-5	0	-4.9303*10^-12	0
4	0	-2.0724*10^-8	0	2.2255*10^-15	0
5	0	0	0	0	0

Table 9-16: CQYmax coefficients for White Potato (Anderson *et al.*, 2015)

	1	2	3	4	5
1	0	0	0	0	0
2	0	4.629*10^-2	0	0	-1.9602*10^-11
3	0	5.0910*10^-5	0	-1.5272*10^-11	0
4	0	-2.1878*10^-8	0	0	0
5	0	0	4.3976*10^-15	0	0

Table 9-17: tA coefficients for Dry Bean (Anderson *et al.*, 2015)

	1	2	3	4	5
1	2.9041*10^5	0	0	0	0
2	1.5594*10^3	15.840	6.1120*10^-3	0	0
3	0	0	0	-3.7409*10^-9	0
4	0	0	0	0	0
5	0	0	0	0	9.6484*10^-19

Table 9-18: tA coefficients for Lettuce (Anderson *et al.*, 2015)

	1	2	3	4	5
1	0	0	1.876	0	0
2	1.0289*10^4	1.7571	0	0	0
3	-3.7018	0	0	0	0
4	0	2.3127*10^-6	0	0	0
5	3.6648*10^-7	0	0	0	0

Table 9-19: tA coefficients for Peanut (Anderson *et al.*, 2015)

	1	2	3	4	5
1	3.7487*10^6	-1.8840*10^4	51.256	-0.05963	2.5969*10^-5
2	2.9200*10^3	23.912	0	5.5180*10^-6	0
3	0	0	0	0	0
4	0	0	0	0	0
5	9.4008*10^-8	0	0	0	0

Table 9-20: tA coefficients for Rice (Anderson *et al.*, 2015)

	1	2	3	4	5
1	6.5914*10^6	-3.748*10^3	0	0	0
2	2.5776*10^4	0	0	4.5207*10^-6	0
3	0	-0.043378	4.562*10^-5	-1.4936*10^-8	-0.043378
4	6.4532*10^-3	0	0	0	0
5	0	0	0	0	0

Table 9-21: tA coefficients for Soybean (Anderson *et al.*, 2015)

	1	2	3	4	5
1	6.7978*10^6	-4.236*10^4	112.63	-0.13637	6.6918*10^-5
2	-4.3658*10^3	33.959	0	0	-2.1367*10^-8
3	1.5573	0	0	0	1.5467*10^-11
4	0	0	-4.911*10^-9	0	0
5	0	0	0	0	0

Table 9-22: tA coefficients for Sweet Potato (Anderson *et al.*, 2015)

	1	2	3	4	5
1	1.2070*10^6	0	0	0	4.0109*10^-7
2	4.9484*10^3	4.2978	0	0	0
3	0	0	0	0	2.0193*10^-12
4	0	0	0	0	0
5	0	0	0	0	0

Table 9-23: tA coefficients for Tomato (Anderson *et al.*, 2015)

	1	2	3	4	5
1	6.2774*10^5	0	0.44686	0	0
2	3.1724*10^3	24.281	5.6276*10^-3	-3.0690*10^-6	0
3	0	0	0	0	0
4	0	0	0	0	0
5	0	0	0	0	0

Table 9-24: tA coefficients for Wheat (Anderson _et al._, 2015)

	1	2	3	4	5
1	$9.5488*10^4$	0	0.3419	$-1.9076*10^{-4}$	0
2	$1.0686*10^3$	15.977	$1.9733*10^{-4}$	0	0
3	0	0	0	0	0
4	0	0	0	0	0
5	0	0	0	0	0

Table 9-25: tA coefficients for White Potato (Anderson _et al._, 2015)

	1	2	3	4	5
1	$6.5773*10^5$	0	0	0	0
2	$8.5626*10^3$	0	0.042749	$-1.7905*10^{-5}$	0
3	0	0	$8.8437*10^{-7}$	0	0
4	0	0	0	0	0
5	0	0	0	0	0

	H0	OPF	BCF	XFRT	tE	tQ	tM	n	CQYmin	CUEmin	CUEmax	gA	Tlight
Dry Bean	12	1.1	0.45	0.97	40	42	63	2	0.02	0.5	0.65	2.5	26
Lettuce	16	1.08	0.4	0.95	1	0	30	2.5	0	0	0.625	2.5	23
Peanut	12	1.19	0.5	0.49	49	65	110	2	0.02	0.3	0.65	2.5	26
Rice	12	1.08	0.44	0.98	57	61	88	1.5	0.01	0	0.64	5.5	29
Soybean	12	1.16	0.46	0.95	46	48	86	1.5	0.02	0.3	0.65	2.5	26
Sweet Potato	18	1.02	0.44	1	33	0	120	1.5	0	0	0.625	2.5	28
Tomato	12	1.09	0.42	0.7	41	56	80	2.5	0.01	0	0.65	2.5	26
Wheat	20	1.07	0.44	1	34	33	62	1	0.01	0	0.64	5.5	23
White Potato	12	1.02	0.41	1	45	75	138	2	0.02	0	0.625	2.5	20

Figure 9-1: MEC parameters arrayed converter values.

9.5.3 MEC Coefficients Module Formulas

Variable Name	Variable Type	Formula/value	Unit
unit neutralizer umol mol	Converter	1	mol/umol
current CO2 per compartment unit neutralized	Converter, arrayed	Gases_Layer.current_CO2_ppm_in_greenhouse* unit_neutralizer_umol_mol	1
CQYmax	Converter, arrayed	IF Crop_Scheduler.scheduler[compartment, cycle, crop_compartment]=0 THEN 0 ELSE (IF current_CO2_per_compartment_unit_neutralized[compartment]=0 THEN 0 ELSE(IF Crop_Scheduler.scheduler[compartment, cycle, PPF_compartment]=0 THEN 0 ELSE(MEC_Parameters.CQYmax_coefficients[Crop_Scheduler.scheduler[compartment, cycle, crop_compartment],1, 1]*1/Crop_Scheduler.scheduler[compartment, cycle, PPF_compartment]*1/current_CO2_per_compartment_unit_neutralized[compartment]+ MEC_Parameters.CQYmax_coefficients[Crop_Scheduler.scheduler[compartment, cycle, crop_compartment],2, 1]*1/Crop_Scheduler.scheduler[compartment, cycle, PPF_compartment]+ MEC_Parameters.CQYmax_coefficients[Crop_Scheduler.scheduler[compartment, cycle, crop_compartment],3,	1

		1]/Crop_Scheduler.scheduler[compartment, cycle, PPF_compartment]*current_CO2_per_compartment_unit_neutralized[compartment]+ MEC_Parameters.CQYmax_coefficients[Crop_Scheduler.scheduler[compartment, cycle, crop_compartment],4, 1]/Crop_Scheduler.scheduler[compartment, cycle, PPF_compartment]*(current_CO2_per_compartment_unit_neutralized[compartment]^2)+ MEC_Parameters.CQYmax_coefficients[Crop_Scheduler.scheduler[compartment, cycle, crop_compartment],5, 1]/Crop_Scheduler.scheduler[compartment, cycle, PPF_compartment]*(current_CO2_per_compartment_unit_neutralized[compartment]^3)+ MEC_Parameters.CQYmax_coefficients[Crop_Scheduler.scheduler[compartment, cycle, crop_compartment],1, 2]*1/current_CO2_per_compartment_unit_neutralized[compartment]+ MEC_Parameters.CQYmax_coefficients[Crop_Scheduler.scheduler[compartment, cycle, crop_compartment],2, 2]+ MEC_Parameters.CQYmax_coefficients[Crop_Scheduler.scheduler[compartment, cycle, crop_compartment],3, 2]*current_CO2_per_compartment_unit_neutralized[compartment]+ MEC_Parameters.CQYmax_coefficients[Crop_Scheduler.scheduler[compartment, cycle, crop_compartment],4, 2]*current_CO2_per_compartment_unit_neutralized[compartment]^2+ MEC_Parameters.CQYmax_coefficients[Crop_Scheduler.scheduler[compartment, cycle, crop_compartment],5, 2]*current_CO2_per_compartment_unit_neutralized[compartment]^3+ MEC_Parameters.CQYmax_coefficients[Crop_Scheduler.scheduler[compartment, cycle, crop_compartment],1, 3]*Crop_Scheduler.scheduler[compartment, cycle, PPF_compartment]/current_CO2_per_compartment_unit_neutralized[compartment]+ MEC_Parameters.CQYmax_coefficients[Crop_Scheduler.scheduler[compartment, cycle, crop_compartment],2, 3]*Crop_Scheduler.scheduler[compartment, cycle, PPF_compartment]+ MEC_Parameters.CQYmax_coefficients[Crop_Scheduler.scheduler[compartment, cycle, crop_compartment],3, 3]*Crop_Scheduler.scheduler[compartment, cycle, PPF_compartment]*current_CO2_per_compartment_unit_neutralized[compartment]+ MEC_Parameters.CQYmax_coefficients[Crop_Scheduler.scheduler[compartment, cycle, crop_compartment],4, 3]*Crop_Scheduler.scheduler[compartment, cycle, PPF_compartment]*current_CO2_per_compartment_unit_neutralized[compartment]^2+ MEC_Parameters.CQYmax_coefficients[Crop_Scheduler.scheduler[compartment, cycle, crop_compartment],5, 3]*Crop_Scheduler.scheduler[compartment, cycle, PPF_compartment]*current_CO2_per_compartment_unit_neutralized[compartment]^3+ MEC_Parameters.CQYmax_coefficients[Crop_Scheduler.scheduler[compartment, cycle, crop_compartment],1, 4]*Crop_Scheduler.scheduler[compartment, cycle, PPF_compartment]^2/current_CO2_per_compartment_unit_neutralized[compartment]+ MEC_Parameters.CQYmax_coefficients[Crop_Scheduler.scheduler[compartment, cycle, crop_compartment],2, 4]*Crop_Scheduler.scheduler[compartment, cycle, PPF_compartment]^2+ MEC_Parameters.CQYmax_coefficients[Crop_Scheduler.scheduler[compartment, cycle, crop_compartment],3, 4]*Crop_Scheduler.scheduler[compartment, cycle,	

| | | PPF_compartment]^2*current_CO2_per_compartment_unit_neutralized[compartment]+
MEC_Parameters.CQYmax_coefficients[Crop_Scheduler.scheduler[compartment, cycle, crop_compartment],4, 4]*Crop_Scheduler.scheduler[compartment, cycle, PPF_compartment]^2*current_CO2_per_compartment_unit_neutralized[compartment]^2+
MEC_Parameters.CQYmax_coefficients[Crop_Scheduler.scheduler[compartment, cycle, crop_compartment],5, 4]*Crop_Scheduler.scheduler[compartment, cycle, PPF_compartment]^2*current_CO2_per_compartment_unit_neutralized[compartment]^3+
MEC_Parameters.CQYmax_coefficients[Crop_Scheduler.scheduler[compartment, cycle, crop_compartment],1, 5]*Crop_Scheduler.scheduler[compartment, cycle, PPF_compartment]^3/current_CO2_per_compartment_unit_neutralized[compartment]+
MEC_Parameters.CQYmax_coefficients[Crop_Scheduler.scheduler[compartment, cycle, crop_compartment],2, 5]*Crop_Scheduler.scheduler[compartment, cycle, PPF_compartment]^3+
MEC_Parameters.CQYmax_coefficients[Crop_Scheduler.scheduler[compartment, cycle, crop_compartment],3, 5]*Crop_Scheduler.scheduler[compartment, cycle, PPF_compartment]^3*current_CO2_per_compartment_unit_neutralized[compartment]+
MEC_Parameters.CQYmax_coefficients[Crop_Scheduler.scheduler[compartment, cycle, crop_compartment],4, 5]*Crop_Scheduler.scheduler[compartment, cycle, PPF_compartment]^3*current_CO2_per_compartment_unit_neutralized[compartment]^2+
MEC_Parameters.CQYmax_coefficients[Crop_Scheduler.scheduler[compartment, cycle, crop_compartment],5, 5]*Crop_Scheduler.scheduler[compartment, cycle, PPF_compartment]^3*current_CO2_per_compartment_unit_neutralized[compartment]^3)
)) | |
| CQY | Converter, arrayed | IF TIME<=Crop_Scheduler.scheduler[compartment, cycle, t_cycle_start] THEN 0 ELSE
IF (Crop_Scheduler.scheduler[compartment, cycle, crop_compartment]=2 OR Crop_Scheduler.scheduler[compartment, cycle, crop_compartment]=6) THEN CQYmax[compartment, cycle] ELSE
IF TIME<= (MEC_Parameters.MEC_parameters[Crop_Scheduler.scheduler[compartment, cycle, crop_compartment], tQ]+Crop_Scheduler.scheduler[compartment, cycle, t_cycle_start]) THEN CQYmax[compartment, cycle] ELSE
IF (TIME>(MEC_Parameters.MEC_parameters[Crop_Scheduler.scheduler[compartment, cycle, crop_compartment], tQ]+Crop_Scheduler.scheduler[compartment, cycle, t_cycle_start]) AND TIME<=(MEC_Parameters.MEC_parameters[Crop_Scheduler.scheduler[compartment, cycle, crop_compartment], tM]+Crop_Scheduler.scheduler[compartment, cycle, t_cycle_start])) THEN CQYmax[compartment, cycle]-(CQYmax[compartment, cycle]-MEC_Parameters.MEC_parameters[Crop_Scheduler.scheduler[compartment, cycle, crop_compartment], CQYmin])*((TIME-(MEC_Parameters.MEC_parameters[Crop_Scheduler.scheduler[compartment, cycle, crop_compartment], tQ]+Crop_Scheduler.scheduler[compartment, cycle, t_cycle_start]))/(MEC_Parameters.MEC_parameters[Crop_Scheduler.scheduler[compartment, cycle, | 1 |

		crop_compartment], tM]-MEC_Parameters.MEC_parameters[Crop_Scheduler.scheduler[compartment, cycle, crop_compartment], tQ])) ELSE 0	
PPFe	Converter, arrayed	IF MEC_Parameters.MEC_parameters[Crop_Scheduler.scheduler[compartment, cycle, crop_compartment], H0]=0 THEN 0 ELSE Crop_Scheduler.scheduler[compartment, cycle, PPF_compartment]*(Crop_Scheduler.scheduler[compartment, cycle, H_compartment]/(MEC_Parameters.MEC_parameters[Crop_Scheduler.scheduler[compartment, cycle, crop_compartment], H0]))	1
tA	Converter, arrayed	IF Crop_Scheduler.scheduler[compartment, cycle, crop_compartment]=0 THEN 0 ELSE (IF PPFe[compartment,cycle]=0 THEN 0 ELSE (IF current_CO2_per_compartment_unit_neutralized[compartment]=0 THEN 0 ELSE(MEC_Parameters.tA_coefficients[Crop_Scheduler.scheduler[compartment, cycle, crop_compartment],1,1]*1/PPFe[compartment,cycle]*1/current_CO2_per_compartment_unit_neutralized[compartment]+ MEC_Parameters.tA_coefficients[Crop_Scheduler.scheduler[compartment, cycle, crop_compartment],2, 1]*1/PPFe[compartment,cycle]+ MEC_Parameters.tA_coefficients[Crop_Scheduler.scheduler[compartment, cycle, crop_compartment],3,1]*current_CO2_per_compartment_unit_neutralized[compartment]/PPFe[compartment,cycle]+ MEC_Parameters.tA_coefficients[Crop_Scheduler.scheduler[compartment, cycle, crop_compartment],4,1]*current_CO2_per_compartment_unit_neutralized[compartment]^2/PPFe[compartment,cycle]+ MEC_Parameters.tA_coefficients[Crop_Scheduler.scheduler[compartment, cycle, crop_compartment],5,1]*current_CO2_per_compartment_unit_neutralized[compartment]^3/PPFe[compartment,cycle]+ MEC_Parameters.tA_coefficients[Crop_Scheduler.scheduler[compartment, cycle, crop_compartment],1, 2]*1/current_CO2_per_compartment_unit_neutralized[compartment]+ MEC_Parameters.tA_coefficients[Crop_Scheduler.scheduler[compartment, cycle, crop_compartment],2, 2]+ MEC_Parameters.tA_coefficients[Crop_Scheduler.scheduler[compartment, cycle, crop_compartment],3,2]*current_CO2_per_compartment_unit_neutralized[compartment]+ MEC_Parameters.tA_coefficients[Crop_Scheduler.scheduler[compartment, cycle, crop_compartment],4, 2]*current_CO2_per_compartment_unit_neutralized[compartment]^2+ MEC_Parameters.tA_coefficients[Crop_Scheduler.scheduler[compartment, cycle, crop_compartment],5, 2]*current_CO2_per_compartment_unit_neutralized[compartment]^3+ MEC_Parameters.tA_coefficients[Crop_Scheduler.scheduler[compartment, cycle, crop_compartment],1,3]*PPFe[compartment,cycle]/current_CO2_per_compartment_unit_neutralized[compartment]+ MEC_Parameters.tA_coefficients[Crop_Scheduler.sched	

		uler[compartment, cycle, crop_compartment],2, 3]*PPFe[compartment,cycle]+ MEC_Parameters.tA_coefficients[Crop_Scheduler.scheduler[compartment, cycle, crop_compartment],3,3]*PPFe[compartment,cycle]*current_CO2_per_compartment_unit_neutralized[compartment]+ MEC_Parameters.tA_coefficients[Crop_Scheduler.scheduler[compartment, cycle, crop_compartment],4,3]*PPFe[compartment,cycle]*current_CO2_per_compartment_unit_neutralized[compartment]^2+ MEC_Parameters.tA_coefficients[Crop_Scheduler.scheduler[compartment, cycle, crop_compartment],5,3]*PPFe[compartment,cycle]*current_CO2_per_compartment_unit_neutralized[compartment]^3+ MEC_Parameters.tA_coefficients[Crop_Scheduler.scheduler[compartment, cycle, crop_compartment],1,4]*PPFe[compartment,cycle]^2/current_CO2_per_compartment_unit_neutralized[compartment]+ MEC_Parameters.tA_coefficients[Crop_Scheduler.scheduler[compartment, cycle, crop_compartment],2, 4]*PPFe[compartment,cycle]^2+ MEC_Parameters.tA_coefficients[Crop_Scheduler.scheduler[compartment, cycle, crop_compartment],3,4]*PPFe[compartment,cycle]^2*current_CO2_per_compartment_unit_neutralized[compartment]+ MEC_Parameters.tA_coefficients[Crop_Scheduler.scheduler[compartment, cycle, crop_compartment],4,4]*PPFe[compartment,cycle]^2*current_CO2_per_compartment_unit_neutralized[compartment]^2+ MEC_Parameters.tA_coefficients[Crop_Scheduler.scheduler[compartment, cycle, crop_compartment],5,4]*PPFe[compartment,cycle]^2*current_CO2_per_compartment_unit_neutralized[compartment]^3+ MEC_Parameters.tA_coefficients[Crop_Scheduler.scheduler[compartment, cycle, crop_compartment],1,5]*PPFe[compartment,cycle]^3/current_CO2_per_compartment_unit_neutralized[compartment]+ MEC_Parameters.tA_coefficients[Crop_Scheduler.scheduler[compartment, cycle, crop_compartment],2, 5]*PPFe[compartment,cycle]^3+ MEC_Parameters.tA_coefficients[Crop_Scheduler.scheduler[compartment, cycle, crop_compartment],3,5]*PPFe[compartment,cycle]^3*current_CO2_per_compartment_unit_neutralized[compartment]+ MEC_Parameters.tA_coefficients[Crop_Scheduler.scheduler[compartment, cycle, crop_compartment],4,5]*PPFe[compartment,cycle]^3*current_CO2_per_compartment_unit_neutralized[compartment]^2+ MEC_Parameters.tA_coefficients[Crop_Scheduler.scheduler[compartment, cycle, crop_compartment],5, 5]*PPFe[compartment,cycle]^3*current_CO2_per_compartment_unit_neutralized[compartment]^3)))	
A	Converter, arrayed	IF Crop_Scheduler.scheduler[compartment, cycle, crop_compartment]=0 THEN 0 ELSE IF tA[compartment, cycle]=0 THEN 0 ELSE IF TIME<Crop_Scheduler.scheduler[compartment, cycle, t_cycle_start] THEN 0 ELSE	1

		IF (TIME>=Crop_Scheduler.scheduler[compartment, cycle, t_cycle_start] AND TIME<(tA[compartment, cycle]+Crop_Scheduler.scheduler[compartment, cycle, t_cycle_start])) THEN MEC_Parameters.Amax*((TIME-Crop_Scheduler.scheduler[compartment, cycle, t_cycle_start])/tA[compartment, cycle])^MEC_Parameters.MEC_parameters[Crop_Scheduler.scheduler[compartment, cycle, crop_compartment], n] ELSE IF (TIME>=(tA[compartment, cycle]+Crop_Scheduler.scheduler[compartment, cycle, t_cycle_start]) AND TIME<=(Crop_Scheduler.scheduler[compartment, cycle, t_cycle_start]+MEC_Parameters.MEC_parameters[Crop_Scheduler.scheduler[compartment, cycle, crop_compartment], tM])) THEN MEC_Parameters.Amax ELSE IF TIME>(Crop_Scheduler.scheduler[compartment, cycle, t_cycle_start]+MEC_Parameters.MEC_parameters[Crop_Scheduler.scheduler[compartment, cycle, crop_compartment], tM]) THEN 0 ELSE 0	
CUE24	Converter, arrayed	IF TIME<=Crop_Scheduler.scheduler[compartment, cycle, t_cycle_start] THEN 0 ELSE IF TIME<=(MEC_Parameters.MEC_parameters[Crop_Scheduler.scheduler[compartment, cycle, crop_compartment], tQ]+Crop_Scheduler.scheduler[compartment, cycle, t_cycle_start]) THEN MEC_Parameters.MEC_parameters[Crop_Scheduler.scheduler[compartment, cycle, crop_compartment], CUE-max] ELSE IF (TIME>(MEC_Parameters.MEC_parameters[Crop_Scheduler.scheduler[compartment, cycle, crop_compartment], tQ]+Crop_Scheduler.scheduler[compartment, cycle, t_cycle_start]) AND TIME<=(MEC_Parameters.MEC_parameters[Crop_Scheduler.scheduler[compartment, cycle, crop_compartment], tM]+Crop_Scheduler.scheduler[compartment, cycle, t_cycle_start])) THEN IF (Crop_Scheduler.scheduler[compartment, cycle, crop_compartment]=1 OR Crop_Scheduler.scheduler[compartment, cycle, crop_compartment]=3 OR Crop_Scheduler.scheduler[compartment, cycle, crop_compartment]=5) THEN MEC_Parameters.MEC_parameters[Crop_Scheduler.scheduler[compartment, cycle, crop_compartment], CUE-max]-(MEC_Parameters.MEC_parameters[Crop_Scheduler.scheduler[compartment, cycle, crop_compartment], CUE-max]-MEC_Parameters.MEC_parameters[Crop_Scheduler.scheduler[compartment, cycle, crop_compartment], CUE-min])*((TIME-(MEC_Parameters.MEC_parameters[Crop_Scheduler.scheduler[compartment, cycle, crop_compartment], tQ]+Crop_Scheduler.scheduler[compartment, cycle, t_cycle_start]))/(MEC_Parameters.MEC_parameters[Crop_Scheduler.scheduler[compartment, cycle, crop_compartment], tM]-MEC_Parameters.MEC_parameters[Crop_Scheduler.scheduler[compartment, cycle, crop_compartment], tQ])) ELSE MEC_Parameters.MEC_parameters[Crop_Scheduler.scheduler[compartment, cycle, crop_compartment], CUE-	1

| | | max]
ELSE 0 | |

9.5.4 MEC Crop Biomass Production Formulas

Variable Name	Variable Type	Formula/value	Unit
DCG unit converter	Converter	0.0036	mol/ (m^2*d)
DCG	Converter, arrayed	DCG_unit_converter*Crop_Scheduler.scheduler[compartment, cycle, H_compartment]*MEC_Coefficients.CUE24[compartment, cycle]*MEC_Coefficients.A[compartment, cycle]*MEC_Coefficients.CQY[compartment, cycle]*Crop_Scheduler.scheduler[compartment, cycle, PPF_compartment]	mol/ (m^2*d)
DOP	Converter, arrayed	DCG[compartment, cycle]*MEC_Parameters.MEC_parameters[Crop_Scheduler.scheduler[compartment, cycle, crop_compartment], OPF]	mol/ (m^2*d)
carbon molecular mass	Converter	12.011	g/mol
CGR	Converter, arrayed	IF Crop_Scheduler.scheduler[compartment, cycle, crop_compartment]=0 THEN 0 ELSE carbon_molecular_weight*DCG[compartment, cycle]/(MEC_Parameters.MEC_parameters[Crop_Scheduler.scheduler[compartment, cycle, crop_compartment], BCF])	g/(m^2*d)
TEB	Converter, arrayed	IF (TIME>=(Crop_Scheduler.scheduler[compartment, cycle, t_cycle_start]+MEC_Parameters.MEC_parameters[Crop_Scheduler.scheduler[compartment, cycle, crop_compartment], tE]) AND TIME<=(Crop_Scheduler.scheduler[compartment, cycle, t_cycle_start]+MEC_Parameters.MEC_parameters[Crop_Scheduler.scheduler[compartment, cycle, crop_compartment], tM])) THEN MEC_Parameters.MEC_parameters[Crop_Scheduler.scheduler[compartment, cycle, crop_compartment], XFRT]*CGR[compartment, cycle] ELSE 0	g/(m^2*d)
TIB	Converter, arrayed	TCB[compartment, cycle]-TEB[compartment, cycle]	g/(m^2*d)
TCB	Converter, arrayed	CGR[compartment, cycle]	g/(m^2*d)

9.5.5 MEC Crop Transpiration Module Formulas

Variable Name	Variable Type	Formula/value	Unit
unit converter umol m2 s	Converter	1	umol/ (m^2*s)
PGross	Converter, arrayed	MEC_Coefficients.A[compartment, cycle]*MEC_Coefficients.CQY[compartment, cycle]*Crop_Scheduler.scheduler[compartment, cycle, PPF_compartment]*unit_converter_umol_m2_s	umol/ (m^2*s)
DPG	Converter	24	1
PNET	Converter, arrayed	PGross[compartment, cycle]*((DPG-Crop_Scheduler.scheduler[compartment, cycle, H_compartment])/DPG+Crop_Scheduler.scheduler[compartment, cycle, H_compartment]*MEC_Coefficients.CUE24[compartment, cycle]/DPG)	umol/ (m^2*s)
current relative humidity per compart-	Converter, arrayed	Humidity_conversions.current_relative_humidity_in_greenhouse	1

ment			
gS	Converter, arrayed	IF MEC_Coefficients.current_CO2_per_compartment_unit_neutralized[compartment]=0 THEN 0 ELSE IF Crop_Scheduler.scheduler[compartment, cycle, crop_compartment]=1 THEN (1.717*MEC_Parameters.MEC_parameters[Dry_Bean, Tlight]-19.96-10.54*VPD[compartment, cycle])*(PNET[compartment, cycle]/MEC_Coefficients.current_CO2_per_compartment_unit_neutralized[compartment]) ELSE IF Crop_Scheduler.scheduler[compartment, cycle, crop_compartment]=2 THEN (1.717*MEC_Parameters.MEC_parameters[Lettuce, Tlight]-19.96-10.54*VPD[compartment, cycle])*(PNET[compartment, cycle]/MEC_Coefficients.current_CO2_per_compartment_unit_neutralized[compartment]) ELSE IF Crop_Scheduler.scheduler[compartment, cycle, crop_compartment]=3 THEN (1.717*MEC_Parameters.MEC_parameters[Peanut, Tlight]-19.96-10.54*VPD[compartment, cycle])*(PNET[compartment, cycle]/MEC_Coefficients.current_CO2_per_compartment_unit_neutralized[compartment]) ELSE IF Crop_Scheduler.scheduler[compartment, cycle, crop_compartment]=4 THEN (0.1389+15.32*current_relative_humidity_per_compartment[1])*(PNET[compartment, cycle]/MEC_Coefficients.current_CO2_per_compartment_unit_neutralized[compartment]) ELSE IF Crop_Scheduler.scheduler[compartment, cycle, crop_compartment]=5 THEN (1.717*MEC_Parameters.MEC_parameters[Soybean, Tlight]-19.96-10.54*VPD[compartment, cycle])*(PNET[compartment, cycle]/MEC_Coefficients.current_CO2_per_compartment_unit_neutralized[compartment]) ELSE IF Crop_Scheduler.scheduler[compartment, cycle, crop_compartment]=6 THEN (1.717*MEC_Parameters.MEC_parameters[Sweet_Potato, Tlight]-19.96-10.54*VPD[compartment, cycle])*(PNET[compartment, cycle]/MEC_Coefficients.current_CO2_per_compartment_unit_neutralized[compartment]) ELSE IF Crop_Scheduler.scheduler[compartment, cycle, crop_compartment]=7 THEN (1.717*MEC_Parameters.MEC_parameters[Tomato, Tlight]-19.96-10.54*VPD[compartment, cycle])*(PNET[compartment, cycle]/MEC_Coefficients.current_CO2_per_compartment_unit_neutralized[compartment]) ELSE IF Crop_Scheduler.scheduler[compartment, cycle, crop_compartment]=8 THEN (0.1389+15.32*current_relative_humidity_per_compartment[compartment])*(PNET[compartment, cycle]/MEC_Coefficients.current_CO2_per_compartment_unit_neutralized[compartment]) ELSE IF Crop_Scheduler.scheduler[compartment, cycle, crop_compartment]=9 THEN (1.717*MEC_Parameters.MEC_parameters[White_Potato, Tlight]-19.96-10.54*VPD[compartment, cycle])*(PNET[compartment, cycle]/MEC_Coefficients.current_CO2_per_compartment_unit_neutralized[compartment]) ELSE 0	mol/ (m^2*s)
VPSAT	Converter, arrayed	IF Crop_Scheduler.scheduler[compartment, cycle, crop_compartment]=0 THEN 0 ELSE 0.611*EXP((17.4*MEC_Parameters.MEC_parameters[	kPa

		Crop_Scheduler.scheduler[compartment, cycle, crop_compartment], Tlight])/(239+MEC_Parameters.MEC_parameters[Crop_Scheduler.scheduler[compartment, cycle, crop_compartment], Tlight]))	
VPAIR	Converter, arrayed	VPSAT[compartment, cycle]*current_relative_humidity_per_compartment[compartment]	kPa
VPD	Converter, arrayed	VPSAT[compartment, cycle]-VPAIR[compartment, cycle]	kPa
unit converter mol m2 s	Converter	1	mol/ (m^2*s)
unit converter h d	Converter	1	h/d
DTR unit converter	Converter	3600	s/h
gC	Converter, arrayed	IF (MEC_Parameters.MEC_parameters[Crop_Scheduler.scheduler[compartment, cycle, crop_compartment], gA]+gS[compartment, cycle])=0 THEN 0 ELSE (MEC_Parameters.MEC_parameters[Crop_Scheduler.scheduler[compartment, cycle, crop_compartment], gA]*gS[compartment, cycle]*unit_converter_mol_m2_s/(MEC_Parameters.MEC_ parameters[Crop_Scheduler.scheduler[compartment, cycle, crop_compartment], gA]*unit_converter_mol_m2_s+gS[compartment, cycle]))	mol/ (m^2*s)
water density at 20°C	Converter	998.23	g/kg
water molecular mass	Converter	18.015	g/mol
DTR	Converter, arrayed	DTR_unit_converter*(water_molecular_weight/water_density_at_20°C)*gC[compartment, cycle]*(VPD[compartment, cycle]/Gases_Layer.greenhouse_nominal_pressure)* Crop_Scheduler.scheduler[compartment, cycle, H_compartment]*unit_converter_h_d	kg/ (m^2*d)

9.5.6 Other Plant Properties Module Formulas

Variable Name	Variable Type	Formula/value	Unit
misc plant properties	Converter, arrayed	See Table 9-26 for values.	-

Table 9-26: Misc plant properties arrayed converter values.

Crop	Harvest Index	Edible biomass water content	Inedible biomass water content	Carbohydrates	Fats	Proteins
Dry Bean	0.4	0.1	0.9	61	1.5	22
Lettuce	0.9	0.95	0.9	3	0.1	0.9
Peanut	0.25	0.056	0.9	16	49	26
Rice	0.3	0.12	0.9	76	3.2	7.5
Soybean	0.4	0.1	0.9	30	20	36
Sweet Potato	0.4	0.71	0.9	20	0.1	1.6
Tomato	0.45	0.94	0.9	3.9	0.2	0.9
Wheat	0.4	0.12	0.9	75	2	11
White Potato	0.7	0.8	0.9	16	0.1	1.7

9.5.7 Crop Water Accumulator Module Formulas

Variable Name	Variable Type	Formula/value	Unit
H2O accumulation rate	Converter, arrayed	IF(Crop_Scheduler.scheduler[compartment, cycle, crop_compartment]=0) THEN 0 ELSE (MEC_Crop_Biomass_Production.TEB[compartment, cycle]/ ((1/Other_Plant_Properties.misc_plant_properties[Crop_Scheduler.scheduler[compartment, cycle, crop_compartment], Edible_biomass_water_content])-1))+(MEC_Crop_Biomass_Production.TIB[compartment, cycle]/ ((1/Other_Plant_Properties.misc_plant_properties[Crop_Scheduler.scheduler[compartment, cycle, crop_compartment], Inedible_biomass_water_content])-1))	g/(m^2*d)

9.5.8 Greenhouse Interface Module Formulas

Variable Name	Variable Type	Formula/value	Unit
compartment cultivation area	Converter, arrayed	See Table 4-19 for values (example).	m^2
O2 molecular mass	Converter	2*15.9994	g/mol
unit converter g to kg	Converter	1000	g/kg
C molecular mass	Converter	12.0107	g/mol
compartment total DOP	Converter, arrayed	SUM(MEC_Crop_Biomass_Production.DOP[compartment, *])*compartment_area_and_volume[compartment, Cultivation_area]/unit_converter_g_to_kg*O2_molecular_weight	kg/d
compartment total DCG	Converter, arrayed	SUM(MEC_Crop_Biomass_Production.DCG[compartment, *])*compartment_area_and_volume[compartment, Cultivation_area]/unit_converter_g_to_kg*C_molecular_weight	kg/d
greenhouse DOP	Converter, summing	SUM(compartment_total_DOP[*])	kg/d
greenhouse DCG	Converter, summing	SUM(compartment_total_DCG[*])	kg/d
compartment total water accumulating	Converter, arrayed	SUM(Crop_Water_Accumulator.H2O_accumulation_rate[compartment, *])*compartment_area_and_volume[compartment, Cultivation_area]/unit_converter_g_to_kg	kg/d
compartment water accumulated per area	Converter, arrayed	compartment_area_and_volume[compartment, Cultivation_area]/unit_converter_g_to_kg*Crop_Water_Accumulator.H2O_accumulation_rate[compartment, cycle]	kg/d
greenhouse water accumulation rate	Converter, summing	SUM(compartment_total_water_accumulating[*])	kg/d
compartment total DTR	Converter, arrayed	SUM(MEC_Crop_Transpiration.DTR[compartment, *])*compartment_area_and_volume[compartment, Cultivation_area]	kg/d
greenhouse DTR	Converter, summing	SUM(compartment_total_DTR[*])	kg/d
compartment total TCB	Converter, arrayed	SUM(MEC_Crop_Biomass_Production.TCB[compartment, *])*compartment_area_and_volume[compartment, Cultivation_area]/unit_converter_g_to_kg	kg/d
greenhouse TCB	Converter, summing	SUM(compartment_total_TCB[*])	kg/d
compartment total TEB	Converter, arrayed	SUM(MEC_Crop_Biomass_Production.TEB[compartment, *])*compartment_area_and_volume[compartment, Cultivation_area]/unit_converter_g_to_kg	kg/d
greenhouse TEB	Converter, summing	SUM(compartment_total_TEB[*])	kg/d
compartment TEB	Converter,	compartment_area_and_volume[compartment, Cultiva-	kg/d

per cycle	arrayed	tion_area]*MEC_Crop_Biomass_Production.TEB[compartment, cycle]/unit_converter_g_to_kg	
compartment total TIB	Converter, arrayed	SUM(MEC_Crop_Biomass_Production.TIB[compartment, *])*compartment_area_and_volume[compartment, Cultivation_area]/unit_converter_g_to_kg	kg/d
greenhouse TIB	Converter, summing	SUM(compartment_total_TIB[*])	kg/d
compartment TIB per cycle	Converter, arrayed	compartment_area_and_volume[compartment, Cultivation_area]*MEC_Crop_Biomass_Production.TIB[compartment, cycle]/unit_converter_g_to_kg	kg/d
water metabolizing	Converter, arrayed	MEC_Crop_Biomass_Production.DCG	mol/(m^2*d)
compartment water metabolizing	Converter, arrayed	SUM(water_metabolizing[compartment, *])*compartment_cultivation_area[compartment, Cultivation_area]*H2O_molecular_mass/unit_converter_g_to_kg	kg/d
H2O molecular mass	Converter	18.01528	g/mol
greenhouse metabolizing water	Converter, summing	SUM(compartment_water_metabolizing[*])	kg/d

9.6 Physical-Chemical Systems Formulas

9.6.1 Incinerator Formulas

Variable Name	Variable Type	Formula/value	Unit
incinerator capacity	Converter	1.266 (example)	kg/d
incineration reactants per kg dry waste	Converter, arrayed	1.969	1
incineration products per kg dry waste	Converter, arrayed	See Table 9-27 for values.	1
incineration O2 consumption	Converter	incineration_reactants_per_kg_dry_waste[O2]* Solids_Layer.total_solid_waste_processing	kg/d
incineration CH4 production	Converter	incineration_products_per_kg_dry_waste[CH4]* Solids_Layer.total_solid_waste_processing	kg/d
incineration CO2 production	Converter	incineration_products_per_kg_dry_waste[CO2]* Solids_Layer.total_solid_waste_processing	kg/d
incineration CO production	Converter	incineration_products_per_kg_dry_waste[CO]* Solids_Layer.total_solid_waste_processing	kg/d
incineration H2O production	Converter	incineration_products_per_kg_dry_waste[H2O]* Solids_Layer.total_solid_waste_processing	kg/d
O2 storage lower threshold	Converter	50 (example)	kg
O2 storage upper threshold	Converter	200 (example)	kg
CO2 storage lower threshold	Converter	50 (example)	kg
solid waste storage lower threshold	Converter	100 (example)	kg
incinerator activity	Converter	IF (Gases_Layer.CO2_Storage<CO2_storage_lower_threshold AND Gases_Layer.O2_Storage>O2_storage_lower_threshold) THEN 1 ELSE IF (Solids_Layer.Solid_Waste_Storage_in_Habitat>solid_waste_storage_upper_threshold AND Gases_Layer.O2_Storage>O2_storage_upper_threshold) THEN 1 ELSE 0	1

Table 9-27: Incineration products arrayed converter values.

Material	Value
CH4	0.008
CO2	1.107
CO	0.075
H2O	0.433

9.6.2 Electrolyzer Formulas

Variable Name	Variable Type	Formula/value	Unit
electrolyzer capacity	Converter	11.82 (example)	kg/d
electrolyzer products per kg H2O	Converter, arrayed	See Table 9-28 for values.	1
electrolyzer H2 production	Converter	electrolyzer_products_per_kg_H2O[H2]* Liquids_Layer.water_consumption_by_electrolyzer	kg/d
electrolyzer O2 production	Converter	electrolyzer_products_per_kg_H2O[O2]* Liquids_Layer.water_consumption_by_electrolyzer	kg/d
O2 storage lower threshold	Converter	50 (example)	kg
potable water storage lower threshold	Converter	10 (example)	kg
electrolyzer activity	Converter	IF Liquids_Layer.Potable_Water_Storage_in_Habitat> potable_water_storage_lower_threshold THEN IF Gases_Layer.O2_Storage< O2_storage_lower_threshold THEN 1 ELSE 0 ELSE 0	1

Table 9-28: Electrolyzer products arrayed converter values.

Material	Value
H2	0.1119
O2	0.8881

9.6.3 Sabatier Reactor Formulas

Variable Name	Variable Type	Formula/value	Unit
sabatier capacity	Converter	7.04 (example)	k/d
sabatier reactants per kg CO2	Converter, arrayed	0.18322	1
sabatier products per kg CO2	Converter, arrayed	See Table 9-29 for values.	1
sabatier H2 consumption	Converter	sabatier_reactants_per_kg_CO2[H2]* Gases_Layer.CO2_consumption_by_sabatier_reactor	kg/d
sabatier CH4 production	Converter	sabatier_products_per_kg_CO2[CH4]* Gases_Layer.CO2_consumption_by_sabatier_reactor	kg/d
sabatier H2O production	Converter	sabatier_products_per_kg_CO2[H2O]* Gases_Layer.CO2_consumption_by_sabatier_reactor	kg/d
CO2 storage upper threshold	Converter	300 (example)	kg
H2 storage lower threshold	Converter	10 (example)	kg
sabatier activity	Converter	IF Gases_Layer.CO2_Storage> CO2_storage_upper_treshold THEN IF Gases_Layer.H2_Storage> H2_storage_lower_threshold THEN 1 ELSE 0 ELSE 0	1

Table 9-29: Sabatier products arrayed converter values.

Material	Value
CH4	0.36452
O2	0.81870

9.6.4 CHX formulas

Variable Name	Variable Type	Formula/value	Unit
habitat CHX capacity	Converter	2 (example)	kg/d
habitat CHX water removal	Converter	IF (SUM(Liquids_Layer.insensible_water_loss_by_crew[*])+ SUM(Liquids_Layer.sensible_water_loss_by_crew[*]))<habitat_CHX_capacity THEN (SUM(Liquids_Layer.insensible_water_loss_by_crew[*])+ SUM(Liquids_Layer.sensible_water_loss_by_crew[*])) ELSE habitat_CHX_capacity	kg/d
greenhouse CHX capacity	Converter	250 (example)	kg/d
greenhouse CHX water removal	Converter	IF Liquids_Layer.total_transpiration_water_production_in_greenhouse<greenhouse_CHX_capacity THEN Liquids_Layer.total_transpiration_water_production_in_greenhouse ELSE greenhouse_CHX_capacity	kg/d

9.6.5 VPCAR formulas

Variable Name	Variable Type	Formula/value	Unit
VPCAR capacity	Converter	15 (example)	kg/d
potable water storage habitat lower threshold	Converter	100 (example)	kg
wastewater storage upper threshold	Converter	100 (example)	kg
wastewater storage lower threshold	Converter	0 (example)	kg
VPCAR activity	Converter	IF (PREVIOUS(SELF, 0)=1 AND Liquids_Layer.Wastewater_Storage<=wastewater_storage_lower_threshold) THEN 0 ELSE IF (Liquids_Layer.Wastewater_Storage>=wastewater_storage_upper_threshold OR (PREVIOUS(SELF, 0)=1) OR (Liquids_Layer.Potable_Water_Storage_in_Habitat<=potable_water_storage_in_habitat_lower_threshold)) THEN 1 ELSE 0	-

9.6.6 Oxygen and Carbon Dioxide Separator Formulas

Variable Name	Variable Type	Formula/value	Unit
O2 separator capacity	Converter	5 (example)	kg/d
O2 separator activity	Converter	IF (PREVIOUS(SELF, 0)=1 AND (Gases_Layer.O2_in_Greenhouse<=Gases_Layer.greenhouse_O2_mass_requirement[nominal] OR Gases_Layer.O2_in_Habitat>Gases_Layer.habitat_O2_mass_requirement[nominal])) THEN 0 ELSE IF ((PREVIOUS(SELF, 0)=1) OR (Gases_Layer.O2_in_Greenhouse>=Gases_Layer.greenhouse_O2_mass_requirement[nominal] AND (Gases_Layer.O2_in_Habitat<Gases_Layer.habitat_O2_mass_requirement[nominal]))) THEN 1 ELSE 0	-

CO2 separator capacity	Converter	2 (example)	kg/d
CO2 separator activity	Converter	IF (PREVIOUS(SELF, 0)=1 AND (Gases_Layer.CO2_in_Habitat<=Gases_Layer.habitat_CO2_mass_requirement[minimum] OR Gases_Layer.CO2_in_Greenhouse>Gases_Layer.greenhouse_CO2_mass_requirement[nominal])) THEN 0 ELSE IF ((PREVIOUS(SELF, 0)=1) OR (Gases_Layer.CO2_in_Habitat>Gases_Layer.habitat_CO2_mass_requirement[nominal] AND Gases_Layer.CO2_in_Greenhouse<Gases_Layer.greenhouse_CO2_mass_requirement[nominal])) THEN 1 ELSE 0	-

9.6.7 Inedible Biomass Processor

Variable Name	Variable Type	Formula/value	Unit
inedible biomass processor capacity per crop	Converter	5 (example)	kg/d
harvested inedible biomass storage upper threshold	Converter	50 (example)	kg
inedible biomass processor activity	Converter	IF (Gases_Layer.CO2_Storage<CO2_storage_lower_threshold AND Gases_Layer.O2_Storage>O2_storage_lower_threshold) THEN 1 ELSE IF (SUM(Solids_Layer.Harvested_Inedible_Dry_Biomass[*])>harvested_inedible_biomass_storage_upper_threshold AND Gases_Layer.O2_Storage>O2_storage_upper_threshold) THEN 1 ELSE 0	-
C in processed inedible biomass	Converter, arrayed	Solids_Layer.inedible_biomass_processing[crop]*MEC_Parameters.MEC_parameters[crop, BCF]	kg/d
CO2 production by inedible biomass processing	Converter, arrayed	C_in_processed_inedible_biomass[crop]*C_to_CO2_converter	kg/d
C to CO2 converter	Converter	44.0095/12.0107	-
C to O converter	Converter	15.9994/12.0107	-
O in processed inedible biomass	Converter, arrayed	C_in_processed_inedible_biomass[crop]*(2-MEC_Parameters.MEC_parameters[crop, OPF]*2+1)*C_to_O_converter	kg/d
O2 consumption by inedible biomass processing	Converter, arrayed	(C_in_processed_inedible_biomass[crop]*C_to_O_converter*2)+(H_in_processed_inedible_biomass[crop]/2*H_to_O_converter-O_in_processed_inedible_biomass[crop])	kg/d
H to O converter	Converter	15.9994/1.007954	-
C to H converter	Converter	1.00794/12.0107	-
H in processed inedible biomass	Converter, arrayed	C_in_processed_inedible_biomass[crop]*2*C_to_H_converter	kg/d
H2O production by inedible biomass processing	Converter, arrayed	H_in_processed_inedible_biomass[crop]*H_to_H2O_converter	kg/d
H to H2O converter	Converter	18.01528/(2*1.00794)	-

10 Appendix C - Nomenclature

ABRS = Advanced Biological Research System

ACMG = Arthur C. Clarke Mars Greenhouse

ADVASC = Advanced Astroculture

ADP = Adenosine Diphosphate

ALS = Advanced Life Support

APC = Air Polarized Concentrator

APH = Advanced Plant Habitat

ASC = Astroculture

ATP = Adenosine Triphosphate

BIO-Plex = Bioregenerative Planetary Life Support Systems Test Complex

BLSS = Bio-regenerative life support systems

BPC = Biomass Production Chamber

BPS = Biomass Production System

BVAD = Baseline Values and Assumptions Document

CEEF = Closed Ecology Experiment Facility

CELSS = Closed Environment Life Support System

CGR = Crop Growth Rate

CHX = Condensing Heat Exchanger

CM = Crew Member

C.R.O.P. = Combined Regenerative Organic Food Production

DCG = Daily Carbon Gain

DLR = German Aerospace Center

DOP = Daily Oxygen Production

DT = Delta Time

DTR = Daily Transpiration Rate

DW = Dry Weight

EC = Energy Cascade *(Chapter 3.8.2 only)*

EC = Electrical Conductivity *(all chapters expect Chapter 3.8.2)*

EDC = Electrochemical Depolarized CO_2 Concentrator

ECLSS = Environment Control and Life Support System

EMCS = European Modular Cultivation System

ESM = Equivalent System Mass

EVA	= Extravehicular Activity
FW	= Fresh Weight
GC	= Growth Chamber
H	= Photoperiod
HPC	= Higher Plant Chamber
ISS	= International Space Station
LGH	= Lunar Greenhouse
LSS	= Life Support System
MDRS	= Mars Desert Research Station
MEC	= Modified Energy Cascade
MET	= Metabolic Equivalent Task
MF	= Multifiltration
MS	= Molecular Sieve
NADP	= Nicotinamide Adenine Dinucleotide Phosphate
NASA	= National Aeronautics and Space Administration
P/C	= Physical-chemical
PAR	= Photosynthetic Active Radiation
PEU	= Plant Experiment Unit
PGF	= Plant Growth Facility
PGU	= Plant Growth Unit
PLC	= Programmable Logic Controller
PPF	= Photosynthetic Photon Flux
PRU	= Plant Research Unit
RH	= Relative Humidity
RLSS	= Regenerative Life Support System
RO	= Reverse Osmosis
SAWD	= Solid Amine Resin CO_2 Removal
SCWO	= Super Critical Water Oxidation
SFWE	= Static-Feed Water Electrolysis
SPWE	= Solid Polymer Water Electrolysis
SIMBOX	= Science in Microgravity Box
SPDT	= Single Pole Dual Toggle
SPFGC	= South Pole Food Growth Chamber

t	= Time
T	= Temperature
TCB	= Total Crop Biomass
TEB	= Total Edible Biomass
TIB	= Total Inedible Biomass
TIMES	= Thermoelectric Integrated Membrane Evaporation System
TLEC	= Top-Level Energy Cascade
VCD	= Vapor Compression Distillation
V-HAB	= Virtual Habitat
V-SUIT	= Virtual Spacesuit
VPCAR	= Vapor Phase Catalytic Ammonia Removal
WO	= Wet Oxidation
WVE	= Water Vapor Electrolysis
XFRT	= Edible Fraction of Total Biomass